TELIDON SYSTEM STUDY

3RD INTERIM REPORT

VOLUME 1 OF 2

MCS MILLER COMMUNICATIONS SYSTEMS LTD.

TELIDON SYSTEM STUDY

3RD INTERIM REPORT

VOLUME 1 OF 2

Contract No: 1ST82-00710
MCS File No: 8342
DSS File No: DSS21ST.36100-2-4380
Date: September 30, 1983
Revised: March 12, 1984

Prepared by: K. W. Moreland, J. H. Lodge
K. W. Moreland, J. H. Lodge

Approved by: R K Tiedemann R G Lyons
R. K. Tiedemann, R. G. Lyons

SUBMITTED BY:

MCS MILLER COMMUNICATIONS SYSTEMS LTD.
300 Legget Drive,
Kanata, Ontario,
Canada K2K 1Y5

TELIDON SYSTEM STUDY
3RD INTERIM REPORT

This interim report details progress made in the areas of multipath channel validation, pulse shaping for teletext, and establishing performance of the existing system in typical noise and multipath environments. The existing system employs a truncated 100% raised cosine transmit pulse shape and a conventional teletext decoder. The most important operational characteristics (slicing level estimation and symbol synchronization) of the conventional teletext decoder have been presented in the Telidon System Study 'Second Interim Report'.

The first section briefly addresses the pulse shaping problem for teletext. The second section deals with multipath channel validation and the generation of realistic channel characteristics to use for system evaluation. The final section discusses the simulated performance of the existing Telidon system in typical multipath and noise environments. Details have been relegated to appendices for the most part.

TABLE OF CONTENTS

VOLUME 1

1.0 PULSE SHAPING FOR TELETEXT

The choice of a suitable pulse shape for teletext has received considerable attention lately [1], [2], [3], [4], [5], [6]. The problem is complicated by the number of objectives that ideally should be simultaneously satisfied. The overall objectives of the pulse shape design are:

(i) to minimize the probability of bit error subject to the other design objectives being satisfied,

(ii) The overshoots, at both the output of the transmitter and the baseband channel of the receiver, should be constrained at acceptable levels,

(iii) the pulse shape design should lead to specifications that are compatible with current television broadcast specifications,

(iv) the overall pulse shape should be reasonably robust in the presence of multipath,

(v) receiver requirements should ideally be kept as simple as possible, (i.e. any necessary complexity and stringent specification should be transferred to the transmit side when possible),

(vi) the bandwidth must be constrained to the 4.2 MHz NTSC video bandwidth.

One possible approach for meeting the above objectives is to define a massive non-linear optimization that attempts to simultaneously achieve the above goals, but this is clearly beyond the scope of the present contract. Furthermore, before such a chore could be undertaken, the pulse shaping problem requires further refinement and formulation. For

example, the acceptable overshoot levels at both the output of the transmitter and the baseband output of the receiver must be determined. This would invariably involve investigating the audio buzz phenomena. Careful thought must be given to choosing an overall performance index, especially when the optimization is to be performed over an ensemble of channel characteristics. Most performance criteria, that would seem reasonable to apply, tend to implicitly weight the poorer members of the ensemble of channels (i.e. those with a relatively high bit error rate) more than good members. Consequently, if one is not careful, the likely result of the optimization might be to sacrifice the performance of the good channels in order to achieve a marginal improvement for the poor channels.

The ultimate guage of the performance of a specific pulse shape is the probability of bit error achieved. Do to intersymbol interference, evaluation of error probability becomes rather involved. A number of techniques for estimating the bounds on the probability of error are presented in [28], [1]. The more accurate bounds are not trivial to evaluate, and often do not have general applicability, due to assumptions about the data correlation properties. In most work that has been done to date on pulse shaping for teletext (Sousa and Pasupathy [2], [3], and S. Ng [6]) certain properties of the eye diagram [i.e. eye height, eye width (time sensitivity), and overshoots] were used as figures of merit for various pulse shapes. A suitable performance criterion to be used as a basis for comparison must be selected and justified.

From the above discussion, it is apparent that deriving an "optimal" pulse shape via nonlinear optimization is a major undertaking, involving considerable effort to formulate and to gather the required data to adequately model system parameters, let alone solve. Another approach to the pulse

shape specification problem is to attempt to decompose it into several smaller, more manageable problems and handle each one separately. In Appendix I, which is primarily concerned with the pulse shaping issue, this is the approach taken. This appendix contains a general discussion about pulse shaping, and the specification of a "reasonable" overall pusle shape, whose transfer function is continuous and therefore realizable. The apportioning of the pulse shape is also discussed along with a reasonable approach to specifying it. Also discussed in Appendix I are the related issues of audio buzz, slicing level, and symbol synchronization. Some of the deficiencies of the existing decoder synchronization circuitry, and possible approaches to overcoming these deficiencies are presented in Appendix I.

Simulation results [15] have shown that a loss of approximately 3 dB can be attributed to the existing slicing level and clock phase circuitry in the Telidon system, even under fairly ideal conditions (i.e. no multipath propagation, ideal carrier recovery, and white gaussian noise). Given the large potential performance gain, improvements to the existing decoder synchronization circuitry should be given the highest priority. As for pulse shape optimization, it is felt that the first step should be a problem definition and tradeoff study. This would provide the opportunity to estimate the potential benefits and risks of performing such an optimization so that a rational decision as to whether or not to persue pulse shape optimization can be made. Areas that such a study should address include:

(i) identifying suitable models for the various uncertainties (i.e. transmitter, receiver, and multipath characteristics) in the teletext transmission path,

(ii) outlining procedures for determining model parameters,

(iii) defining a tractable optimization problem and estimating the associated costs (in terms of money and amount of computation).

2.0 MULTIPATH CHANNEL VALIDATION AND GENERATION

Considerable effort by members of CRC (in particular Robert Bultitude and Mike Sablatash) has been devoted to measuring channel impulse responses in the Ottawa area. The purpose of this section is to analyze the CRC measurements, and make some comparisons with results generated by the Telidon RF propagation model simulation program. For developing multipath channels for use in the Telidon system performance simulation, the VHF multipath simulation program allows more flexability and control. For example, with the simulation program, the carrier frequency can be easily modified to characterize channels in frequency bands where measurements were not conducted.

The simulation program has been very instructive in yielding insight into the behaviour of VHF multipath propagation as a function of frequency and environment. The severity of multipath components as a function of delay for various frequencies and reflector characteristics are discussed and presented in [15] and [18]. An important conclusion that can be drawn from the simulation results is that the statistics of the channel are wildly non-stationary, and are very sensitive to frequency and receiver locality. As indicated in [18], when the frequency is 55.25 MHz (channel 2), multipath all but disappears, even with 30m x 30m reflectors. However, when the carrier frequency is 211.25 MHz (channel 13), multipath is much more severe, and significant echoes with delays of 10 μsec are possible for large 30m x 30m reflectors. The propagation model has indicated these meaningful trends with regards to frequency sensitivity of the VHF multipath channel.

The cumulative distribution function for channel 13 (f = 211.25 MHz) with randomized reflector width, height, and thickness is presented in Figure 1. In fact, the thickness was randomly selected between 10 cm and 30 cm, and the width and height were independently and randomly selected between 7.6m and 30m. It is apparent from Figure 1, that for VHF, it should not be necessary to consider multipath delays greater than 10 μsec. The delay spread shown in Figure 1 is thought to be a conservative upper bound as it is unlikely that many structures can produce a specular reflection comparable to that of the di-electric slabs (up to 30m x 30m) used in the simulation. One would expect the delay spread to be strongly dependent on reflector sizes, as the ratio of the scattered to incident field strengths, in the direction of specular reflection, provided in [19] and reproduced here for convenience:

$$\left|\frac{E_s}{E_i}\right| \simeq \frac{2\pi\ r_o^2\ \sin\psi\ R_v'\ H^3 W}{\lambda^2 r^2 r_1^2} \qquad (1)$$

where

r_o is the distance between transmitter and receiver

r_1 is the distance between transmitter and scatterer

r is the distance between the scatterer and receiver

ψ is the surface grazing angle

λ is the carrier wavelength

R_v' is the reflection coefficient

H is the reflector height

TELIDON RF PROPAGATION MODEL -- ANALYSIS OF SCATTER DIAGRAM PAR9B

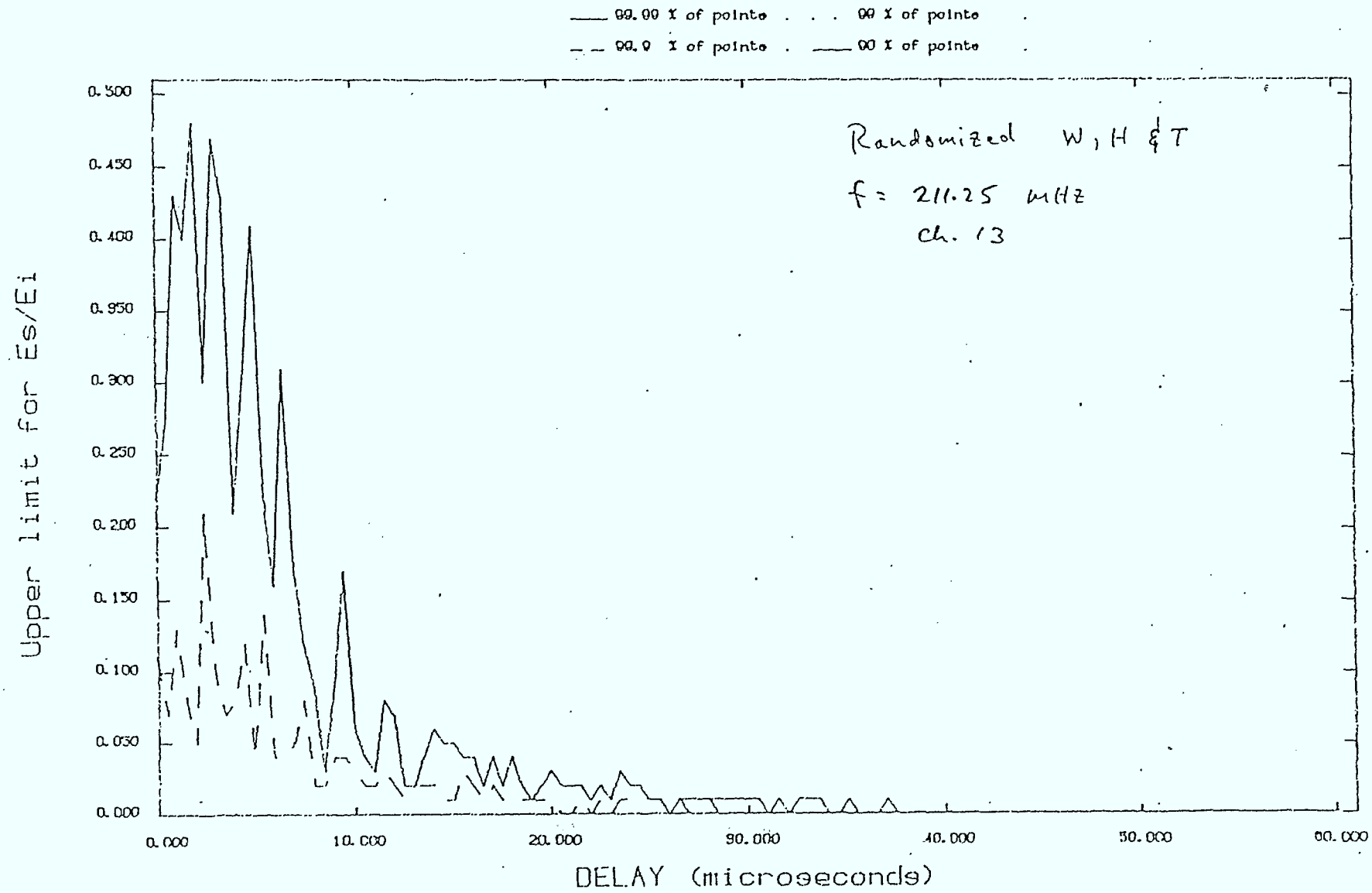

Figure 1

W is the reflector width,

is proportional to H^3W. Hence, if the reflector area is reduced by a factor of '2', in the far-field, echoes are reduced by 12 dB, thereby decreasing the delay spread of significant echoes.

In analyzing the CRC measurements, attention must be restricted to the subset of channels which provide acceptable video quality. There is absolutely no need attempting to provide Broadcast Telidon service to customers that do not receive useful television pictures over the air. A prescreening procedure for discarding channels not providing usable television pictures is presented and discussed in detail in Appendix II. A brief summary will be provided here for completeness.

2.1 Channel Classification

A procedure for weighting multiple ghosts to obtain an estimate of subjective picture quality, proposed in [21], was adopted for channel classification. To estimate the subjective quality of a television picture, a "perceived DU (desired to undesired) ratio, denoted by PDUR, is computed. It is essentially the ratio of the power of the desired signal to the power sum of individual ghost images (Signal to Clutter Ratio), with appropriate weighting applied to each echo to account for the effects of delay (τ) and r.f. phase (ψ).

The degree of quality degradation is dependent on the phase, ψ, and delay, τ, of the ghost. The perceived DU ratio of a particular individual ghost with delay, τ, and phase, ψ, is the DU ratio of a positive ghost with standard delay that provides equivalent degradation.

The perceived DU ratio of the i-th ghost is given by:

$$P_{i[dB]} = \frac{D}{U}(i) + W_{\psi}(i) + W_{\tau}(i)_{[dB]} \qquad (2)$$

where

$\frac{D}{U}(i)$ is the DU ratio of the ghost

W_{ψ} is the phase weighting function (see Figure 2)

W_{τ} is the delay weighting function. (see Figure 3)

In [21], the standard delay for a ghost is 5 μsec.

The perceived DU ratio, which provides an indication of the degree of quality degradation of a picture impaired by multiple ghosts, is:

$$PDUR = -10 \log_{10} \sum_{i=1}^{n} 10^{-P_i/10} \ [dB] \qquad (3)$$

where

n = the number of ghosts.

The relationship between PDUR and subjective picture quality is shown graphically in Figure 4. The subjective picture evaluation was made using the 5 point comment scale shown in Table 1. In fact, experiments conducted by the authors of [21] indicate that the correlation coefficient between the numerical PDUR and subjective quality assessment is very high. In fact, the PDUR is probably the best gauge of subjective picture quality available at present.

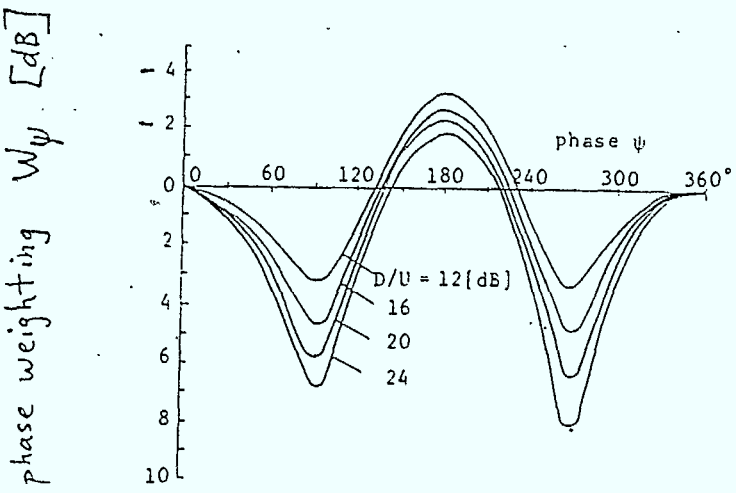

Figure 2 : Phase Weighting Curve

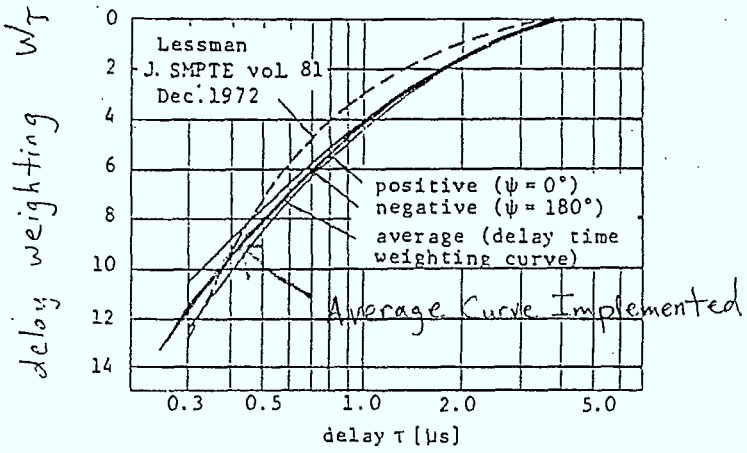

Figure 3 : Delay time weighting curves

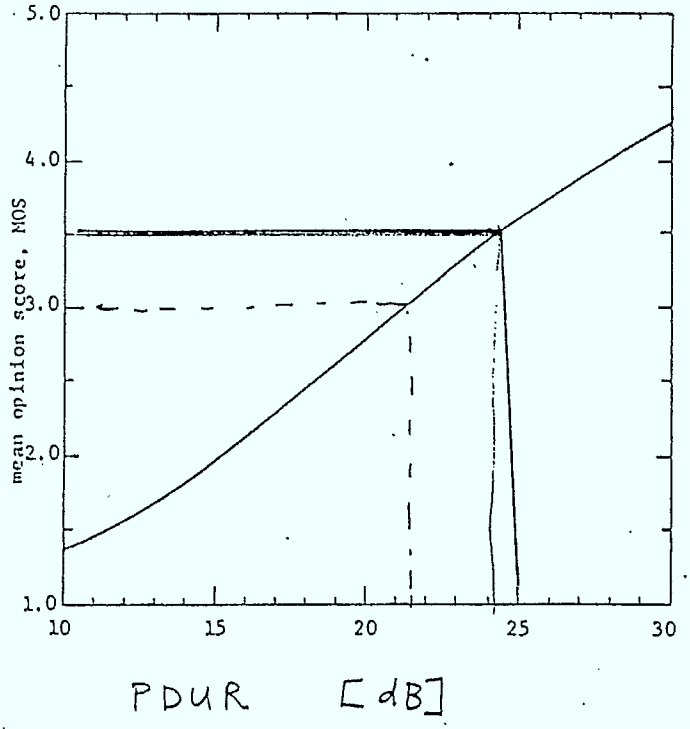

Figure 4 : Relationship between PDUR and mean opinion score for picture quality

Comment Number	Description
5	imperceptible
4	perceptible but not annoying
3	somewhat annoying
2	severely annoying
1	unusable

Table 1: 5-point comment scale used in [21] for subjective picture evaluation

Using Figure 4 and the comment scale of Table 1, the following thresholds were selected for acceptable and good video channels:

PICTURE QUALITY	COMMENT SCALE THRESHOLD	PDUR THRESHOLD
Unacceptable	≤ 1.5	≤ 11 dB
Good	≥ 3.5	≥ 24 dB

2.2 Developing Channel Statistics Using The Simulation Program

The VHF propagation model simulation program can be used to generate realistic multipath channels to use for establishing Telidon system performance. To do so, one must establish the number of echo paths, N, comprising the channel impulse response. This parameter is strongly dependent on the density of buildings and extent of the urban area. In the simulation, one simply has to combine N Monte Carlo cycles into an impulse response, specifying the delay, magnitude, and a uniform phase angle on the interval $[-\pi, \pi]$ for each component path. The channel can then be classified using the PDUR classification scheme discussed in the previous section. Only acceptable channels are retained, and statistical analysis performed on the acceptable and the good channels. The PDUR, and consequently, the classification procedure will be a

function of the number of echo paths comprising a channel impulse response. The sensitivity of this parameter will be investigated. With the simulation program, the generation of impulse responses of acceptable video channels is relatively easy. At present, we collect impulse responses that have PDUR's between specific limits (i.e. '13 - 15 dB', '19 - 20 dB', etc). This gives one better control over the quality of the channel under investigation. However, it must be emphasized that good video quality does not necessarily imply good teletext performance.

2.2.1 Generating CDF Contours With The Simulation Program

Generating and classifying channels to use for evaluating system performance is relatively straight-forward. An extremely important parameter is the number of echoes (reflectors), N. Phase weighting is also important, as the subjective effect of an echo does depend on the phase of the echo. To statistically characterize channels with acceptable video, we would like to develop cdf contours of magnitude versus delay. Consequently we would like to decondition with respect to phase.

Originally, the proposed channel characterization procedure involved assigning a uniform phase [0°, 360°] to each path, estimating the phase weighting from implementations of the phase weighting curves (see Figure 2), estimating the delay weighting (see Figure 3), and determining the PDUR ratio. The average delay weighting function can be approximated as follows:

$$W_{\tau\,[dB]} = \begin{cases} 11.5 - 15.78\ \log_{10}(\tau/0.3) & \text{for } \tau \leq 0.5\mu\text{sec} \\ 8 - 13.29\ \log_{10}(2\tau) & \text{for } 0.5\mu\text{sec} \leq \tau \leq 1\mu\text{sec} \\ 4 - 8.3\ \log_{10}(\tau) & \text{for } 1\mu\text{sec} \leq \tau \leq 2\mu\text{sec} \\ 1.5 - 5.68\ \log_{10}(\tau/2) & \text{for } 2\mu\text{sec} \leq \tau \leq 3\mu\text{sec} \\ 0.5 - 4\ \log_{10}(\tau/3) & \text{for } 3\mu\text{sec} \leq \tau \leq 4\mu\text{sec} \\ 0 & \text{for } \tau \geq 4.0\ \mu\text{sec} \end{cases} \quad (4)$$

Implementing the phase weighting curves, which are indexed according to DU ratio, is more involved. Consequently, a simpler procedure has been adopted.

2.2.2 Phase Weighting

The subjective effect of a ghost depends on its r.f. phase. However, the r.f. phase is a volatile parameter that can change dramatically with small perturbations in the position of the antenna. A channel that is classified as acceptable may be so only because of fortunate phases on dominate echoes. Perturbations in these phases would provide a channel that does not give acceptable video quality. Channels that are certain to provide acceptable video quality can be guaranteed by assuming worst case phases (ψ=180°) for each path.

It must be emphasized that the mean opinion score of '1.5' (which corresponds to a PDUR of 11 dB) was established as a conservative estimate of the threshold of acceptability. Variations of ± 2 dB about the PDUR threshold, do not

greatly improve or degrade mean opinion scores on subjective quality. For example increasing the threshold by 2.5 dB translates into an increase of only 0.25 on the comment scale. As a result, there does not really exist a clear cut threshold, and the choice is rather arbitrary.

For an impulse response defined by a number of echo paths with delays, τ_i, and magnitudes, u_i, an infinite number of potential channels can be defined by assigning uniform phases to each path. One could classify the channel based on an average phase weighting, worst case phase assumption, or assuming zero phase (positive) echoes. The PDUR's computed using these assumptions are related as follows:

$$PDUR_{(ave)} \simeq PDUR_{(zero\ phase)} + 0.46\ dB$$

$$PDUR_{(worst\ case)} \simeq PDUR_{(zero\ phase)} - 2\ dB$$

The average phase weighting was evaluated assuming the phase weighting curve for a DU ratio of 12 dB, and the mean worst case weighting is approximately 2 dB.

The difference between average and worst case phase weighting is 2.5 dB, which translates ito only a 0.25 change in the quality comment scale in the neighbourhood of the threshold. Consequently, we will require that each channel have a PDUR exceeding 11 dB, for worst case phase weighting. This can be evaluated assuming positive echoes (avoiding the need for considering phase weighting) by increasing the thresholds by 2 dB, i.e.

Channel Classification	PDUR Threshold
Unacceptable	$\leq$ 13 dB
Good	$\geq$ 26 dB

2.2.3 Statistics Gathering and Sensitivity Versus 'N'

A scatter table for acceptable channels (this includes good channels) and a scatter table for good channels are maintained. When an impulse response is classified, the magnitude and delay for each path comprising that impulse response is entered into the appropriate scatter table. The scatter tables are then analyzed to generate cumulative distribution functions of magnitude versus delay. The cdf contours of the ensemble of paths belonging to acceptble channels are generated to obtain an indication of the delay spread that an adaptive equalizer must content with, and to allow a comparison with channel measurements. One could select channel responses from the cdf contours. However, there is no guarantee that the channel response selected would in fact be a channel providing acceptable picture quality. One would have to compute the PDUR to be certain. Since channels are generated and classified during the statistics gathering process, storing these (and indexing them according to PDUR value) for future use is much better than generating channels from the cdf contours.

The PDUR is dependent on the number of echoes, N. As N increases, the background clutter level increases. This tends to reduce the PDUR ratio, resulting in a higher percentage of rejected channels.

2.3 Simulation Runs And Results

The major purpose of these preliminary runs was to establish the sensitivity of the cdf contours with respect to the number of echoes in the channel impulse response. Furthermore, one can establish the effect of the acceptability criterion on the cdf contours by comparing the results with those previously obtained [15], [18]. The model that was used was the same as that specified in [18], i.e.

frequency	selectable
ε_r	3.0
σ	3×10^{-4} mho/m
T	randomly selected between 10-30 cm
W, H	randomly selected between 7.6m and 30m
Occupational Domain	6 km x 6 km, centered on the receiver
Transmitter Height, h_1	60m
Receiver Height, h_2	8.3m
Path Length	16 km
Reflector Orientation	Randomized

Table 3 contains a summary of the simulation results, and the corresponding figure numbers of the appropriate CDF contours. As expected, as the number of impulse response components increases, the percentage of channels rejected increases and the percentage of good channels decreases. This is simply due to the increased background clutter level. As indicated in Table 3, when the number of significant reflectors in the 6 km x 6 km occupational domain is dense (800) for channel 13, over 50% of the channels are rejected (PDUR's less than 13 dB). The number of reflectors in the occupational domain can be related to the frontage density [18] of significant reflectors (as seen from the street) as follows:

Frequency (MHz)	Number of Channels Classified	Number of Paths Per Channel	Percentage Rejected	Percentage Accepted	Percentage Good	CDF Contour Figures
211.25 (channel 13)	5,000	100	5.1	94.9	54.9	5, 6
	2,000	200	10.8	89.2	18.6	7, 8
	2,000	400	22.6	77.4	0.45	9, 10
	1,000	800	51.8	48.2	0.0	11
55.25 (channel 2)	10,000	100	0.0	100	98	12, 13
	2,500	400	0.0	100	91	14, 15
201 (corresponds to frequency used in CRC measurements)	10,000	100	4.5	95.5	57.5	16, 17
	5,000	200	9.58	90.42	21.5	18, 19

Table 3: Preliminary Simulation Results

N (number of reflectors)	FRONTAGE DENSITY
100	3.13%
200	4.43%
400	6.27%
800	8.87%

The CDF contours for acceptable and good channels for a carrier frequency of 211.25 MHz and various values of N are provided in Figures 5 through 11. As the number of rejected channels increases with increasing N, the general trend is a reduction in the magnitude contours for the acceptable channels. However, the changes are not that dramatic, and it is safe to conclude that the magnitude versus delay contours are not very sensitive to the number of reflectors (echo paths).

It is interesting to compare the results obtained employing the acceptability criterion (see Figure 5 for N=100 paths) with those obtained earlier (see Figure 1). It is apparent is that 99.99% contour is reduced. The echoes in the 1-5 μsec region are above -8 dB in Figure 1, and this corresponds to channels providing unacceptable video quality. As is evident in Figure 5, the 99.99% contour is in the vicinity of -9.4 dB out to roughly 1 μsec, at which point it begins to fall. There is little difference for longer delays (greater than or equal to 5 μsec).

ANALYSIS OF SCATTER DIAGRAM PAR100 - ACCEPTABLE CHANNELS

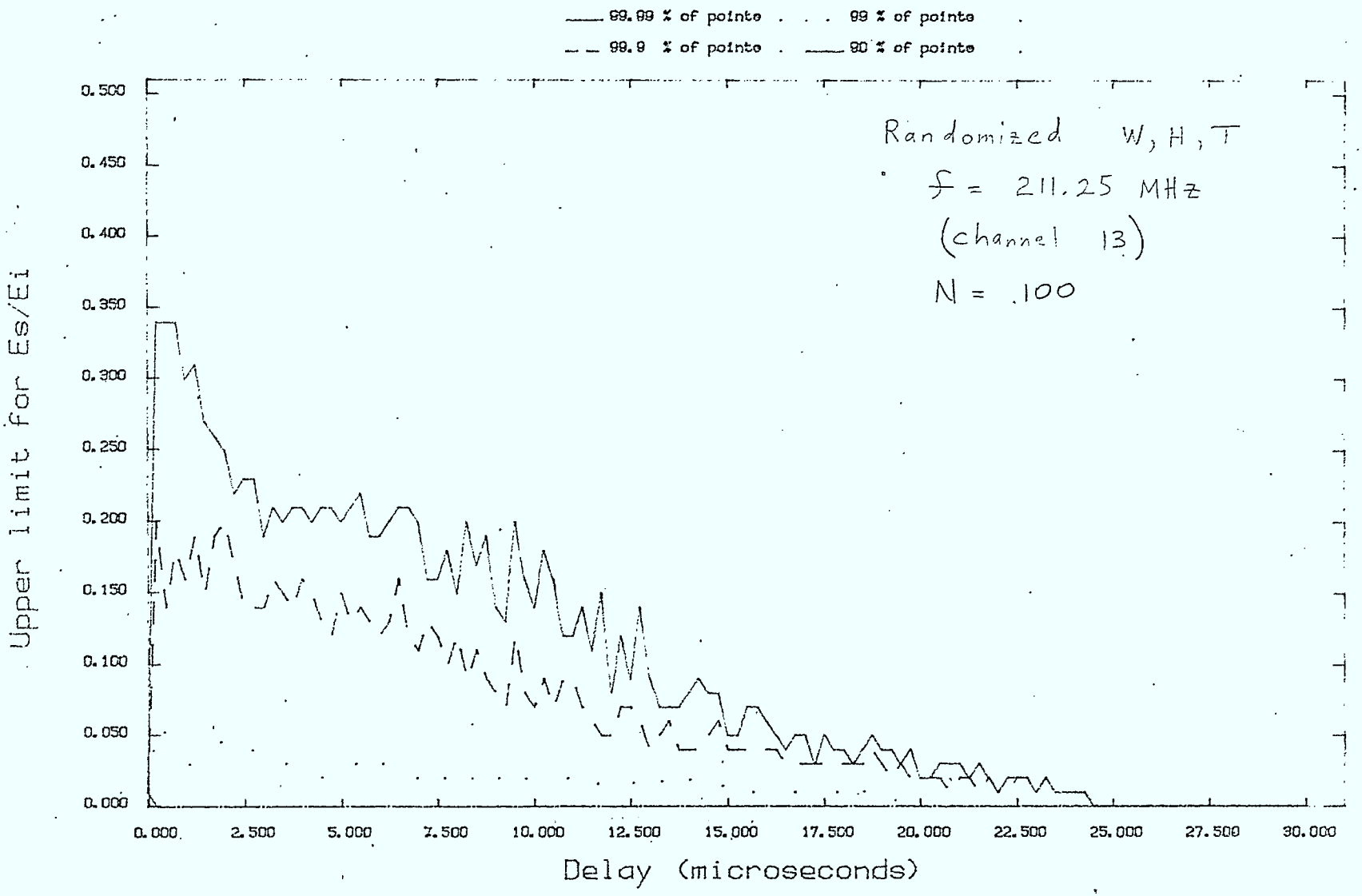

Figure 5

ANALYSIS OF SCATTER DIAGRAM PAR100 - GOOD CHANNELS

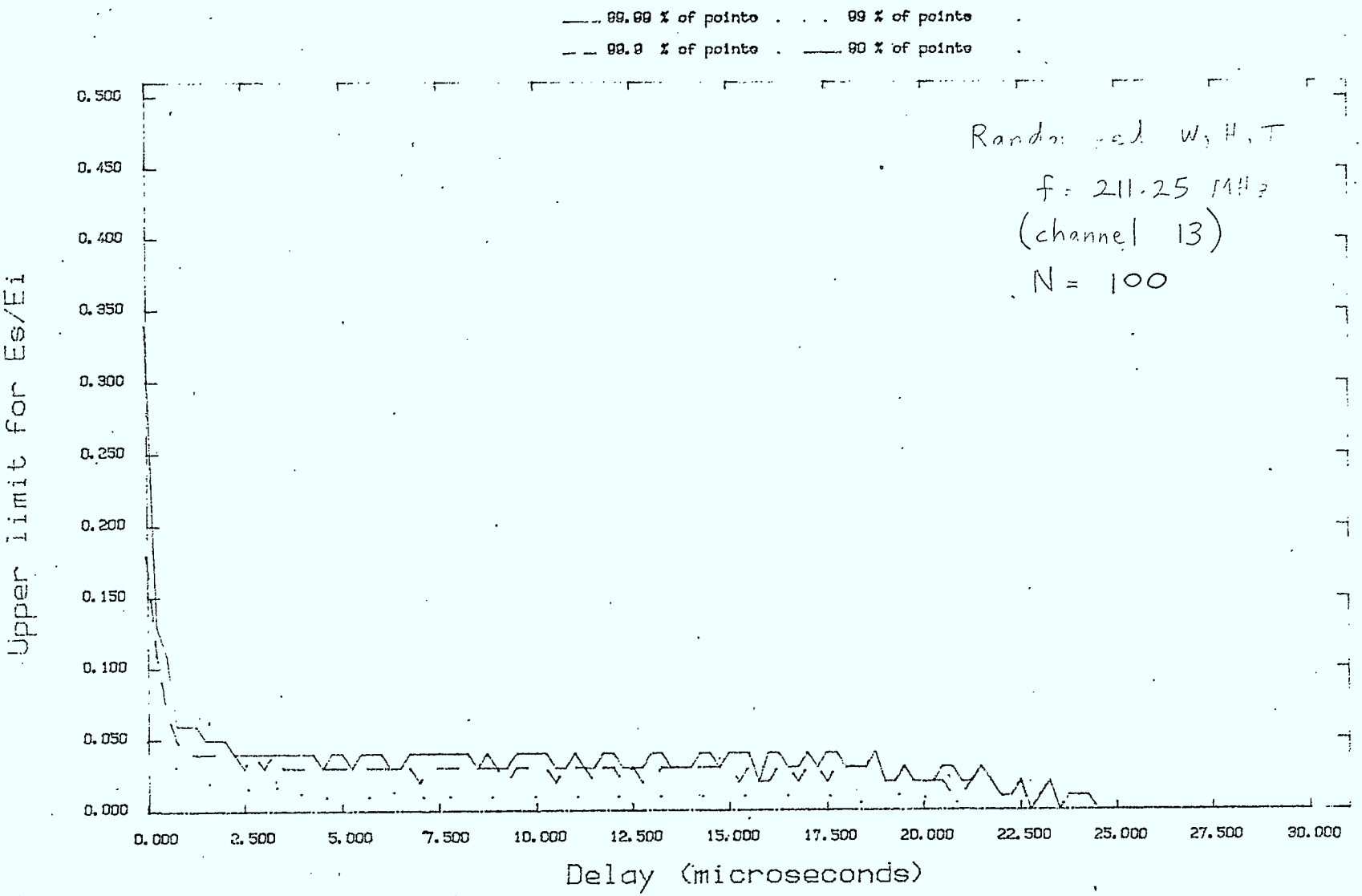

Figure 6

ANALYSIS OF SCATTER DIAGRAM PAR200 - ACCEPTABLE CHANNELS

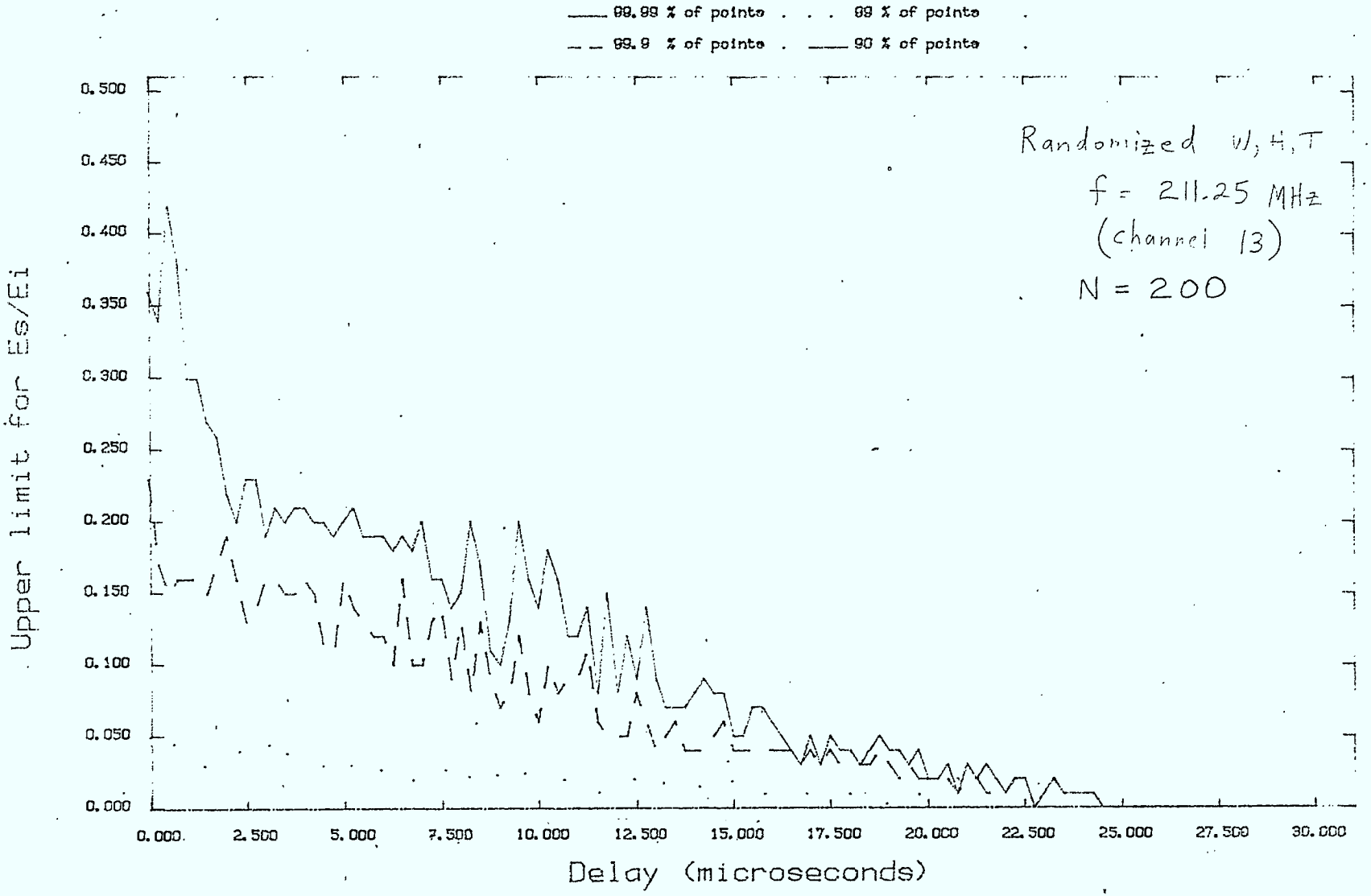

Figure 7

ANALYSIS OF SCATTER DIAGRAM PAR200 - GOOD CHANNELS

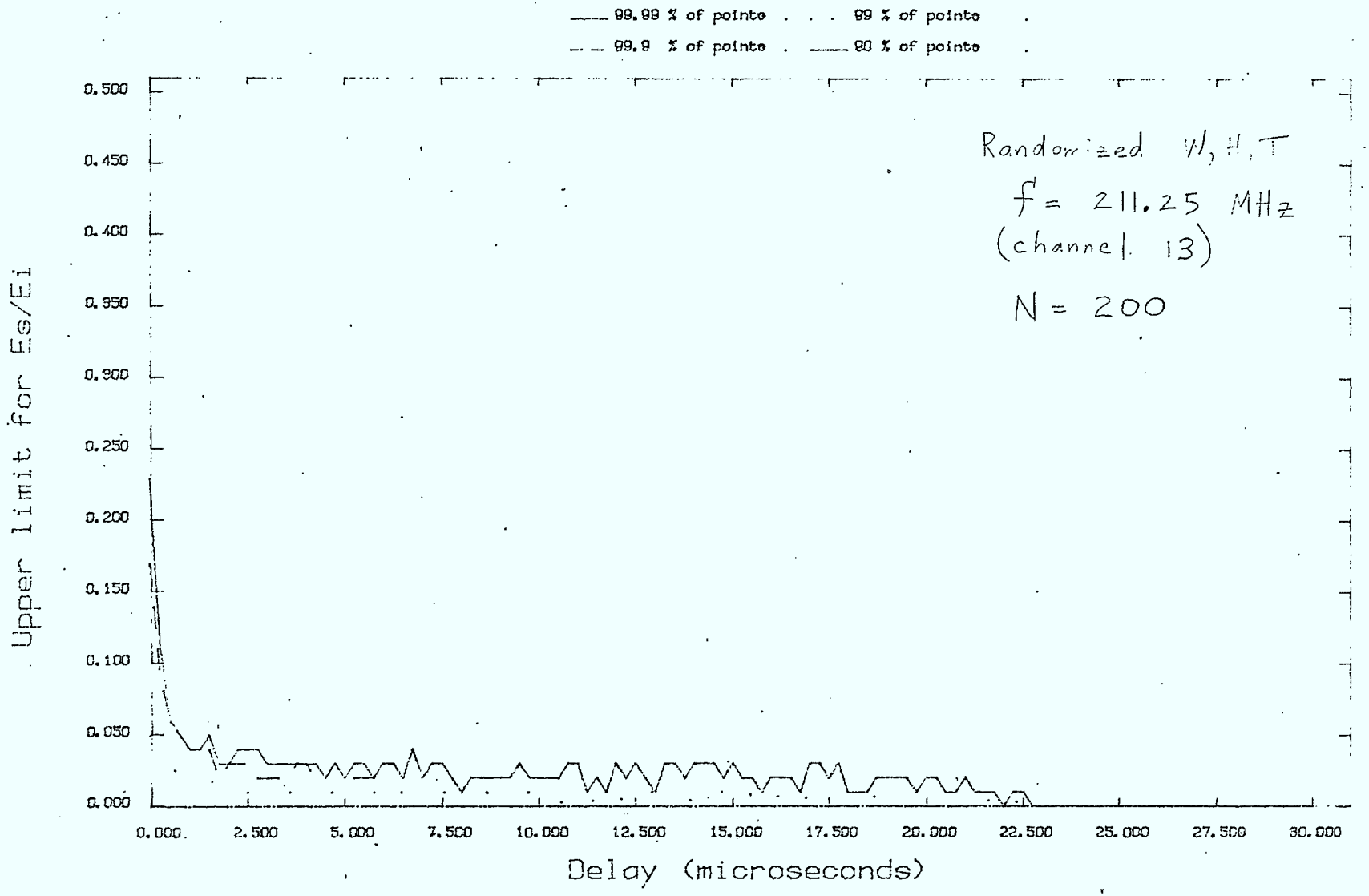

Figure 8

ANALYSIS OF SCATTER DIAGRAM PAR400 - ACCEPTABLE CHANNELS

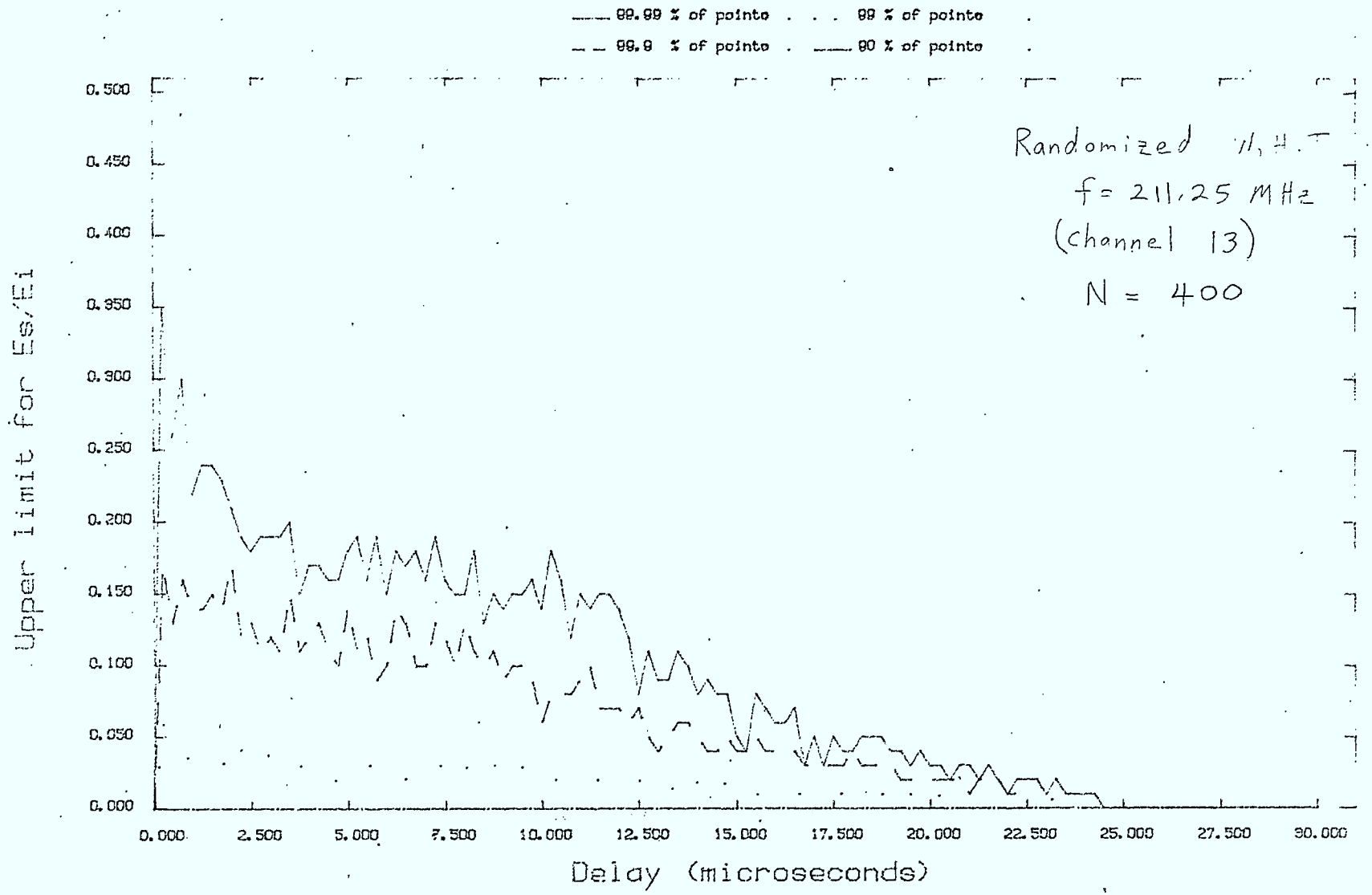

Figure 9

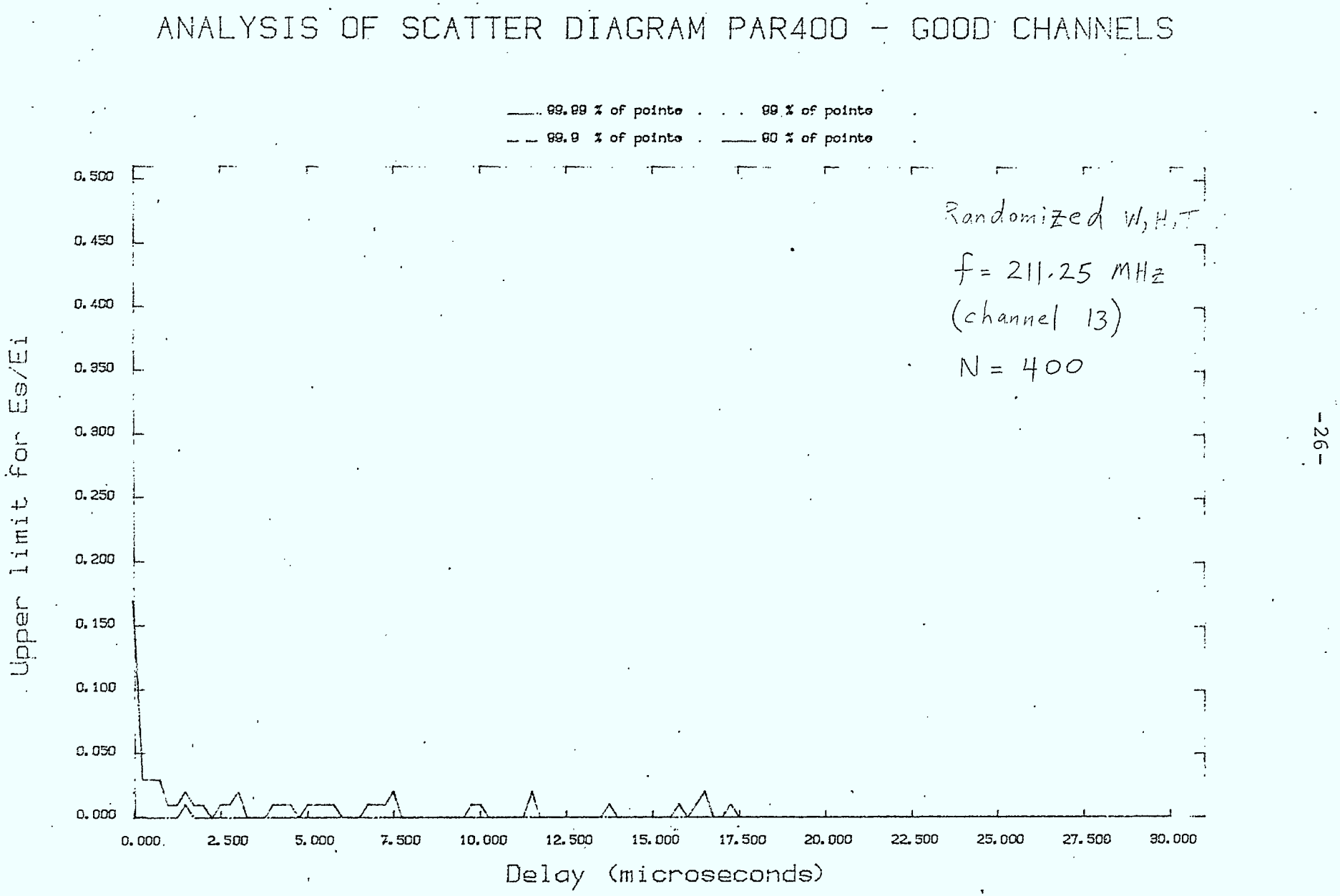
ANALYSIS OF SCATTER DIAGRAM PAR400 - GOOD CHANNELS
99.99 % of points
99 % of points
99.9 % of points
90 % of points
Randomized W,H,T
f = 211.25 MHz
(channel 13)
N = 400
Upper limit for Es/Ei
0.500
0.450
0.400
0.350
0.300
0.250
0.200
0.150
0.100
0.050
0.000
0.000
2.500
5.000
7.500
10.000
12.500
15.000
17.500
20.000
22.500
25.000
27.500
30.000
Delay (microseconds)

Figure 10

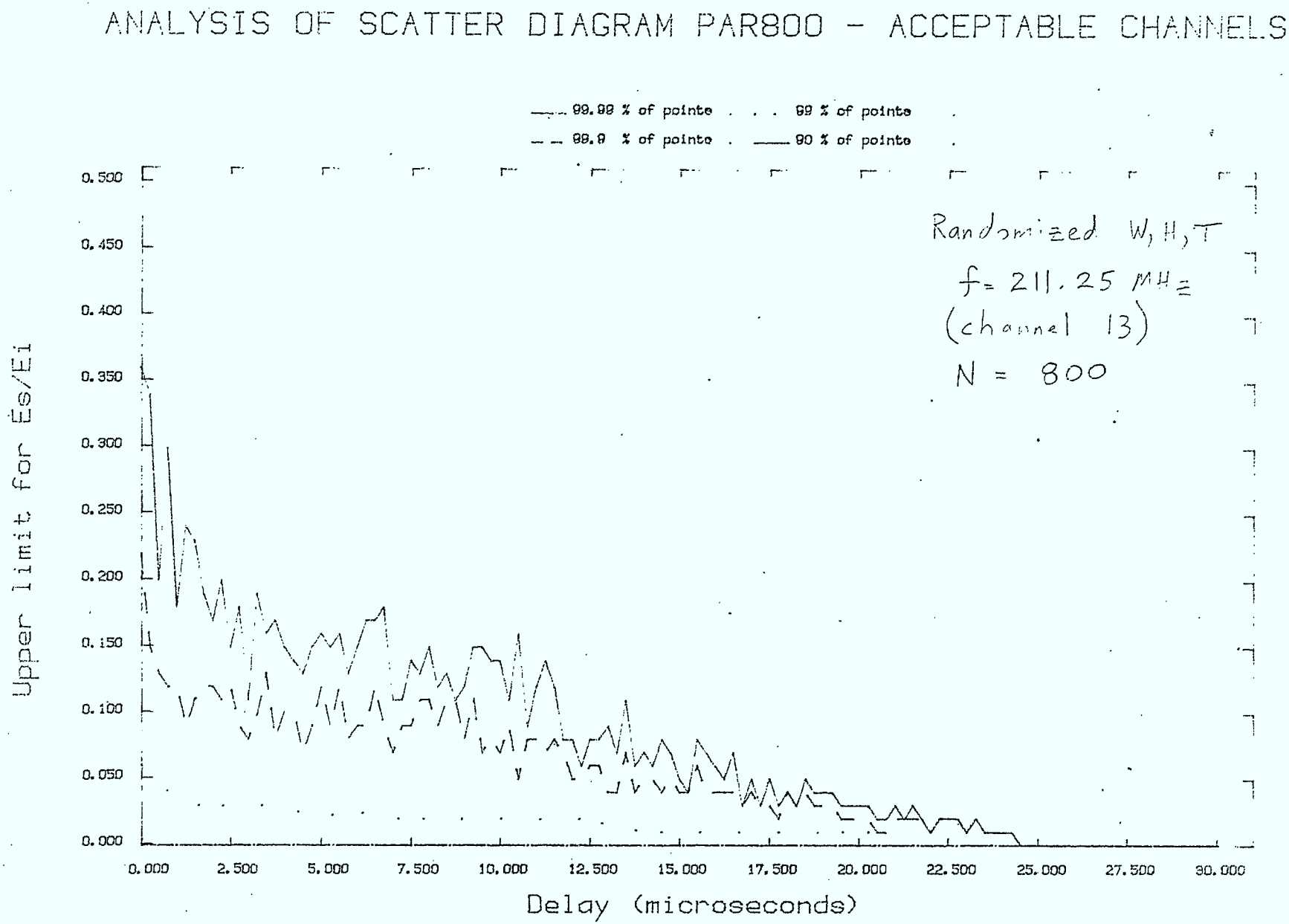
ANALYSIS OF SCATTER DIAGRAM PAR800 - ACCEPTABLE CHANNELS
99.99 % of points
99 % of points
99.9 % of points
90 % of points
Randomized W, H, T
f = 211.25 MHz
(channel 13)
N = 800
Upper limit for Es/Ei
0.500
0.450
0.400
0.350
0.300
0.250
0.200
0.150
0.100
0.050
0.000
0.000
2.500
5.000
7.500
10.000
12.500
15.000
17.500
20.000
22.500
25.000
27.500
30.000
Delay (microseconds)

Figure 11

In examining the contours for good channels it is not surprising to find that significant multipath components can arise for short delays (≤ 0.5 μsec). Such close in echoes, while not troublesome for video, can be troublesome for teletext. For longer delays, the magnitudes of echoes are below -26 dB.

The results for channel 2 (f = 55.25 MHz) are not at all surprising in light of the frequency sensitivity of the multipath channel discussed previously, and immediately evident from Figure 10 of reference [18]. In fact, we observed that no channels were rejected, and that most channels ($\geq 90\%$) are good video channels. It is also apparent that the cdf contours of the acceptable and good channels are not very sensitive to the number of impulse response components, N, or echo paths. It is also apparent from Figure 13 and 15, that the good video channels are also reasonably good teletext channels. An equalizer with the capability of handling delays of 2.5 μsec would be sufficient for channel 2.

Results were also gathered from f = 201 MHz, which corresponds to the frequency used in the CRC measurements. There are small changes in the percentage of rejected and good channels relative to the channel 13 results. There is also a small reduction in the cdf contour levels relative to the corresponding channel 13 results. The relative insensitivity of the cdf contours as a function of the number of reflectors is apparent in Figures 16 - 19.

With the incorporation of the channel prescreening algorithm, the multipath simulation program can be used to generate realistic multipath channels for consideration. Given the variability of the multipath channel demonstrated by the simulation program and observed during the CRC channel measurements, the channels generated by the

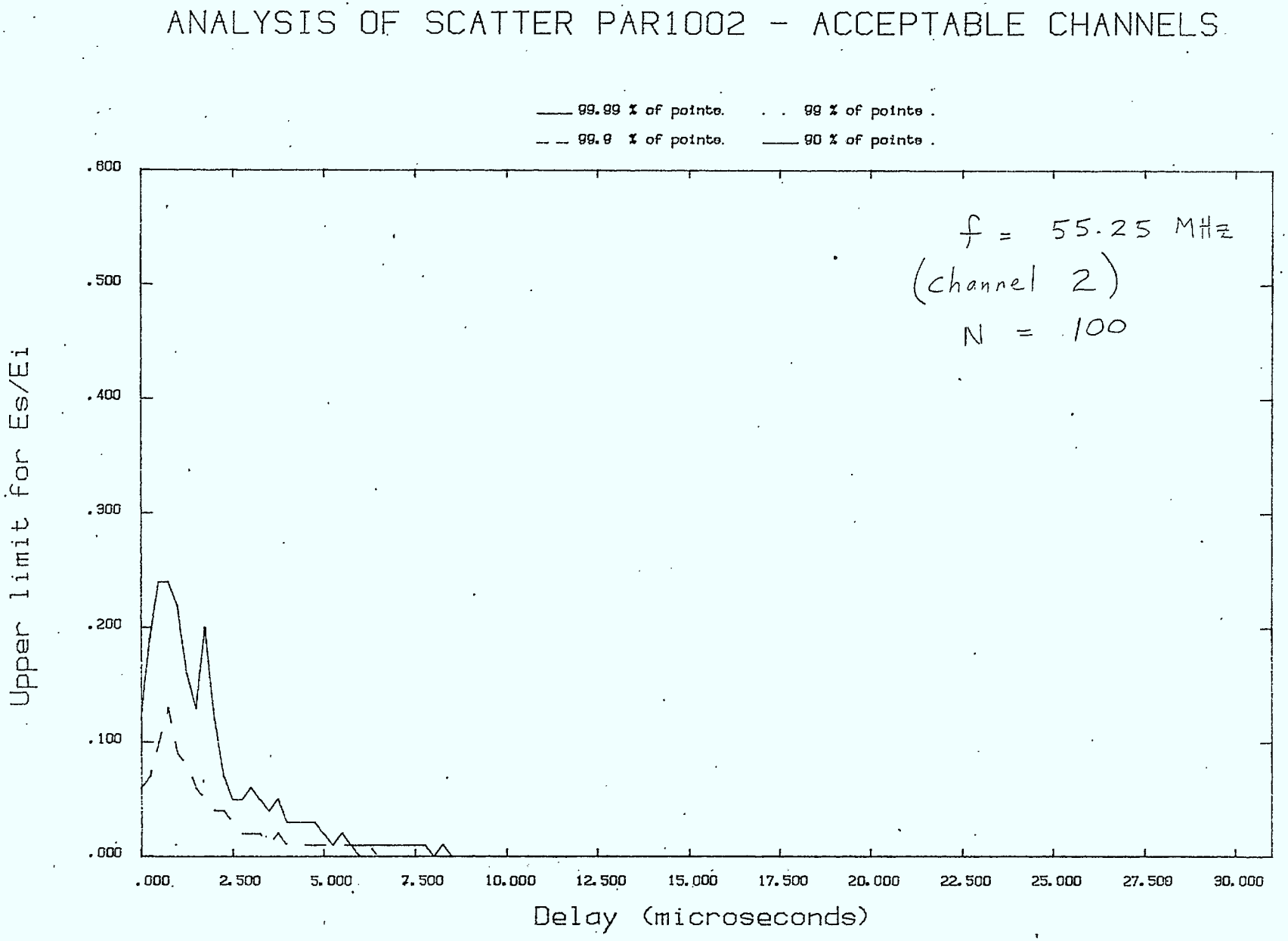
ANALYSIS OF SCATTER PAR1002 - ACCEPTABLE CHANNELS
99.99 % of points
99 % of points
99.9 % of points
90 % of points
f = 55.25 MHz
(channel 2)
N = 100
Upper limit for Es/Ei
.600
.500
.400
.300
.200
.100
.000
.000
2.500
5.000
7.500
10.000
12.500
15.000
17.500
20.000
22.500
25.000
27.500
30.000
Delay (microseconds)

Figure 12

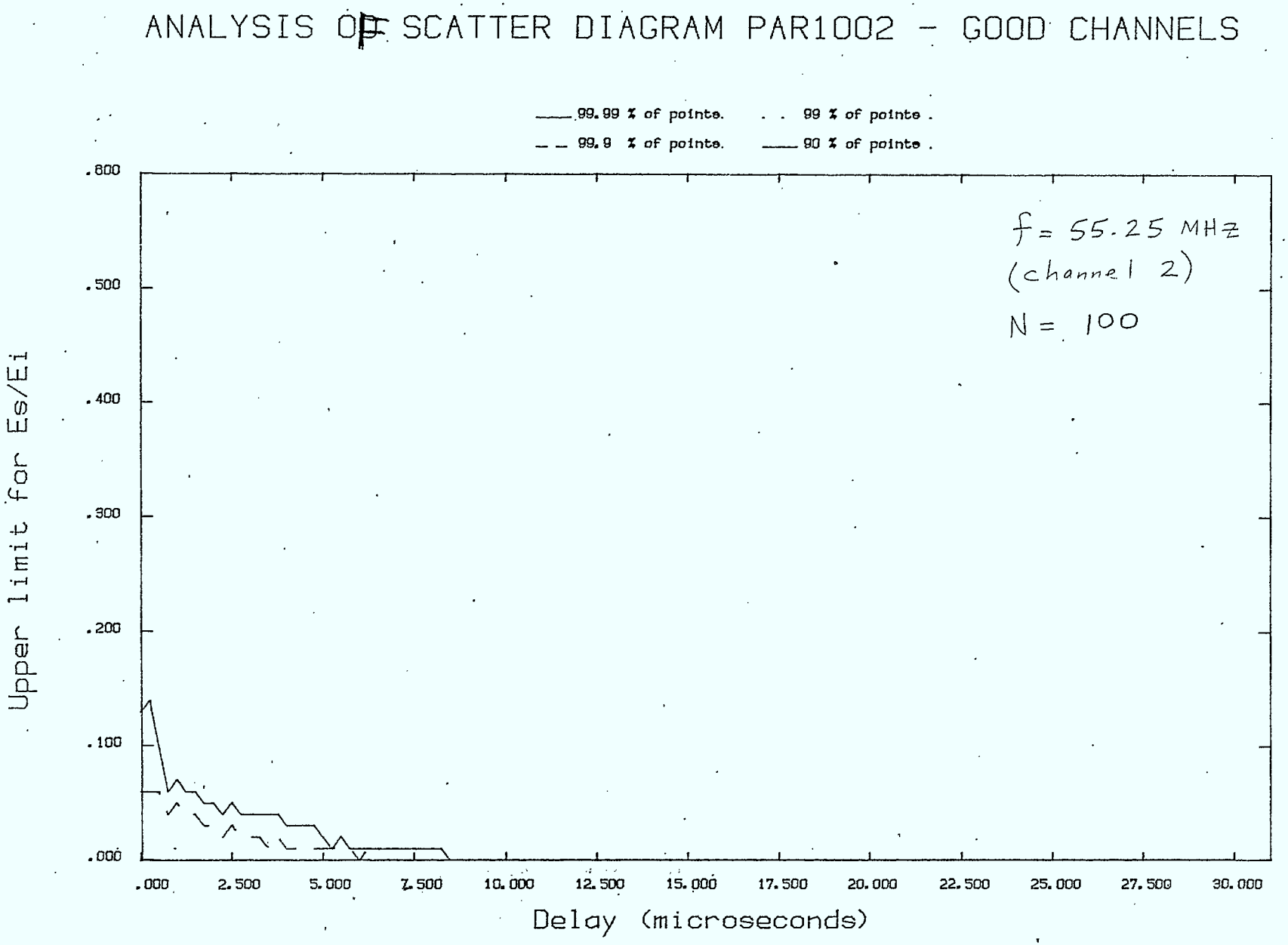
ANALYSIS OF SCATTER DIAGRAM PAR1002 - GOOD CHANNELS
99.99 % of points
99 % of points
99.9 % of points
90 % of points
f = 55.25 MHz
(channel 2)
N = 100
Upper limit for Es/Ei
.800
.500
.400
.300
.200
.100
.000
.000
2.500
5.000
7.500
10.000
12.500
15.000
17.500
20.000
22.500
25.000
27.500
30.000
Delay (microseconds)

Figure 13

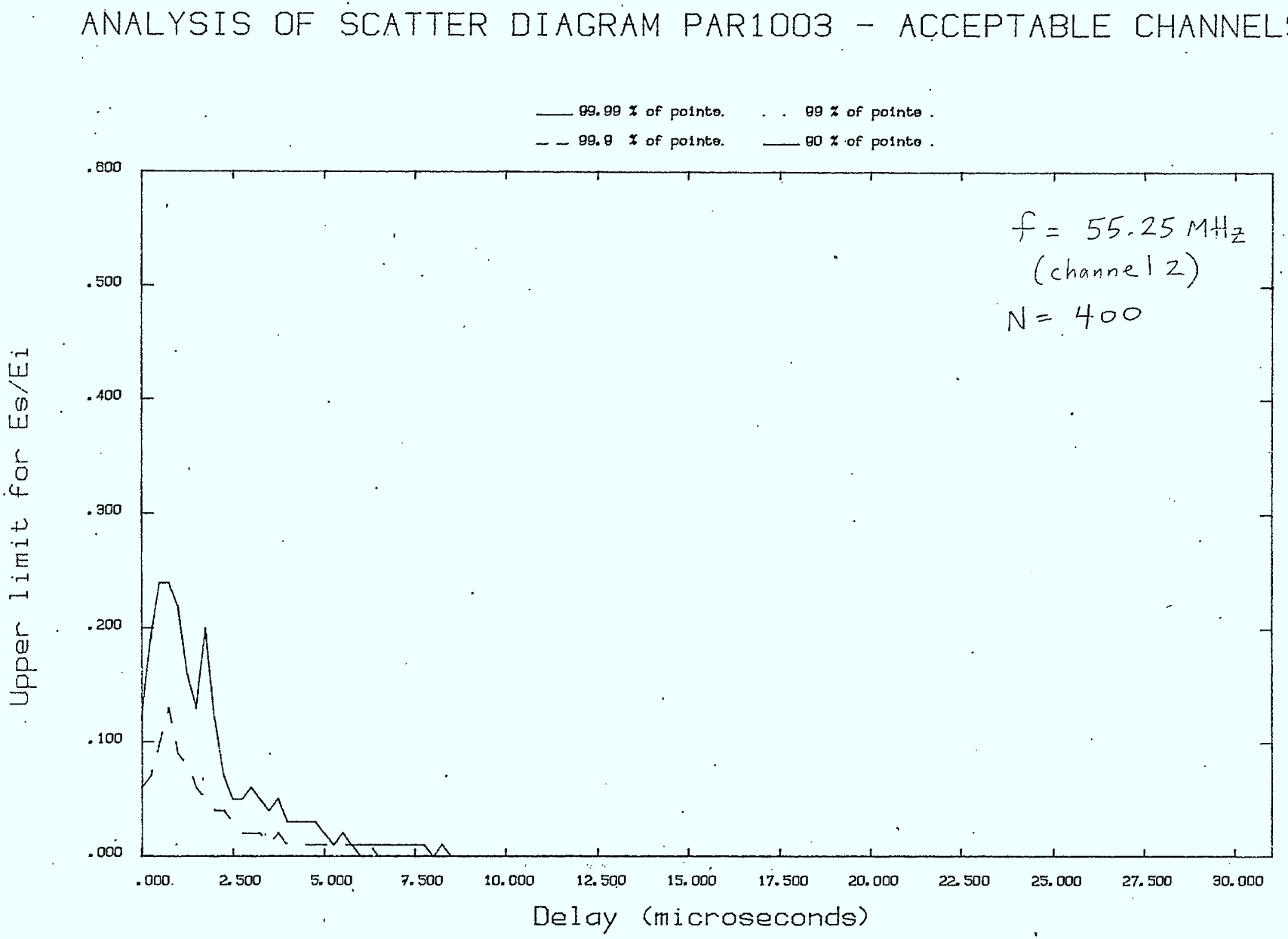
ANALYSIS OF SCATTER DIAGRAM PAR1003 - ACCEPTABLE CHANNELS
99.99 % of points
99 % of points
99.9 % of points
90 % of points
f = 55.25 MHz
(channel 2)
N = 400
Upper limit for Es/Ei
.600
.500
.400
.300
.200
.100
.000
.000
2.500
5.000
7.500
10.000
12.500
15.000
17.500
20.000
22.500
25.000
27.500
30.000
Delay (microseconds)

Figure 14

ANALYSIS OF SCATTER DIAGRAM PAR1003 - GOOD CHANNELS

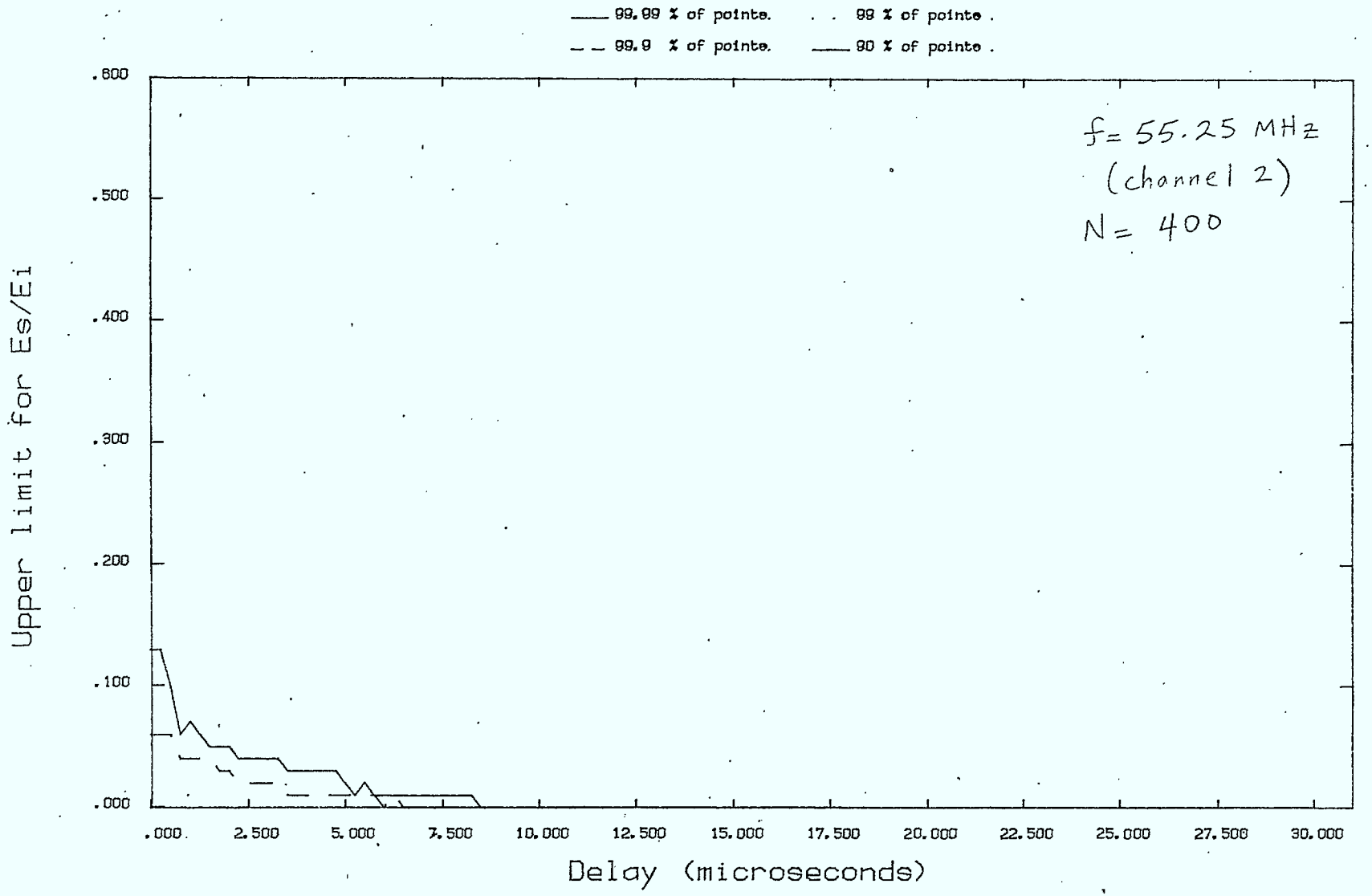

Figure 15

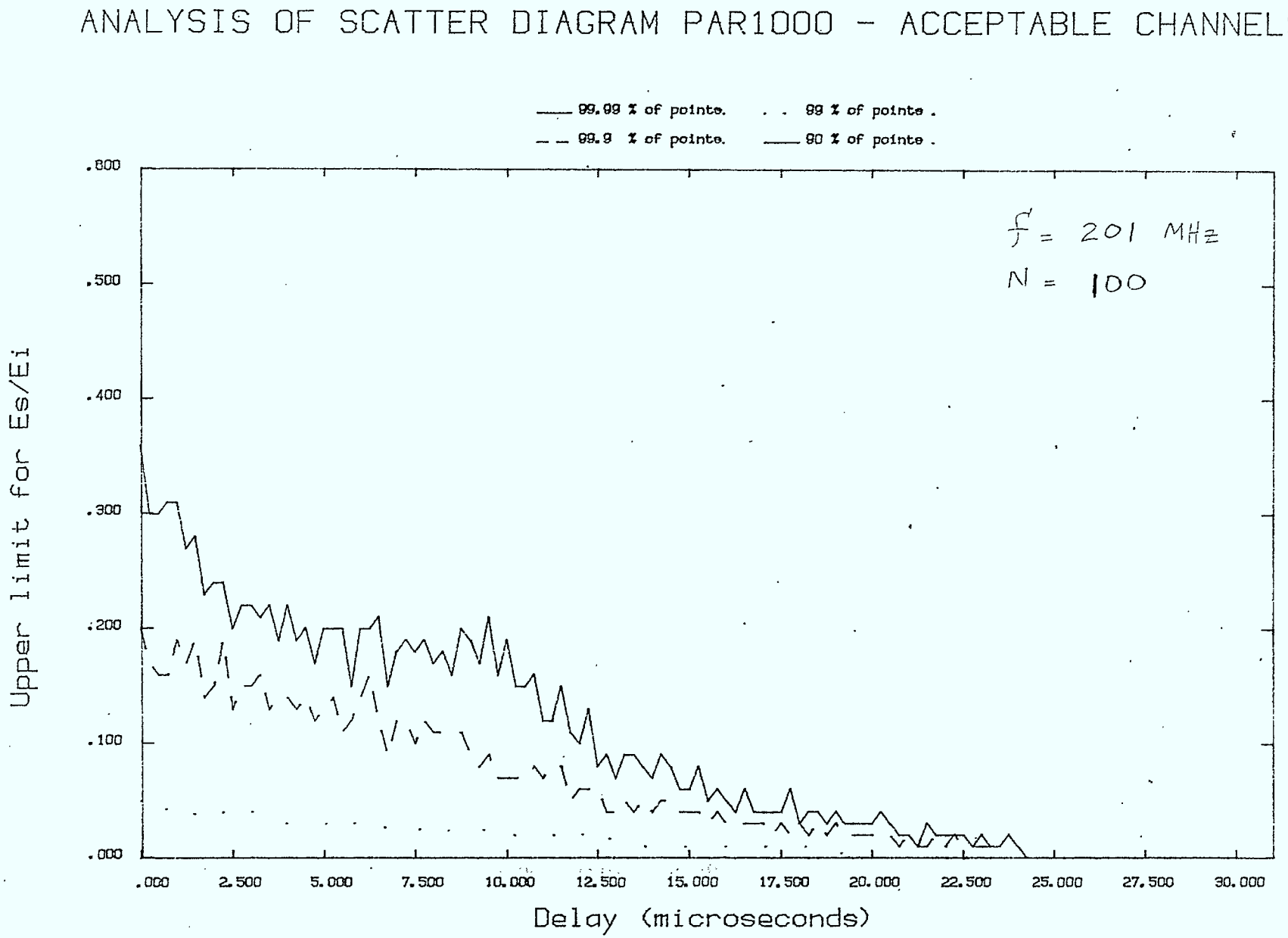
ANALYSIS OF SCATTER DIAGRAM PAR1000 - ACCEPTABLE CHANNELS
99.99 % of points
99 % of points
99.9 % of points
90 % of points
f = 201 MHz
N = 100
Upper limit for Es/Ei
.800
.500
.400
.300
.200
.100
.000
.000
2.500
5.000
7.500
10.000
12.500
15.000
17.500
20.000
22.500
25.000
27.500
30.000
Delay (microseconds)

Figure 16

ANALYSIS OF SCATTER DIAGRAM PAR1000 - GOOD CHANNELS

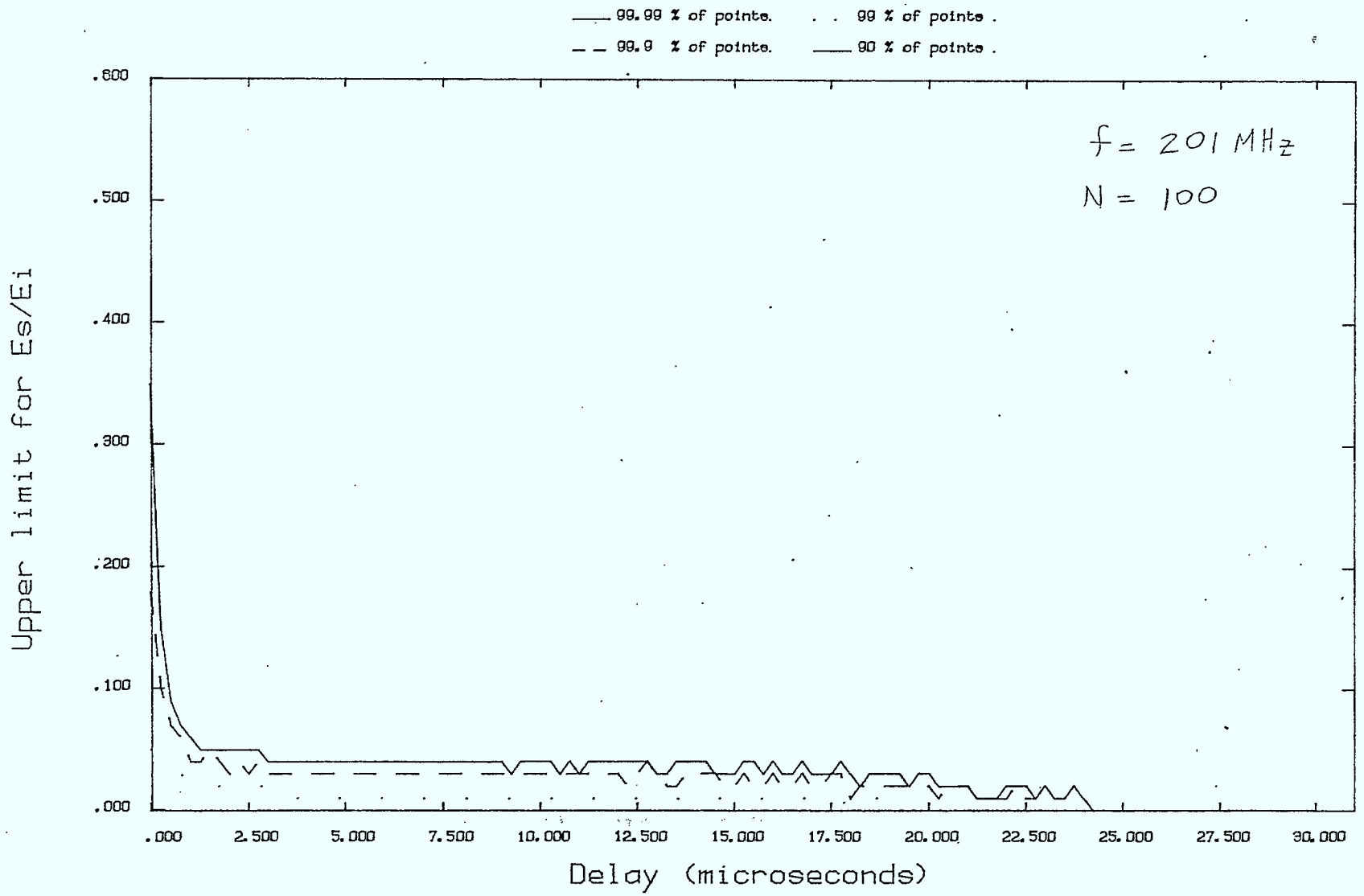

Figure 17

ANALYSIS OF SCATTER DIAGRAM PAR1001 - ACCEPTABLE CHANNELS

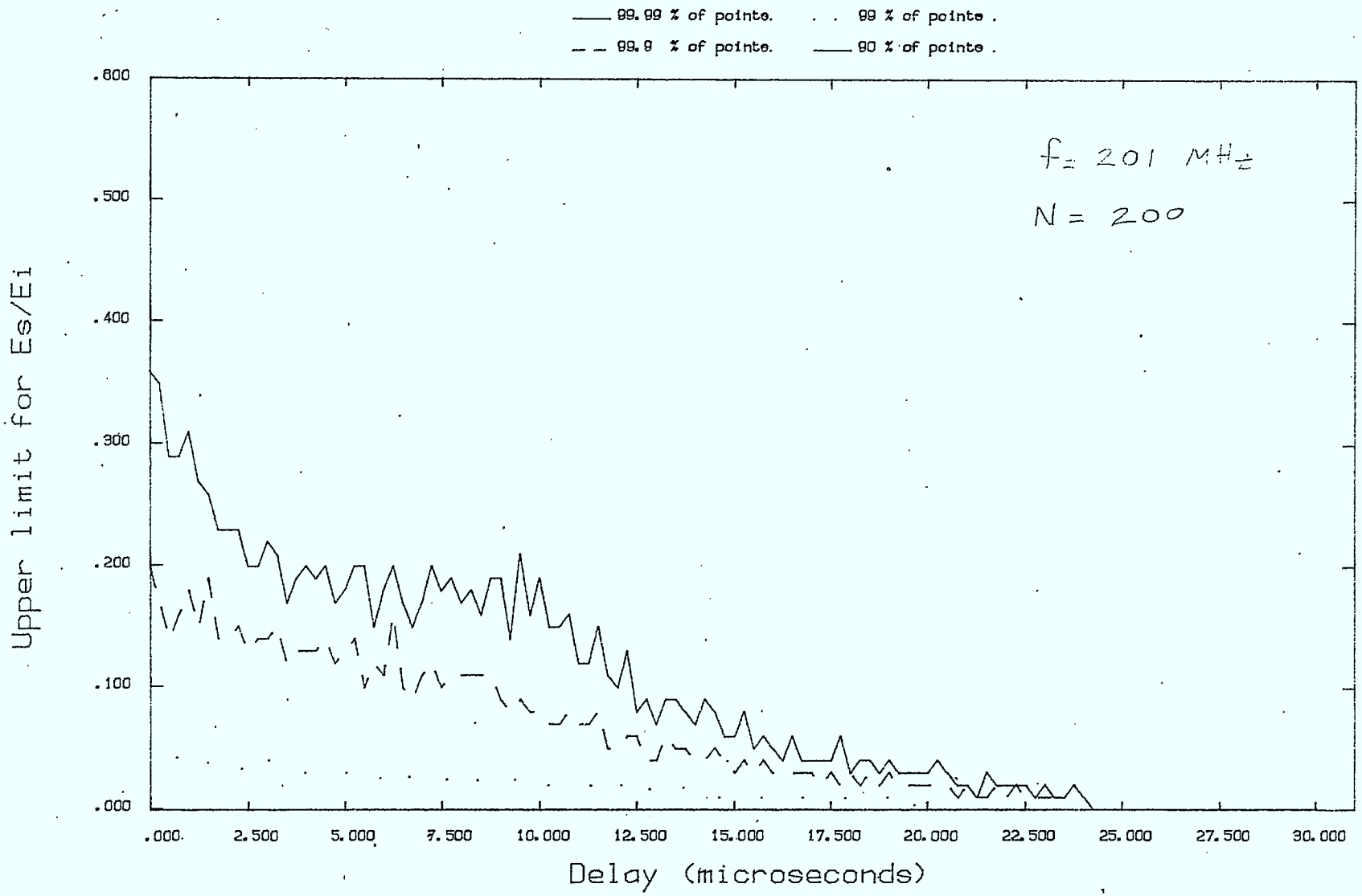

Figure 18

ANALYSIS OF SCATTER DIAGRAM PAR1001 - GOOD CHANNELS

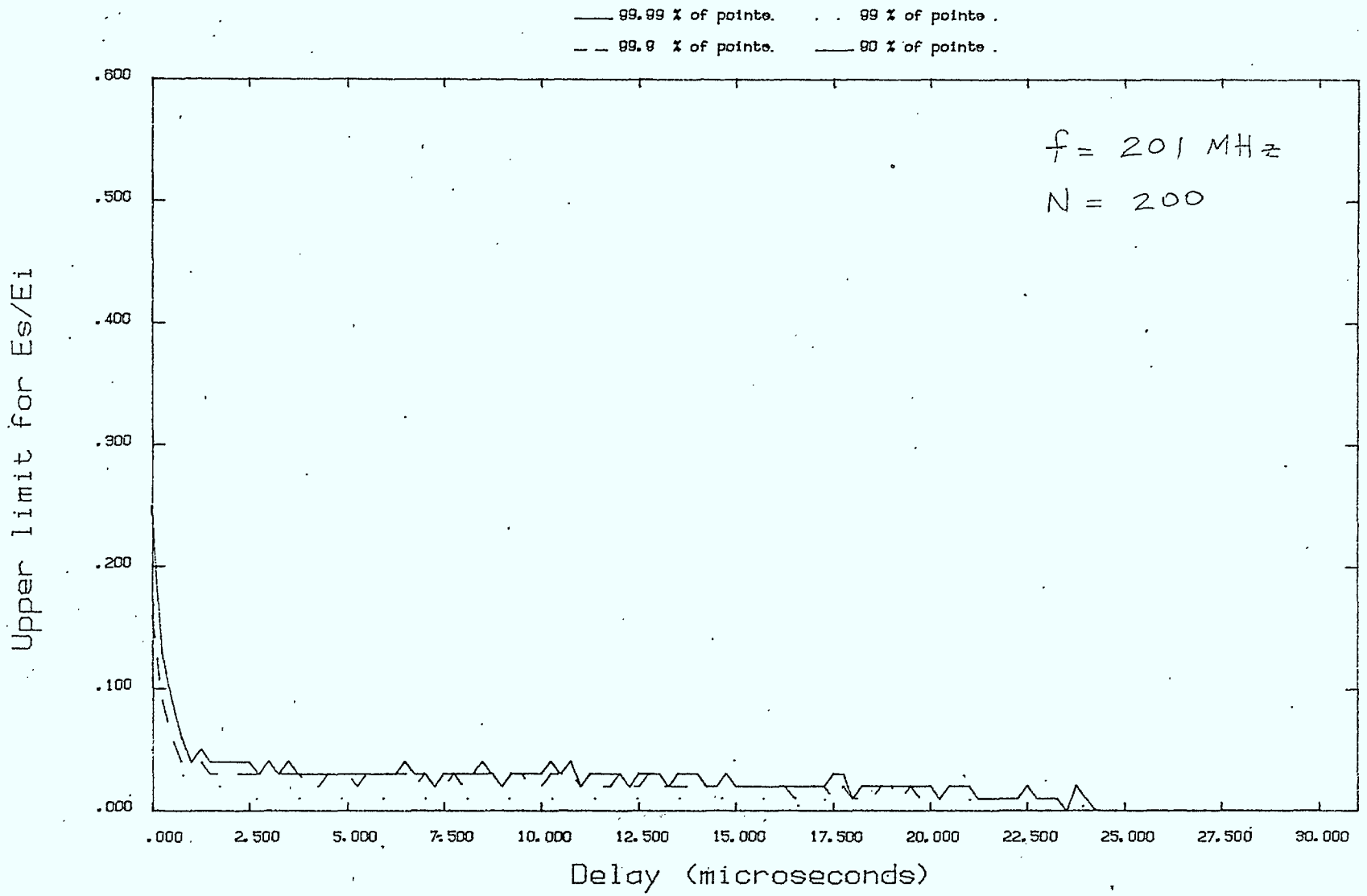

Figure 19

multipath program are clearly possible candidates. One could argue that if enough measurements were taken, a particular channel characteristic would eventually be observed. Combining this with the obvious advantages and flexabilities afforded by the simulation program, the multipath channels used for system evaluation will be generated by the simulation program.

2.4 Analyzing The CRC Measurements

Plots of the inphase, quadrature, and squared envelope (sum of squared inphase and quadrature components) components for 160 channel impulse response measurements, including a back-to-back measurement, have been obtained. The procedure for classifying channels involved visually extracting the magnitudes and delays of individual multipath components and computing the PDUR. Since there is no carrier phase recovery in the impulse response measurement system, extracting the absolute phase of echoes is not possible. Assuming zero phase echoes, channels were rejected whenever the PDUR happened to be less than 11 dB, for these measurements. The tedious information extraction and classification process has been completed and the details are presented in Appendix III.

The file numbers of the channel measurements providing acceptable video quality and those that were rejected are provided in Table 4. Of the 159 channels classified, 83 channels would provide acceptable video quality (52.2%), while 76 channels would be unacceptable for television pictures (47.8%). Furthermore, the majority of measurements were conducted in downtown Ottawa. Of the 107 downtown measurements, over 50% of the channels were rejected (54). Many of the downtown channels, especially along Bay, Slater, and Metcalfe Streets, were terrible

	ACCEPTABLE CHANNELS		REJECTED CHANNELS	
	2	96	3	130
	4	98	16	132
	5	99	17	134
	6	100	18	135
	7	101	19	136
	8	104	25	140
	9	105	29	141
	10	106	32	142
	11	107	33	144
	12	108	34	145
West-end	15	109	35	146
measurements	20	110	36	147
	21	111	38	148
	22	112	43	149
	23	113	44	150
	24	114	45	151
	30	116	46	152
	31	117	47	153
	37	118	48	155
	39	119	49	156
	40	121*	50	158
	41*	122	51	161
	42	128	63	162
	52	131*	68	163
	53	133	71	164
	54	137	75	165
	55	138	79	166
	56	139	80	
	57	143	81	
	58	154*	82	
	59	157*	83	
	60	159	84	
Downtown	61	160	86	
measurements	62	167	87	
	66		90	
	67		91	
	69		92	
	70		93	
	72		97	
	73		102	
	74		103	
	76		115	
	77		120	
	78*		123	
	85		124	
	88		125	
	89		126	
	94		127	
	95		129	

* non-minimum phase channels with acceptable video quality

Table 4: Channel Classification

channels, with echoes stronger than the main path (non-minimum phase channels). In some locals (i.e. along Nepean Street near Kent) the channel characteristics were wildly varying.

In analyzing the CRC channel measurements, it is important to keep in mind the intended purpose, which was to obtain some measurement data on representative multipath channels in the Ottawa area. These measurements were to indicate the typical multipath spreads that would have to be handled by an adaptive equalizer. The purpose was not to gather an enormous number of randomly selected channel measurements in an attempt to statistically categorize the multipath channel.

The extremely high percentage of rejected channels obtained, in spite of the fact that a relatively low acceptability threshold, (PDUR $\leq$ 11 dB) was used, tends to suggest that the measurements were biased somewhat towards extreme multipath channels. This is in part due to the linear display used, where small but <u>not</u> insignificant multipath is barely noticable. Multipaths that are clearly noticable on the display (i.e. magnitudes between 0.2 - 0.5 which correspond to -14 dB to -6 dB echoes) are typically severe multipath channels. Incorporating a logarithmic display would provide a better indication of the severity of the multipath channels, and would prevent the discarding of channels that appear to have insignificant multipath. In gathering channel data for use in the constrained pulse optimization problem, random sampling of measurement sites should be followed to prevent biasing the measurement data towards very poor channel characteristics. A significant reduction in the percentage of rejected channels should occur.

A large number of measurements were conducted in the Bay, Slater, James, Metcalf, Albert, and Queen Street areas. The majority of channels were terrible, as evidenced by the impulse response plots (Files 123 through 166) in Appendix III. Of the last 26 measurements, which were conducted along Albert and Queen streets, only 5 channels were acceptable (19.2%). Primarily in the downtown area, channels with reflected paths stronger than the main path (which is primarily due to blockage) were observed. Most of these non-minimum phase channels were very bad television channels. In fact, only six were deemed acceptable. The propagation model used in the simulation does not incorporate blockage, and will result in minimum phase channel characteristics. Given that the vast majority of measured channels providing usable televison pictures were minimum phase channels, this is not a major deficiency.

Because of the severe multipath suffered in many downtown regions, televison signals, and consequently Telidon, must be received from cable systems. Even in areas removed from the downtown core, such as Carlingwood, severe multipath was observed. Of the 15 channel measurements conducted in the Carlingwood area, 10 channels were rejected (66.7%). These preliminary measurements indicate that the majority Broadcast Telidon subscribers will be in suburban and rural areas, which is not at all surprising.

For the acceptable channels, statistics on the number of significant echo paths were gathered. A significant echo path was defined as one with a DU ratio less than or equal to 24 dB. The mean number of signficiant echoes was 3.33, with a standard deviation of 1.97.

The magnitudes and delays of the echoes comprising the acceptable video channels have been accumulated in a

"scatter table" in Figure 20. As a rough comparison, smoothed 99.99% and 99% contours from Figure 16 (assuming 100 impulse response components) were sketched on. It must be emphasized that the threshold of acceptability was different for the classification of the CRC measurement data, being 2 dB lower than that used in generating Figure 16. This can be roughly accounted for by shifting the upper contour up by 2 dB. If this were done, only a few (4) observations would be above this threshold, and the majority would be between the 99.99% and 99% contours. It is also apparent from the measurements that the vast majority of echoes have delays less than 3 μsec. All echoes with long delays had magnitudes below the 99.99% contour. The longest delay observed was 8 μsec with a DU of approximately 19 dB. The delay spread, with the model parameters presented in Section 2.3, is seen to be roughly 10 μsec from Figure 16, which is somewhat greater than that observed from measurement results.

As alluded to earlier, the multipath propagation model is quite sensitive to the size of the reflector. In fact the ratio of the amplitude of the reflected signal to the desired signal is proporational to H^3W. By fiddling with model parameters such as average width, height, and size of the occupational domain, the simulation could be forced to closely match values appropriate for Ottawa. To demonstrate the extreme sensitivity to reflector area, consider reducing the average reflector area by a factor of 4. This will reduce $|E_s/E_i|$ by 24 dB on average, and will reduce the delay spread considerably. The results are summarized in Table 5 and Figures 21 - 26. For these simulation runs the threshold of acceptability was the same as that used for classifying the measured channels. It is

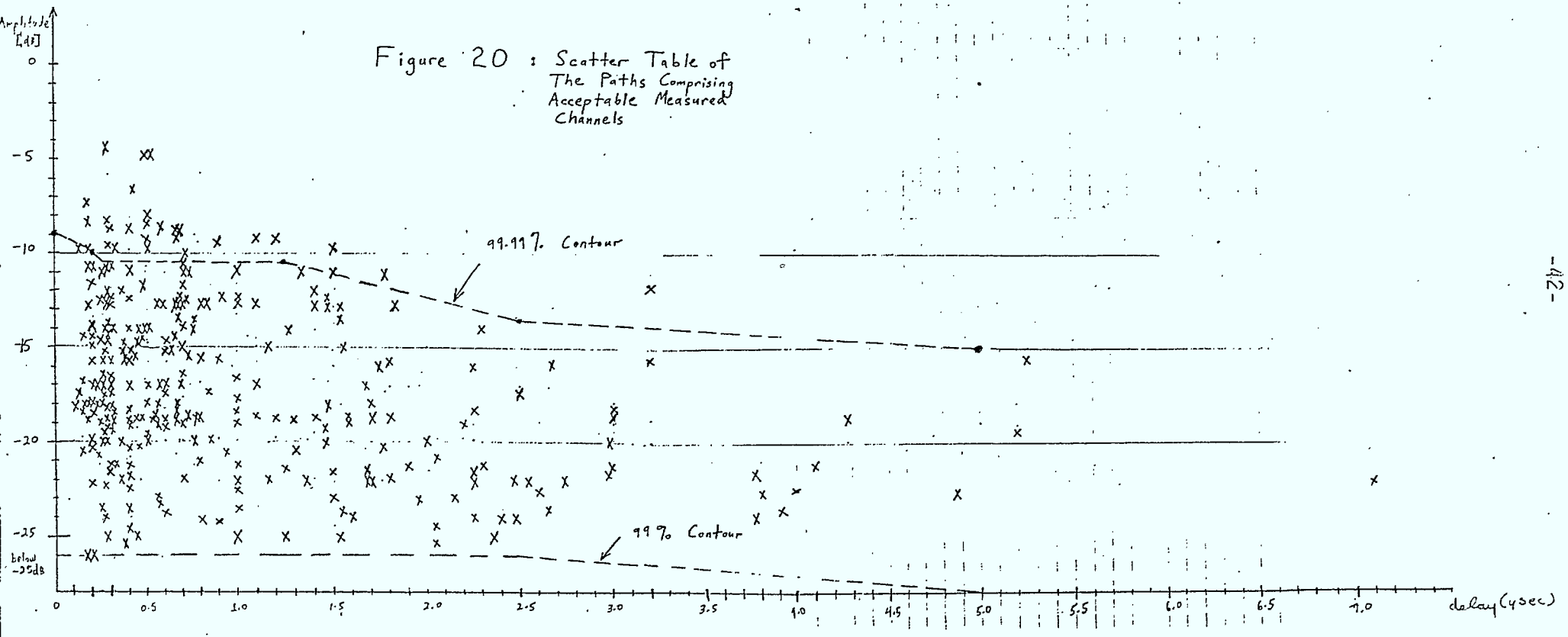

Figure 20 : Scatter Table of The Paths Comprising Acceptable Measured Channels

apparent that the majority of channels are good video channels, with a delay spread of only 2.5 μsec, and a much reduced magnitude contour. The cdf contours are not sensitive functions of the number of echo paths.

A similar set of runs was conducted with the average reflector area selected to be 63.6% of the typical average area which is 353.44 m^2. The results are summarized in Table 6 and Figures 27 - 32. From the cdf contours for the channels classified as acceptable, the delay spread, referenced to echoes at least 20 dB down, is roughly 6 μsec. A significant reduction in the delay spread is accomplished by a relatively small change in reflector dimensions. Smoothed versions of the 99.99% and 99% contours of Figures 29 and 31 are shown on the scatter table of measurement data in Figure 33. It is apparent that the delay spread of the simulation model now corresponds better with the delay spread of the measurements.

It is also evident that for short delays, one observes measured echo strengths greater than the 99.99% simulation contour ($\tau \leq 0.6$ μsec). They are reasonably close to the contour however. The reason for this can be attributed to the approximations used in the simulation model for the near field region [15], [18], which is one of the known weaknesses of the model. To take proper account of the near field region would be rather difficult and increase the complexity considerably. With large reflectors (as used in the simulation), and for frequencies in the neighbourhood of 201 MHz, the near field region is rather substantial (i.e. paths with delays less than 1 μsec will be the near field region). However, given that the vast majority of measurements do fall within the contour bounds, the simulation program is a good working model.

Frequency (MHz)	Number of Channels Classified	Number of Paths Per Channel	Percentage Rejected	Percentage Accepted	Percentage Good	CDF Contour Figures
201	5,000	100	0.42	99.58	88.2	27, 28
	10,000	50	0.25	99.75	95.1	29, 30
	25,000	20	0.07	99.93	98	31, 32

Table 6: Average Reflector Size is 63.6% of Typical Value

Frequency (MHz)	Number of Channels Classified	Number of Paths Per Channel	Percentage Rejected	Percentage Accepted	Percentage Good	CDF Contour Figures
201	5,000	100	0.0	100	99.3	21, 22
	10,000	50	0.0	100	99.8	23, 24
	25,000	20	0.0	100	99.9	24, 25

Table 5: Average Reflector Area Reduced By a Factor of 4

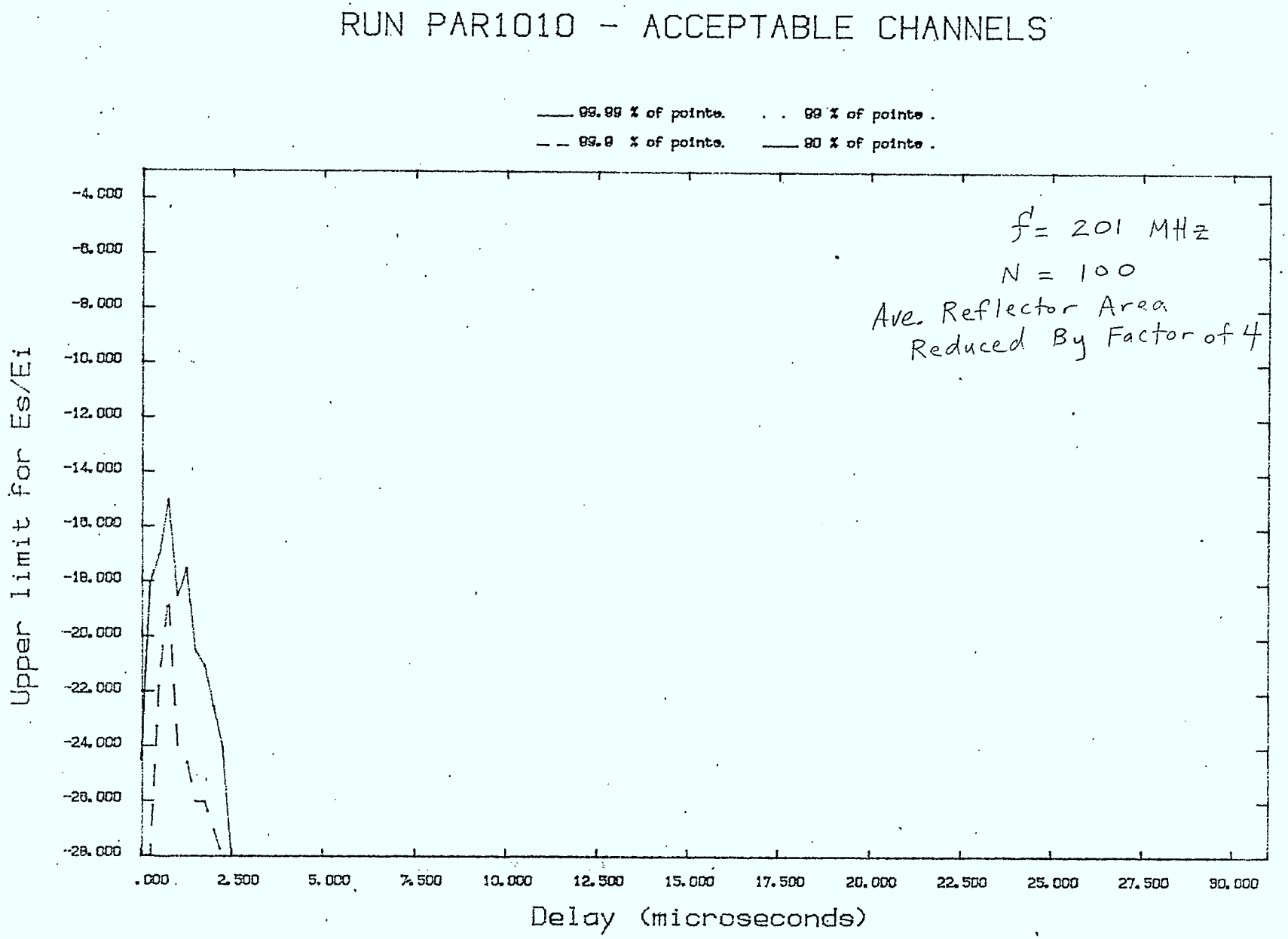
RUN PAR1010 - ACCEPTABLE CHANNELS
99.99 % of points.
99 % of points.
99.9 % of points.
90 % of points.
f = 201 MHz
N = 100
Ave. Reflector Area
Reduced By Factor of 4
Upper limit for Es/Ei
-4.000
-6.000
-8.000
-10.000
-12.000
-14.000
-16.000
-18.000
-20.000
-22.000
-24.000
-26.000
-28.000
.000
2.500
5.000
7.500
10.000
12.500
15.000
17.500
20.000
22.500
25.000
27.500
30.000
Delay (microseconds)

Figure 21

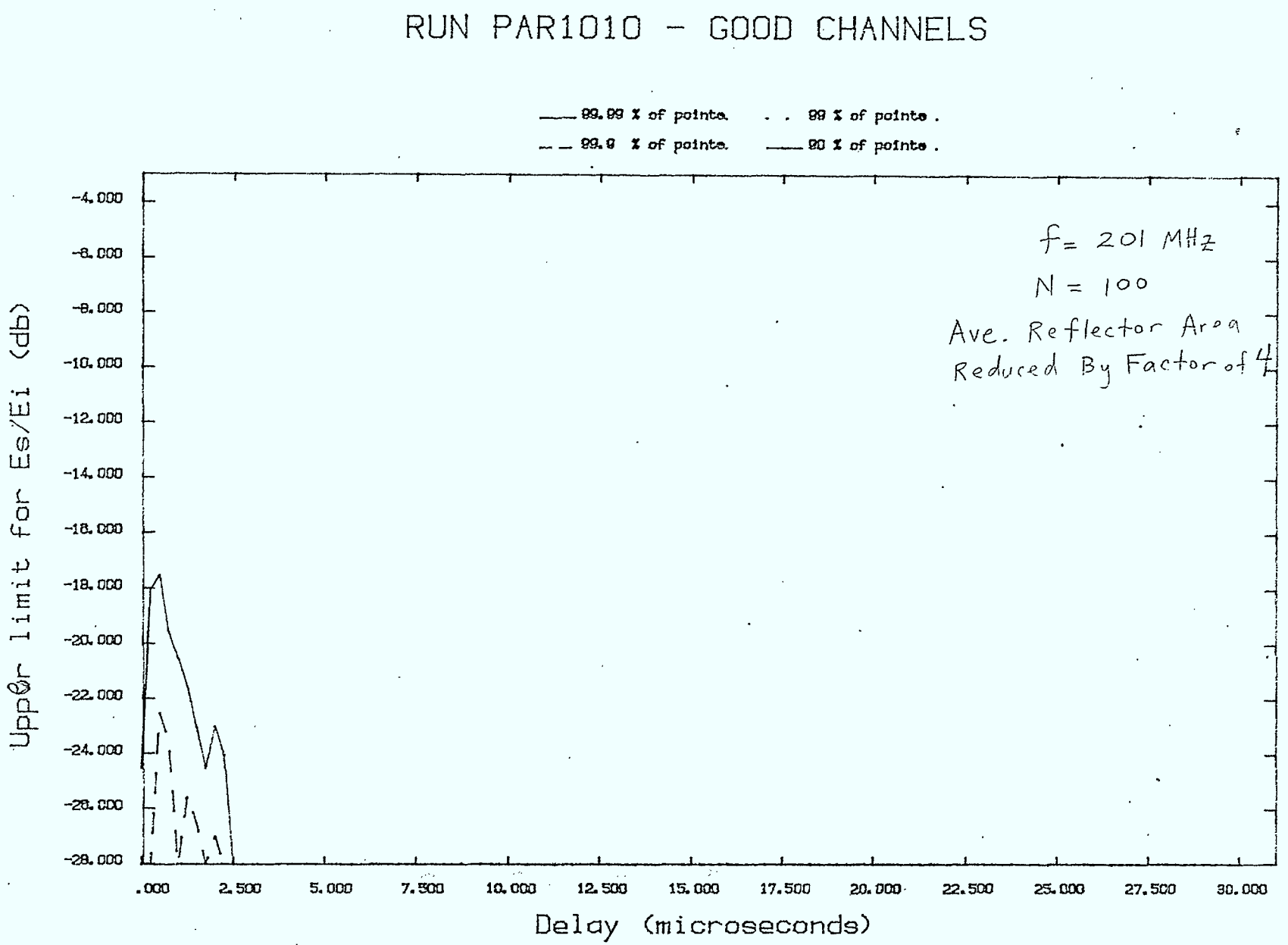
RUN PAR1010 - GOOD CHANNELS
99.99 % of points
99 % of points
99.9 % of points
90 % of points
f = 201 MHz
N = 100
Ave. Reflector Area
Reduced By Factor of 4
Upper limit for Es/Ei (db)
-4.000
-6.000
-8.000
-10.000
-12.000
-14.000
-16.000
-18.000
-20.000
-22.000
-24.000
-26.000
-28.000
.000
2.500
5.000
7.500
10.000
12.500
15.000
17.500
20.000
22.500
25.000
27.500
30.000
Delay (microseconds)

Figure 22

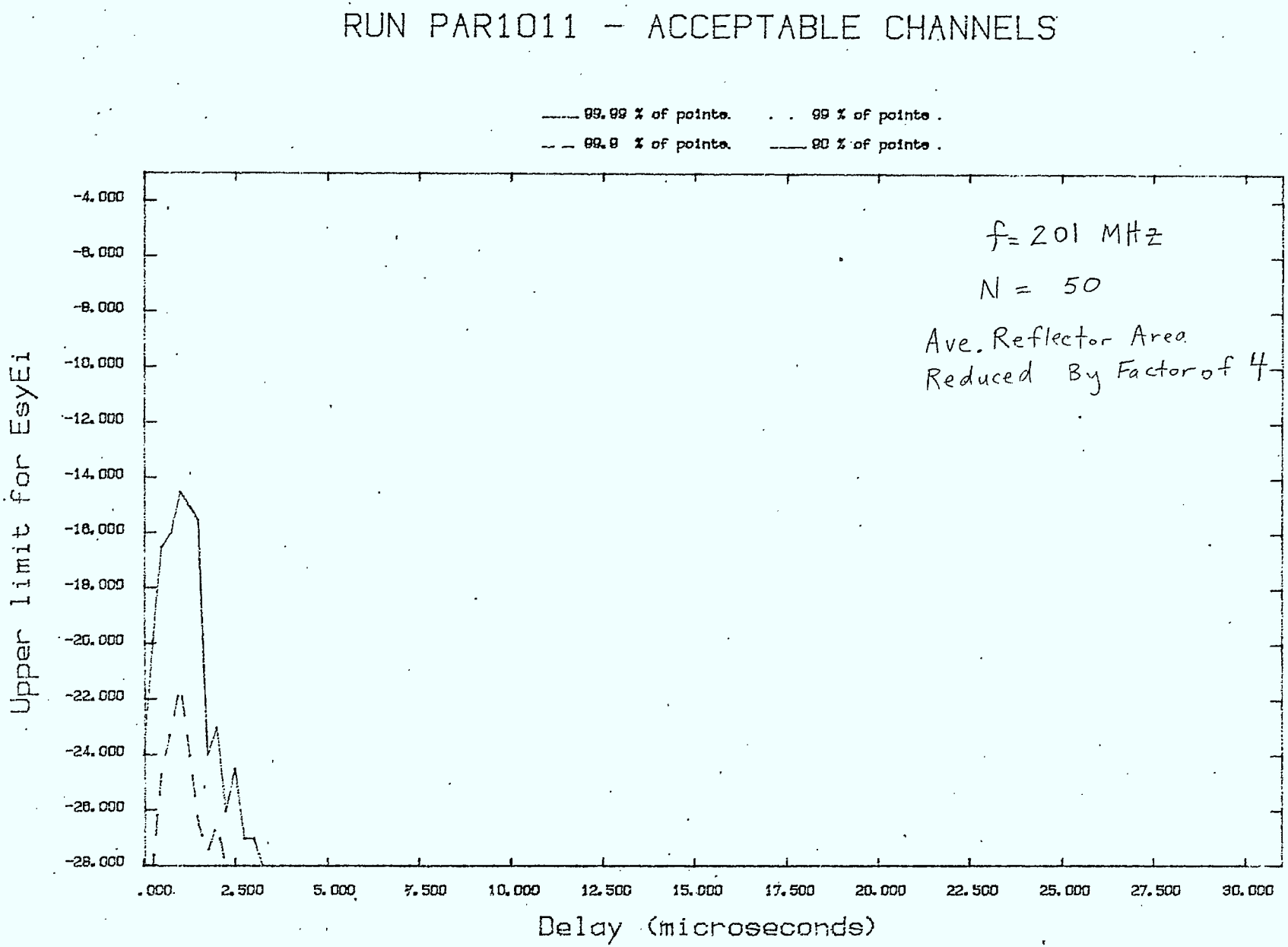
RUN PAR1011 - ACCEPTABLE CHANNELS
99.99 % of points.
99 % of points.
99.9 % of points.
90 % of points.
f= 201 MHz
N = 50
Ave. Reflector Area
Reduced By Factor of 4
Upper limit for EsyEi
-4.000
-6.000
-8.000
-10.000
-12.000
-14.000
-16.000
-18.000
-20.000
-22.000
-24.000
-26.000
-28.000
.000
2.500
5.000
7.500
10.000
12.500
15.000
17.500
20.000
22.500
25.000
27.500
30.000
Delay (microseconds)

Figure 23

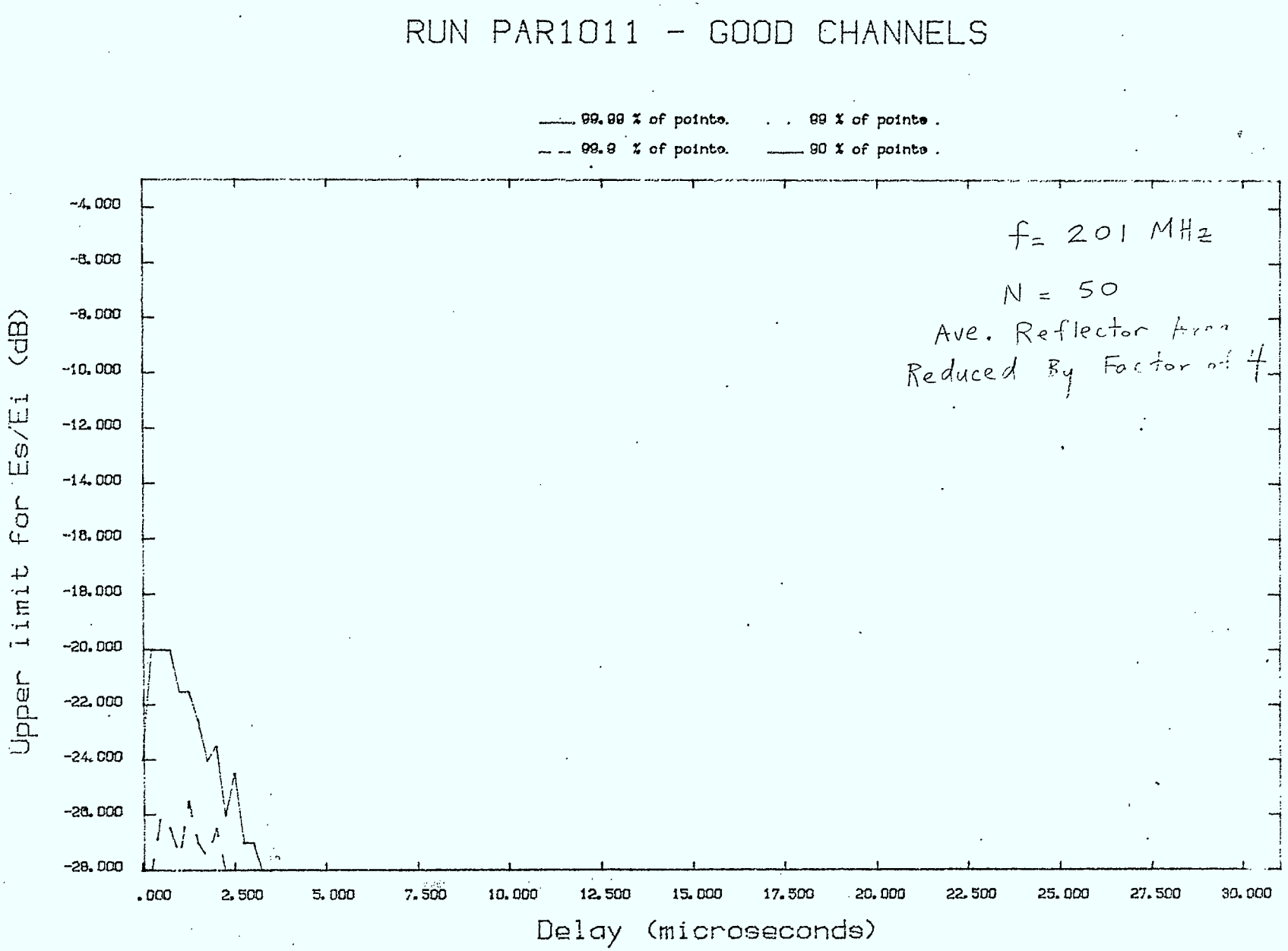
RUN PAR1011 - GOOD CHANNELS
99.99 % of points
99 % of points
99.9 % of points
90 % of points
f= 201 MHz
N = 50
Ave. Reflector Area
Reduced By Factor of 4
Upper limit for Es/Ei (dB)
-4.000
-6.000
-8.000
-10.000
-12.000
-14.000
-16.000
-18.000
-20.000
-22.000
-24.000
-26.000
-28.000
.000
2.500
5.000
7.500
10.000
12.500
15.000
17.500
20.000
22.500
25.000
27.500
30.000
Delay (microseconds)

Figure 24

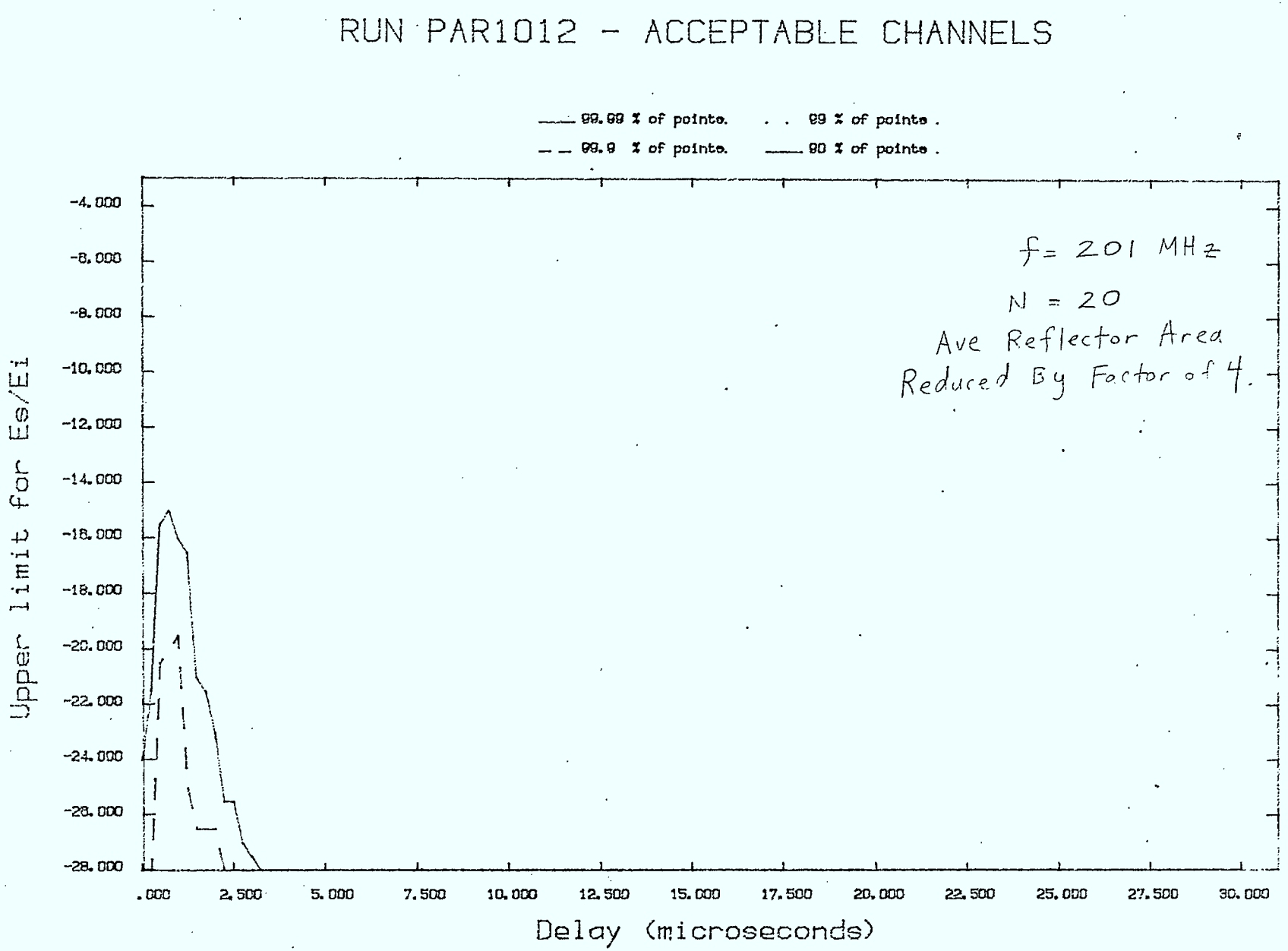
RUN PAR1012 - ACCEPTABLE CHANNELS
99.99 % of points
99 % of points
99.9 % of points
90 % of points
f= 201 MHz
N = 20
Ave Reflector Area
Reduced By Factor of 4.
Upper limit for Es/Ei
-4.000
-6.000
-8.000
-10.000
-12.000
-14.000
-16.000
-18.000
-20.000
-22.000
-24.000
-26.000
-28.000
.000
2.500
5.000
7.500
10.000
12.500
15.000
17.500
20.000
22.500
25.000
27.500
30.000
Delay (microseconds)

Figure 25

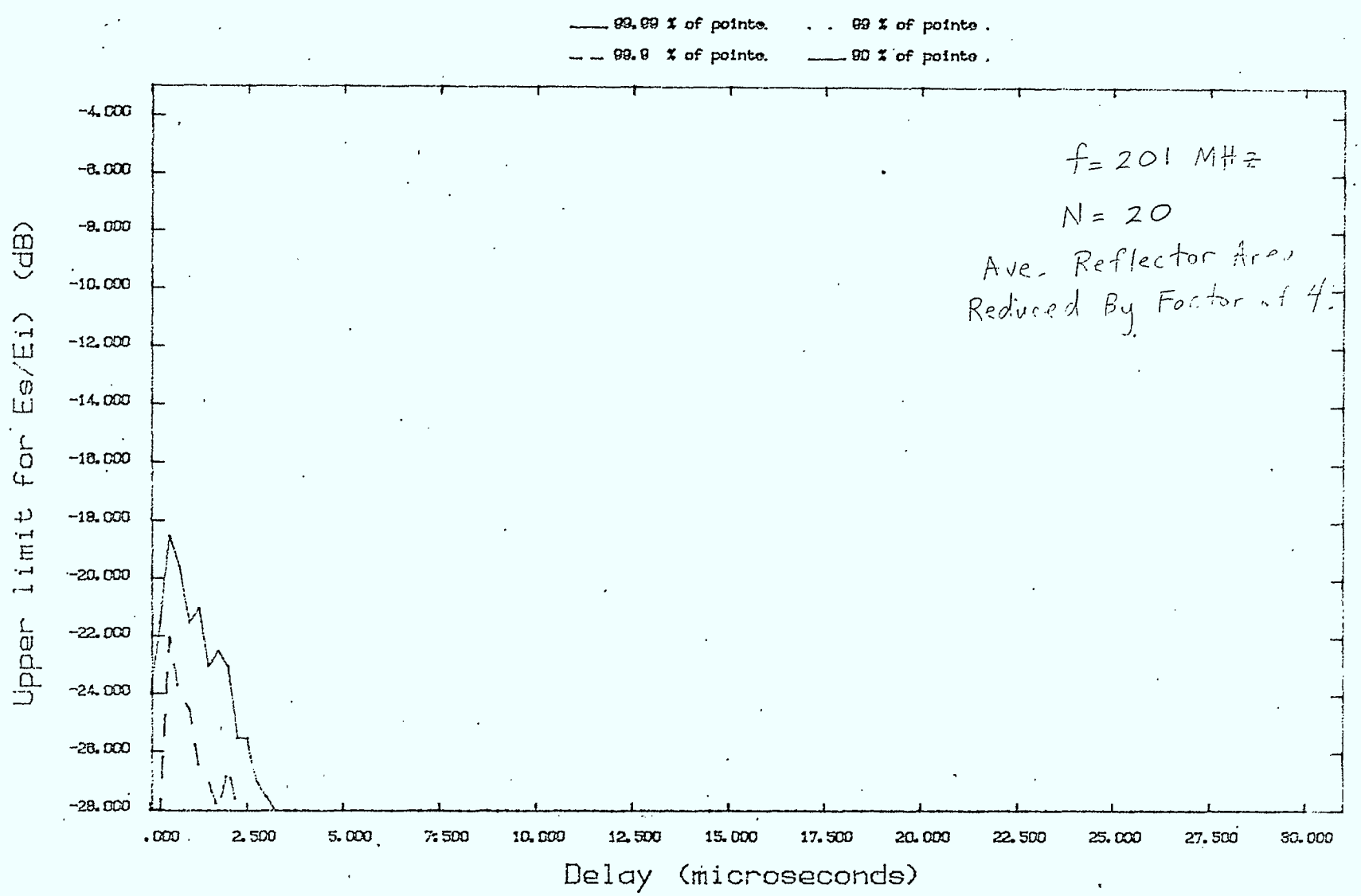
RUN PAR1012 - GOOD CHANNELS
99.99 % of points
99 % of points
99.9 % of points
90 % of points
f = 201 MHz
N = 20
Ave. Reflector Area
Reduced By Factor of 4.
Upper limit for Es/Ei) (dB)
-4.000
-6.000
-8.000
-10.000
-12.000
-14.000
-16.000
-18.000
-20.000
-22.000
-24.000
-26.000
-28.000
.000
2.500
5.000
7.500
10.000
12.500
15.000
17.500
20.000
22.500
25.000
27.500
30.000
Delay (microseconds)

Figure 26

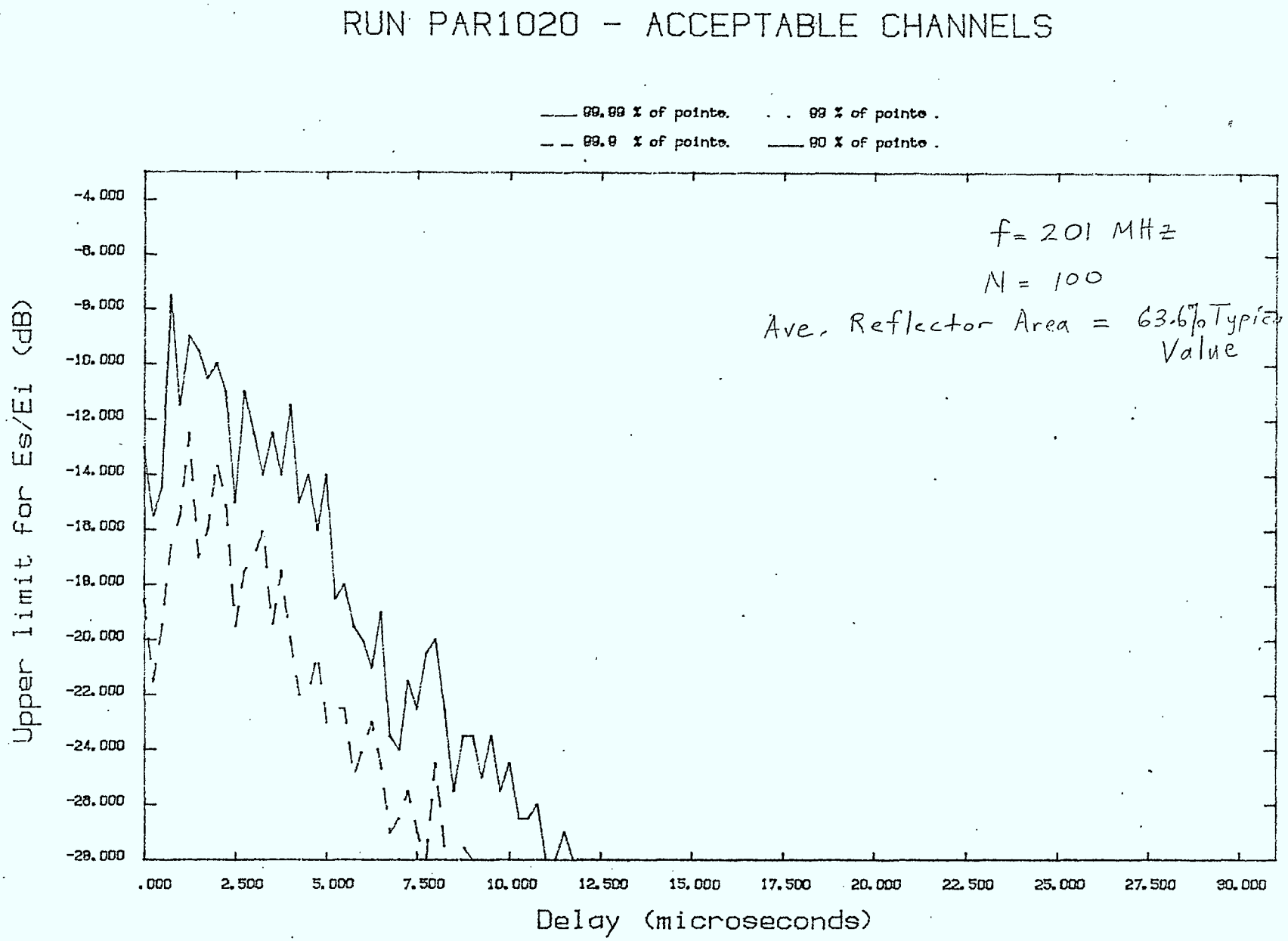
RUN PAR1020 - ACCEPTABLE CHANNELS
99.99 % of points
99 % of points
99.9 % of points
90 % of points
f = 201 MHz
N = 100
Ave. Reflector Area = 63.6% Typical Value
Upper limit for Es/Ei (dB)
-4.000
-6.000
-8.000
-10.000
-12.000
-14.000
-16.000
-18.000
-20.000
-22.000
-24.000
-26.000
-28.000
.000
2.500
5.000
7.500
10.000
12.500
15.000
17.500
20.000
22.500
25.000
27.500
30.000
Delay (microseconds)

Figure 27

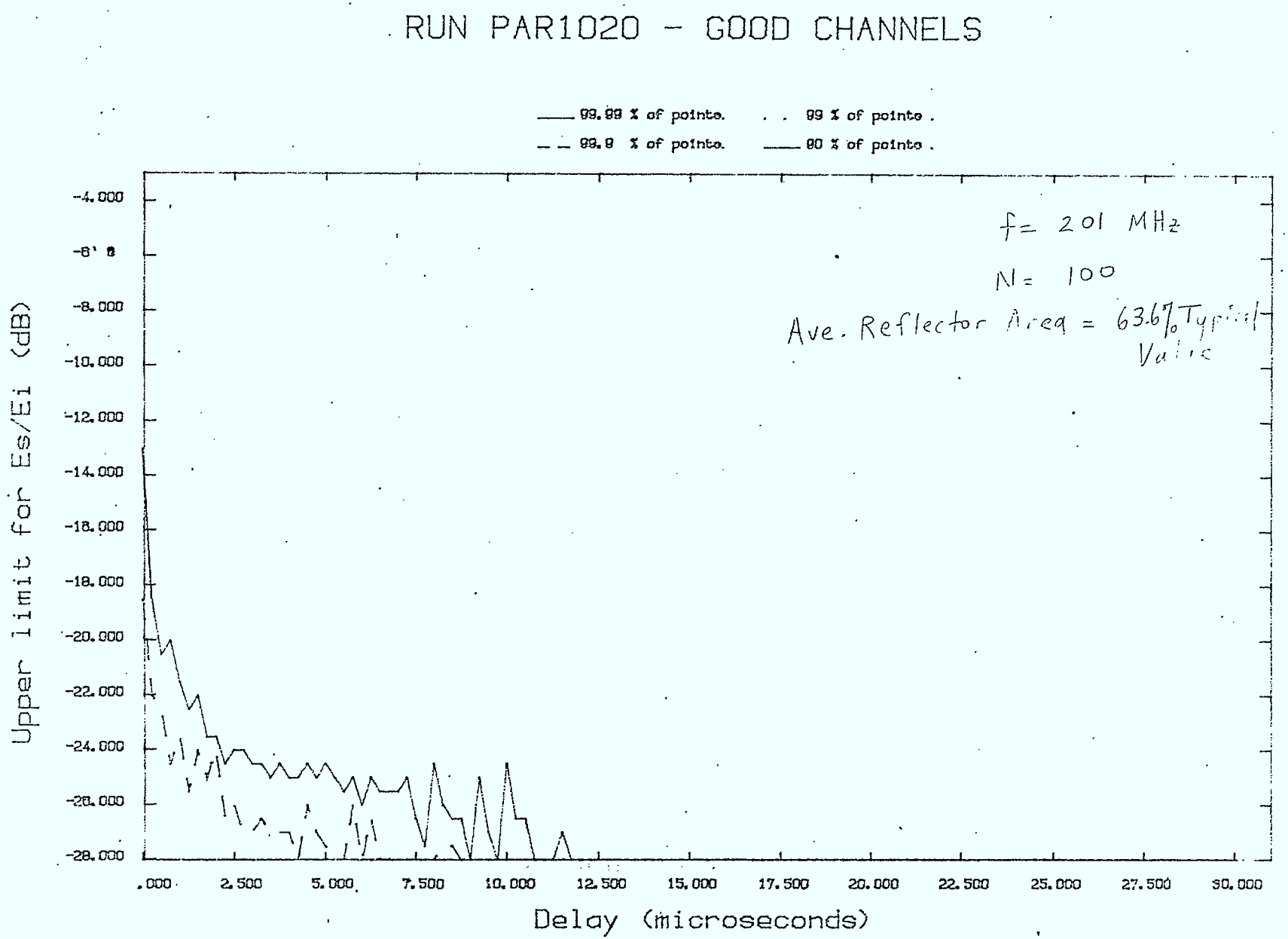
RUN PAR1020 - GOOD CHANNELS
99.99 % of points
99 % of points
99.9 % of points
80 % of points
f= 201 MHz
N= 100
Ave. Reflector Area = 63.6% Typical Value
Upper limit for Es/Ei (dB)
-4.000
-8.000
-10.000
-12.000
-14.000
-16.000
-18.000
-20.000
-22.000
-24.000
-26.000
-28.000
.000
2.500
5.000
7.500
10.000
12.500
15.000
17.500
20.000
22.500
25.000
27.500
30.000
Delay (microseconds)

Figure 28

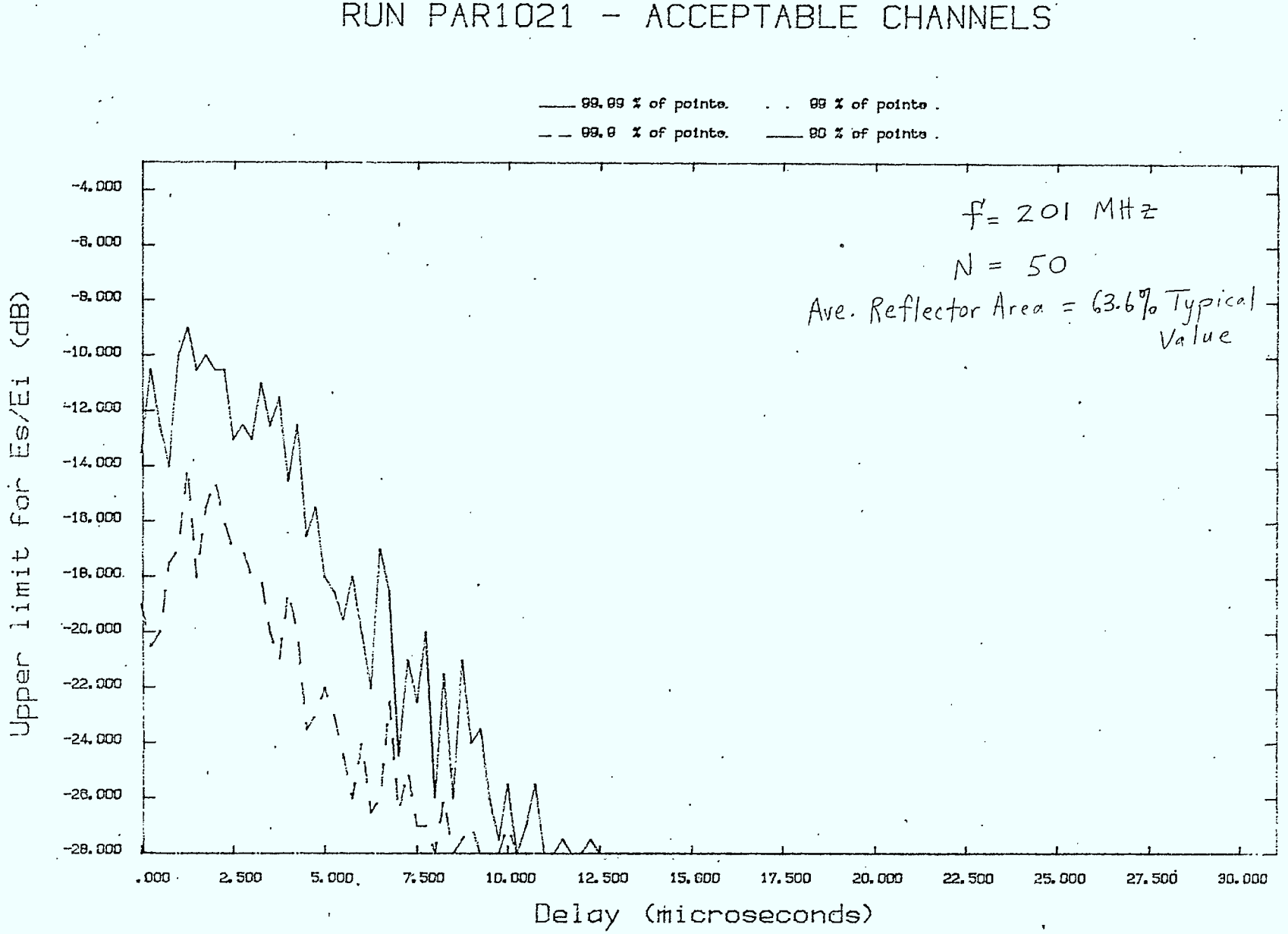
RUN PAR1021 - ACCEPTABLE CHANNELS
99.99 % of points
99 % of points
99.9 % of points
90 % of points
f = 201 MHz
N = 50
Ave. Reflector Area = 63.6% Typical Value
Upper limit for Es/Ei (dB)
-4.000
-6.000
-8.000
-10.000
-12.000
-14.000
-16.000
-18.000
-20.000
-22.000
-24.000
-26.000
-28.000
.000
2.500
5.000
7.500
10.000
12.500
15.000
17.500
20.000
22.500
25.000
27.500
30.000
Delay (microseconds)

Figure 29

RUN PAR1021 - GOOD CHANNELS

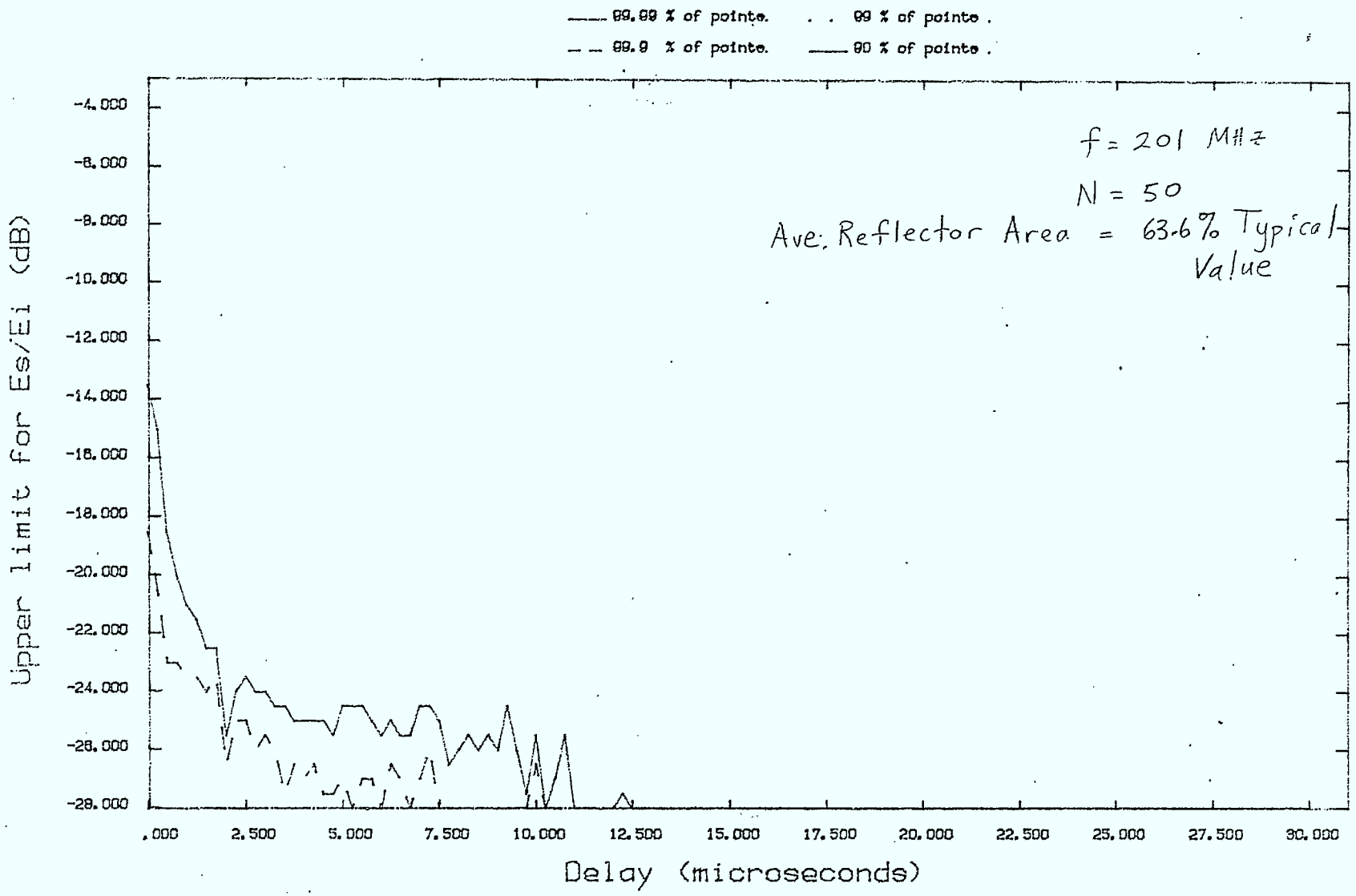

Figure 30

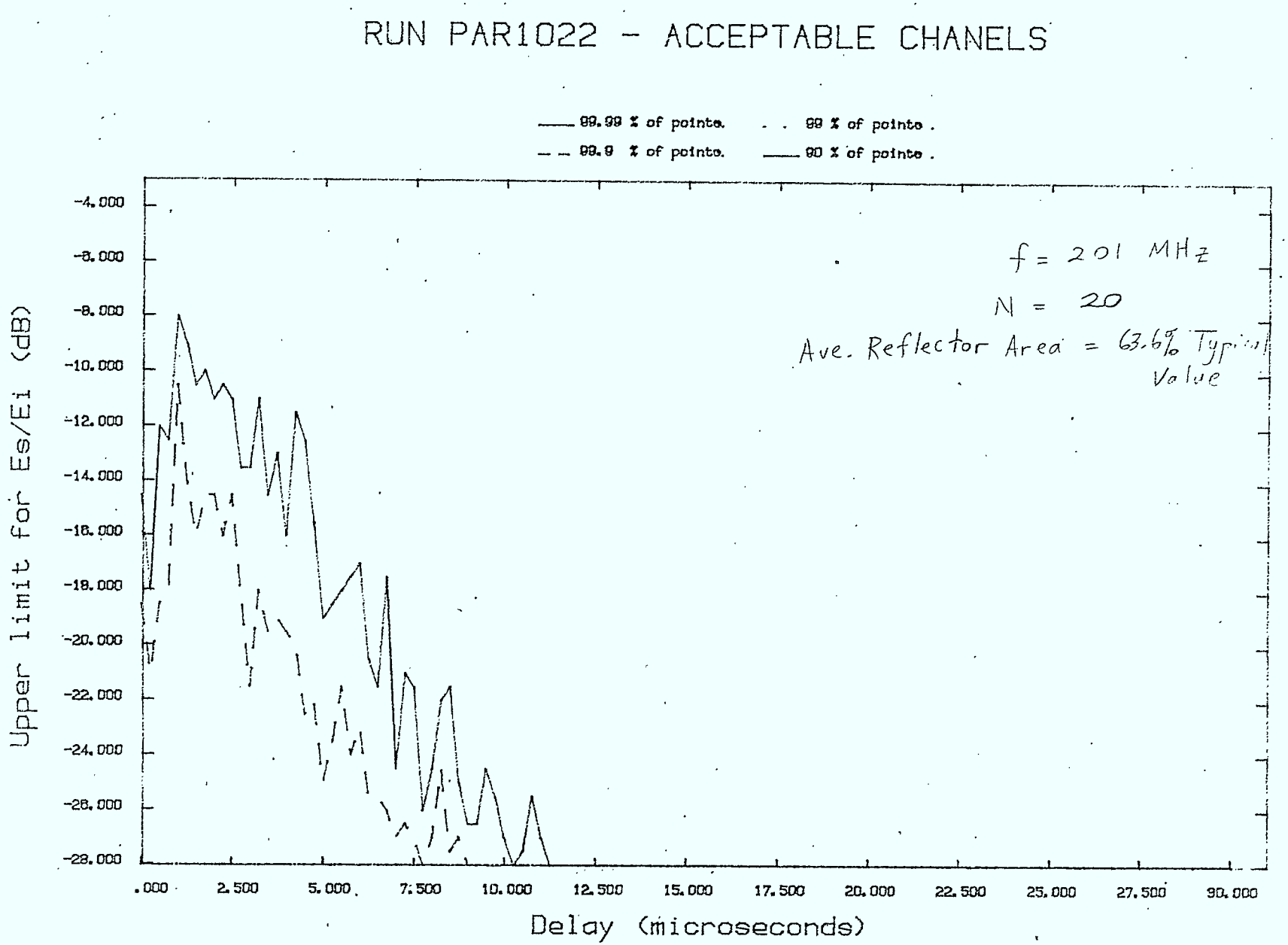
RUN PAR1022 - ACCEPTABLE CHANELS
99.99 % of points
99 % of points
99.9 % of points
90 % of points
f = 201 MHz
N = 20
Ave. Reflector Area = 63.6% Typical Value
Upper limit for Es/Ei (dB)
-4.000
-6.000
-8.000
-10.000
-12.000
-14.000
-16.000
-18.000
-20.000
-22.000
-24.000
-26.000
-28.000
.000
2.500
5.000
7.500
10.000
12.500
15.000
17.500
20.000
22.500
25.000
27.500
30.000
Delay (microseconds)

Figure 31

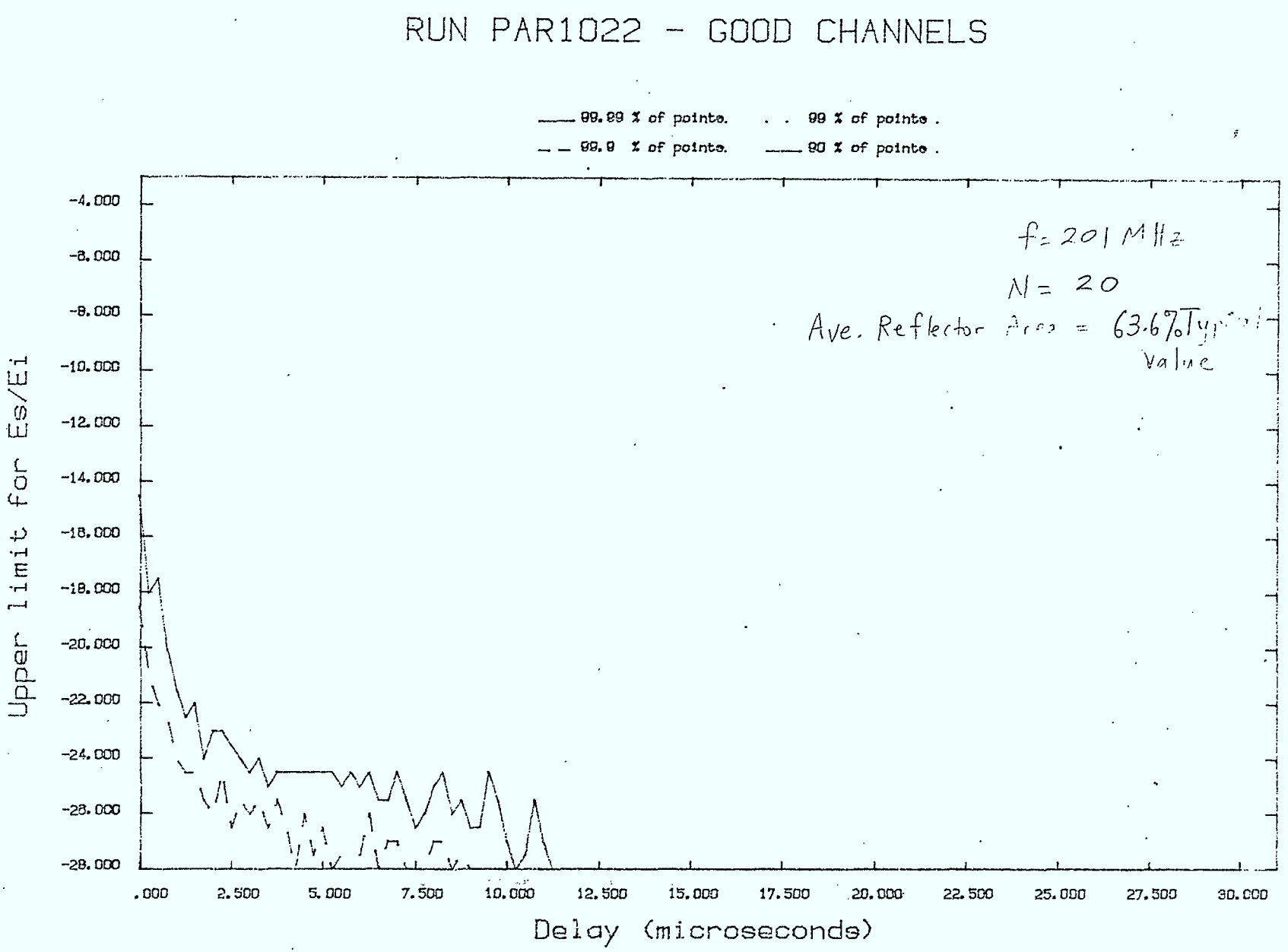
RUN PAR1022 - GOOD CHANNELS
99.99 % of points.
99 % of points.
99.9 % of points.
90 % of points.
f = 201 MHz
N = 20
Ave. Reflector Area = 63.67% Typical Value
Upper limit for Es/Ei
-4.000
-8.000
-8.000
-10.000
-12.000
-14.000
-18.000
-18.000
-20.000
-22.000
-24.000
-28.000
-28.000
.000
2.500
5.000
7.500
10.000
12.500
15.000
17.500
20.000
22.500
25.000
27.500
30.000
Delay (microseconds)

Figure 32

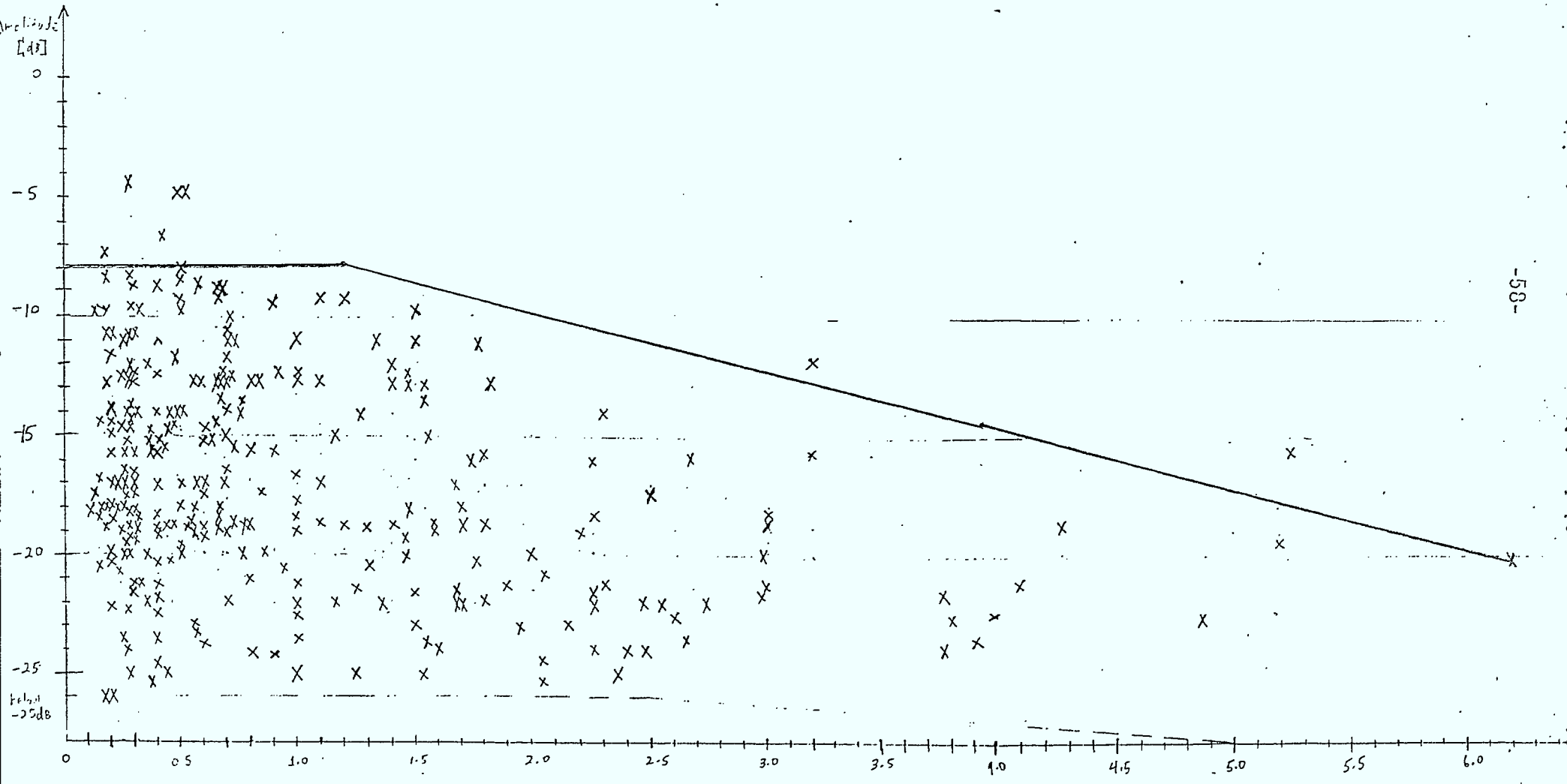

Figure 33 : Scatter Table of Measured Data With 99.9% Contour From Experiment With 63.6% Charge In Reflector Area.

Plots of the significant echoes of impulse responses for channels used to generate Figure 27 (N=100), for various PDUR's, are shown in Figures 34 - 39. On these figures, note that there is a 0 dB main path at t=0. One thing that is apparent is that the average number of significant echoes is less than 3, which is the approximate average among acceptable measured channels.

With the reflector sizes unchanged from the previous scenario, and by simply reducing the occupational domain to a 3 km x 3 km rectangle centered about the receiver, and having 400 impulse response components (number of reflectors) we were able to get a better match between the number of significant echoes generated by the simulation program and the average number observed for the channel measurements. Sample impulse response plots for this situation are provided in Figures 40-50. The cdf contours for this situation are shown in Figure 51. The delay spread is roughly 7 μsec. A smoothed 99.99% contour is drawn on the scatter diagram for the measured data in Figure 52. The delay spread seems to agree reasonably well with the measured data, and the previously mentioned deficiency of the simulation model in the near field region is evident. In generating the statistics, 2000 channels were classified, with 15.9% rejected, 84.1% acceptable, and only 0.25% deemed to be good video channels. One would expect that with an expanded set of random measurements, that the measured channel rejection rate would fall to a value closer to 15-20%, as opposed to the present value in the neighbourhood of 50%. As has been previously discussed, there was a tendancy "to look for multipath" during these measurements, and this is responsible for the results being biased towards bad channels (very strong multipath).

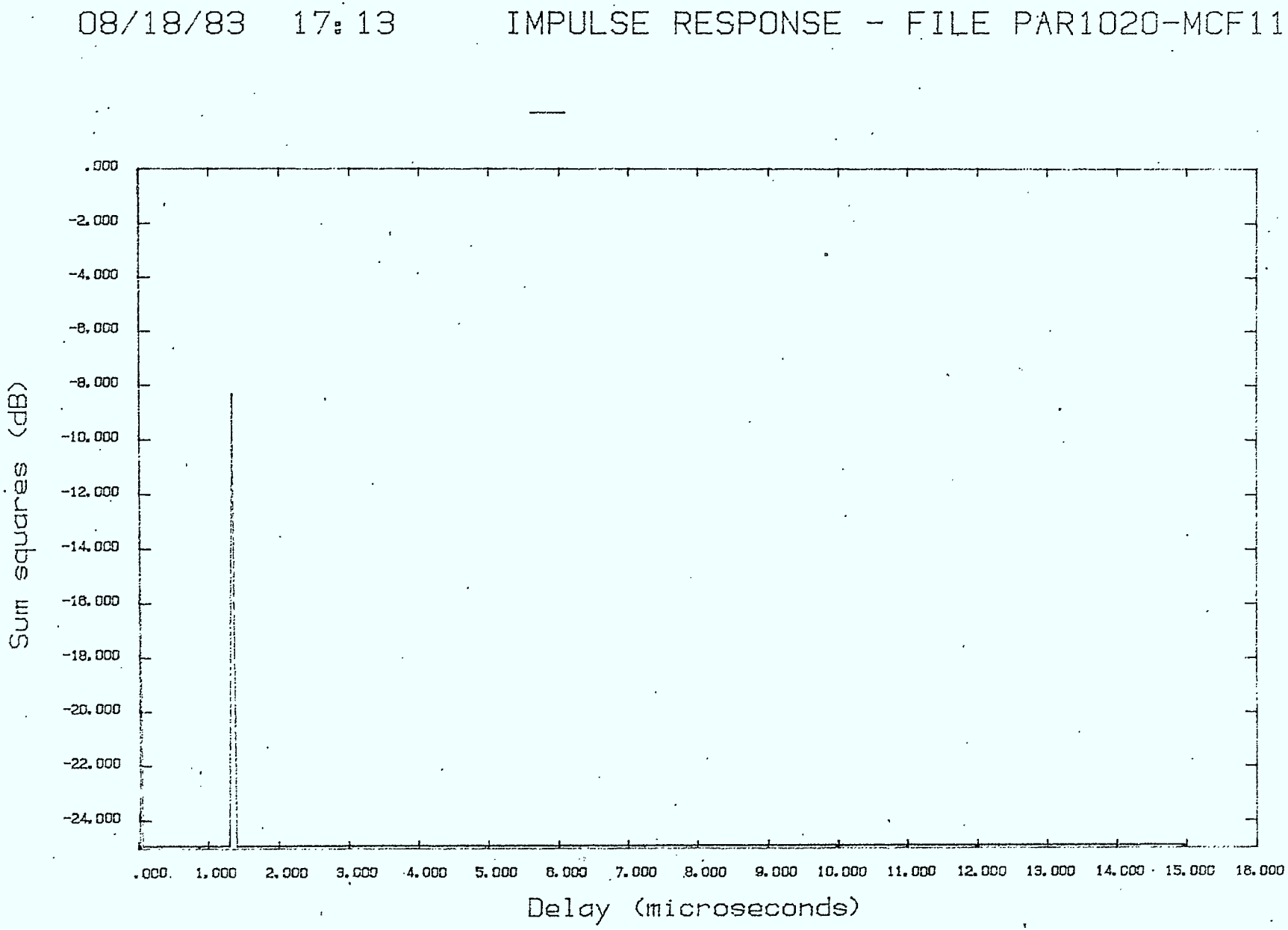

Figure 34 : Impulse Response Plot (PDUR = 11 dB)

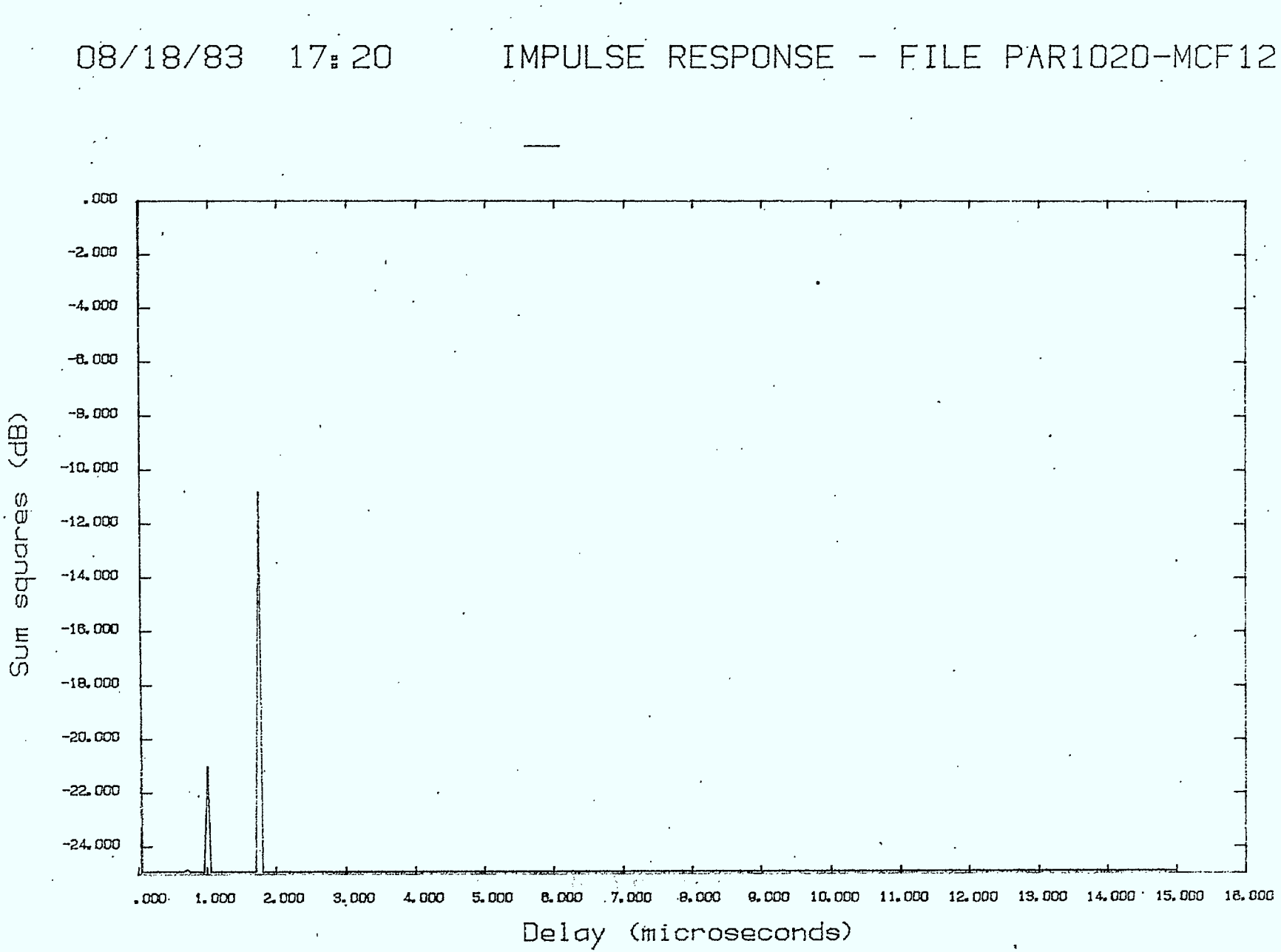

Figure 35 : Impulse Response Plot (PDUR = 12 dB)

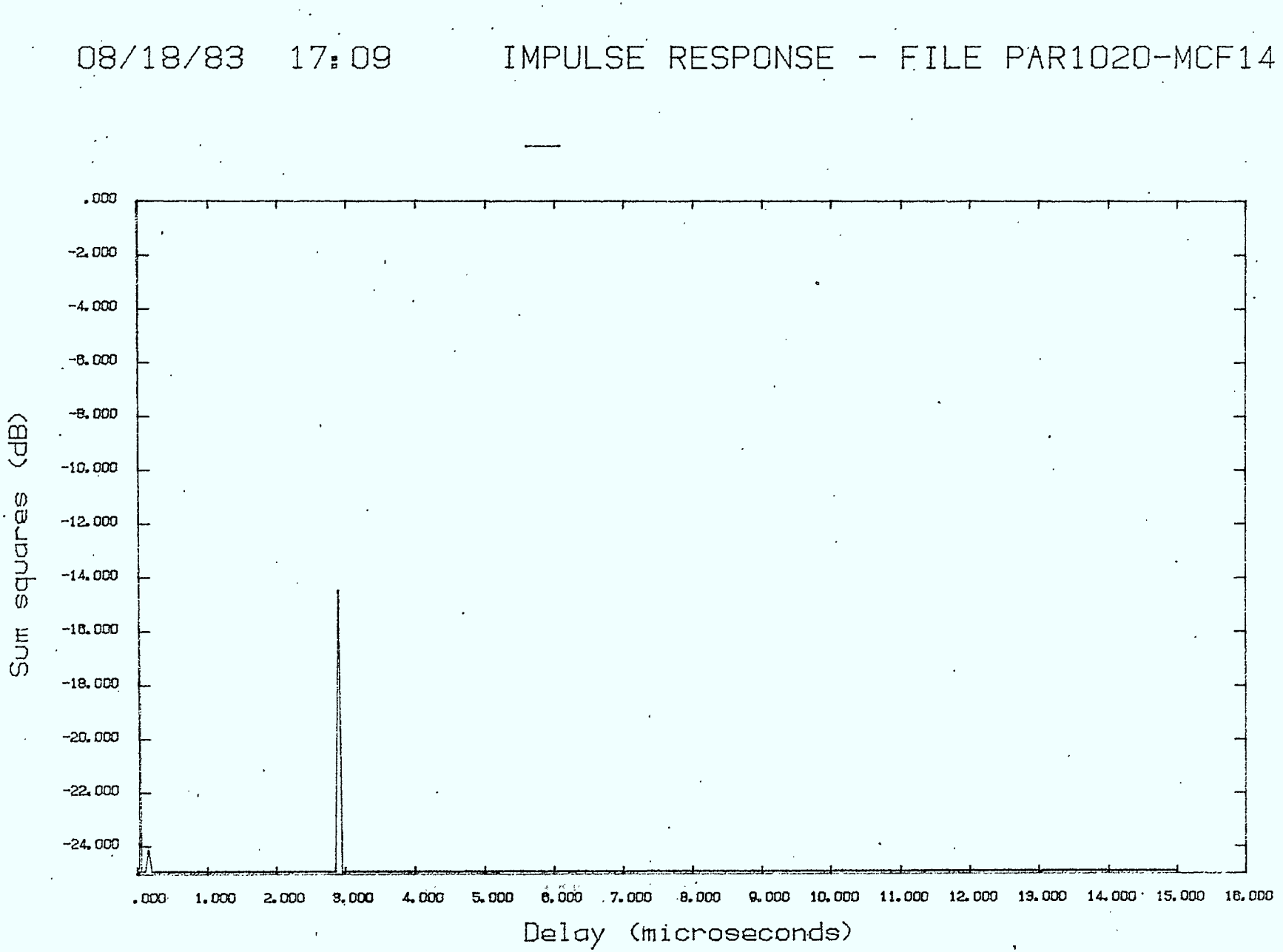

Figure 36 : Impulse Response Plot (PDUR = 14 dB)

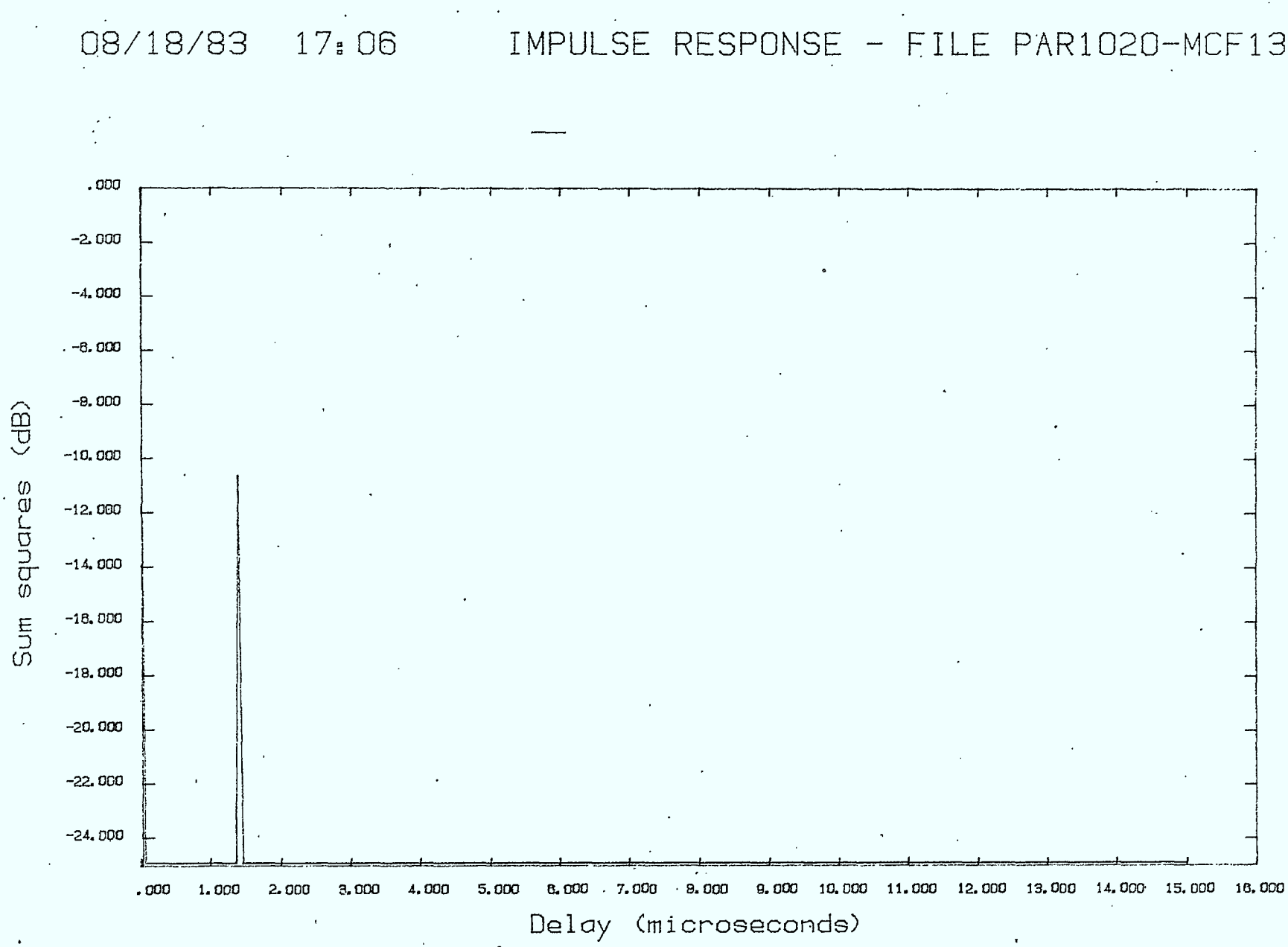

Figure 37 : Impulse Response Plot (PDUR = 13 dB)

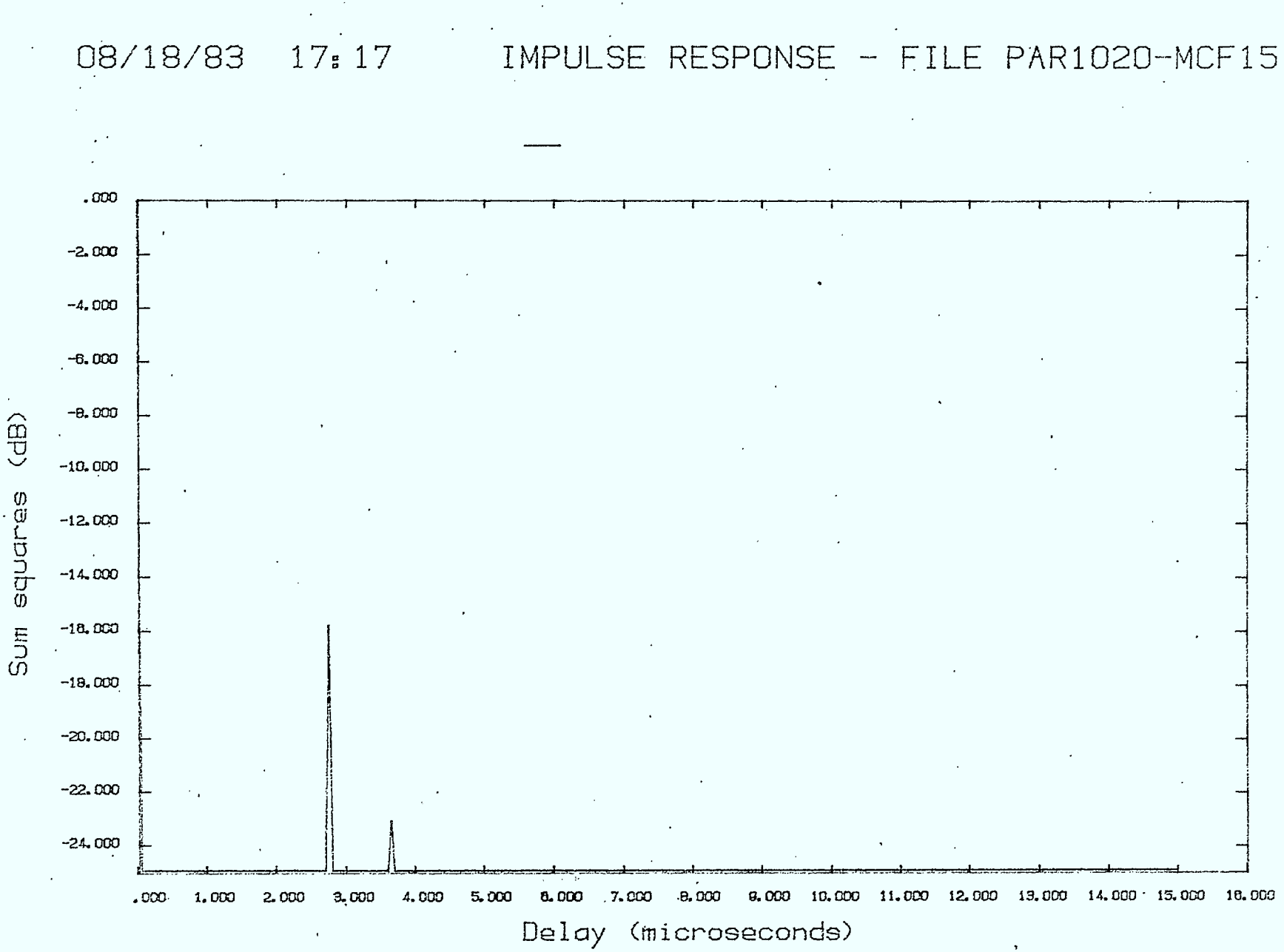

Figure 38 : Impulse Response Plot (PDUR = 15dB)

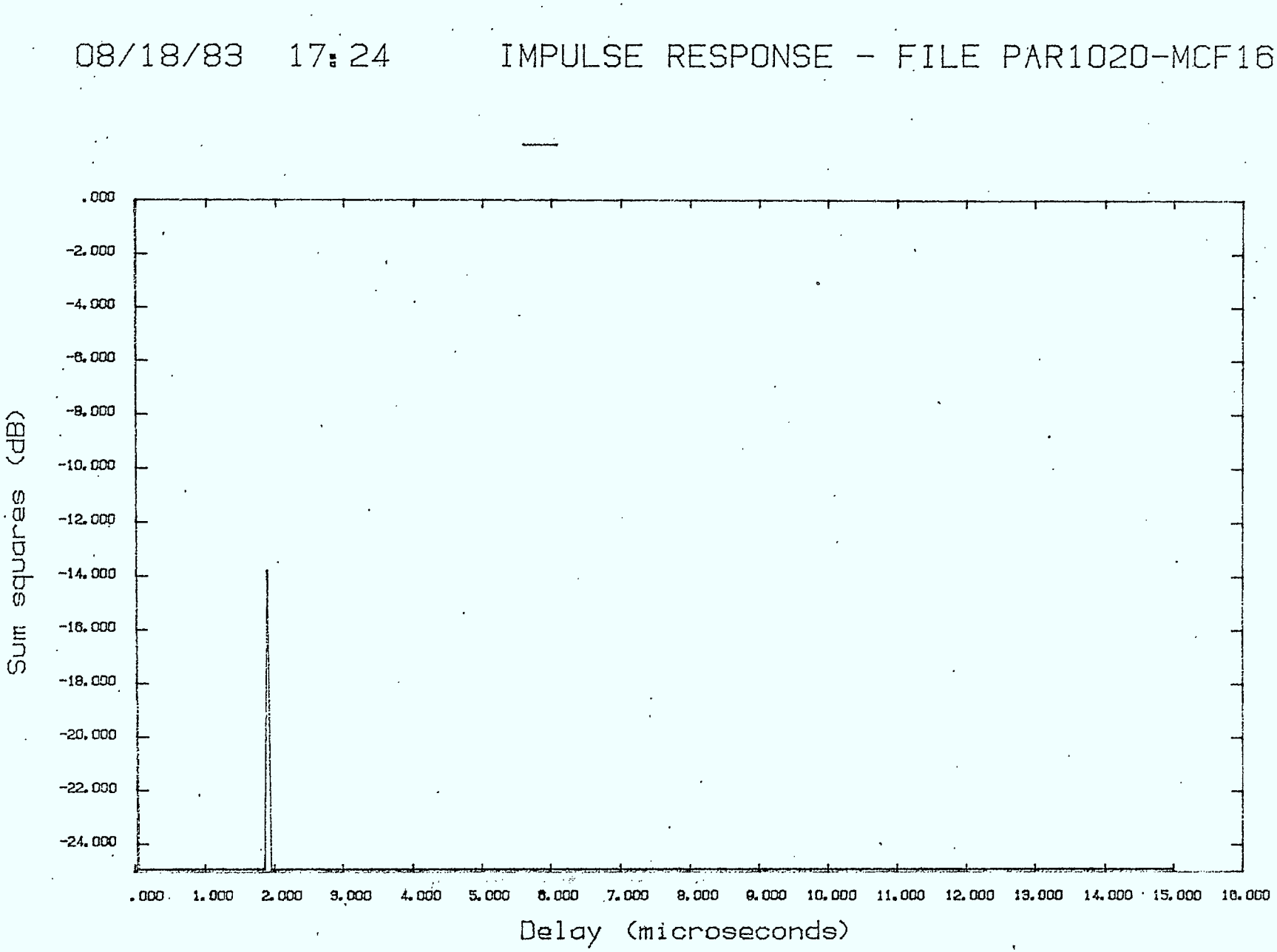

Figure 39 : Impulse Response Plot (PDUR = 16 dB)

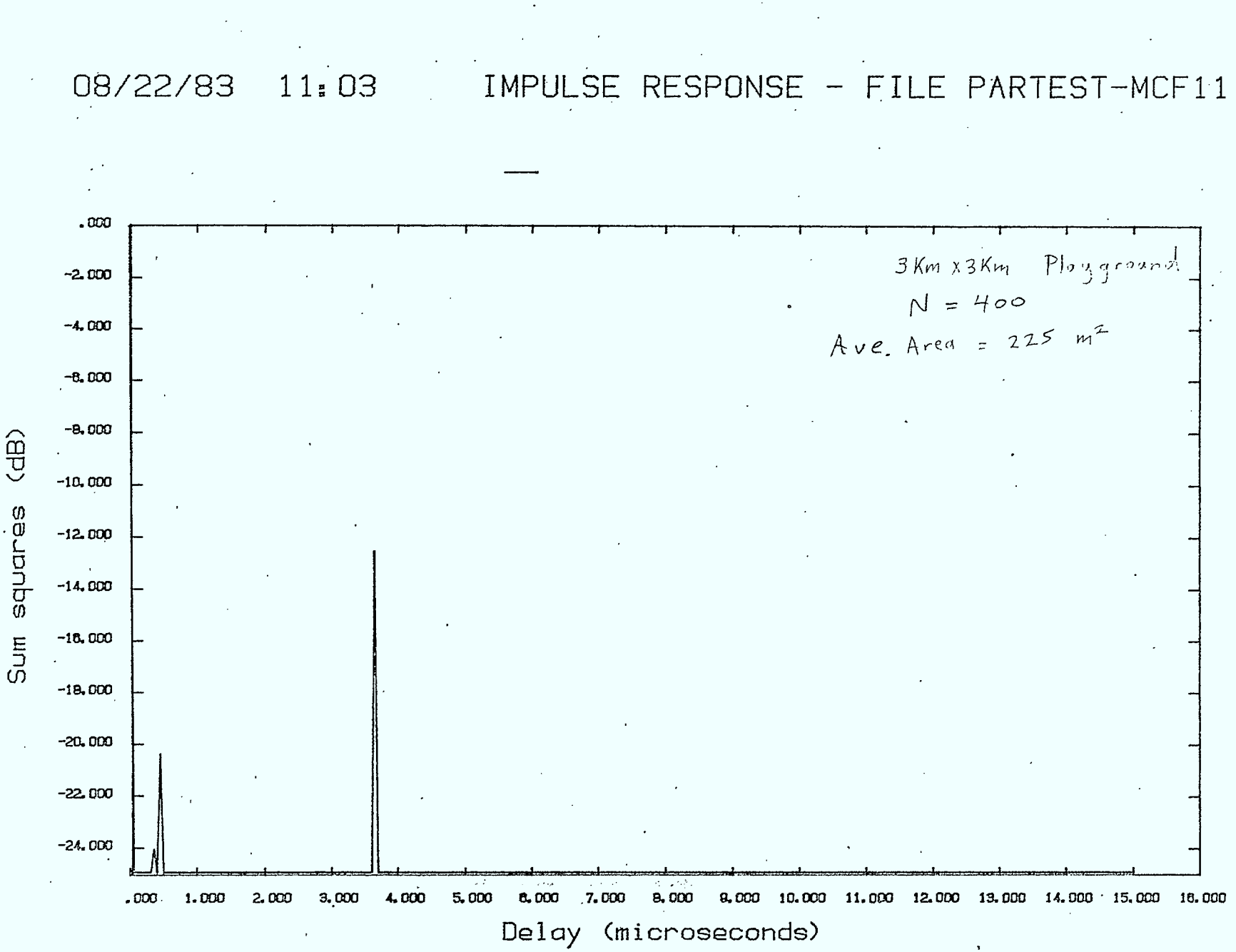

Figure 40 : Impulse Response Plot (PDUR = 11 dB)

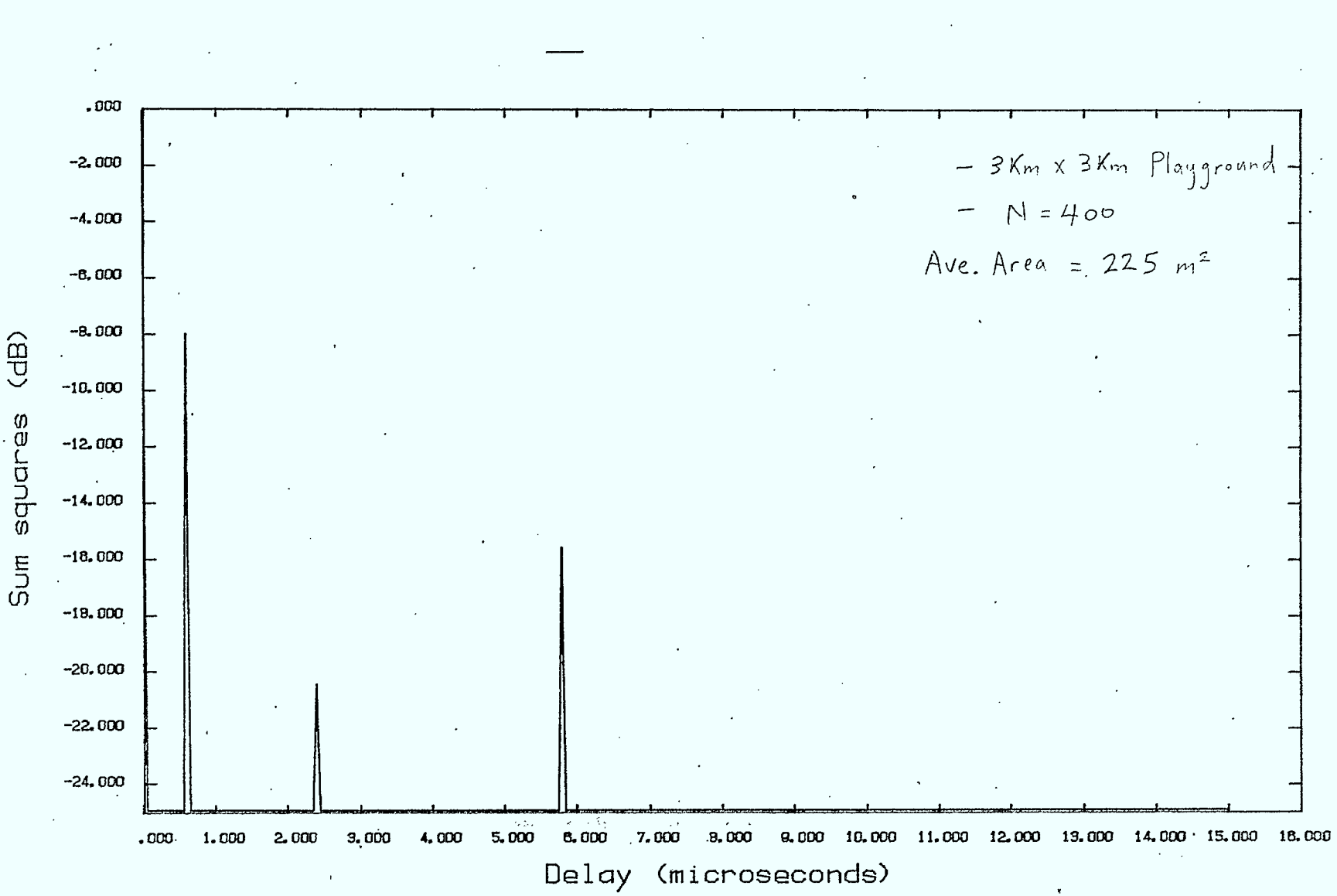

Figure 41 : Impulse Response Plot (PDUR = 11 dB)

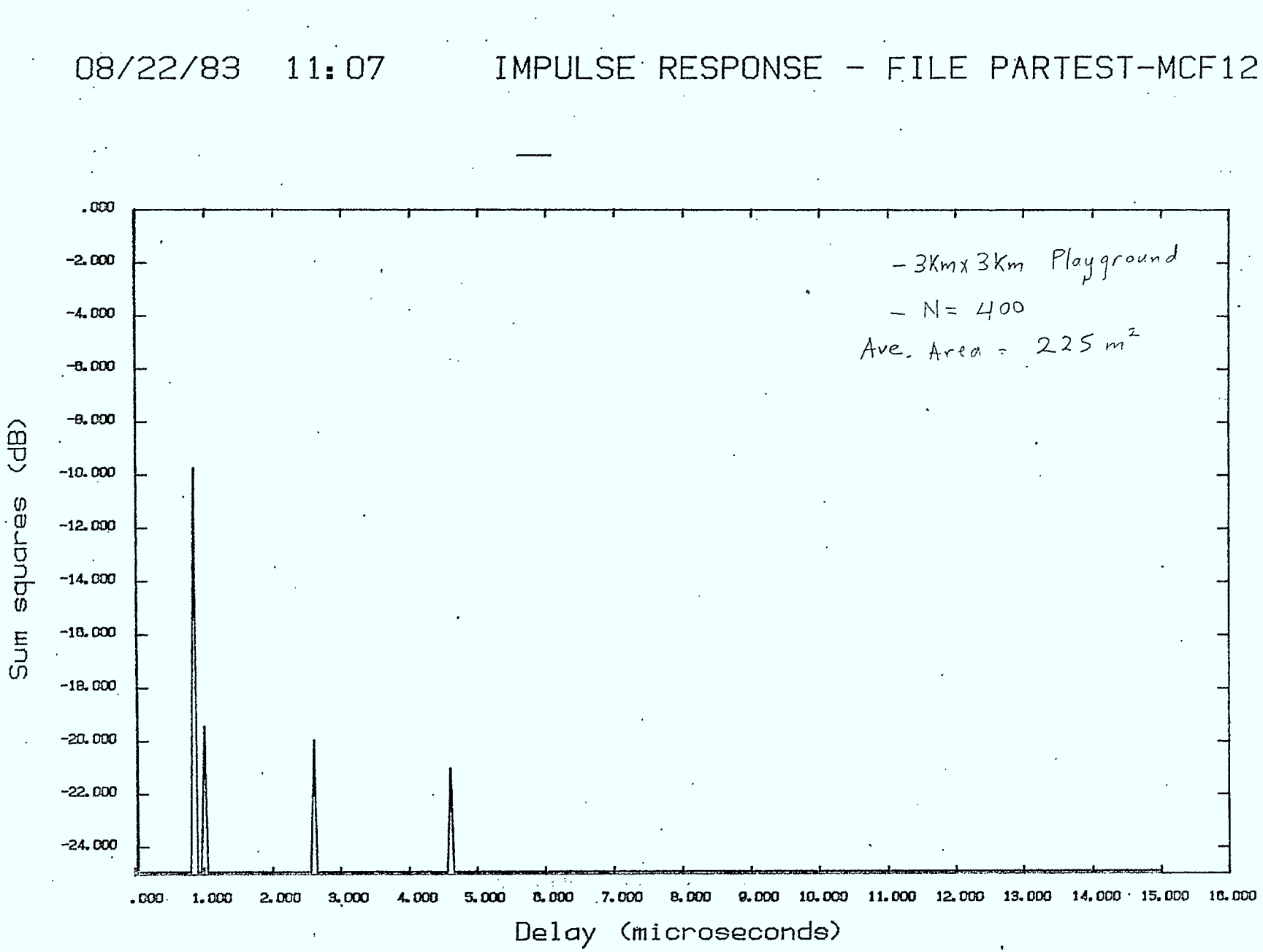

Figure 42: Impulse Response Plot (PDUR = 12 dB)

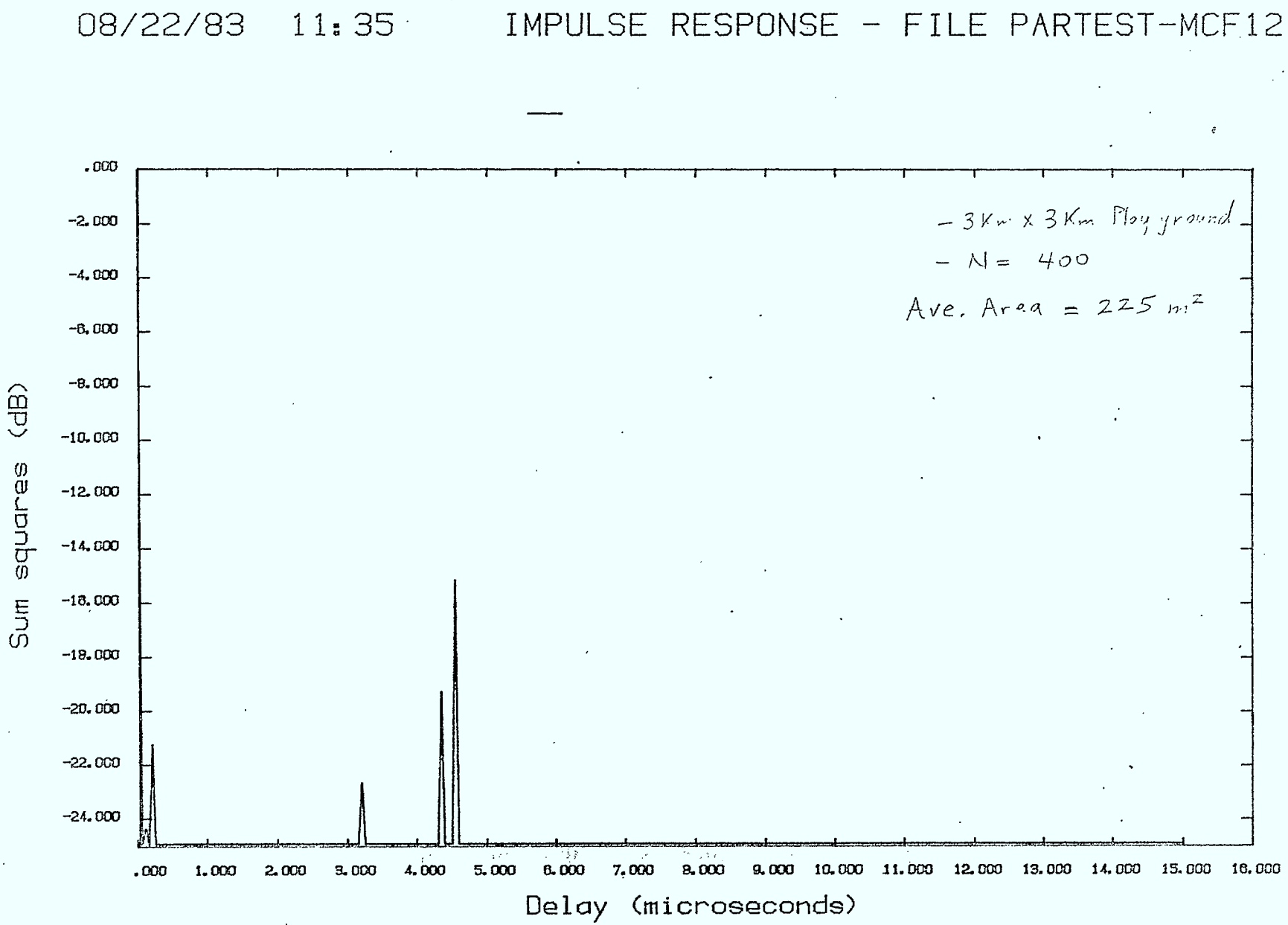

Figure 43 : Impulse Response Plot (PDUR = 12.dB)

08/22/83 11:49 IMPULSE RESPONSE - FILE PARTEST-MCF12

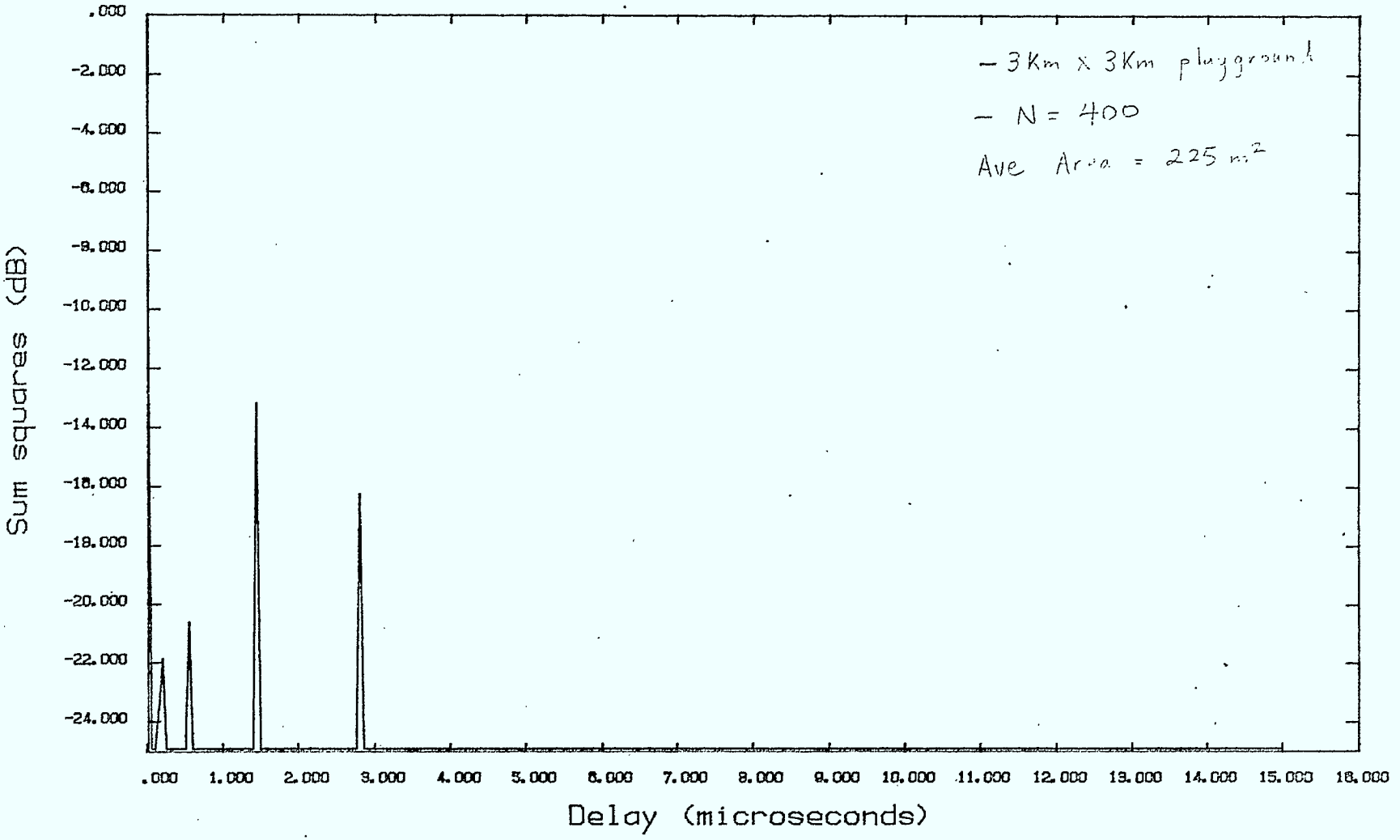

Figure 44 : Impulse Response Plot (PDUR = 12 dB)

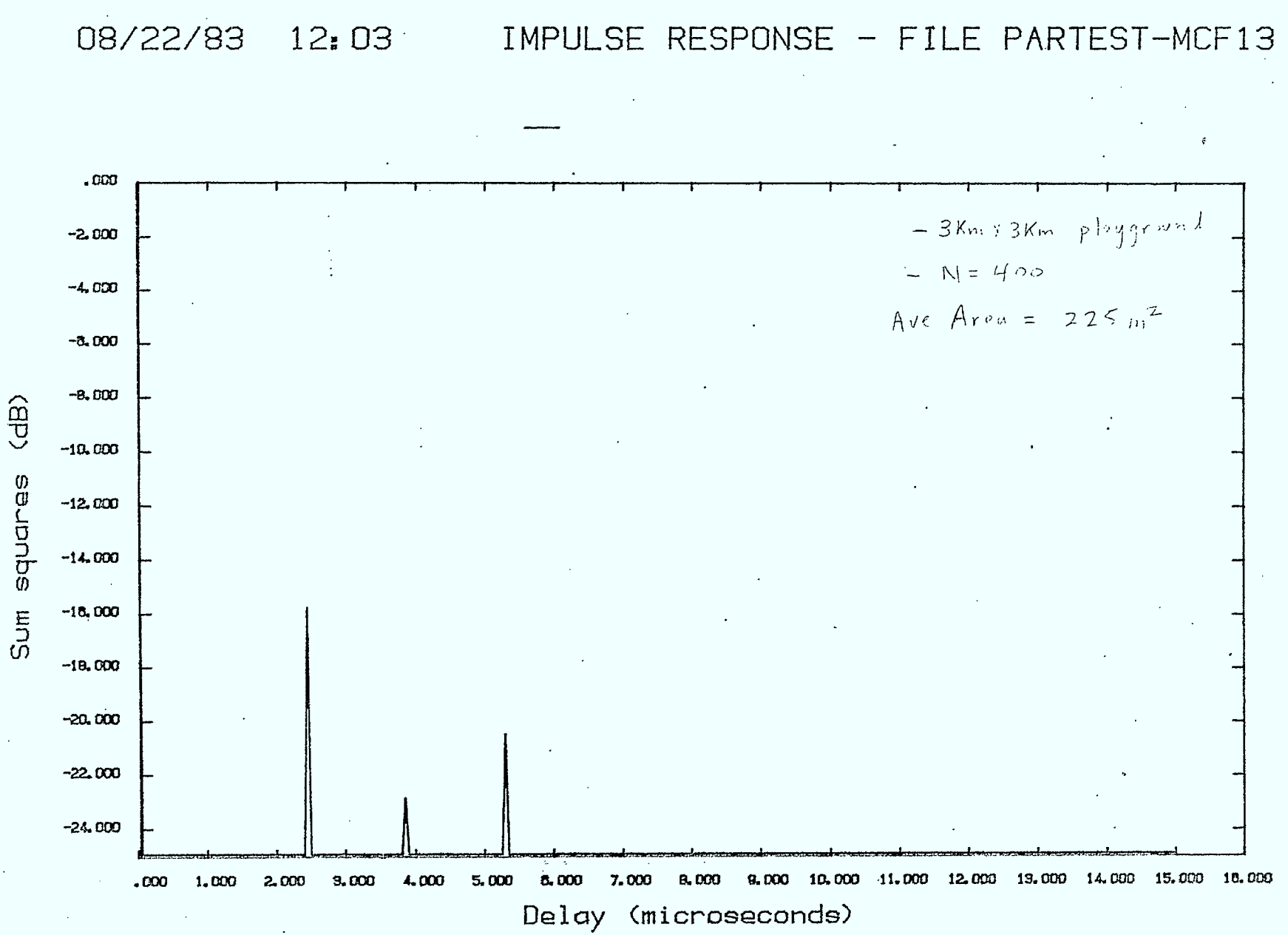

Figure 45 : Impulse Response Plot (PDUR = 13 dB)

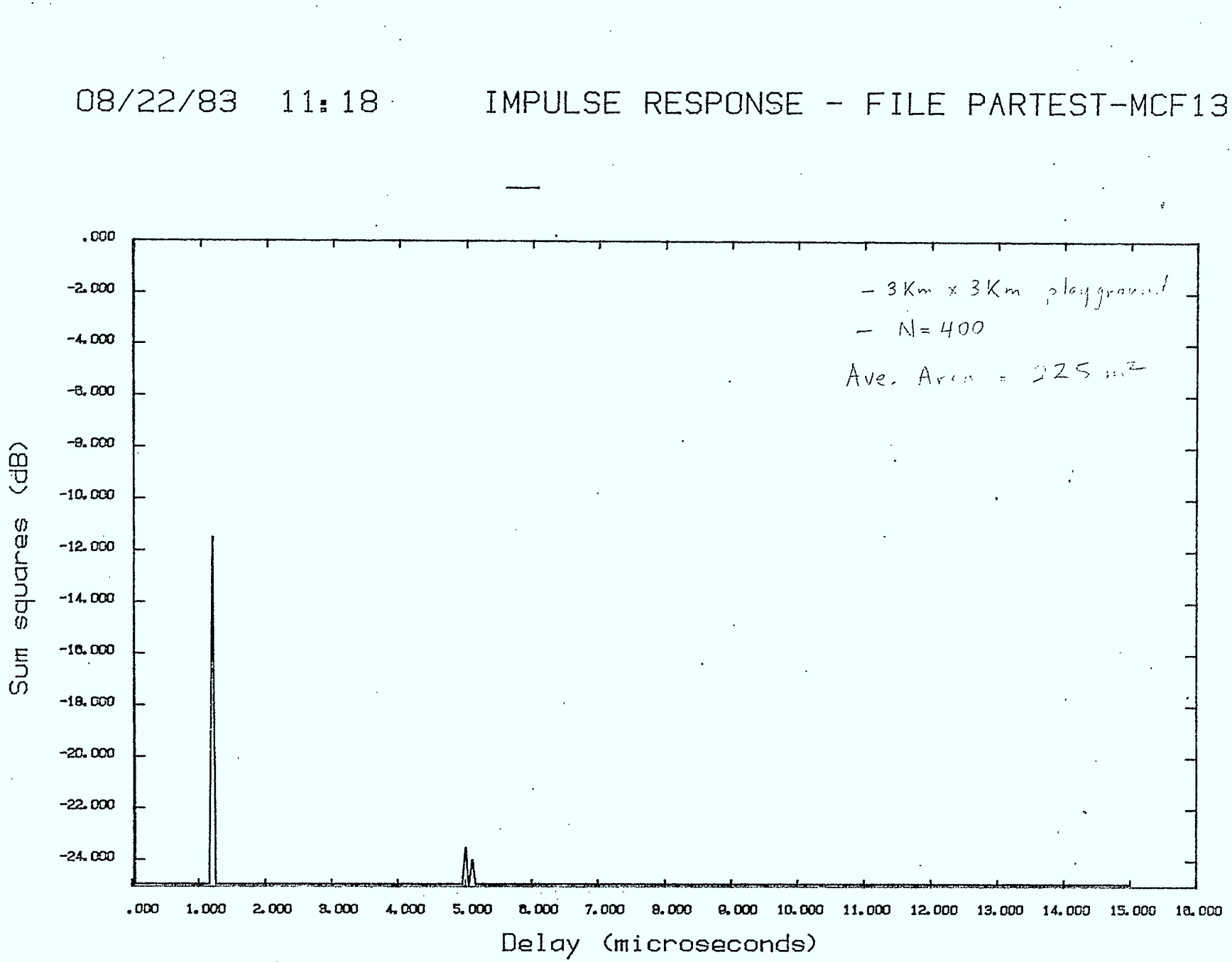

Figure 46 : Impulse Response Plot (PDUR = 13 dB)

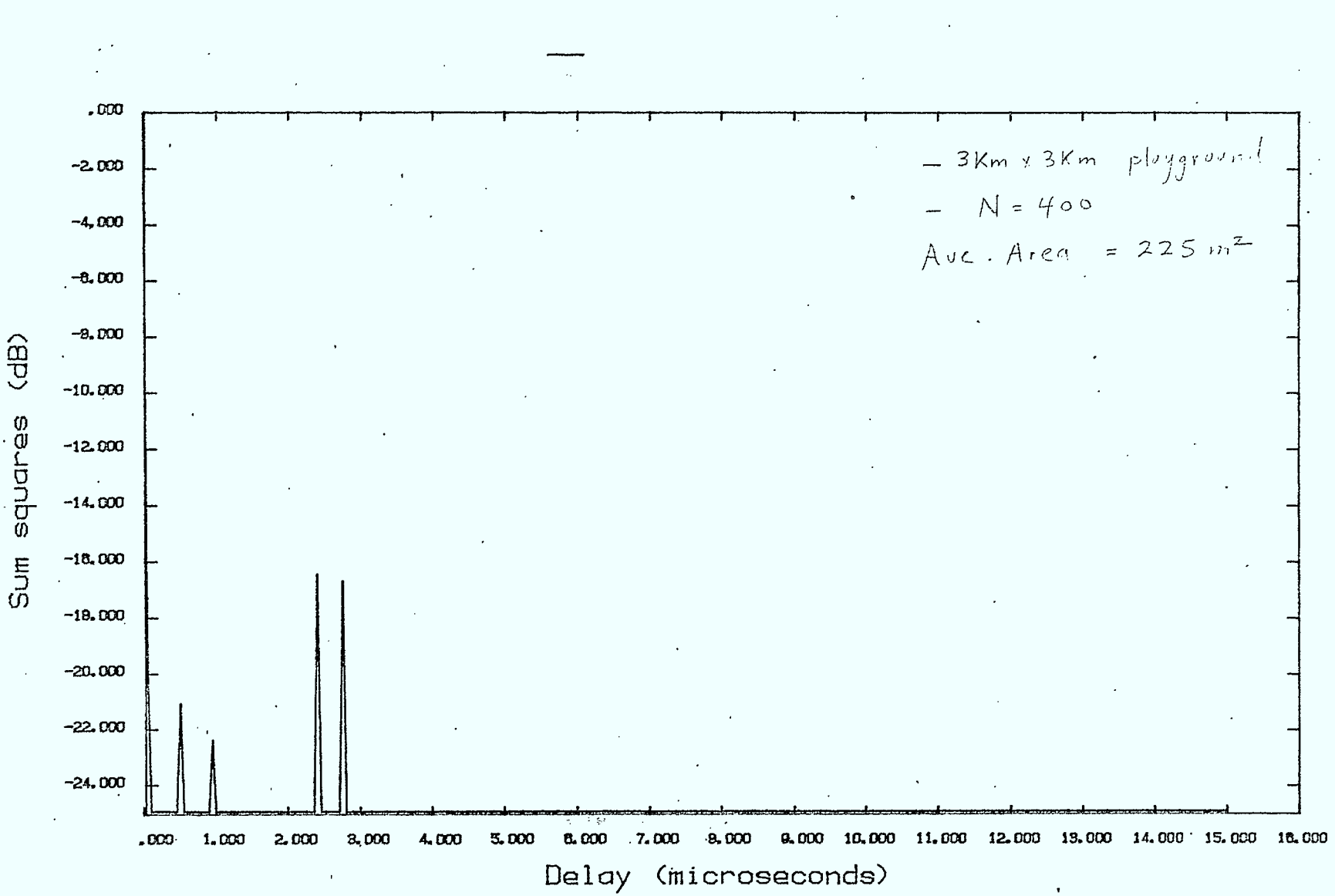

Figure 47 : Impulse Response Plot (PDUR = 13 dB)

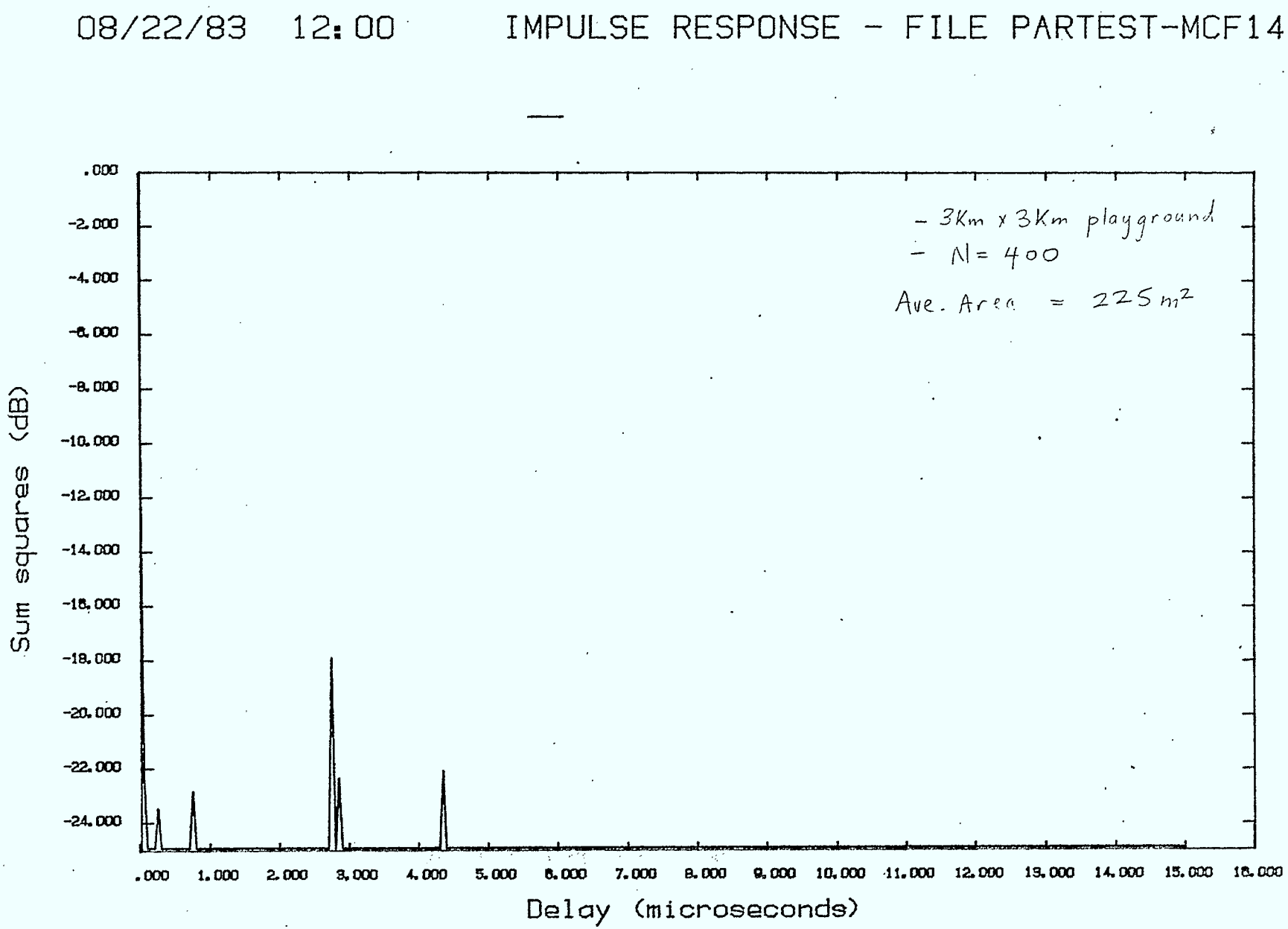

Figure 48 : Impulse Response Plot (PDUR = 14 dB).

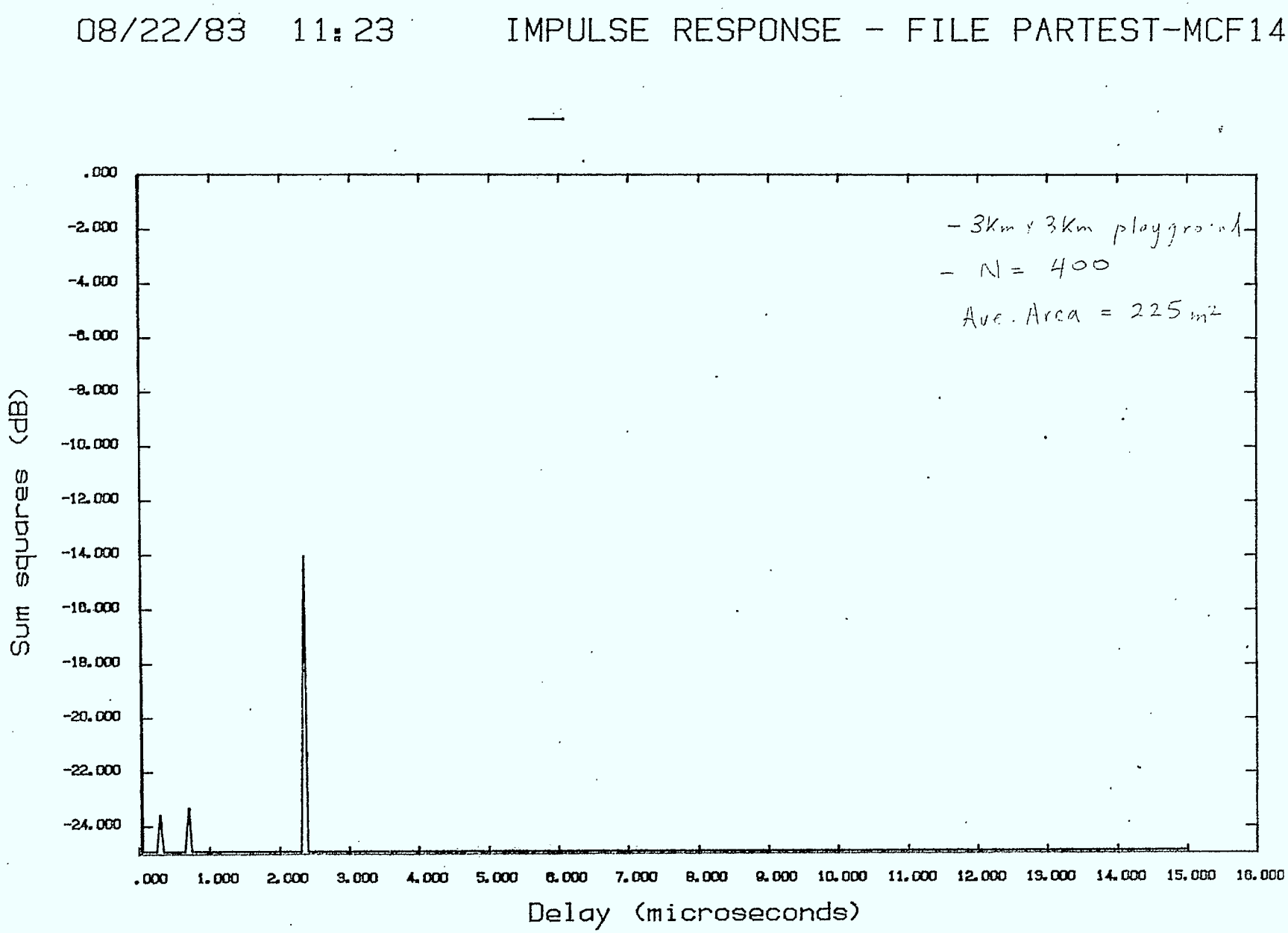

Figure 49 : Impulse Response Plot (PDUR = 14 dB)

08/22/83 11:13 IMPULSE RESPONSE - FILE PARTEST-MCF14

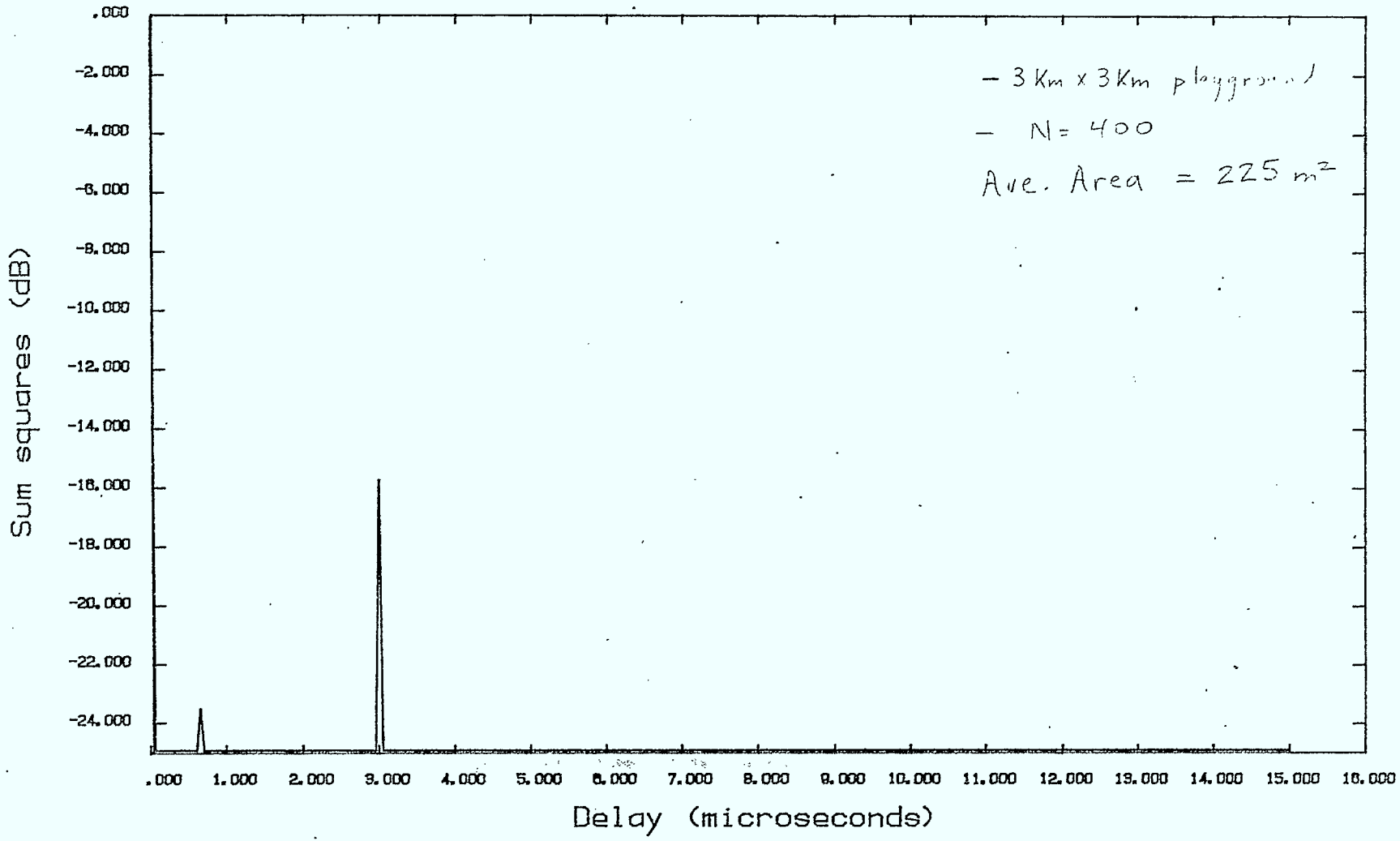

Figure 50 : Impulse Response Plot (PDUR = 14 dB)

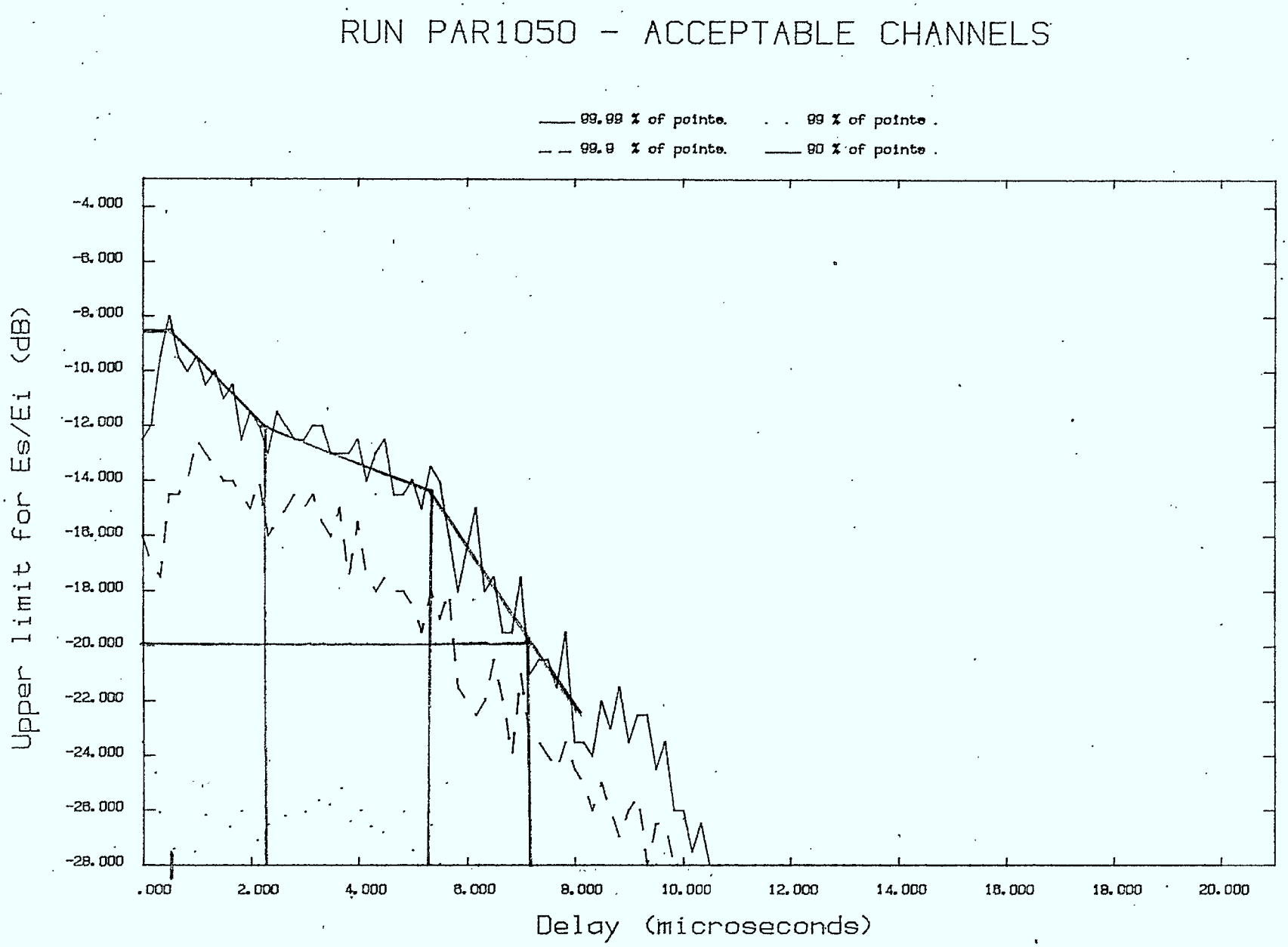

Figure 51: CDF contours (reflector area 225 m², N = 4[illegible], reduced occupational domain (3Km x 3Km))

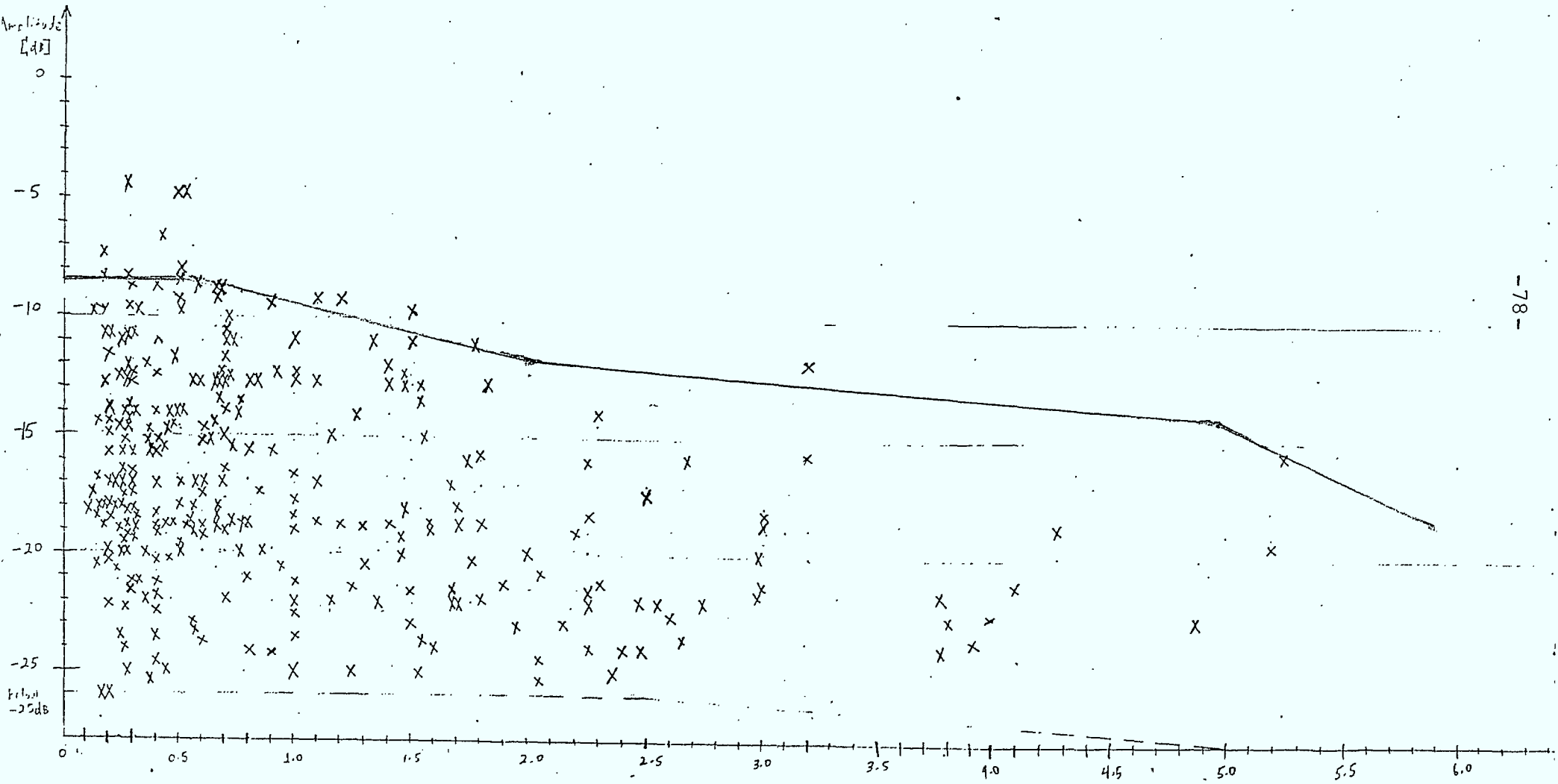

Figure 52 : Scatter Table For Measured Acceptable Video Channels With Smoothed 99.99% Contour From Figure 51.

2.5 Concluding Remarks on Multipath Channel Validation

The extreme sensitivity of the VHF multipath channel to important parameters such as frequency and reflector dimensions has been demonstrated. It is apparent that by fiddling with model parameters, a reasonable fit with measured data can be obtained. After a satisfactory fit is established, the simulation program allows one to examine the characteristics of the multipath channels in different frequency regions.

A reasonable fit with the measured data (scatter table of magnitudes versus delay, and average number of significant echo paths) was obtained by adjusting the average reflector area, number of scatterers per channel impulse response, and the size of the occupational domain. The channel rejection rate of the CRC measurements is much higher than one would anticipate. The measurements seem to be biased towards poor (very strong multipath) channels. There are many reasons for this, but in defense of the measurements, their purpose was not to statistically categorize the multipath channel, but rather to provide some indication of the severity of multipath in suburban and urban environments.

The extreme variability of the multipath channel is evident from the measured channel impulse responses and from simulated channel impulse responses. As a result, in any given locality, the number of potential channels is virtually boundless, and the absolute accuracy of any specific candidate in this subset is of relatively little concern. The existance of a meaningful "average" channel for a specific region is questionable, considering the wildly non-stationary characteristics of the multipath channel. One would expect that a substantial number of

channels would have frequency responses considerably different from that of the "average" channel characteristic.

In spite of deficiencies in the near field region, the Telidon RF propagation model is a useful working model, and has provided considerable insight into the nature of VHF multipath propagation. With the addition of the channel prescreening capability, attention can be restricted to those channels which provide usable television pictures, and one cannot dispute the fact that the generated channel responses are valid possibilities. Given the extreme variability of the multipath channel, one could argue that if measurements were conducted over a prolonged period, that eventually one would discover a channel with the characteristics of the simulated channel. Due to the ease with which multipath channels can be generated and categorized with the Telidon RF propagation simulation program, and its increased flexability, it will be used to develop prospective channels for system evaluation.

3.0 ESTABLISHING BASELINE SYSTEM PERFORMANCE

In this section the simulated baseline performance of the existing Telidon system in typical multipath and noise environments is presented. A simplified system block diagram is presented in Figure 53. The data signal is a bipolar pulse amplitude modulated waveform. The baseband transmit pulse shape is a truncated 100% raised cosine pulse. The data signal is inserted into its appropriate place (i.e. timing and dc offset) in the television line (see Figure 54). Incorporating the synchronization components of the television line (i.e. the sync pulse and colour burst) is extremely important, especially when investigating the performance in multipath environments. The appropriate signal orientation and carrier level are applied to simulate the modulation type and modulation index selected. Television signals are typically transmitted using negative modulation (peak signal levels correspond to sync pulse tips and darker video signals) which is discussed in considerable detail in Appendix VIII of [15]. Incorporating the modulation technique is important for non-linear envelope detectors but not for synchronous detection. Attention has been restricted to synchronous detection for the results discussed in this section.

The Telidon system simulation is performed at a complex baseband. That is, all bandpass filtering operations are replaced by equivalent baseband filtering operations. The transmit and receive filters presently used in the simulation have ideal characteristics. The amplitude responses are shown in Figures 55 and 56, and the phase responses are assumed to be zero. The receiver filter response is characteristic of the responses of TV station demodulators. Typical home receivers have IF filters with responses that are down 6 dB at the colour subcarrier, as illustrated in Figure 57 [29]. The decreased bandwidth of

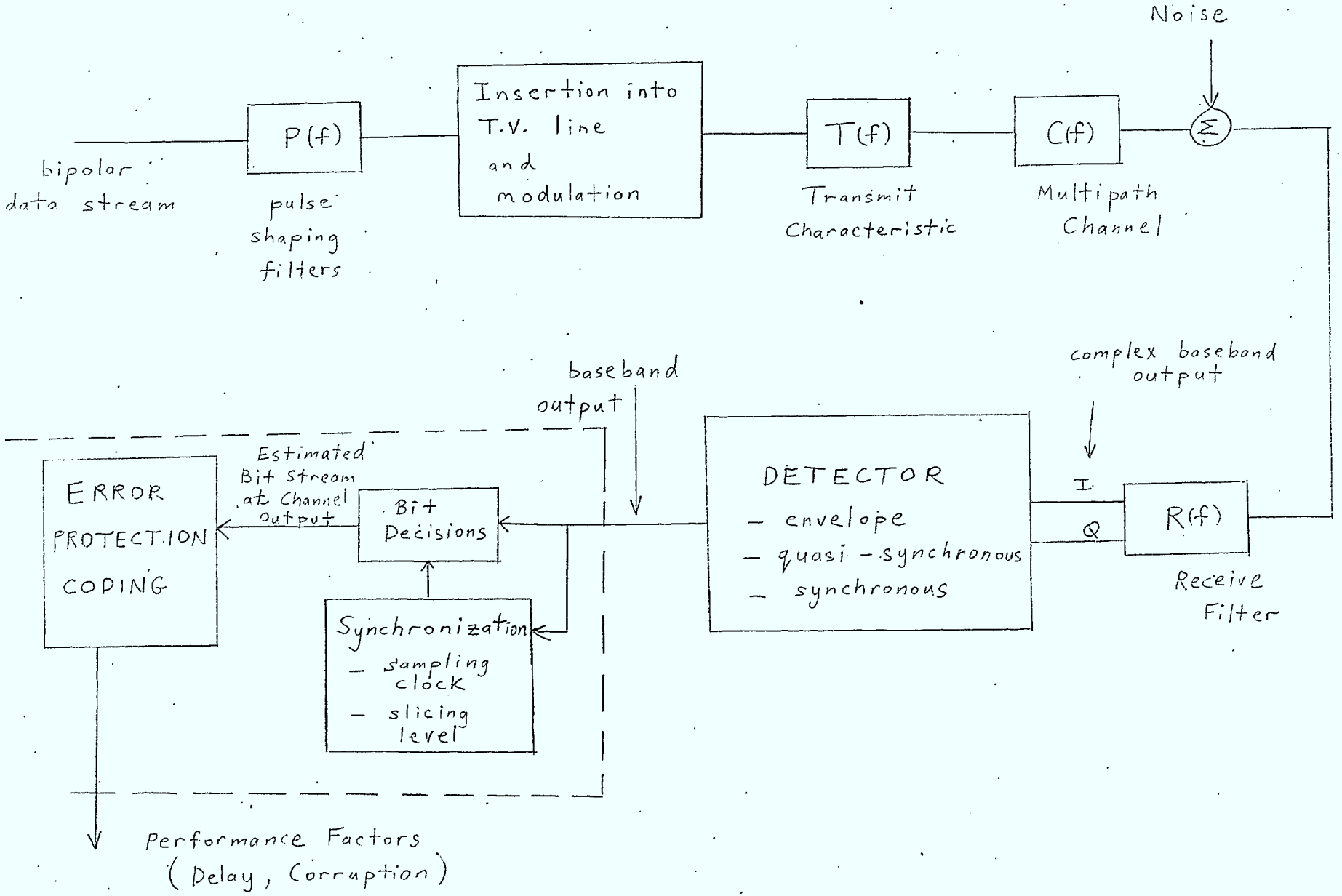

Figure 53 : Telidon system block diagram

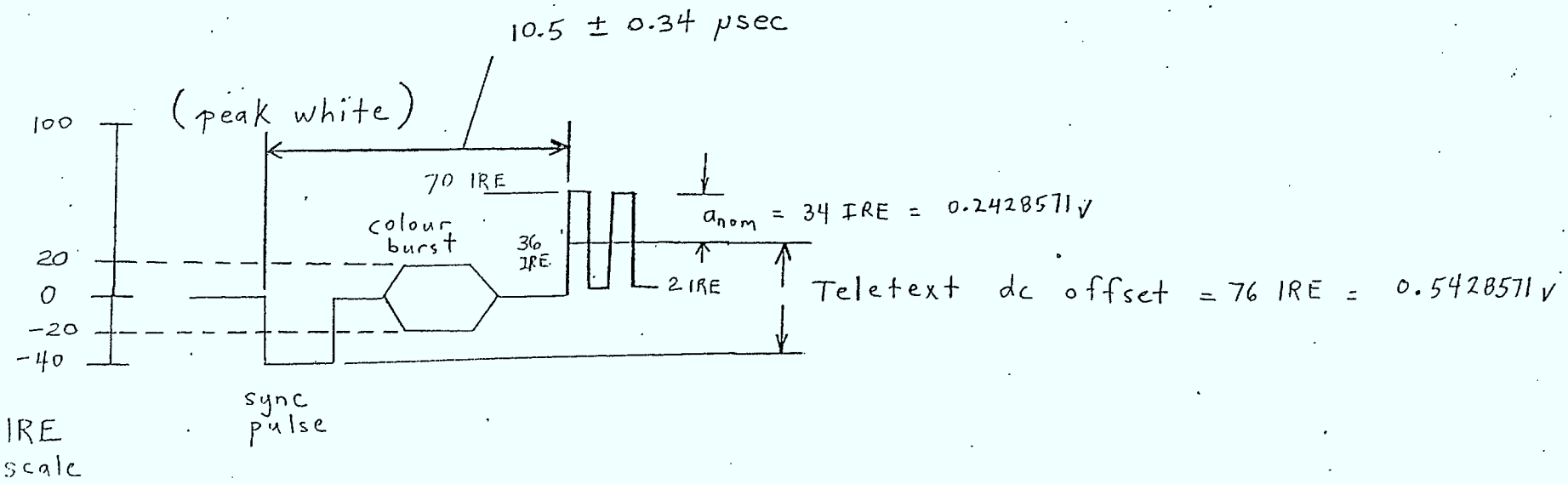

Figure 54 : Teletext levels from BS-14 [7]

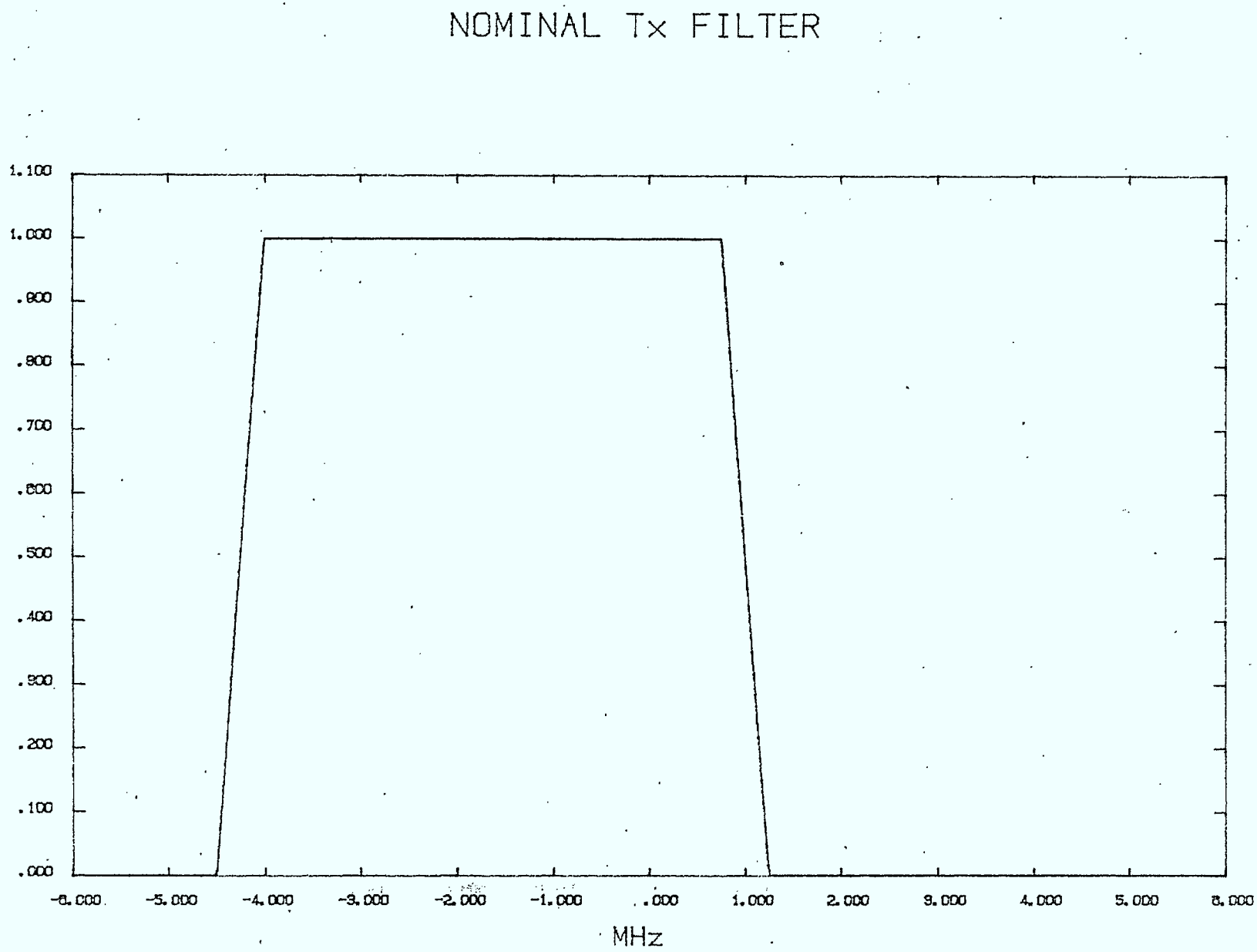

Figure 55 : Amplitude response of nominal transmit filter

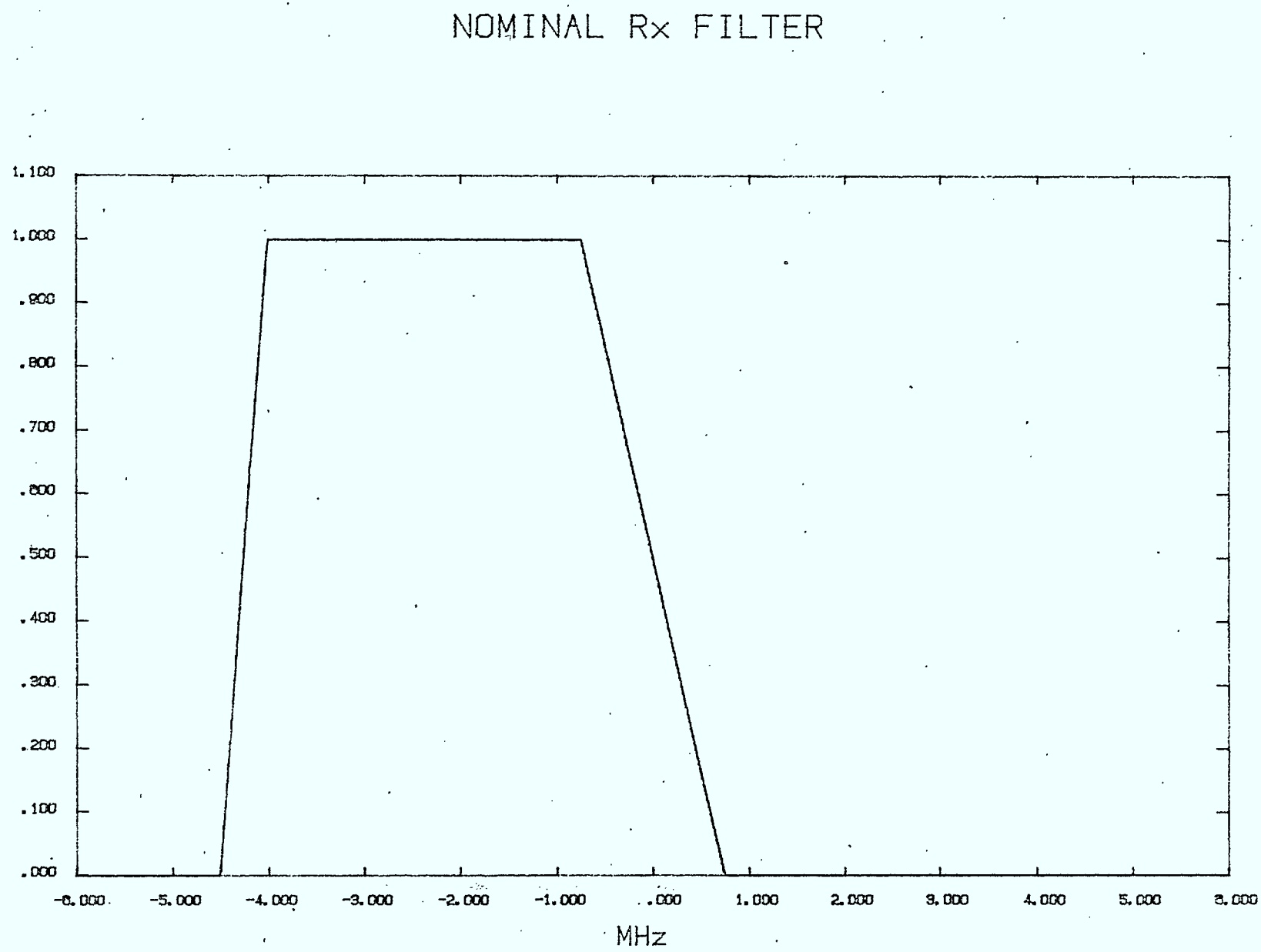

Figure 56 : Amplitude response of nominal receiver filter

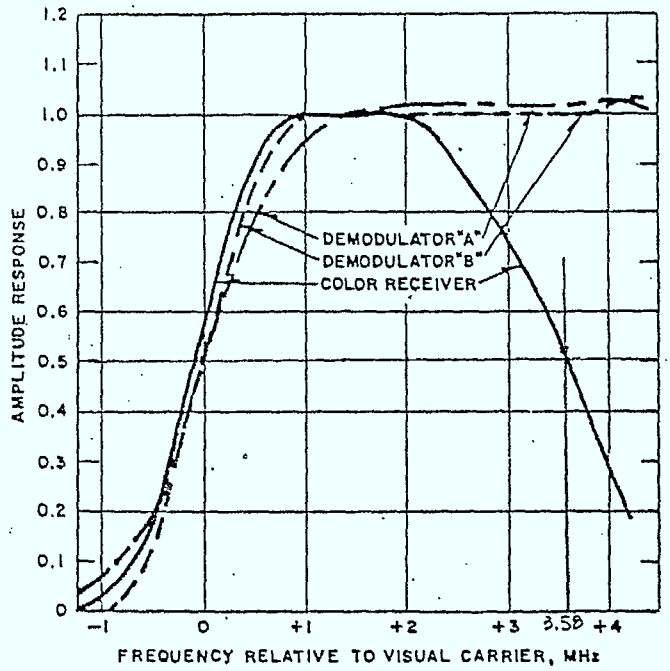

Figure 57 : Amplitude response of station demodulators and a colour home receiver [29]

the home receiver imposes a performance degradation for teletext, as intersymbol interference worsens (eye height is reduced) [3]. There is also the strong possibility that overshoots would increase with such a bandwidth reduction. Although there seems to be considerable data available on the amplitude responses of typical home receivers, there is not much available concerning the phase or group delay responses. A program that computes the phase response from the amplitude response, under the assumption that the transfer function is minimum phase, has been developed. Although it is planned to conduct runs with typical transmit and receive filter characteristics, baseline performance can be established using idealized responses. Performance with representative transmit and receive filter profiles will invariably be worse.

The simulated system presently employs synchronous detection, where carrier recovery is essentially perfect. Carrier recovery systems for synchronous detectors employ phase locked loop circuits with a relatively narrow bandwidth. However, most television receiver carrier recovery systems use phase locked loop circuits with a fairly wide loop bandwidth. This is made necessary by some television applications such as tracking phase variations produced by video game modulators or resulting from incidental phase modulation due to a poor television transmitter. The recovered carrier from the wideband loop is used to demodulate the receiver IF output to obtain a baseband video signal. This process is commonly referred to as "quasi synchronous" detection.

Phase offsets in the carrier recovery process result in quadrature distortion. This can introduce significant intersymbol interference, even though the overall ("inphase") pulse shape satisfies Nyquist's first criterion. This is because the quadrature component will

not in general satisfy Nyquist's first criterion and will not have zero crossings in the desired locations. It is apparent that a quasi-synchronous detector is likely to exhibit performance that is far from optimal. Incorporating quasi-synchronous detection, in order to assess the degree of degradation, is an important future objective.

The transmit pulse shape specified in [7] is a truncated (low-pass filtered) 100% raised cosine pulse. One of the major deficiencies is that there is no specification given for the critically important low pass filter, which will have a major impact on the attainable overshoot level. It seems that this lowpass filter, responsible for reducing interference with the sound channel, has a nominal 4.0 MHz bandwidth [34]. The characteristics of a commercially available, phase equalized 4 MHz lowpass filter [34] are shown in Figure 58, and have been incorporated in the pulse shaping process in the simulation. This "truncated" 100% raised cosine pulse is presently used in the Telidon system.

Establishing the baseline performance of the existing Telidon system is crucial for assessing coding objectives and assessing the need for system improvements such as "adaptive equalization, better synchronization techniques, and using an "optimized" transmit pulse shape. The performance of the relatively ideal system simulated (idealized filter profiles and carrier recovery) will provide an upper bound for actual system performance.

As has been mentioned earlier [15], the synchronization techniques employed presently in the Telidon system have many deficiencies. It is believed that the performance degradations imposed by non-ideal filter characteristics and quasi-synchronous carrier recovery are small compared

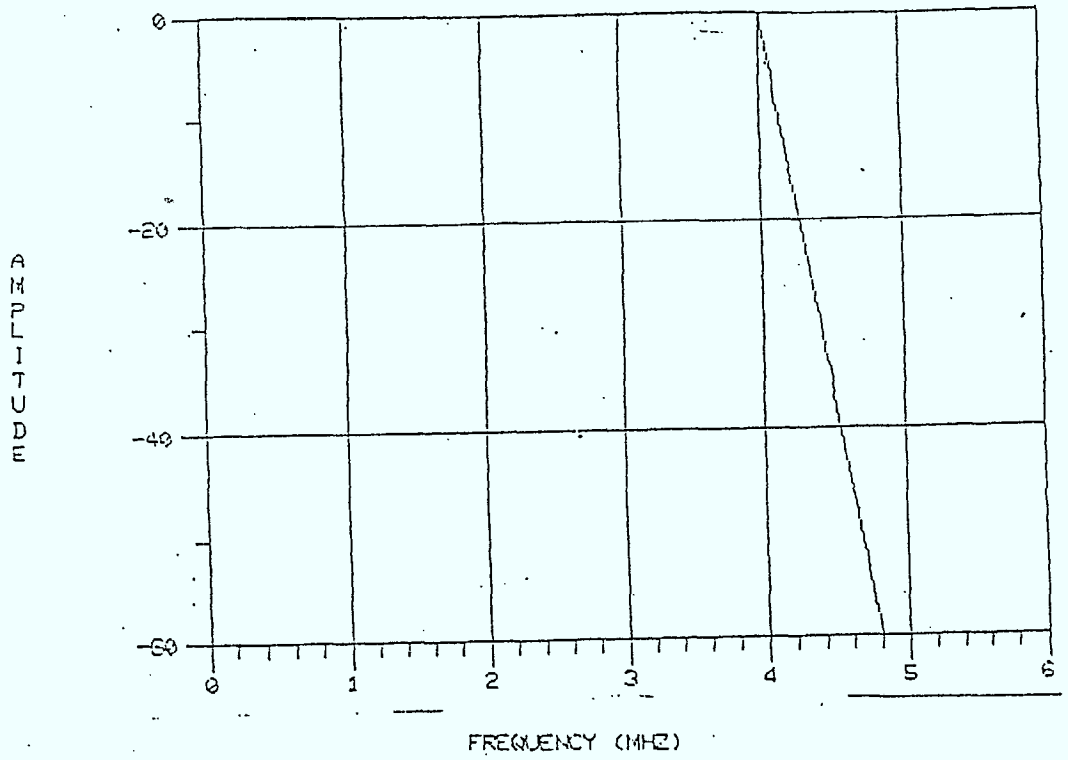

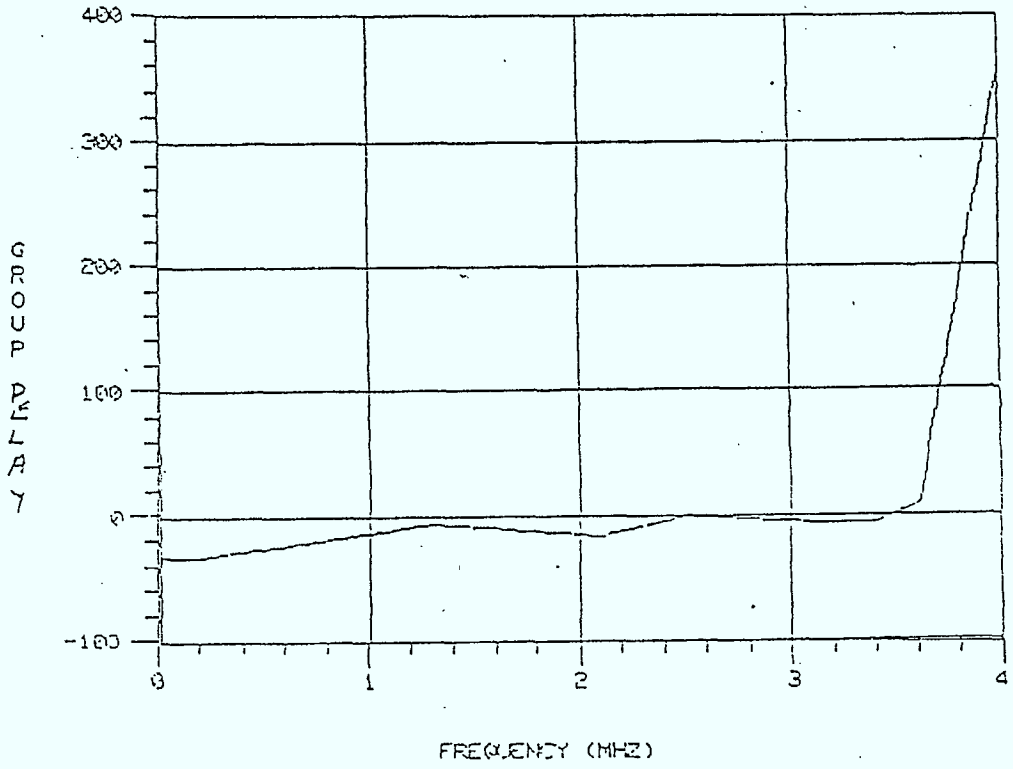

Figure 58 : Amplitude and Group Delay Responses of the 4 MHz Lowpass Filter Used In The MCS simulation

to those that can be attributed to these suboptimal synchronization techniques. Because such a significant performance degradation can be attributed to the weak slicing level and clock phase determination approaches, it is appropriate at this point to discuss some of these deficiencies. The approach presently employed in the Telidon system will be briefly described. For a more detailed discussion, see Section 3.3 of [15]. The present system uses the two byte clock sync signal to serially estimate the slicing level and clock phase. It first estimates the slicing level, using two peak detection circuits, one following the most positive signal excursions and the other, the least positive signal excursions. These peak detection circuits have a short charging time and a long decay time. The peak detector outputs are smoothed, and the slicing level taken to be midway between the two peak valves. Once the slicing level is established, the decoder uses a single zero crossing to choose one of five possible clock phases. There are several weaknesses in the procedure that can result in performance falling far short of optimum. Some of these problems are:

(1) The peak detector circuits are sensitive to noise peaks. Consequently, in impulse noise environments, loss of synchronization is likely when an impulse occurs during the portion of the clock sync signal preceding the freezing of the slicing level. An obvious improvement is to average or integrate (approximated by low pass filtering) the received signal to obtain an estimate of the slicing level. Averaging will clearly reduce the sensitivity to impulsive interference. Also, it is not difficult to show that for a data signal with equal numbers of ones and zeros, corrupted by white gaussian noise, that the maximum likelihood estimate of the dc level of the data signal is given by the average of the

received signal over the observation period. This averaging principle should be used in future decoders.

(2) Even relatively modest multipath can introduce significant error in the slicing level. This is because the signal level immediately preceding the clock sync signal is at the blanking level (0 IRE) and the average level during the clock sync signal is significantly different (roughly 36 IRE) [7], (see Figure 59). Consequently any multipath propagation will result in an apparent shift in level for a duration corresponding to the multipath differential delay. The situation gets even worse when the delay spread is large enough that a delayed version of the sync pulse or the colour burst gets superimposed on the clock sync signal. The effects are clearly demonstrated in Figures 60 and 61. In Figure 60, we have a filtered version of a portion of the teletext line received under ideal conditions. In Figure 61, the clock sync signal illustrated was received over a multipath channel with a single -6 dB positive echo with a delay spread of 5μsec. The corrupting effect of the sync pulse is evident during the early segment, and the superposition of the colour burst introduces some overshoots and undershoots.

In multipath environments, the slicing level determined by an averaging slicer will also be in error, but is likely to outperform the present technique simply because it is much less peak sensitive. Note that if the slicing level were determined later in the burst (at a time exceeding the largest multipath spread), a better estimate of the dc level would be obtained. As a result, a system that does not freeze the slicing level, but

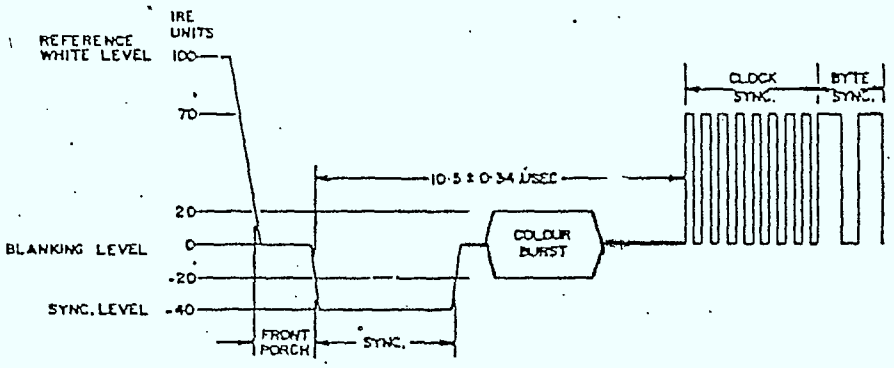

Figure 59 : Inserted Teletext Signal [7]

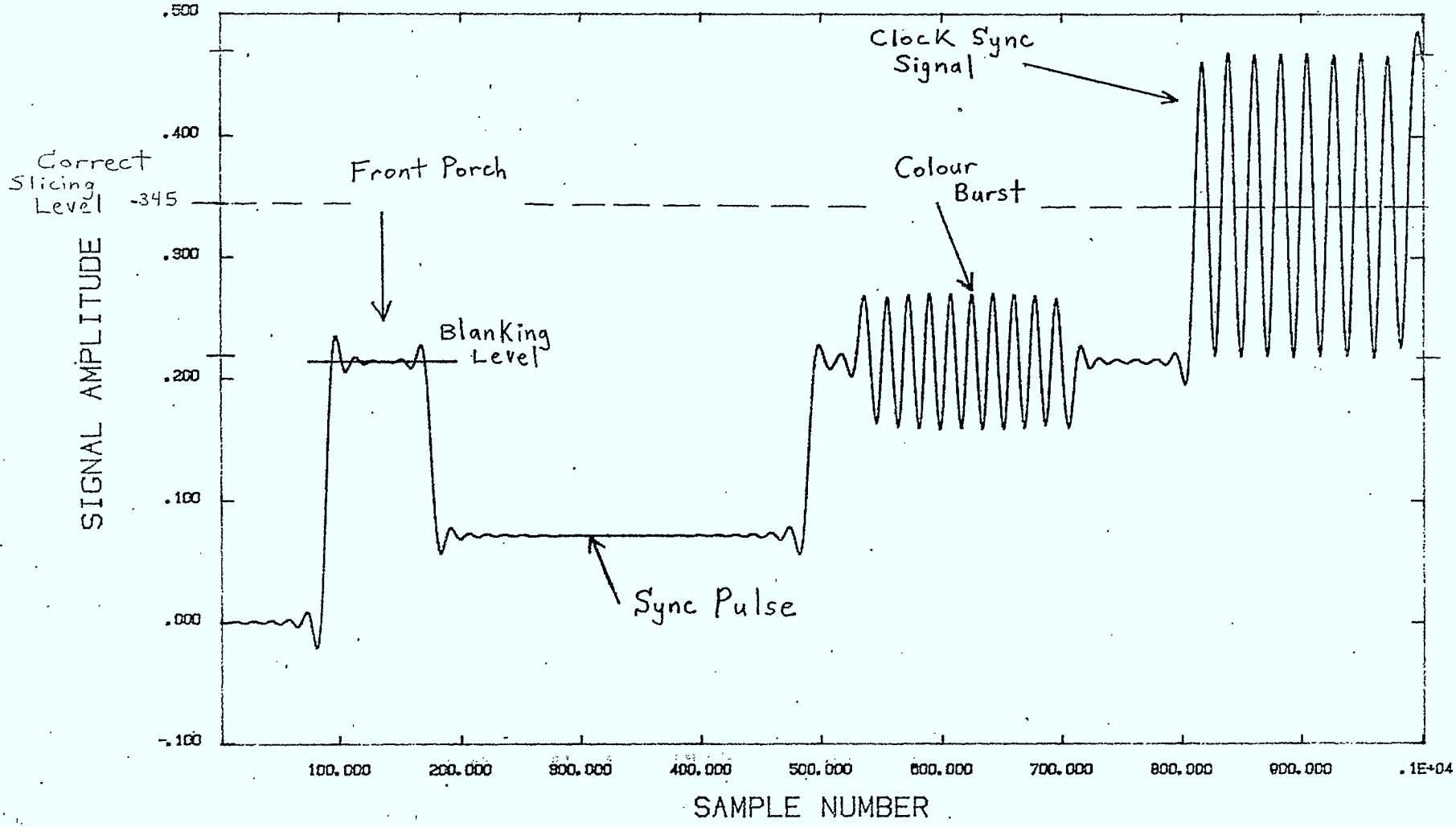

Figure 60 : Filtered Received Teletext Line

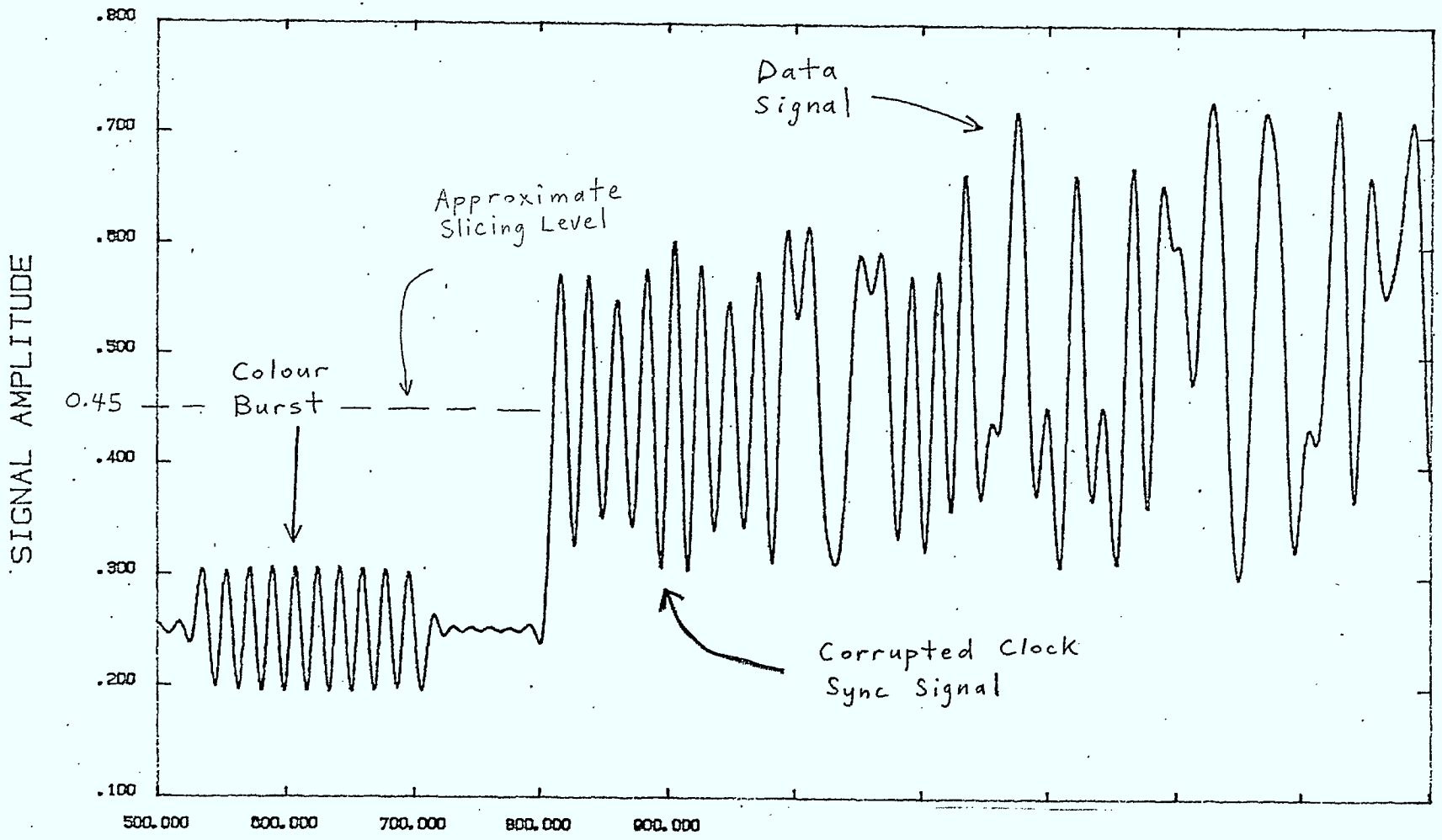

Figure 61 : Received Clock Sync Signal over A Multipath Channel With A Single -6 dB Positive Echo. With Delay Spread of 5 μsec.

tracks it along the burst, would have superior performance. Because the data burst can itself introduce a dc component (i.e. there is no guarantee or protection against a long string of bits with the same polarity), adaptive slicing level determination ideally must be decision directed. This requirement severely impacts implementation and circuit complexity.

(3) The optimum slicing level may be time varying due to time varying phase errors in the recovered carrier. This is further evidence that adaptive slicing level circuitry may be required.

Some serious problems exist with the technique presently used to estimate clock phase. These are:

(1) An error in slicing level results in an error in clock phase. There is really no reason why bit timing recovery should be so dependent on the slicing level estimation. They are clearly independent problems and should be treated as such. Consequently, in the next decoder phase, a parallel as opposed to serial synchronization technique should be designed.

(2) The sampling clock phase is estimated from only a single zero crossing, and will tend to be very sensitive to noise and other interference.

A recommended improvement for symbol synchronization, which is closely related to the cross-correlation time delay estimation technique (which is optimal in white gaussian noise), is presented in Section 5 of Appendix I. Time does not permit the implementation of such improvements to the synchronization procedure in the simulation program.

An improved version of the existing decoder that estimates the slicing level by averaging rather than using peak detection circuits, but still uses the inferior timing recovery technique, has been implemented.

3.1 Simulation Validation

To validate the simulation, a 30% raised cosine pulse shape was used with an ideal (no multipath) white gaussian noise channel. In this case Nyguist's first criterion is satisfied. Consequently, the theoretical performance bound (which requires ideal slicing level determination and ideal bit timing recovery to achieve) is given by:

$$p_e = Q(\sqrt{SNR_o})$$

where $SNR_o = \frac{d^2}{\sigma_o^2}$

d = the deterministic amplitude at the optimum sampling instant

σ_o^2 = the output noise variance

$$Q(\alpha) = \int_{\alpha}^{\infty} \frac{1}{\sqrt{2\pi}} e^{-t^2/2}\, dt$$

The interrelationships between the TV signal to noise ratio (SNR_{TV}) and SNR_o are discussed in detail in Appendix VII of [15].

The simulated performance with ideal recovery is presented in Figure 62. Close agreement with theoretical performance is observed. Also shown in Figure 62 is the performance

-97-

FIG 62 : BIT ERROR RATE vs SNR_{TV} FOR RC30

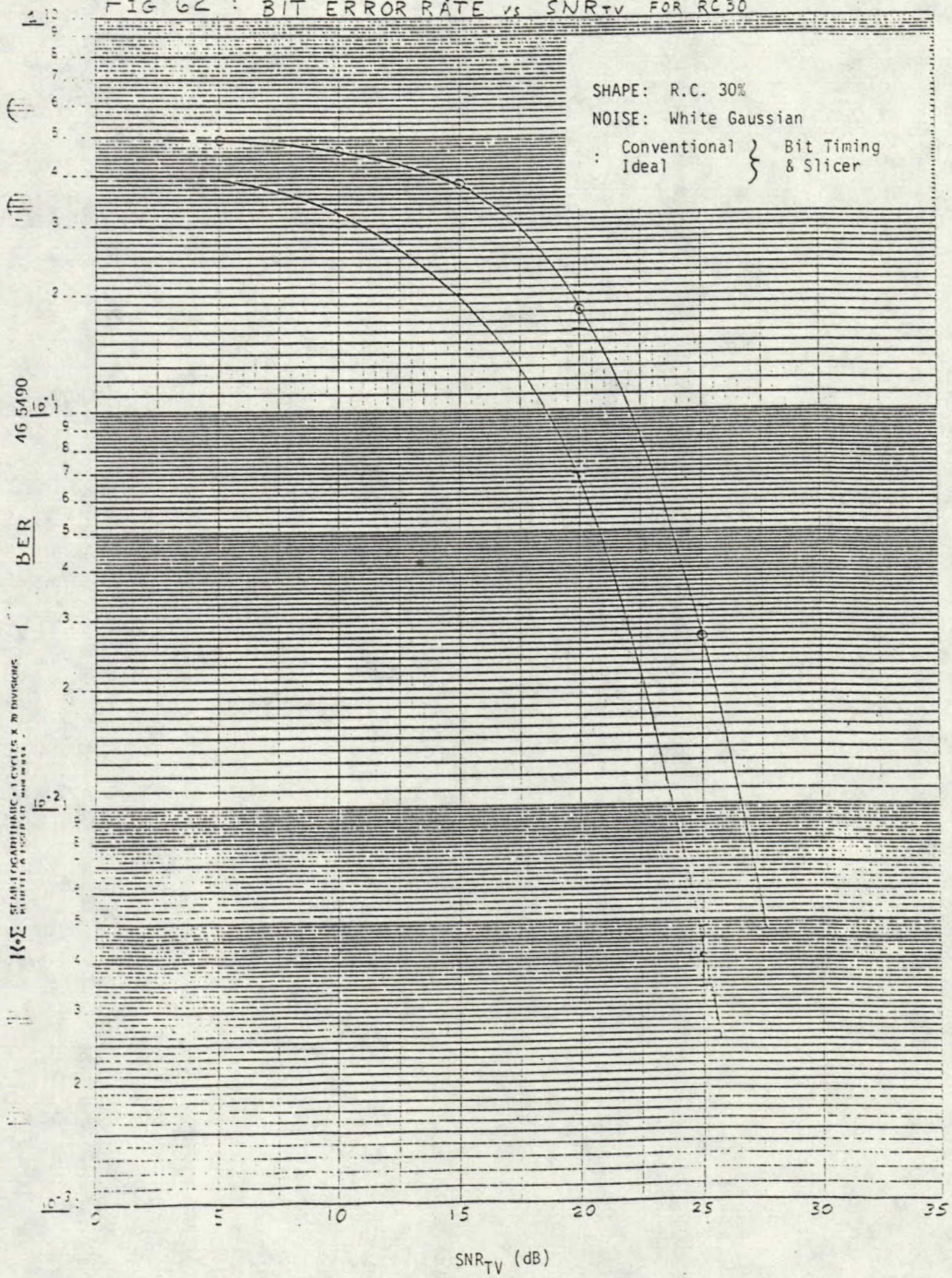

using the existing recovery procedure. The existing recovery procedure used in the Telidon system will be referred to as "conventional" on figures displaying performance. Over the signal to noise ratio region investigated, roughly a 3dB loss can be attributed to the present synchronization techniques of the Telidon system.

A comparison of the performance of the decoder presently used and an ideal decoder, for a low-pass filtered 100% raised cosine transmit pulse shape (the BS-14 specified pulse shape [7]) with an ideal white gaussian noise channel is provided in Figure 63. A 3dB performance degradation is evident. Also, note that the performance with the 100% raised cosine pulse is not very different than that obtained with a 30% raised cosine pulse.

3.2 Comparison of Performance in Various Noise Environments

In this section the performance of the baseline Telidon system is examined in various impulse noise environments, white gaussian noise environments and mixtures of impulse and white gaussian noise environments. The video signal to noise ratios used in the simulation are weighted (see Appendix VII of [15] for details). The best relationship between television picture quality and video S/N for random noise is provided by the Television Allocation Study Organization (TASO) rating [6], [25]. The video signal to noise ratios required to provide specific TASO grades are illustrated in Table 7. These TASO SNR's are unweighted [6], [25]. However, it is becoming customary to specify weighted SNR's, because in this case, subjective performance is independent of the random noise spectral characteristics [26], [27]. The unweighted video SNR's for the TASO grades are referenced to white (thermal) baseband noise. To convert these to weighted SNR's one must add a weighting factor of 6.1 dB [26], [27]. In [23], the subjective picture quality versus video S/N provided is:

FIG 63 : BIT ERROR RATE vs. SNR_{TV} FOR RC 100

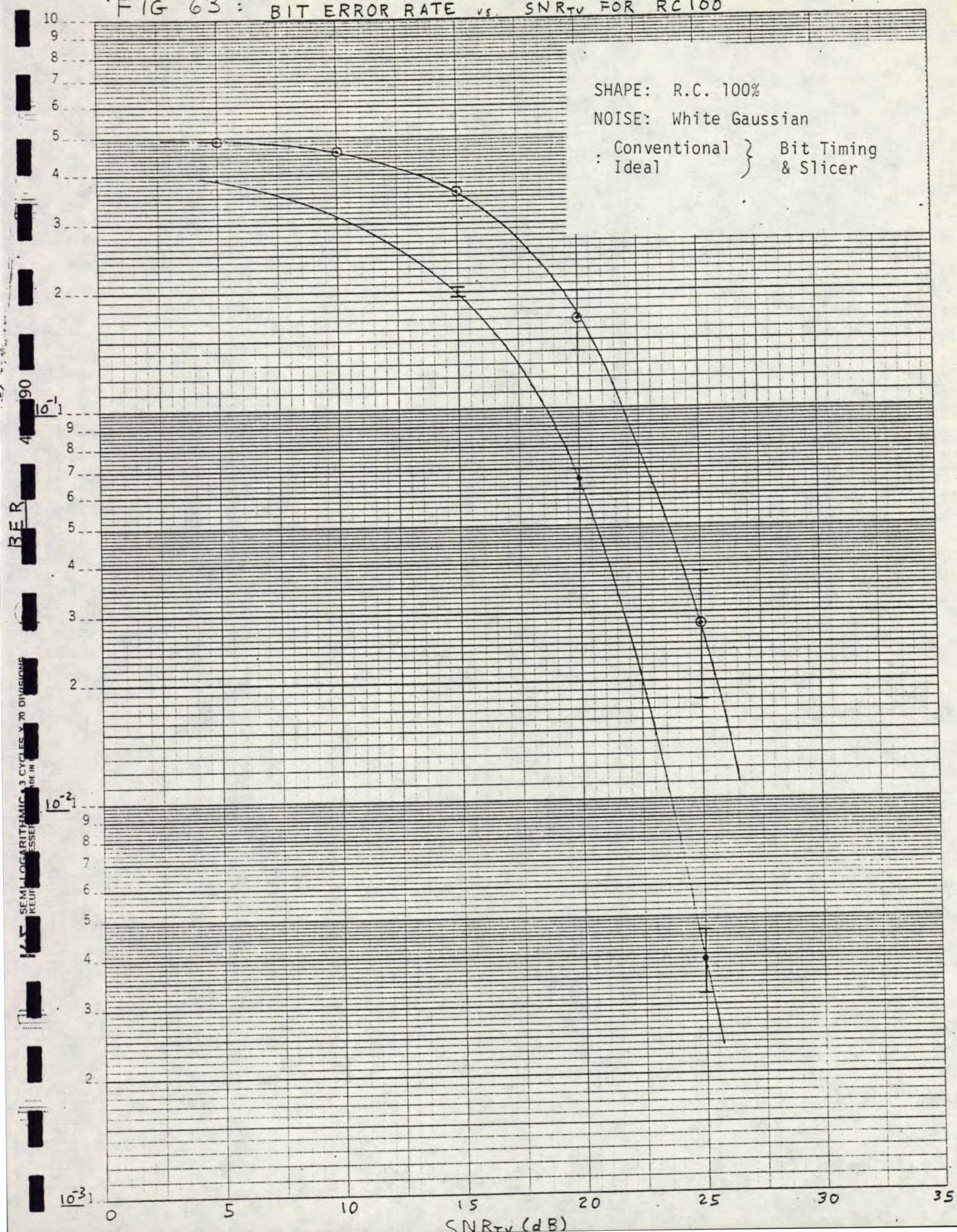

TASO Grade	Unweighted Video SNR (dB)	Weighted Video SNR (dB)
Excellent	42	48.1
Fine	33	39.1
Passable	27	33.1
Marginal	23	29.1
Inferior	16	22.1

Table 7: TASO grades versus video S/N

Unweighted Video S/N [dB]	Subjective Picture Quality
12	Bad
18	Poor
24	Fair

Although not explicitly stated, these values are likely unweighted (they agree well with the TASO assessment of picture quality). From Table 7, the weighted SNR region of greatest interest is between 25-36 dB, where acceptable but not exceptionally good video grades are obtained.

The impulse noise process implemented has Poisson arrivals at rate λ. The impulse amplitudes can have either a generalized Rayleigh distribution with parameter α, i.e.:

$$f_u(u) = \frac{\alpha}{2R_o^{\alpha}} u^{\alpha-1} \exp\{\frac{-u^{\alpha}}{2R_o^{\alpha}}\}$$

where $0 \leq \alpha \leq 2$ and $u \geq 0$,

or a log-normal distribution, i.e.

$$f_u(u) = \frac{1}{\sqrt{2\pi}\ \sigma\ u} \exp\{-\frac{1}{2}\ (\frac{\ell n\ u}{\sigma})^2\}$$

where $u \geq 0$. The parameters R_o and σ in the two distributions above must be selected to provide the desired impulse noise power [15]. Video signal power to noise

power ratios are not appropriate for assessing subjective picture quality. As discussed in [26], in impulse noise environments, the signal to noise ratio most commonly used is the peak-to-peak amplitude of the picture signal to the peak-to-peak amplitude of the noise. For transmission systems, the threshold SNR for impulsive noise is 11 dB [26]. Unfortunately, this is not related to subjective picture quality at the receiver. Furthermore, for realistic impulse arrival rates of 3,000 to 30,000 per sec (justification provided in Appendix IX of reference [15]), and for video SNR's as great as 45 dB, the peak SNR will be in the neighbourhood of the above mentioned 11 dB threshold. As a result, the peak SNR used for assessing transmission systems is not really appropriate. Although not complete at this time, an approach for assessing the threshold impulse arrival rate and video S/N for acceptable picture quality is being derived. It is based on a perceived percentage of the picture that can be corrupted by impulses, and still yield a useable picture.

To characterize performance, five runs were conducted at TV signal to noise ratios of 25 dB, 29 dB, 33 dB, and 45 dB, with an ideal channel, nominal transmitter and receiver filters, using the truncated 100% raised cosine pulse shape. The noise types considered are summarized below:

Noise Type	Impulse Arrival Rate λ (per sec)	Impulse Amplitude Distribution
Impulse	30,000	Rayleigh (α=1)
Impulse	30,000	Rayleigh (α=2)
Impulse	30,000	Log-Normal
Impulse	3,000	Rayleigh (α=2)
50/50 Mixture of White Gaussian and Impulse	30,000	Rayleigh (α=2)
White Gaussian	--	--

Performance was investigated for both the present decoder employed in the Telidon system (referred to as the "conventional" decoder throughout the remainder of this report), and an improved version which uses an averaging slicer.

The results for the conventional decoder are shown in Figure 64. Several interesting observations can be made. In impulse noise, performance is strongly dependent on the impulse arrival rate, λ. At low SNR_{TV} there is close to an order of magnitude difference in error rate for λ=3,000 compared to λ=30,000. This is expected, however, because each impulse is likely to cause an error at either of the above impulse arrival rates, and there is an order of magnitude difference in arrival rate. As the SNR_{TV} increases, the power in each impulse decreases, and is an order of magnitude less for λ=30,000. Consequently, there is less than an order of magnitude difference in error rate at SNR_{TV} = 30 dB and 35 dB. In fact, in the neighbourhood of 45 dB, the performance curves cross-over, and performance is worse with λ=3,000. This behaviour is exactly what one would expect at high SNR_{TV} because there is more power concentrated in the impulses with λ=3,000. With the same impulse arrival rate (λ=30,000) it is noted that there is little difference in performance with impulse amplitude distributions belonging to the generalized Rayleigh family (α=1 and α=2). However, performance is noticeably better with the log-normal amplitude distribution. This is not surprising either, because the log-normal distribution tends to have a greater proportion of smaller amplitudes than does the Rayleigh distribution for the range of impulse noise powers considered (see Appendix IV for details). The performance with Gaussian noise is considerably better than that for impulse noise for $SNR_{TV} \geq 29$ dB. The performance crossover at roughly SNR_{TV} = 25 dB is not unexpected, and is due to the rather

Figure 64: Performance of the Conventional Decoder With an Ideal Channel In Various Noise Environments.

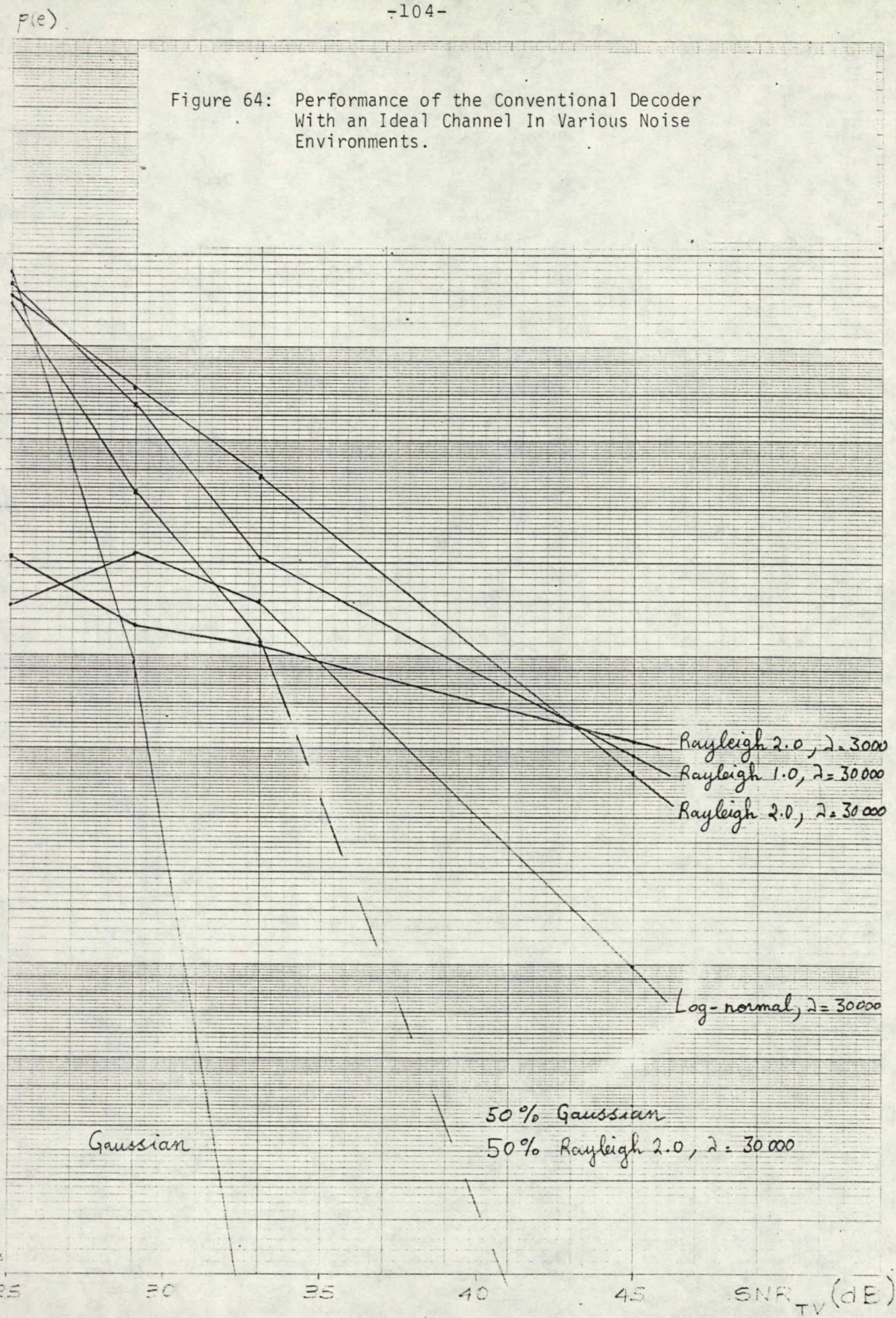

infrequent occurrance of impulses compared to the significant, ever present thermal noise. Note also that the 50/50 mixture of gaussian and impulse noise results in a considerable performance degradation relative to thermal noise environments, but performance is considerably better than it is in impulse noise environments. It is apparent that in strong impulse noise environments, the SNR_{TV} must be in the neighbourhood of 40 dB to provide bit error rates less than 1×10^{-3}, which is not exceptional performance.

The performance using the averaging slicer decoder is presented in Figure 65. A rather significant improvement in performance is apparent. In impulse noise, bit error rates less than 1×10^{-3} can be achieved for SNR_{TV}'s exceeding 36 dB, which corresponds roughly to a 4 dB improvement. This is not at all unexpected, and is the result of the decreased peak sensitivity of averaging slicer. Note also that there is not as much difference between the performance obtained with the log-normal and Rayleigh impulse amplitude distributions, although, as anticipated, performance is better with the log-normal distribution. With the gaussian and impulse noise mix, performance at lower SNR_{TV}'s is somewhat better with the averaging slicer. With regards to impulse noise the same fundamental trends hold, and there is a significant degradation relative to thermal noise. In gaussian noise the averaging slicer decoder also outperforms the conventional decoder. To allow a better comparison, the number of runs conducted at each signal to noise ratio was increased to ten. The performance results are summarized in Figure 66. Error bars on the averaging slicer results are provided to give an indication on the variability. The averaging slicer decoder provides a significant performance improvement (roughly 2 dB in the 30-33 dB video signal to noise ratio region).

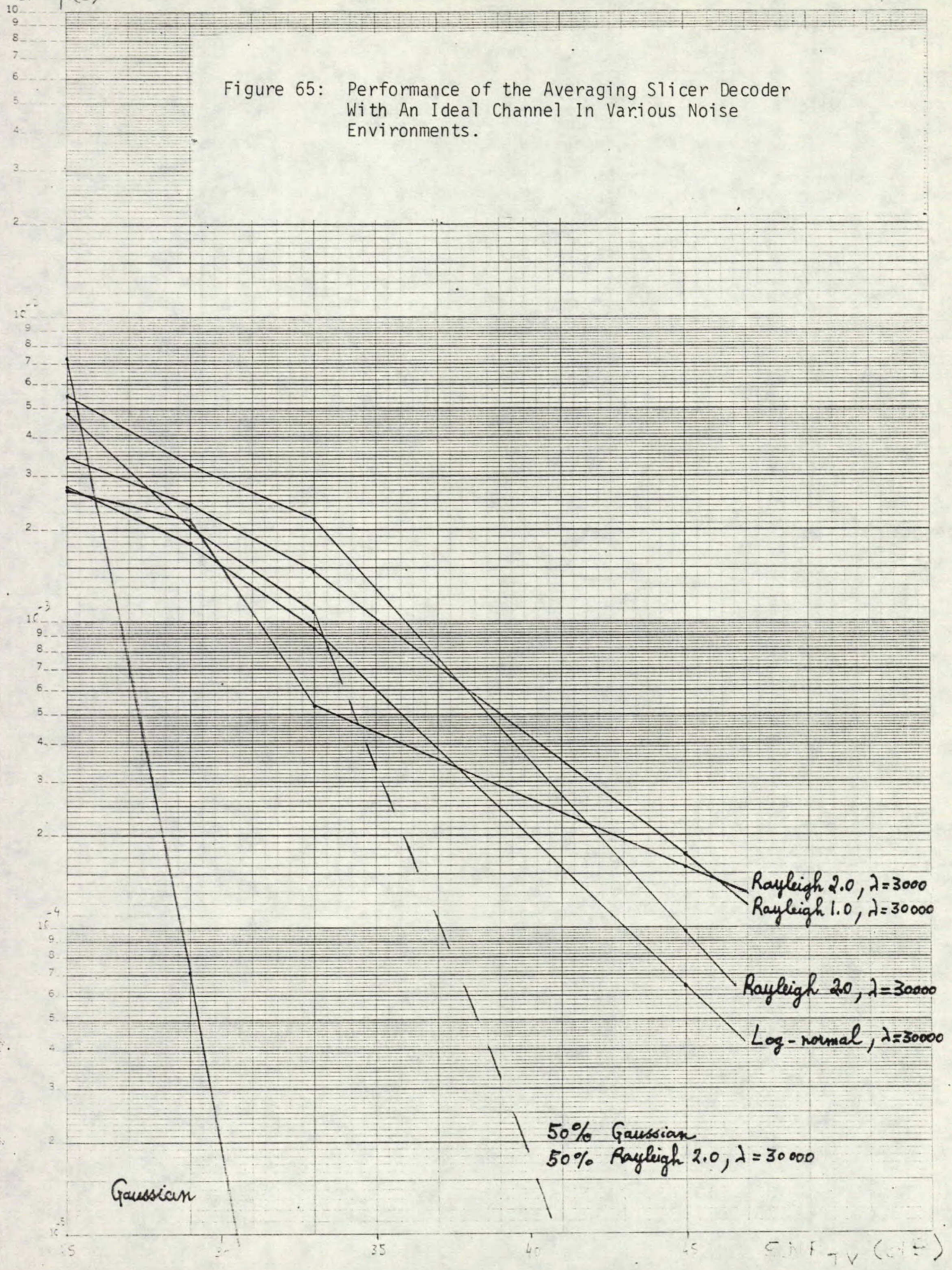

Figure 65: Performance of the Averaging Slicer Decoder With An Ideal Channel In Various Noise Environments.

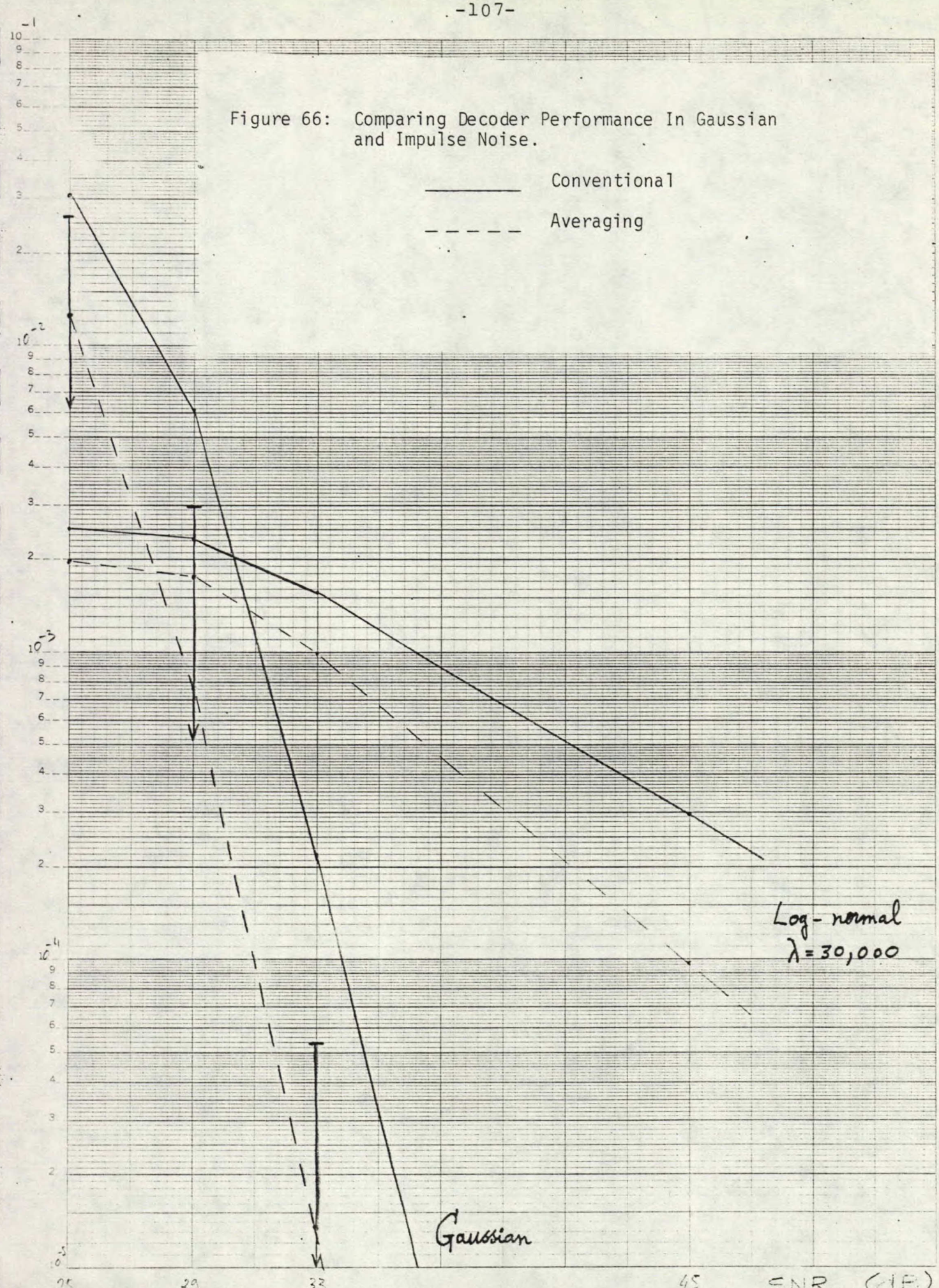

Figure 66: Comparing Decoder Performance In Gaussian and Impulse Noise.

3.3 Characterizing Performance In Multipath Environments

When characterizing system performance in multipath environments, attention must be restricted to the subset of channels which provide acceptable video quality. There is absolutely no need attempting to provide Broadcast Telidon service to customers that cannot receive useful television pictures over the air. A procedure for estimating the subjective picture quality of a multipath channel is presented in Section 2.1 and discussed in detail in Appendix II. This technique uses a perceived DU ratio which is essentially a signal to clutter ratio that takes into account the delay spread influence. Close in echoes are much less annoying than similar strength ghosts with longer delays. As an example, a PDUR of 13 dB implies an annoying but usable picture (taken as the acceptability threshold for assessing Telidon System performance). A PDUR of 20 dB corresponds to noticeable but only somewhat annoying echoes. It must be emphasized that acceptable video quality does not guarantee acceptable teletext performance.

The multipath simulation program was used to generate impulse response files, defined by a vector of delays and magnitudes. These impulse responses were generated with the parameters (average reflector area, and reflector density) that provided the best match to the measured impulse responses obtained in the Ottawa area. The multipath channel subroutine uses this impulse response file, and creates a frequency domain sampled version of the channel frequency response:

$$C(f) = 1 + \sum_{i=1}^{N} m_i e^{j\phi_i} e^{-j2\pi f d_i}$$

where ϕ_i is the random phase $[-\pi,\pi]$ assigned to each path

m_i is the relative magnitude associated with the i-th echo path

d_i is the relative delay associated with the i-th echo path

N is the number of reflectors (echo paths) comprising the impulse response

A plot of dominant paths of the channel impulse responses that were used are provided in Figures 67, 68, 69, and have PDUR's of 13 dB, 14 dB, and 20 dB respectively. As has been mentioned earlier, multipath components can distort the clock sync portion of the teletext signal by superimposing delayed and attenuated versions of the signal preceding the teletext data (i.e. blanking level, colour burst, and sync tips). The degree of slicing level error is a strong function of the phase assigned to the dominant echoes. For example, quadrature echoes (ϕ = 90° or 270°) are much less serious than inphase echoes (ϕ = 0° or 180°).

To restrict ourselves to a manageable number of simulation runs, we considered only the three multipath channels mentioned above. To characterize performance for each channel, we conducted 5 different runs, selecting different echo phases each time, and repeated the same runs for different signal to noise ratios and decoder models. Selecting different echo phases on each run is equivalent to selecting a different channel, although one with the same delay spread and echo magnitudes. Due to the impact

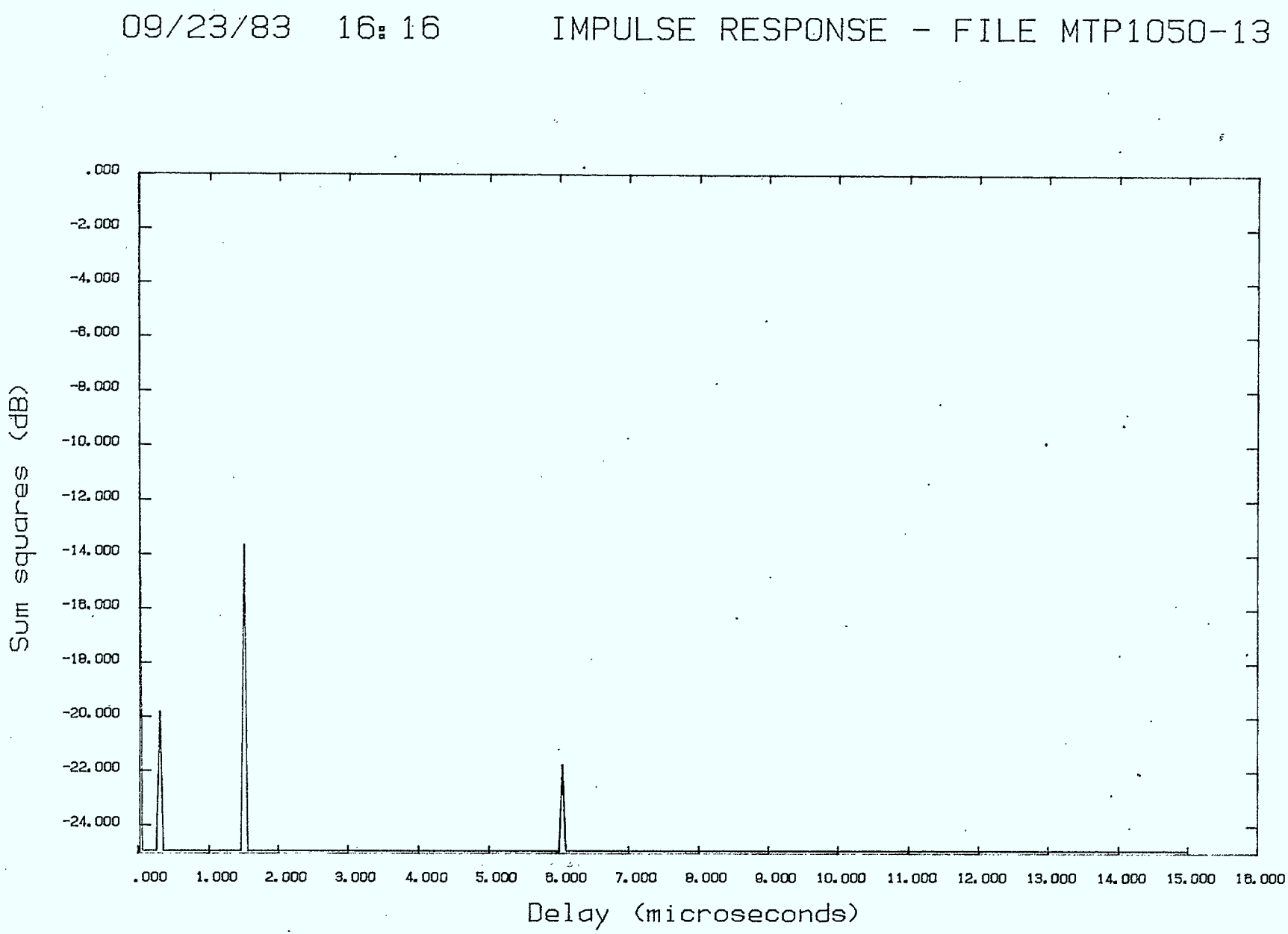

Figure 67 : Dominant Echoes Of Multipath Channel With PDUR = 13 dB

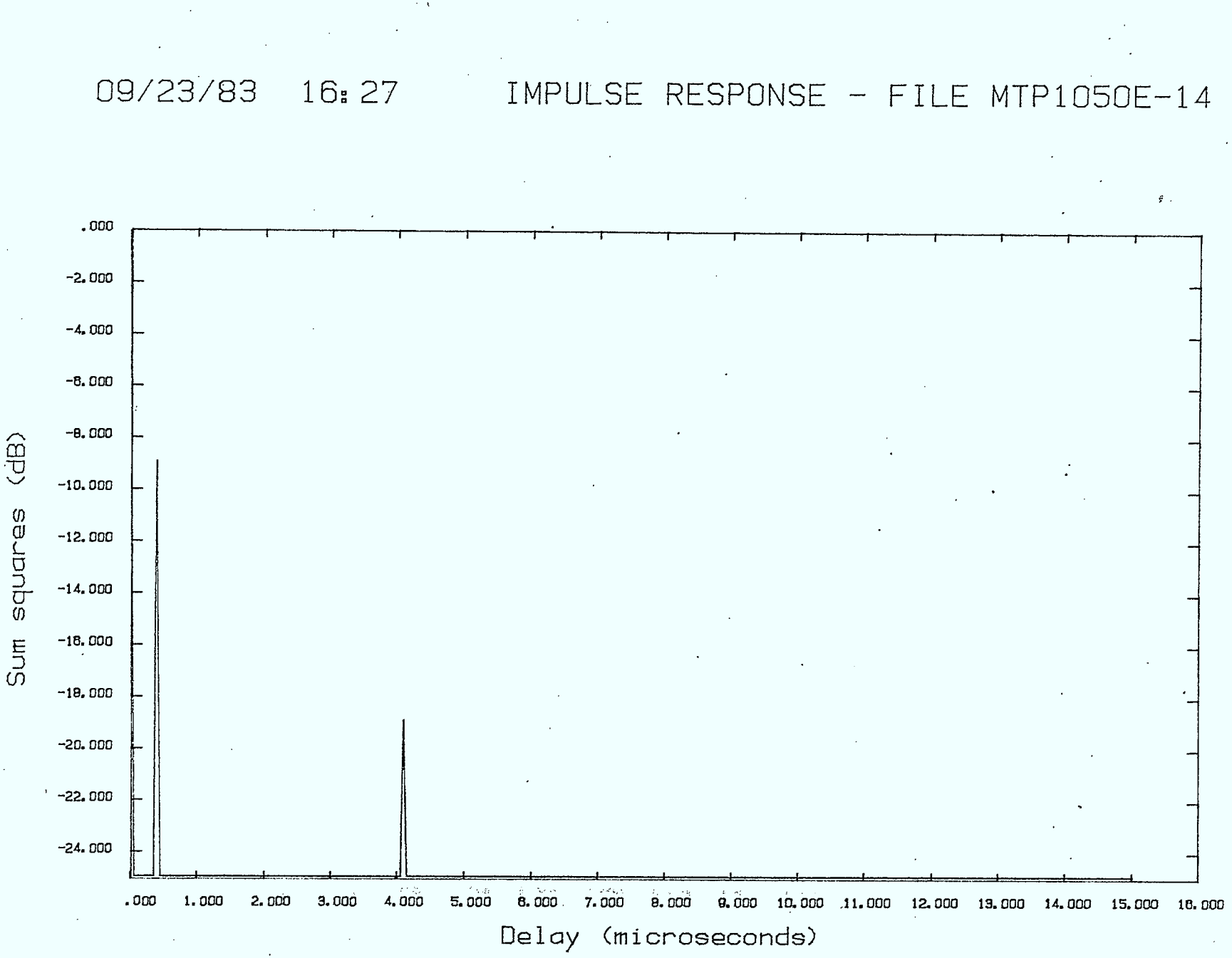

Figure 68 : Dominant Echoes Of Multipath Channel With PDUR = 14 dB

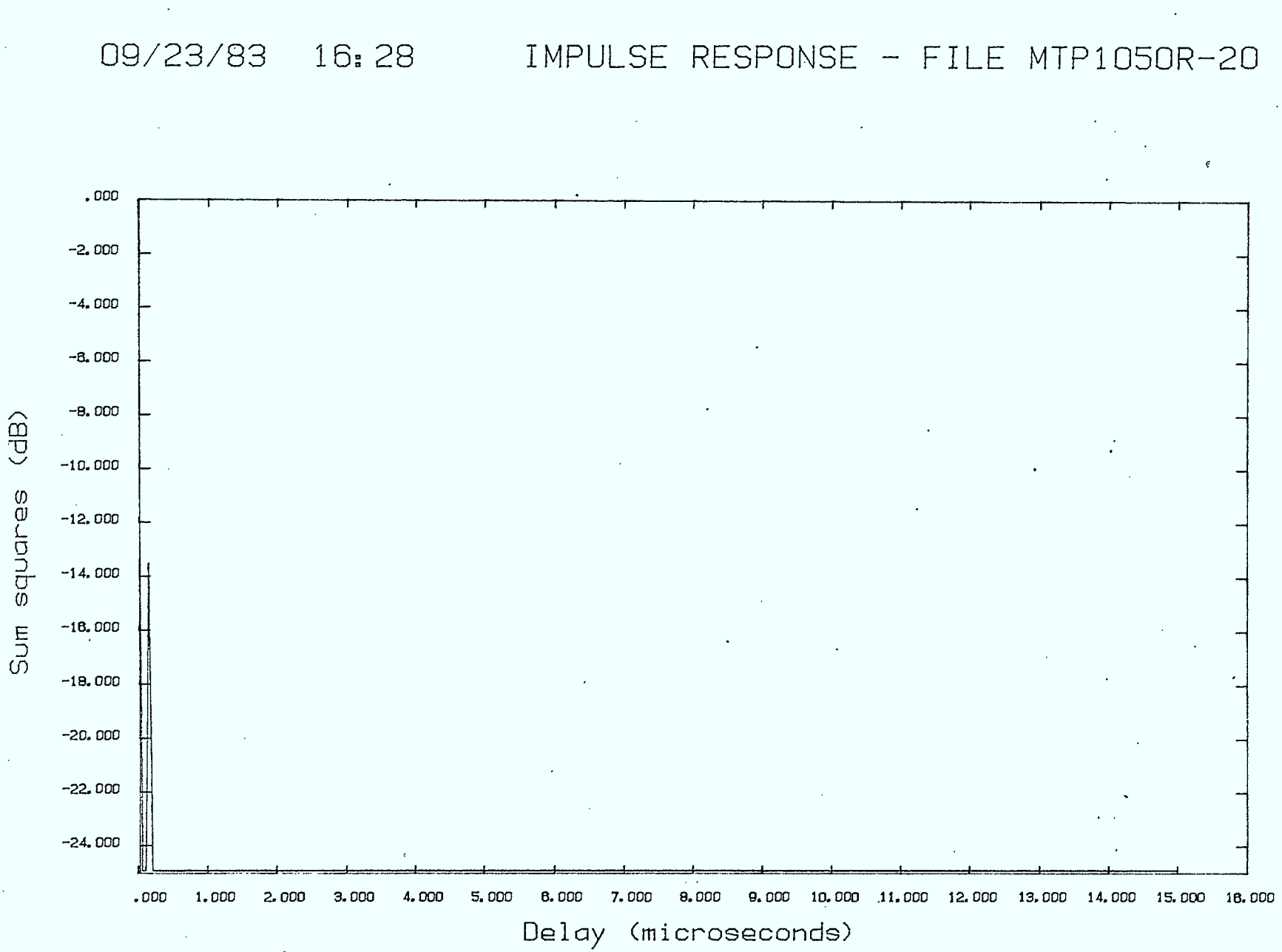

Figure 69 : Dominant Echoes of Multipath Channel With PDUR = 20 dB

of channel variation on slicing level error (different phases being assigned to the echoes), significant variation in the output results is observed from run to run (see Tables 8 and 9). However, on the graphs summarizing performance, only the mean performance over the ensemble of 5 runs (channels) is supplied. Error bars are not included because they would spoil the clarity and add little of value.

Performance of the conventional and averaging slicer decoders has been determined with the above mentioned multipath channels in white gaussian noise and "impulse and gaussian noise" mixtures. Determining the appropriate mix of impulse and thermal noise is hampered by the lack of measurement data. The other problem is that, in practice, it would be so variable and dependent on measurement sites (similar to the multipath channel variability problem) that any choice is likely to valid somewhere, at some time. However, to reduce the degrees of freedom somewhat, a fixed value has been selected using Figure 70 [30]. AT 200 MHz, urban man-made noise is roughly 24 dB (251.2 times) stronger than typical thermal noise. Suburban man-made noise is roughly 10 dB worse than thermal noise. Taking an average yields impulse noise being 21 dB (125.89 times) greater than typical receiver noise. This is the value we used for the ratio of impulse to gaussian noise, and we assumed that the impulse amplitude distribution was truly Rayleigh ($\alpha = 2.0$). We conducted runs with $\lambda = 30{,}000$ and $\lambda = 3{,}000$, using both the conventional and averaging slicer decoder models.

The average bit error rate performance for the multipath channel shown in Figure 67, with PDUR = 13 dB, in a white gaussian noise environment, is summarized in Figure 71. The performance of both decoder models for an ideal white

Multipath Delay (μsec)	Amplitude	Phase (deg)
0.0424	0.0825	- 84.2
0.411	0.331	- 17.8
4.125	0.105	- 74.7

Averaging Slicer Decoder

RAW BIT ERROR RATE, BASED ON 40 + 224 = 264 BITS/PACKET:	.3787879E-03
PROB (1 MISSED ERROR IN 5 PREFIX BYTES, NO ERROR DETECTION):	0.000000
PROB (MORE THAN 1 MISSED ERROR IN 5 PREFIX BYTES, NO ERROR DETECTION):	0.000000
PROB (AT LEAST 1 MISSED ERROR IN 33 PREFIX+HEADER BYTES, NO ERROR DETECTION):	0.000000
PROB (AT LEAST 1 ERROR DETECTED IN 5 PREFIX BYTES):	0.000000
PROB (AT LEAST 1 ERROR DETECTED IN 33 PREFIX+HEADER BYTES):	0.000000
PROB (PACKET REJECTED DUE TO PDI ERROR DETECTION) ,BASED ON 28 PDI/PACKET:	.7500000E-01
AVERAGE NUMBER OF POST-DECODER PDI ERRORS/PACKET, BASED ON 28 PDI/PACKET:	0.000000
NUMBER OF PACKETS LOST (PACKET LOST WHEN MORE THAN 30 % OF ERRORS):	0

Conventional Decoder

RAW BIT ERROR RATE, BASED ON 40 + 224 = 264 BITS/PACKET:	.2386364E-02
PROB (1 MISSED ERROR IN 5 PREFIX BYTES, NO ERROR DETECTION):	0.000000
PROB (MORE THAN 1 MISSED ERROR IN 5 PREFIX BYTES, NO ERROR DETECTION):	0.000000
PROB (AT LEAST 1 MISSED ERROR IN 33 PREFIX+HEADER BYTES, NO ERROR DETECTION):	0.000000
PROB (AT LEAST 1 ERROR DETECTED IN 5 PREFIX BYTES):	0.000000
PROB (AT LEAST 1 ERROR DETECTED IN 33 PREFIX+HEADER BYTES):	.5000000E-02
PROB (PACKET REJECTED DUE TO PDI ERROR DETECTION) ,BASED ON 28 PDI/PACKET:	.4150000
AVERAGE NUMBER OF POST-DECODER PDI ERRORS/PACKET, BASED ON 28 PDI/PACKET:	.1785714E-03
NUMBER OF PACKETS LOST (PACKET LOST WHEN MORE THAN 30 % OF ERRORS):	0

Table 8: Simulation Results With 14 dB PDUR Channel In Gaussian Noise.

Multipath Delay (μsec)	Amplitude	Phase (deg.)
0.0424	0.0825	- 23
0.411	0.331	- 70.3
4.125	0.105	77.8

Averaging Slicer Decoder

```
RAW BIT ERROR RATE, BASED ON 40 + 224 = 264 BITS/PACKET:                          .2670455E-02
PROB (1 MISSED ERROR IN 5 PREFIX BYTES, NO ERROR DETECTION):                      0.000000
PROB (MORE THAN 1 MISSED ERROR IN 5 PREFIX BYTES, NO ERROR DETECTION):            0.000000
PROB (AT LEAST 1 MISSED ERROR IN 33 PREFIX+HEADER BYTES, NO ERROR DETECTION):     0.000000
PROB (AT LEAST 1 ERROR DETECTED IN 5 PREFIX BYTES):                               .1500000E-01
PROB (AT LEAST 1 ERROR DETECTED IN 33 PREFIX+HEADER BYTES):                       .4350000
PROB (PACKET REJECTED DUE TO PDI ERROR DETECTION) ,BASED ON 28 PDI/PACKET:        .5357143E-03
AVERAGE NUMBER OF POST-DECODER PDI ERRORS/PACKET, BASED ON 28 PDI/PACKET:
NUMBER OF PACKETS LOST (PACKET LOST WHEN MORE THAN 30 % OF ERRORS):               0
```

Conventional Decoder

```
RAW BIT ERROR RATE, BASED ON 40 + 224 = 264 BITS/PACKET:                          .1062500E-01
PROB (1 MISSED ERROR IN 5 PREFIX BYTES, NO ERROR DETECTION):                      0.000000
PROB (MORE THAN 1 MISSED ERROR IN 5 PREFIX BYTES, NO ERROR DETECTION):            0.000000
PROB (AT LEAST 1 MISSED ERROR IN 33 PREFIX+HEADER BYTES, NO ERROR DETECTION):     0.000000
PROB (AT LEAST 1 ERROR DETECTED IN 5 PREFIX BYTES):                               .2000000E-01
PROB (AT LEAST 1 ERROR DETECTED IN 33 PREFIX+HEADER BYTES):                       .3500000E-01
PROB (PACKET REJECTED DUE TO PDI ERROR DETECTION) ,BASED ON 28 PDI/PACKET:        .7750000
AVERAGE NUMBER OF POST-DECODER PDI ERRORS/PACKET, BASED ON 28 PDI/PACKET:         0.000000
NUMBER OF PACKETS LOST (PACKET LOST WHEN MORE THAN 30 % OF ERRORS):               1
```

Table 9: Simulation Results With 14 dB PDUR Channel In Gaussian Noise

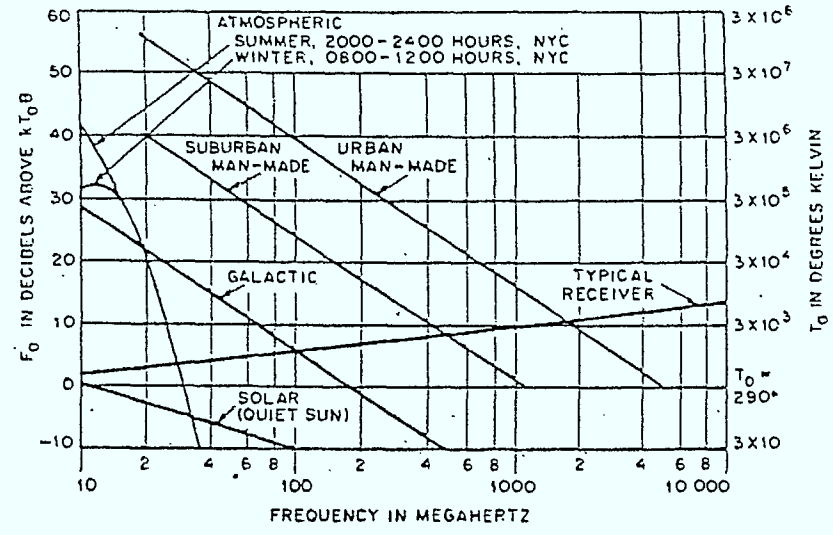

Figure 70 : Median values of average noise power expected from various sources. (after [30] p. 27-2)

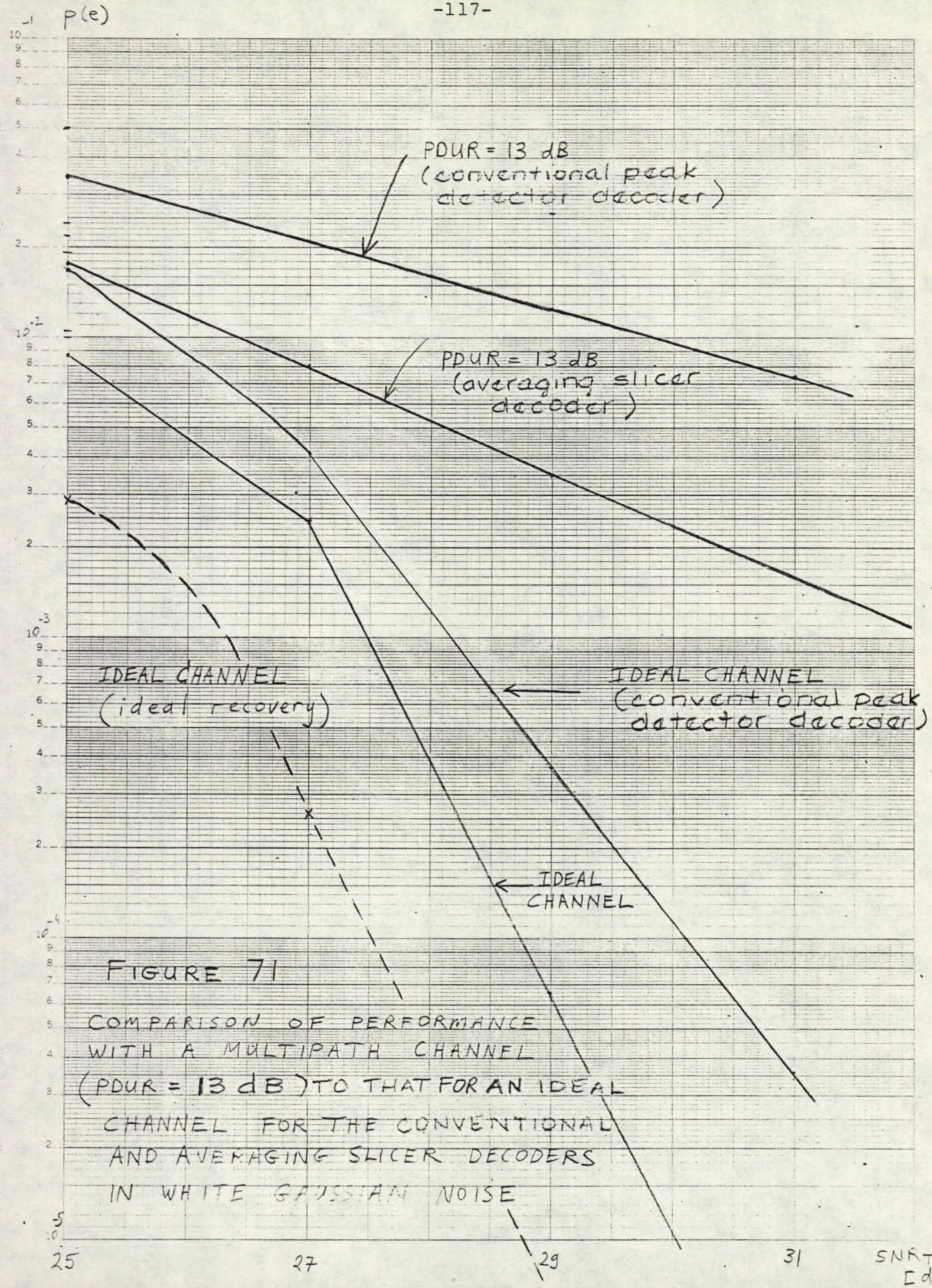

FIGURE 71

COMPARISON OF PERFORMANCE WITH A MULTIPATH CHANNEL (PDUR = 13 dB) TO THAT FOR AN IDEAL CHANNEL FOR THE CONVENTIONAL AND AVERAGING SLICER DECODERS IN WHITE GAUSSIAN NOISE

gaussian noise channel is also presented to provide an indication of the degradation imposed by multipath. It is apparent that the averaging slicer provides a significant average improvement in bit error rate relative to the conventional decoder (roughly 3.5 dB) in this multipath environment. It is also readily apparent that performance, with this multipath channel, is significantly worse than that obtained with an ideal channel, for both decoder models. For example, with an ideal channel at a weighted video S/N of 29 dB, which corresponds to a marginal TASO subjective assessment grade, error rates of 6.5×10^{-5} for the averaging slicer and 3.7×10^{-4} for the conventional decoder are obtained. This corresponds to fairly reasonable teletext performance. With the 13 dB PDUR multipath channel, the corresponding error rates are 3.5×10^{-3} for the averaging slicer and 1.25×10^{-2} for the conventional decoder, which is relatively poor performance. With an ideal channel, the conventional decoder is roughly 1 dB worse than the averaging slicer decoder over the signal to noise region examined. The performance curve for ideal recovery, with an ideal channel, for video S/N's between 25-29 dB is also shown on Figure 71. Note that for this signal to noise region, the degradation of the conventional decoder relative to ideal recovery is roughly 2.25 dB. The averaging slicer decoder is approximately 1.25 dB worse than ideal recovery, indicating that there is still an appreciable performance gain to be exploited. Improving the clock phase recovery procedure of the Telidon system is the next logical step.

Performance of the two decoder models with the 13 dB PDUR channel in a mixture of impulse and gaussian noise (impulse noise has Rayleigh amplitude distribution) is summarized in Figure 72. The superiority of the averaging slicing level decoder is clearly evident. In fact, the performance of the averaging slicing level decoder, for the high impulse arrival rate ($\lambda = 30{,}000$), is very similar to that

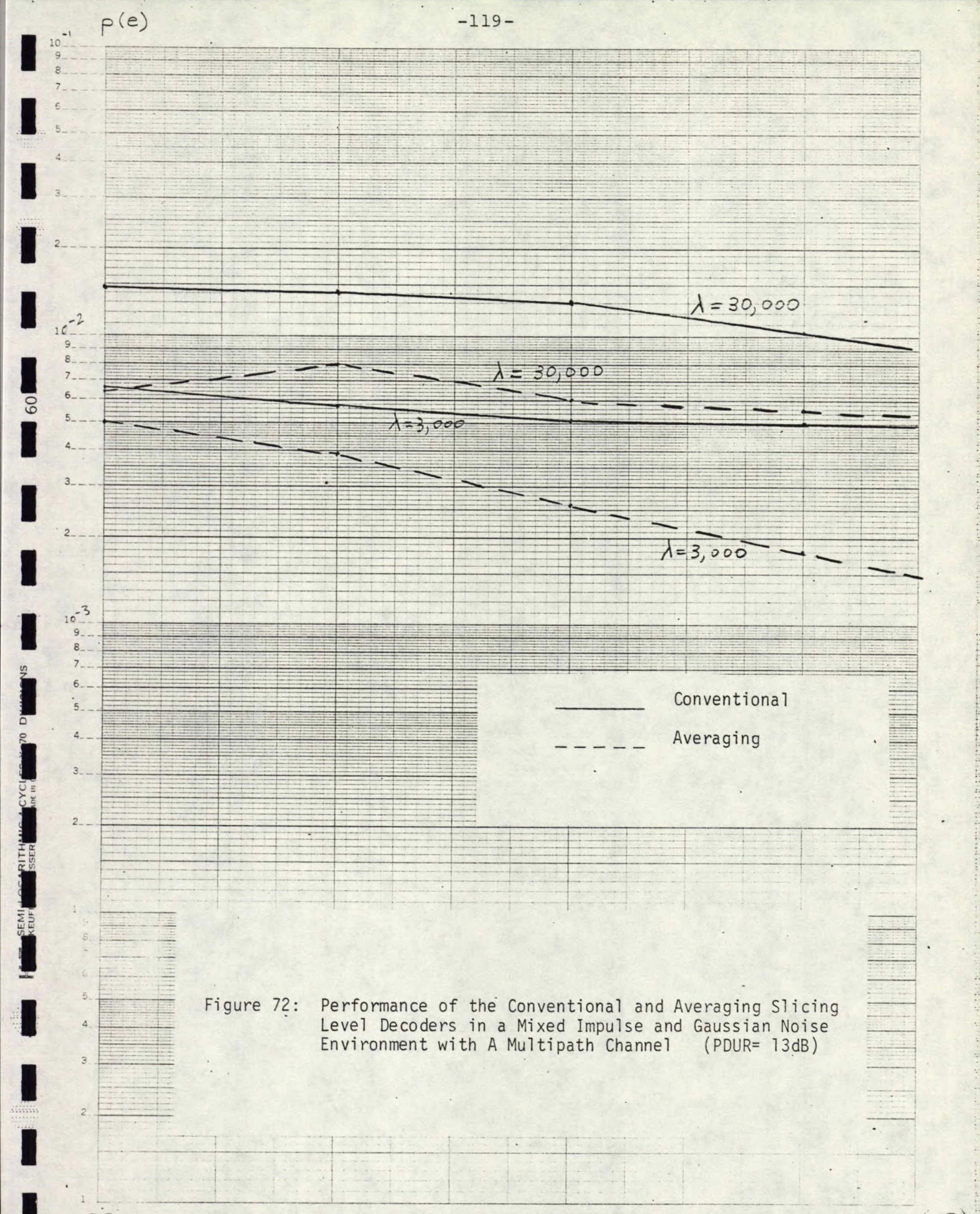

Figure 72: Performance of the Conventional and Averaging Slicing Level Decoders in a Mixed Impulse and Gaussian Noise Environment with A Multipath Channel (PDUR= 13dB)

achieved with the conventional decoder, for a much less severe impulse noise environment (λ = 3,000). Over such a small SNR_{TV} range, there is little improvement in performance with increasing SNR_{TV} (curves are rather flat). It is also interesting to compare the performance of the conventional decoder in gaussian noise and the impulse-gaussian noise mixture (λ = 30,000). In fact, for $SNR_{TV} \leq 29$ dB, performance is better in the impulse-gaussian noise mixture. Performance is quite bad, however, with the error rate being in the 1×10^{-2} neighbourhood. It must also be emphasized that this is a channel that is very close to the video quality acceptability borderline.

Performance of the two decoder types in a gaussian noise environment with a multipath channel with a PDUR of 14 dB, is presented in Figure 73. It is apparent from the impulse response plot presented in Figure 68, that this channel has a very significant close in echo (much more servere than that of the 13 dB PDUR channel in Figure 67). The PDUR, which is used to estimate subjective video quality, cannot be used directly to estimate teletext quality. The subjective effect of close in echoes is not as annoying as those with larger delay spreads for subjective video quality. Consequently, strong close-in echoes, which will cause trouble for teletext, can be tolerable from a video quality viewpoint. In fact, a comparison of Figures 71 and 73 reveals that the performance with the 14 dB PDUR multipath channel is worse than that obtained with the 13 dB PDUR multipath channel. Note that there is a significant degradation relative to the performance with an ideal channel. This degradation is a result of the intersymbol interference introduced by the channel and the slicing level error introduced by multipath. It is interesting to note that the averaging slicer has a significant advantage over the peak sensitive conventional decoder. Note also that the performance of the conventional decoder does not improve significantly as

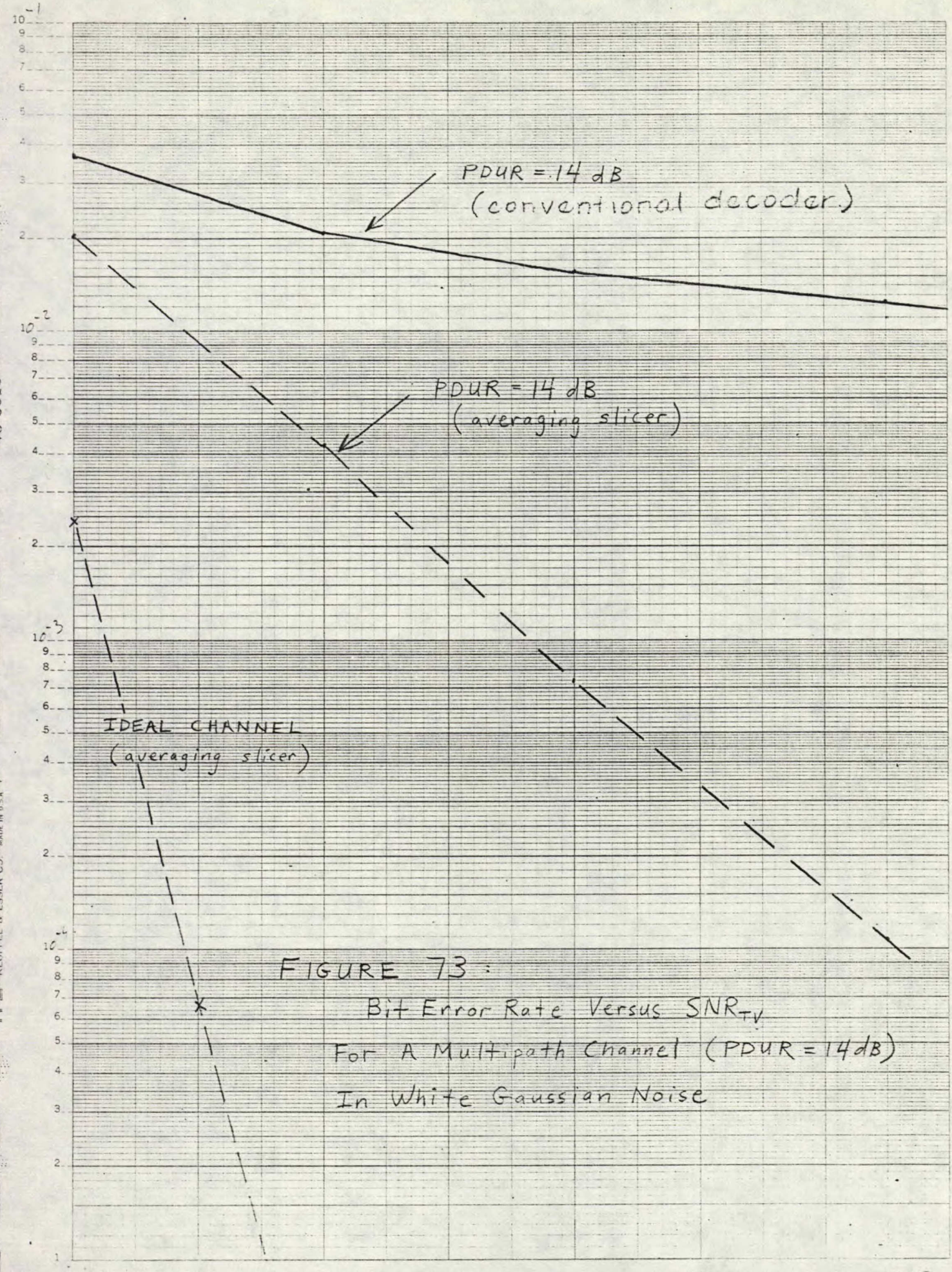

FIGURE 73:
Bit Error Rate Versus SNR_{TV}
For A Multipath Channel (PDUR = 14dB)
In White Gaussian Noise

the video signal to noise ratio increases. (Note that SNR_{TV} = 33 dB corresponds to a passable TASO grade and SNR_{TV} = 39 dB corresponds to a fine grade). Even with a SNR_{TV} = 40 dB, the error rate is still above 1×10^{-2}. This is exactly the sort of error rate behaviour one would expect from a significant slicing level error (i.e. the error rate for bits with the same polarity as the slicing level error decreases much slower than it would in the absence of a slicing level error). The performance with the averaging slicer is considerably better. To achieve a bit error rate of 8×10^{-4} or lower, the video S/N must exceed 35 dB.

A comparison of the performance achieved by the two decoders in the impulse-gaussian noise mixture for the same multipath channel is presented in Figure 74. The superiority of the averaging slicer decoder is clearly evident. As indicated in Figure 74, the performance of the decoder with the averaging slicer for the worst case impulse arrival rate, λ = 30,000 per sec, is considerably better than that achieved by the conventional decoder in a much less severe noise environment with an impulse arrival rate of 3,000 per sec. In comparable noise environments, there is roughly an order of magnitude difference in the performance between the two decoders. For what seems like a fairly realistic impulse arrival rate (λ = 3,000 per sec), one can achieve error rates that are better than 1×10^{-3} for TV SNR's exceeding 35 dB with the averaging slicing level decoder. Making a comparison between the performance in gaussian noise (Figure 73) and that for an impulse-gaussian noise mixture with λ = 3,000 per sec (Figure 74), it is evident that performance is better in the mixed noise environment for SNR_{TV}'s less than 34 dB with the averaging slicer decoder. However, for SNR's above 34 dB, there is a much greater improvement with increasing signal to noise ratios in the gaussian noise environment.

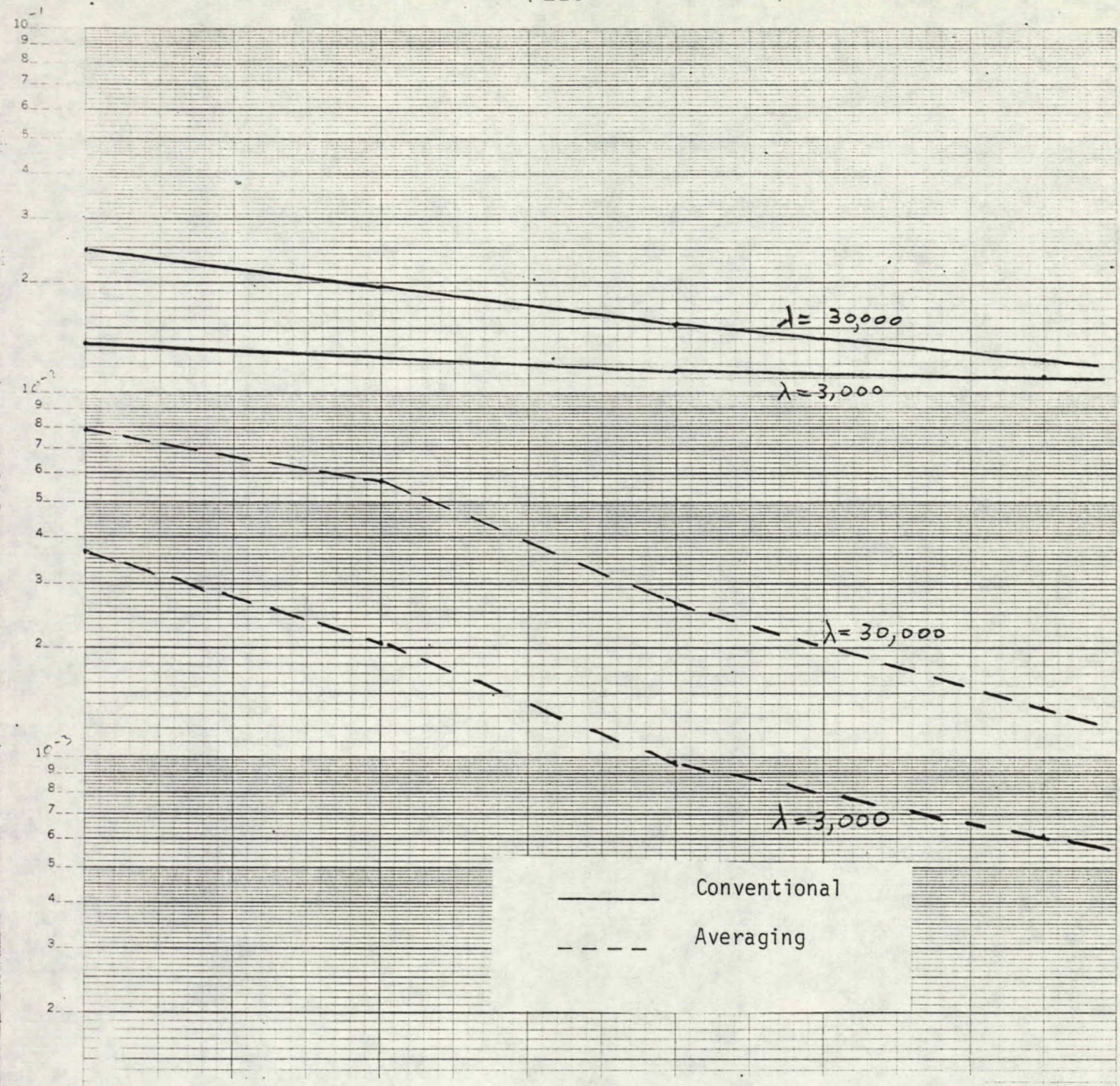

Figure 74: Bit Error Rate Versus SNR_{TV} for a Multipath Channel (PDUR = 14 dB) In An Impulse - Gaussian Noise Environment.

The multipath channel with PDUR = 20 dB, shown in Figure 69, has a significant close in echo. The performance of the conventional and averaging slicing level decoders in various noise environments with this multipath channel is summarized in Figure 75. In a Gaussian noise environment, the loss relative to an ideal channel is considerably less than what was observed previously for the 13 dB and 14 dB PDUR multipath channels. The averaging slicer has approximately a 1.8 dB advantage over the conventional decoder in this multipath environment. In the mixed impulse-gaussian noise environment, the averaging slicing level decoder is clearly superior, but its margin is not quite as great as it was for the more severe multipath channels. As is characteristic, at low SNR_{TV}, performance in impulse noise dominated environments is better than in gaussian noise. The opposite is true at high signal to noise ratios. At SNR_{TV}'s exceeding 33 dB (TASO quality grade is passable as a minimum) performance is quite good (error rate less than or equal to 1×10^{-4}) with the decoder which estimates the slicing level via averaging.

Because error correction and detection coding is to be employed in the Telidon system, the input error rate that can be handled can be relaxed somewhat. However, it is unlikely that the input error rate can exceed 1×10^{-3} without imposing some severe penalty, in terms of either delay or missed errors. The type of noise influences the burstiness of errors (impulse noise is thought to cause bursts of errors) and thereby the choice of error protection coding required to combat errors. Taking 1×10^{-3} as the threshold error rate, it is apparent that the existing system (employing peak detection circuits for slicing level estimation) cannot achieve this performance level with multipath channels near the video acceptability threshold, even for video signal to noise ratios corresponding to TASO Grades Fine and Excellent.

Figure 75: Bit Error Rate Versus SNR_{TV} for a Multipath Channel With PDUR = 20 dB In Various Noise Environments.

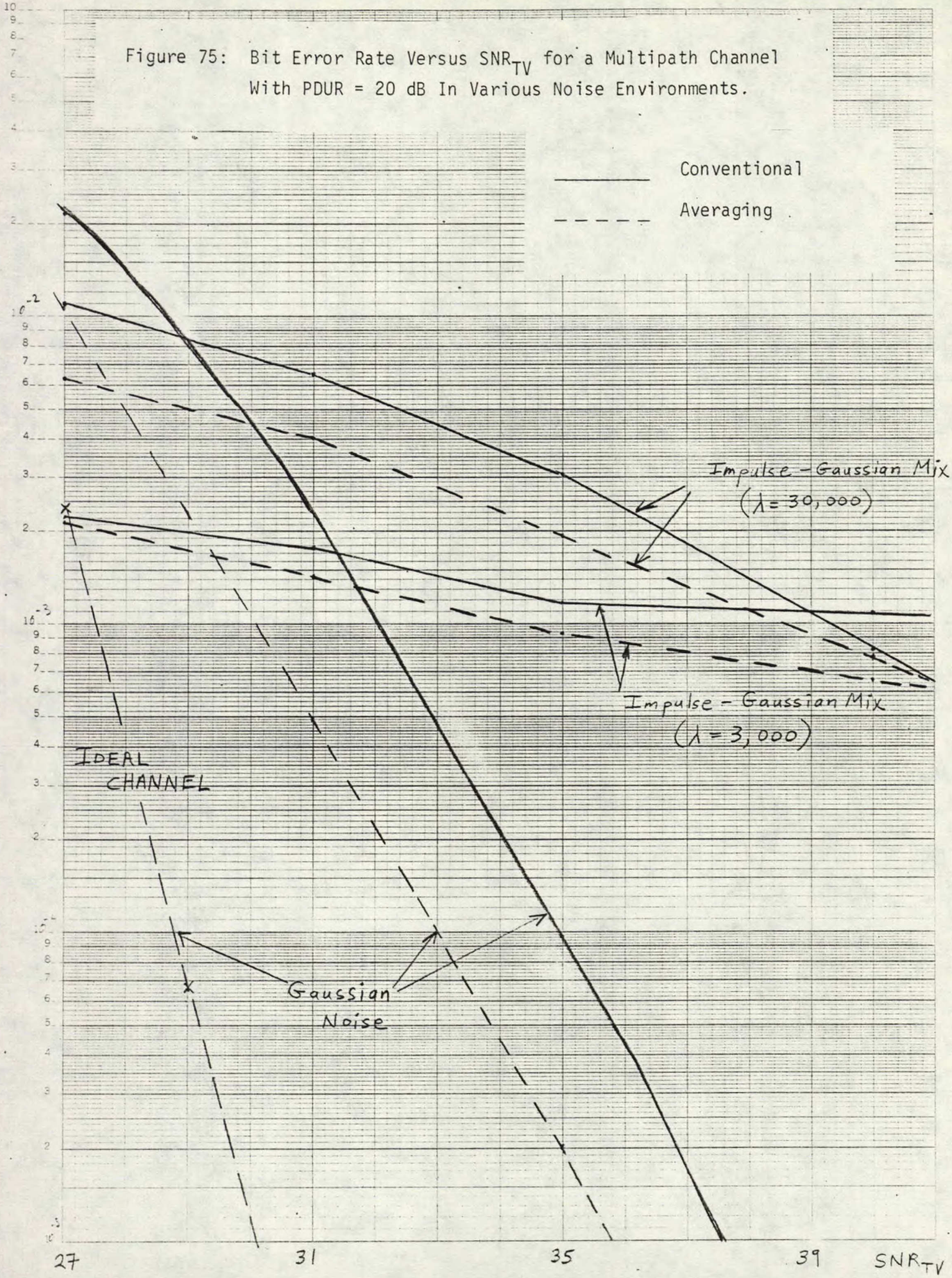

Furthermore, in mixed impulse-gaussian noise environments, with impulse noise power 21 dB greater than the gaussian noise component and with a Rayleigh impulse amplitude distribution, this performance level cannot be attained for the multipath channels investigated with PDUR's near the acceptable limit. With these channels, the averaging slicing level decoder improves performance considerably. The performance threshold is surpassed for signal to noise ratios corresponding to TASO grades Passable, Fine, and Excellent.

Performance with the PDUR = 20 dB multipath channel is considerably better. The performance threshold can be achieved for realistic video S/N (corresponding to a Passable TASO grade) in thermal noise environments with the conventional decoder. In predominately impulse noise, the threshold is attained for SNR_{TV}'s greater than 40 dB. Significant increases in coverage area will be realized if the present peak detector slicing level technique is replaced by a low pass filter (averaging). Improved timing recovery procedures will also have a significant impact on coverage area. It is also apparent that to achieve an error rate of less than 1×10^{-3} for all SNR_{TV}'s greater than or equal to 29 dB (corresponding to marginal video quality or better), channel equalization will be essential for channels with poor subjective picture quality. The value of equalization in impulse noise dominated environments is debatable.

3.4 Evaluating The Effectiveness of The Error Protection Coding Presently Employed in Telidon

Error protective codes for use with the data block are based on the odd parity of every byte in the block. The Hamming (8,4) symbols of the headers and prefixes also have odd parity. Presently, either no suffix byte or only one suffix byte is used. When no suffix is included, PDI

error protection is simply a byte by byte parity check, capable of detecting an odd number of errors in each byte. When one suffix byte is included, it contains a longitudinal parity check for the entire Data Block, as shown in Figure 76. This scheme, often referred to as the "product" code, permits the correction of only one error in the data block, the detection of some even numbered bit errors per byte, and the detection of all odd numbered errors per byte.

With our simulation program, the errors in the bit stream at the channel output (input to the error correction and detection decoder) are logged. These error sequences can then be analyzed to determine the error autocorrelation function, gap length and burst length distribution functions, and other typical error statistics. These error sequences (after being Exclusive OR'ed with an appropriate [odd parity] zero data sequence) can then be decoded by a series of potential coding techniques to assess their relative performance.

In order to evaluate possible channel and decoder enhancements, a procedure for relating errors to performance degradation (corruption and delay) was developed. To do so, errors had to be categorized as to their severity, which requires knowledge of the Telidon message structure and error protection in use. A proposed categorization of errors is presented in Appendix VI of [15], where an attempt to predict the effects of errors within different sections of the Telidon message is discussed. A brief summary will be presented here for completeness. Errors can either be corrected, detected, or missed. Detected errors result in delays (waiting to re-receive the packet) while missed errors can result in either delay or image corruption, depending on their position. By assuming an average record composition (a

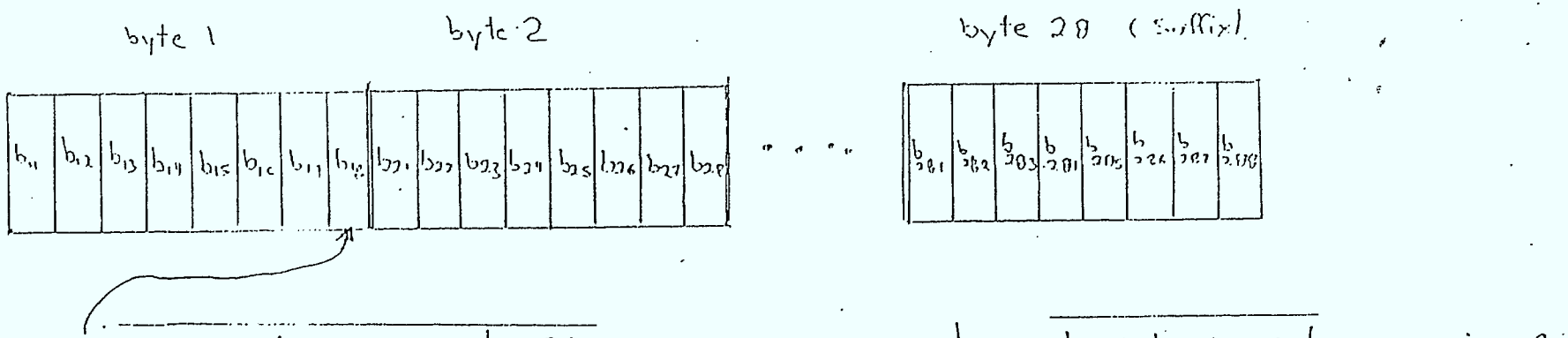

Figure 76 : Present Single Suffix Encoding

record was assumed to consist of a 33 byte header block followed by 50 data blocks including prefix segments) expressions were developed for the packet rejection probability, R, and the average number of PDI errors per record, Nc. To evaluate these expressions for R and N_c, an error analysis program was developed to measure the following quantities:

a) $\alpha_1 = P_{HAM}(1,5)$ = the probability of 1 missed byte error in 5 bytes (not detected)

b) $\alpha_2 = \sum_{\ell=2}^{5} P_{HAM}(\ell,5)$ = the probability of more than 1 missed byte error in 5 byte (no error detection)

c) $\alpha_3 = \sum_{\ell=2}^{33} P_{HAM}(\ell,33)$ = the probability of at least 1 missed byte error in 33 bytes (no error detection)

d) $\beta_1 = D_{HAM}(5)$ = the probability that at least 1 error is detected in 5 bytes

e) $\beta_2 = D_{HAM}(33)$ = the probability that at least 1 error is detected in 33 bytes

f) P_{DD} = the probability that the packet is rejected due to PDI error detection (post-decoding PDI rejection rate with selected block code)

g) N_D = Average number of post decoder PDI errors that were not detected per packet.

Note that the subscript HAM refers to Hamming (8,4) protected bytes.

These fundamental quantities are used to determine the following important parameters:

a) P_{HC} = the probability of a header corrupting error situation in a packet

b) P_{PC} = the probability of packet corruption due to missed errors in the prefix

c) P_{PD} = the probability that the packet is rejected due to the prefix

d) P_{HD} = the probability that the packet is rejected due to detected errors in the header

We will not go into the justification details (see Apppendix VI of [15]), but it can be shown that:

$$P_{HC} = \frac{\alpha_3}{2}$$

$$P_{PC} = 0.2\,\alpha_1$$

$$P_{PD} = 0.8\,\alpha_1 + \alpha_2 + \beta_1$$

$$P_{HD} = \frac{\alpha_3}{2} + \beta_2$$

The overall packet rejection rate, R, and the number of PDI errors per record, NC, (for a record containing 50 data packets) can be approximated by:

$$R \approx \frac{P_{HD}}{51} + 0.98\,(P_{PD} + P_{DD}\,[1-P_{PD}])$$

$$Nc \approx 24.5\,(P_{HC} + P_{PC}\,[1-P_{DD}]) + 50\,N_D(1-[P_{PC} + P_{PD}])$$

The error analysis program computes the above packet rejection rate and number of PDI errors per record for both the byte parity check case and the product code. Some other useful quantities that are output include:

(i) the pre-decoder bit error rate,

(ii) the number of bit errors corrected,

(iii) the number of bit errors introduced by false correction,

(iv) after correction bit error rate (this includes packets which have errors that could be detected ... we are simply ignoring the detection capability),

(v) after correction and detection bit error rate (excludes those packets which have detectable errors),

for the various block codes employed. The format is illustrated in Table 10.

3.4.1 Establishing Realistic Bounds For Acceptable Packet Rejection Rates and Number of PDI Errors Per Record

Ideally, acceptable limits on R and Nc should be established by subjective testing, as the values are likely to be highly variable due to differing personal opinions. However we must establish realistic bounds without the benefit of the results of such subjective tests.

In [15], a rough bound on the packet rejection rate was established. It was based on the results of an MCS study "Comparison of Error Correction", where it was found that the mean waiting time increased dramatically for bit error rates greater than 10^{-4}. This was based on random error statistics and a similar block length to that used in Telidon (i.e. 256 bits). Assuming that essentially all errors can be detected, the packet rejection rate is given by:

$$R \simeq 1 - (1-p_e)^{256}$$

$$\simeq 256\, p_c = 2.5 \times 10^{-2}$$

To get a better feel for the average amount of time between retransmissions, we can compute the mean number of records between retransmissions, N_{RR}, which is given by:

$$N_{RR} = \frac{(1-R)}{RL} *$$

where L = the number of packets per record (assumed to be 50).

Using $R = 2.5 \times 10^{-2}$ and L = 50, the average number of records between retransmissions is 0.78, which is not very good performance. Consequently, when R exceeds 2.5×10^{-2}, it is safe to classify this as unacceptable performance. In fact, some limited subjective testing should be conducted to either support or contradict this bound, and if the latter, provide data that could be used to derive a reasonably tight bound.

In [15], a maximum number of byte errors per picture (15.5) is derived based on the maximum bit error rate of 5.5×10^{-4} quoted in Treurniet's subjective tests [31] and the average number of bits per picture (page) which was 28,228 [31]. Assuming 50 data packets per record, with 28 data bytes per packet, the average number of records per picture is approximately 2.5. Therefore a reasonable bound on the number of PDI errors per record is:

$$N_C(max) = 6.2$$

It must be emphasized that subjective quality in [31] was established using pictures (maps) as opposed to textual

*In [33], there are obvious errors on page 28, equations (2.17) and (2.18).

information. Because the subjective tests were based on only one specific type of graphical image, one must be cautious of the above figure. Clearly subjective tests, with a variety of pictures and mixes of graphical and textual information, should be performed to ensure realistic limits on PDI error rate and the tolerance to delay. However without the benefit of such information, we will use $R_{(max)} = 2.5 \times 10^{-2}$ and N_c (max) = 6.2.

It is interesting to examine some of the requirements of the Japanese Teletext system presented in [32]. Their major objective was achieving a page error rate of 5×10^{-2}, and they make no distinction between errors that can be detected (which result in retransmission) and missed errors (which result in corruption). It is remarked in [32] that the above page error rate is considered to be rather severe compared to those for other systems developed in other countries.

In the Japanese system, a page consists of 8 packets of 34 bytes each (total of 272 data & control bytes). Consequently, one of our records, composed of packets with 33 control & data bytes, corresponds to roughly 6 Japanese pages. First let us assume that the majority of errors can be detected, in which case the page rejection rate (P_R) is 5×10^{-2}. The average number of pages between retransmissions is $\frac{1-P_R}{P_R} = 19$. Converting this to our standard record, we obtain:

Average Number of Records Between Retransmission ≈ 3.2

which is significantly better than what was obtained using R (max). In fact the above corresponds to a equivalent packet rejection rate, R_{eq}, of 6.2×10^{-3}, which is a factor of 4 better than R (max). Since this is supposed to be a stringent requirement, one should be able to find a reasonable value between 2.5×10^{-2} and 6.2×10^{-3}.

The page error definition used in the Japanese calculations [32] is somewhat bizarre. If a packet has more than 2 error bits it is regarded as an error block. If there are two or more error blocks in the page of eight blocks, the page is referred to as an error page. Note that these errors could be detectable errors. Acceptable pages can be guaranteed if the upper limit on the number of errors per line is one, which corresponds to one byte error per packet. The threshold bit error rate for the Japanese system was 5×10^{-3}. At this error rate, the probability of error detection is much greater than data corruption (by at least an order of magnitude) for most codes. On page 22 of [33], the validity of the above assumption for the SAB and S&S codes for bit error rates exceeding 4.96×10^{-3} is clearly demonstrated. Consequently we can take $\frac{1}{10}$ byte errors per packet as an upper limit on the number corrupting errors (undetected). This translates into

$$N_c = \frac{1}{10} * 8 \text{ packets/Jap. page} * 6 \text{ Jap. pages/MCS record}$$

$$= 4.8 \text{ PDI errors/record.}$$

This upper limit is in reasonably close agreement with the limit of 6 PDI errors/record extrapolated from the subjective tests conducted by Treurniet [31]. The only major question mark is whether or not the bound on R is tight enough.

3.4.2 System Performance with the Product Code

As mentioned earlier, the existing Telidon system uses either byte parity, which only detects errors, or the product code, which has weak correction but strong detection capabilities, for error protection. Unfortunately, the capability of storing error sequences was not available when the simulation runs for the multipath channels with PDUR's of 13 dB and 14 dB were conducted. Error analysis was conducted for the 20 dB PDUR multipath channel (pre-correction results summarized in Figure 75) and for the ideal channel (pre-correction results summarized in Figures 64 and 65) for the log-normal and Rayleigh (α = 2) impulse noise environments with an impulse arrival rate of 30,000 per sec. The most important quantities for assessing performance are the overall packet rejection rate, and the number of PDI errors per record. The tedious task of evaluating the mean rejection rate, and mean number of PDI errors per record at each signal to noise ratio has been completed, and the results presented graphically.

To begin we will examine the results for the 20 dB PDUR multipath channel. The packet rejection rate versus SNR_{TV} for gaussian noise is presented in Figure 77. As expected, the product code (with its limited correction capabilities) is better than using only the byte parity (which only detects errors). Because of a lower input error rate, the performance with the averaging slicing level decoder is superior to that of the conventional decoder. The acceptability threshold ($R_{max} = 2.5 \times 10^{-2}$) is achieved with the product code at the following SNR_{TV}:

Figure 77: Packet Rejection Rate Vs SNR_{TV} for Gaussian Noise
(20dB PDUR Channel)

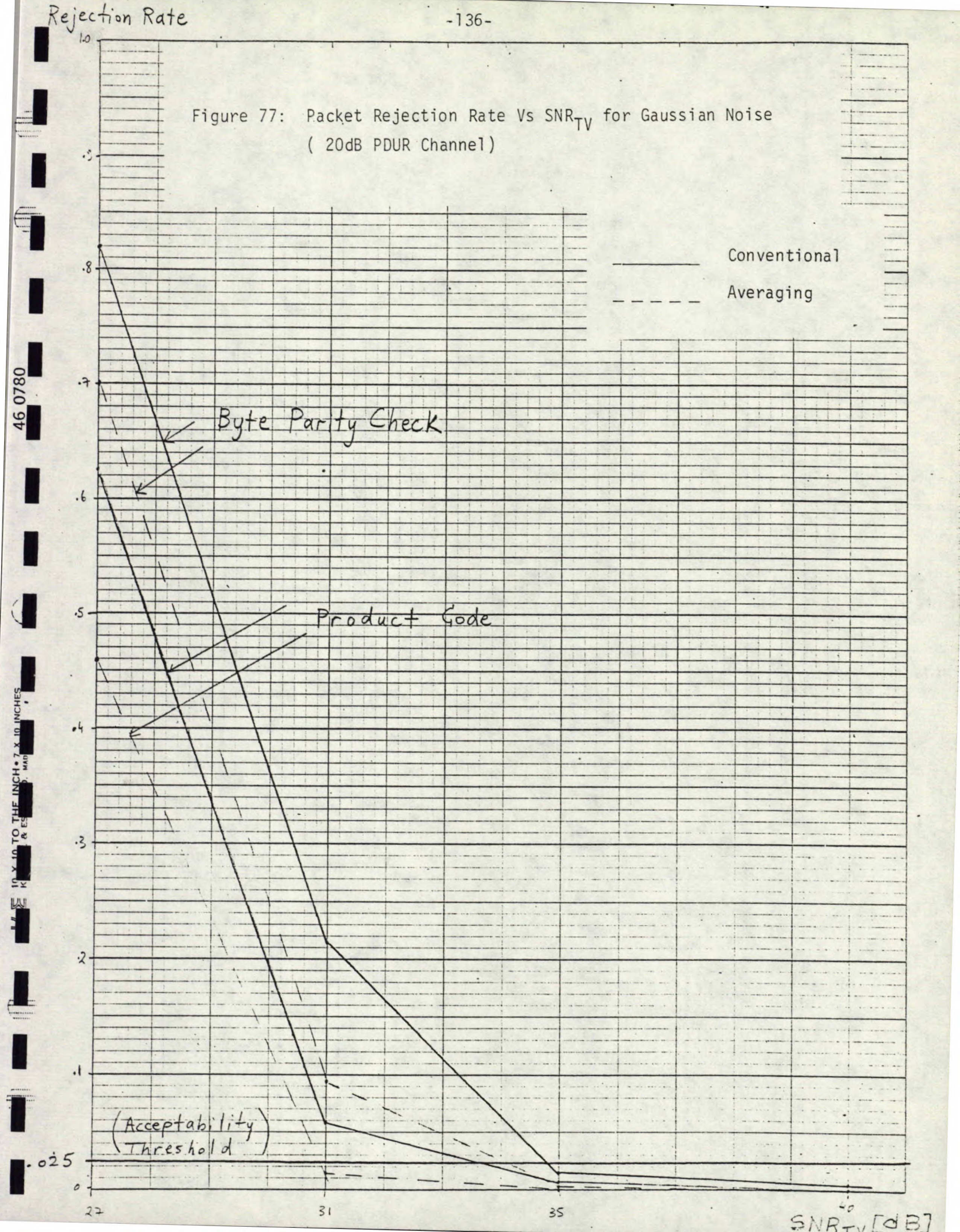

Decoder	SNR_{TV}	TASO Grade
Conventional (peak detector slicing circuitry)	33.6	Passable
Averaging (slicing level estimated via averaging)	31	Marginal-Passable

Furthermore, with the conventional decoder, the packet rejection rate at SNR_{TV} = 35 dB is 7×10^{-3} (which is close to the stringent Japanese requirement). It is apparent that reasonable rejection rates with the existing Telidon system can be attained for SNR_{TV}'s that provide "Passable" TASO signal grades with this multipath channel. It is very unlikely that the same will be true for more severe multipath channels, as the error rate at the input to the decoder is at least a factor of three higher with the 13 dB and 14 dB PDUR channels in this signal to noise ratio region.

The packet rejection rate versus SNR_{TV} for the most severe impulse - gaussian noise mix (λ = 30,000) is shown in Figure 78. Note that there is really not a tremendous difference between the results for both decoder types. Using only byte parity is clearly inadequate and with the product code the acceptability threshold is attained around SNR_{TV} = 40 dB. Similar statements hold with less severe impulse noise (λ = 3,000), except that there is not such a dramatic difference between the product code and using only byte parity (see Figure 79).

FIGURE 78

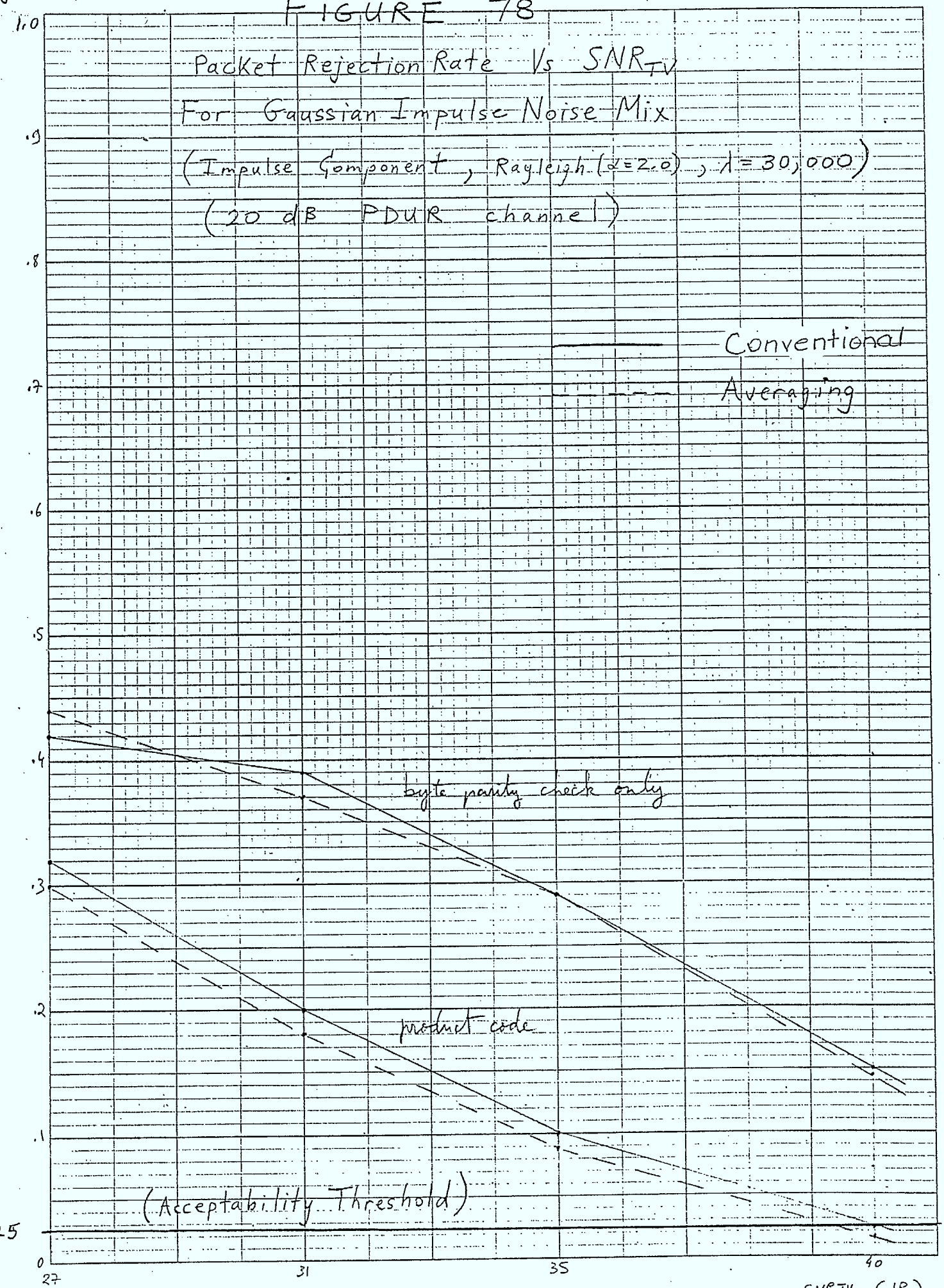

Rejection Rate

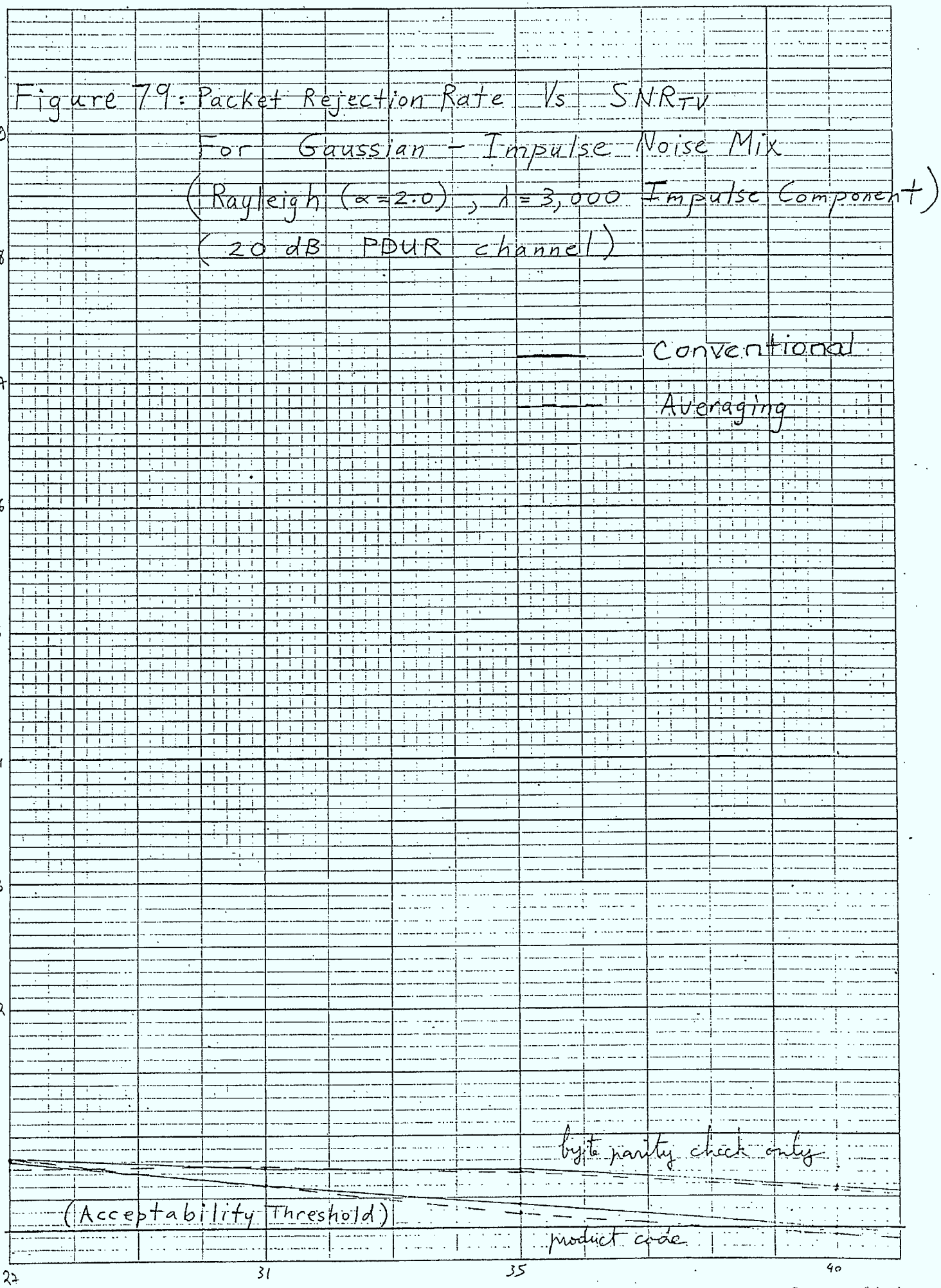

Figure 79: Packet Rejection Rate Vs SNR_{TV}
For Gaussian + Impulse Noise Mix
(Rayleigh ($\alpha = 2.0$), $\lambda = 3,000$ Impulse Component)
(20 dB PDUR channel)

In gaussian noise environments, the average number of PDI errors per record for both the averaging and conventional decoders, was well below $N_c(max) = 6.2$, for both the product code and byte parity check. In fact, the worst case average (at $SNR_{TV} = 27$ dB) was 1.4. This can be attributed to the error detection capabilities of the above techniques, as well as the isolated, random nature of errors in guassian noise environments. In the most severe mixture of impulse and gaussian noise, one can see from the results presented in Figure 80 that the average number of PDI errors per record is well below the threshold value (6.2) with the product code. The product code, with its weak correction capabilities, is as expected, superior to the byte parity check. In less severe impulse and gaussian noise, there is little difference between the conventional and and modified averaging slicer decoders, and the average number of PDI errors per record is well below the threshold $N_c(max) = 6.2$ (see Figure 81). The after-correction bit error rate, which gives an indication of the correction capabilities of a code, is presented in Figure 82. Comparing this with the pre-decoder bit error rate (see Figure 75) one notices only a very slight improvement. Given the weak correction capabilities of the product code this is not surprising.

Error sequences for runs conducted with an ideal channel in a rather severe ($\lambda = 30,000$) impulse noise environment, with log-normal and Rayleigh ($\lambda = 2.0$) amplitude distributions, were analyzed. The packet rejection rate results for the Rayleigh amplitude distribution are presented in Figure 83. Note that SNR_{TV} must exceed 43 dB in order to surpass the 2.5×10^{-2} threshold. As expected, the results for the averaging slicing level decoder are better than those for the conventional decoder. As expected (lower input error rate), the packet rejection

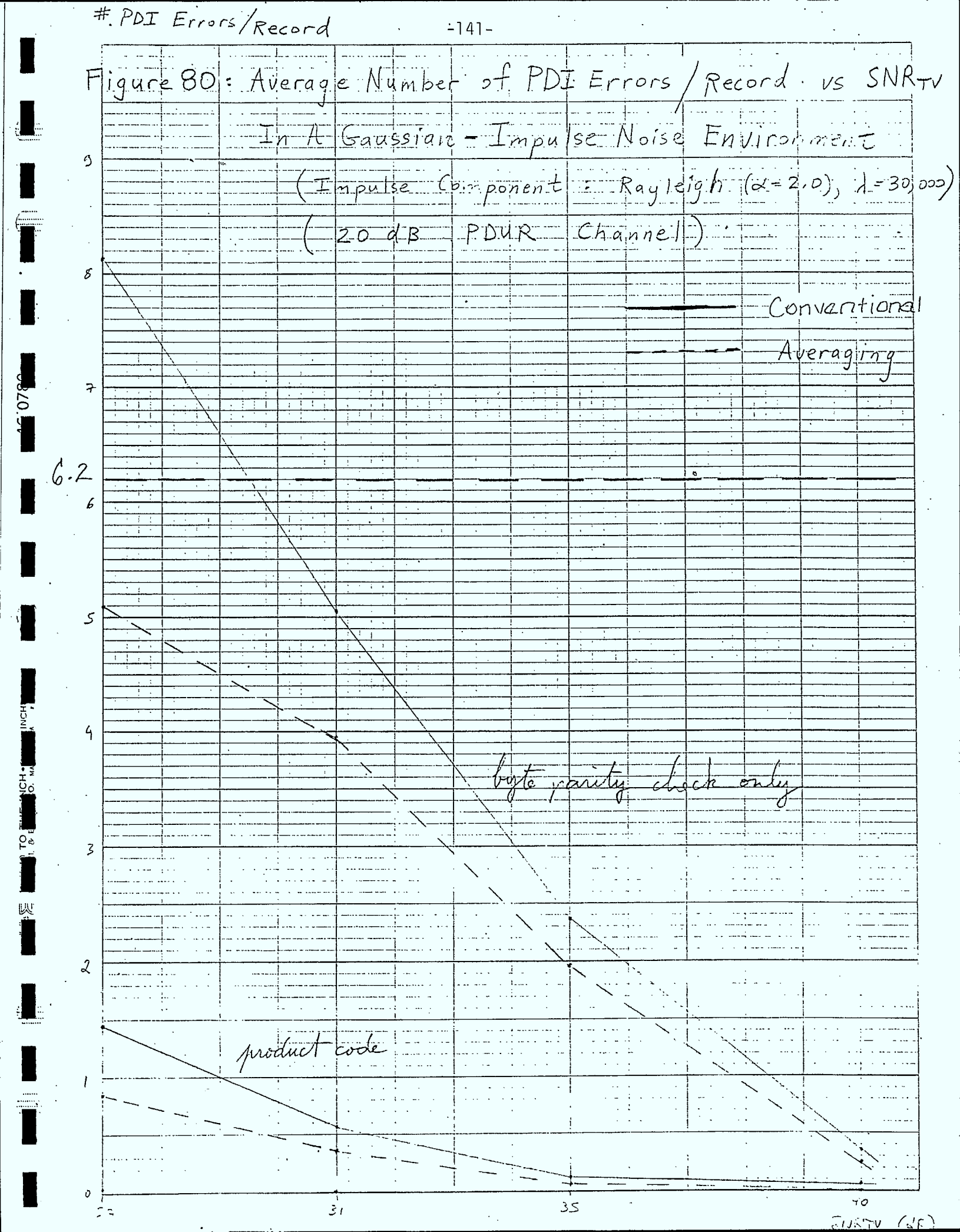
PDI Errors/Record
Figure 80: Average Number of PDI Errors/Record vs SNR_TV
In A Gaussian-Impulse Noise Environment
(Impulse Component: Rayleigh (α=2.0), λ=30,000)
(20 dB PDUR Channel)
Conventional
Averaging
6.2
byte parity check only
product code
9
8
7
6
5
4
3
2
1
0
31
35
40
SNR_TV (dB)

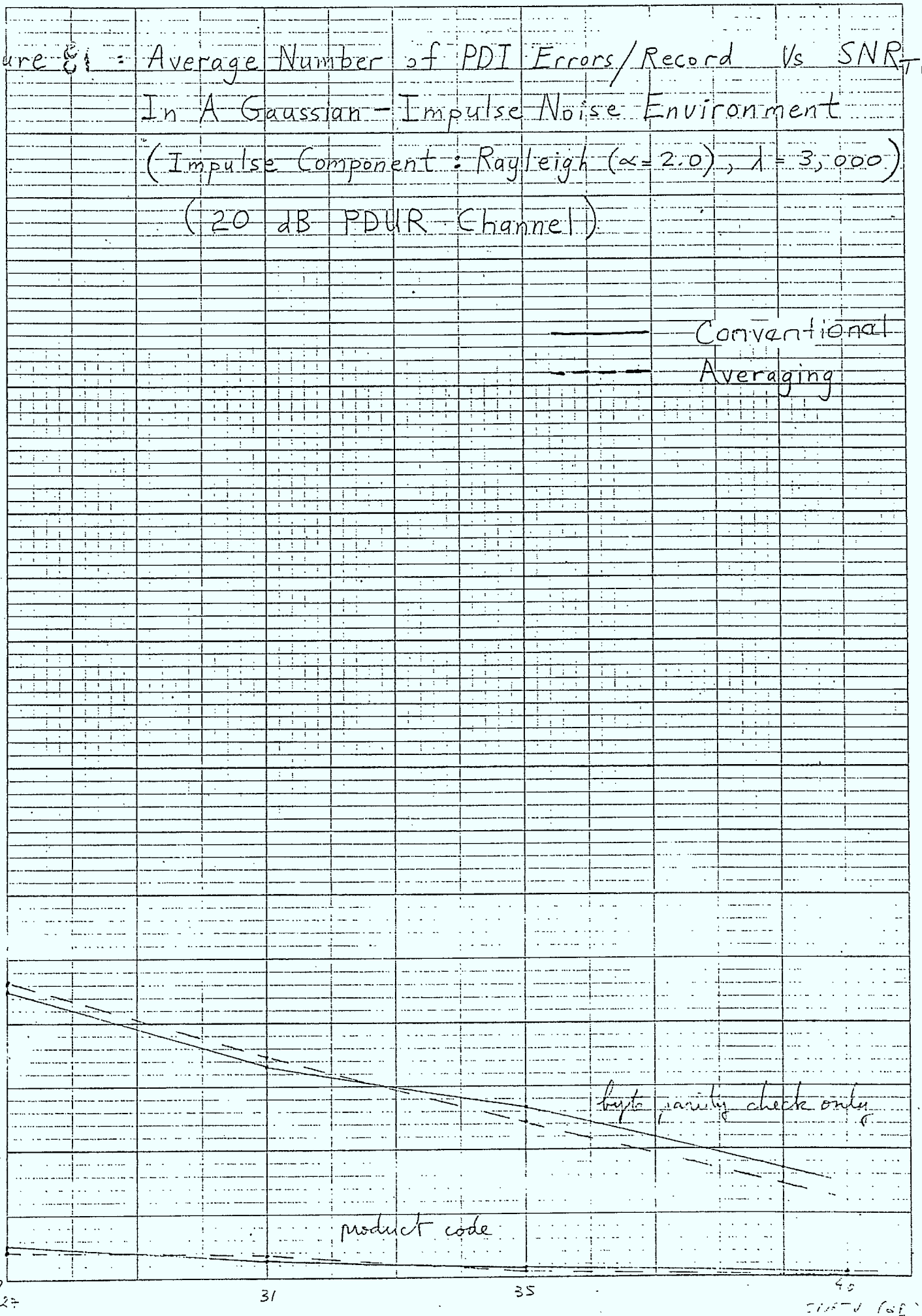
PDI Errors/Record
Figure 61 : Average Number of PDI Errors/Record Vs SNR_{TV}
In A Gaussian-Impulse Noise Environment
(Impulse Component : Rayleigh ($\alpha = 2.0$), $\lambda = 3,000$)
(20 dB PDUR Channel)
Conventional
Averaging
byte parity check only
product code
9
8
7
6
5
4
3
2
1
0
27
31
35
39

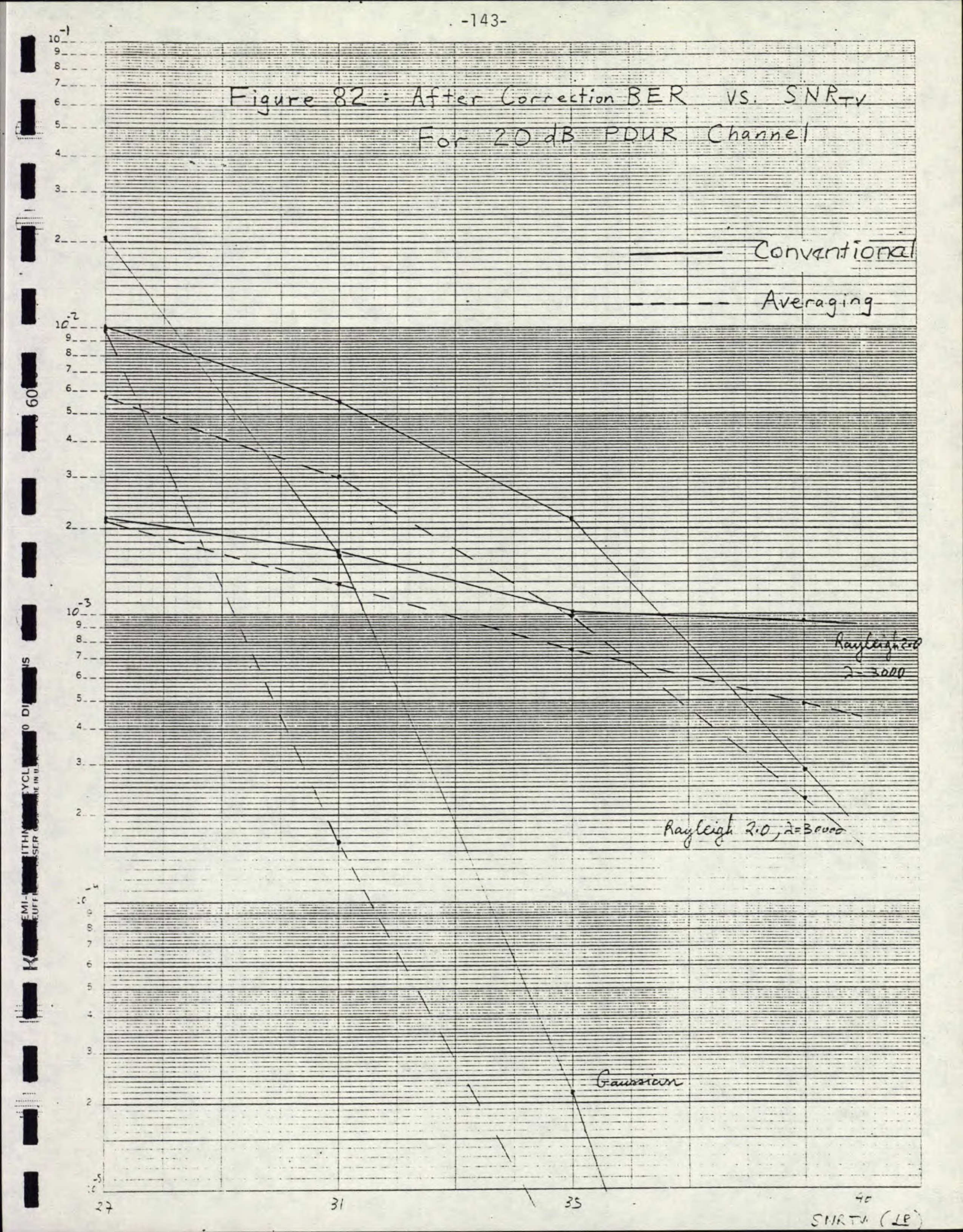
Figure 82 : After Correction BER vs. SNR_TV
For 20 dB PDUR Channel
Conventional
Averaging
Rayleigh 2.0, 2=3000
Rayleigh 2.0, 2=3000
Gaussian
10^-1
10^-2
10^-3
10^-4
10^-5
27
31
35
40
SNRTV (dB)

Figure 83

Packet Rejection Rate Versus SNR_{TV}

For An Ideal Channel In Impulse Noise

($\lambda = 30,000$, Rayleigh ($\alpha = 2.0$))

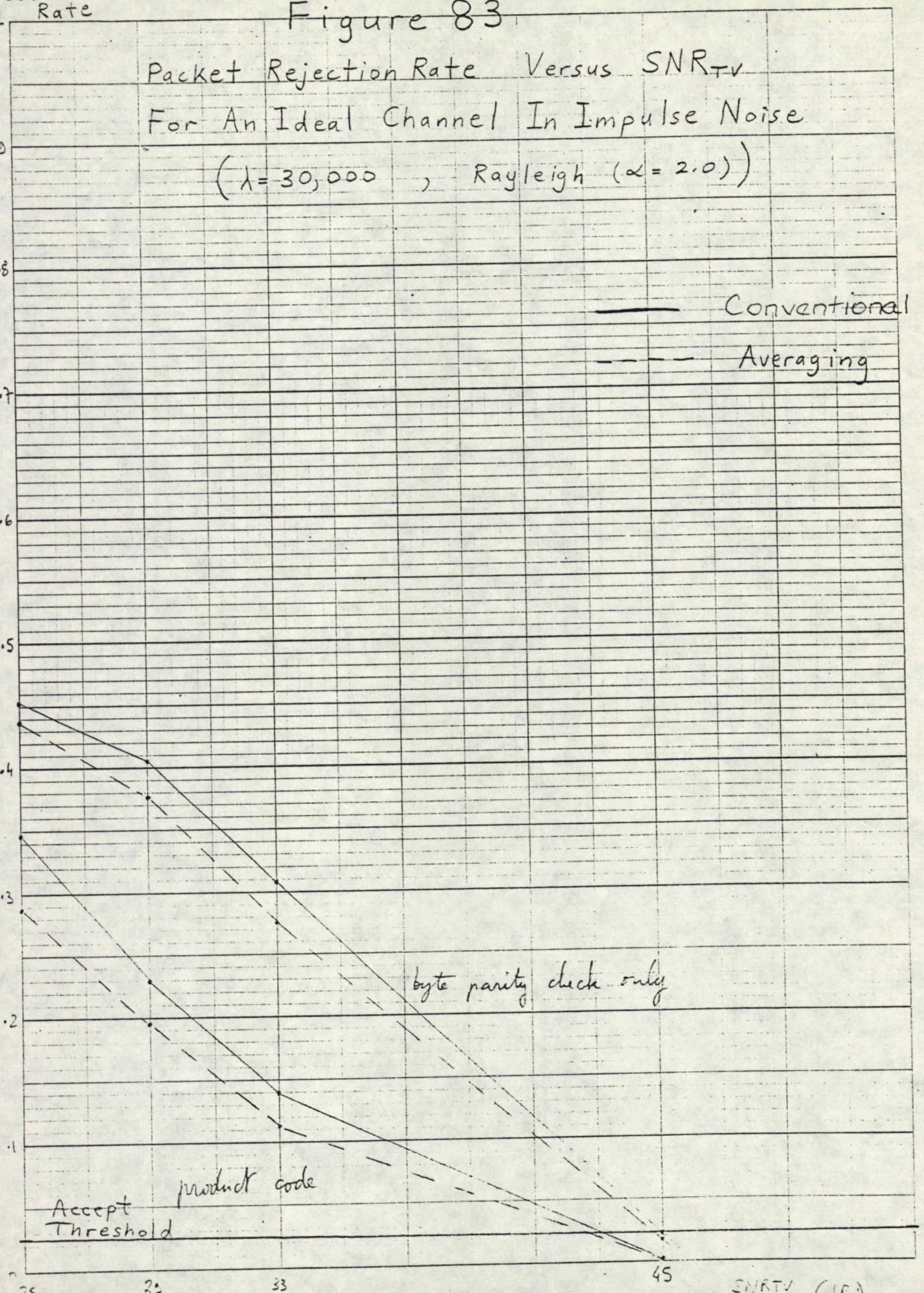

rates are lower in log-normal impulse noise (see Figure 84). For the product code, the rejection rate threshold is crossed at SNR_{TV} = 40 dB. One really must be able to assess the subjective picture quality in such levels of impulse noise before one can determine whether the performance of the existing system is adequate or deficient. The average number of PDI errors per record, for Rayleigh and log-normal impulse noise, are presented in Figures 85 and 86, respectively. As is evidenced, the values for the product code are well below $N_c(max) = 6.2$ over the complete signal to noise ratio range investigated. This can be attributed to the strong error detection capabilites of this code. The after-correction bit error rates are shown in Figure 87. It is interesting to compare these results with the pre-coding error rate, illustrated in Figure 64 and 65. There is a marginal improvement in Rayleigh impulse noise with error sequences from the conventional decoder. A much more dramatic improvement is noted for Rayleigh impulse noise with the averaging slicing level decoder and in both cases for log-normal impulse noise, at high SNR_{TV}. The correcting capabilities improve dramatically as the input error rate approaches 1×10^{-4}.

3.5 Concluding Remarks

The clear superiority of the modified decoder (which determines the slicing level by averaging) in gaussian and impulse noise environments, with and without multipath, has been demonstrated. Still, there remains a significant degradation (roughly 1 dB) relative to ideal recovery. It is anticipated that implementing the recommended clock phase recovery procedure will improve performance considerably. Given the potential gain, this should be given high priority.

Figure 84

Packet Rejection Rate Versus SNR-v

For An Ideal Channel In Impulse Noise

(λ = 30,000 , Log-normal)

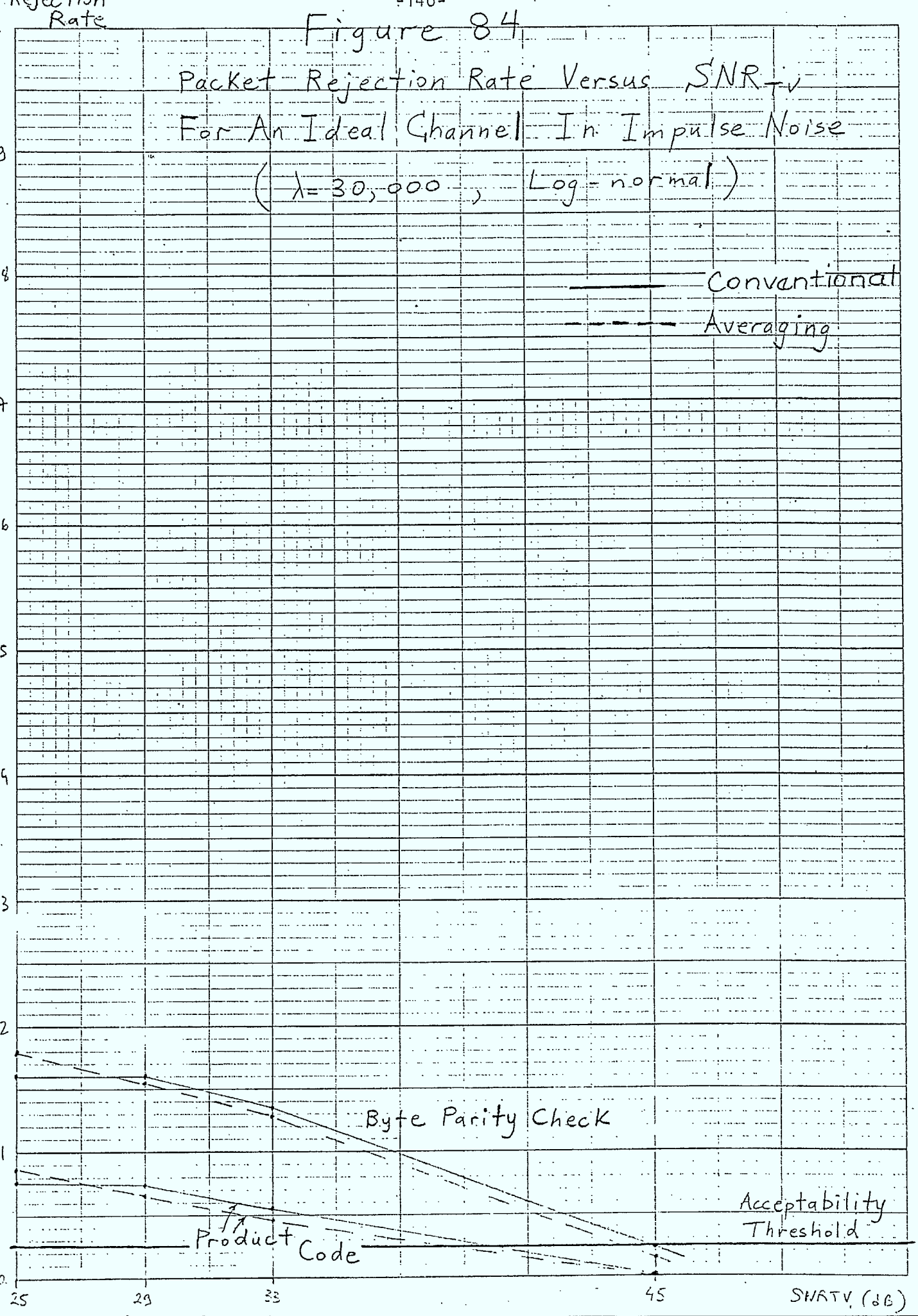

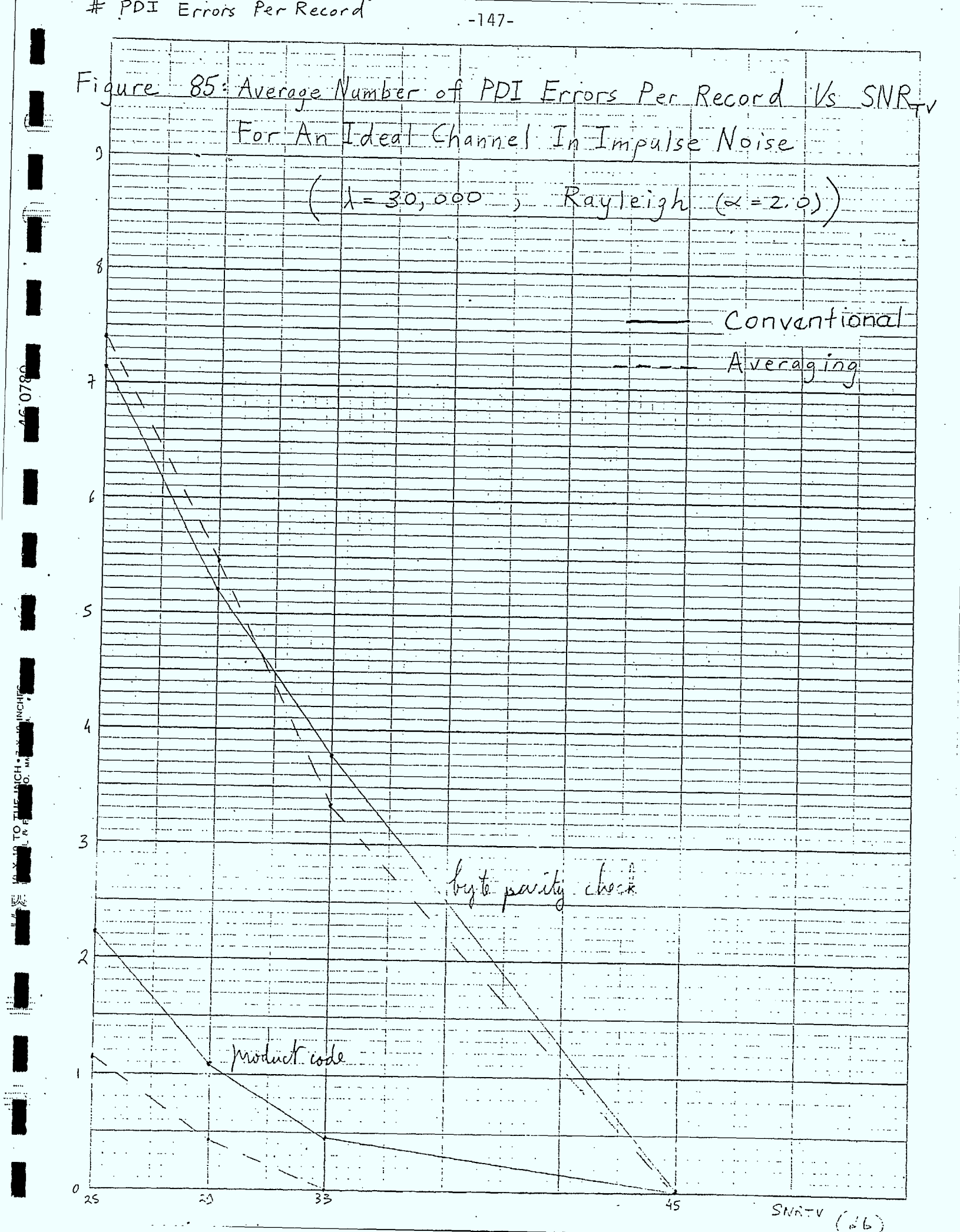

Figure 85: Average Number of PDI Errors Per Record Vs SNR_{TV} For An Ideal Channel In Impulse Noise ($\lambda = 30,000$; Rayleigh ($\alpha = 2.0$))

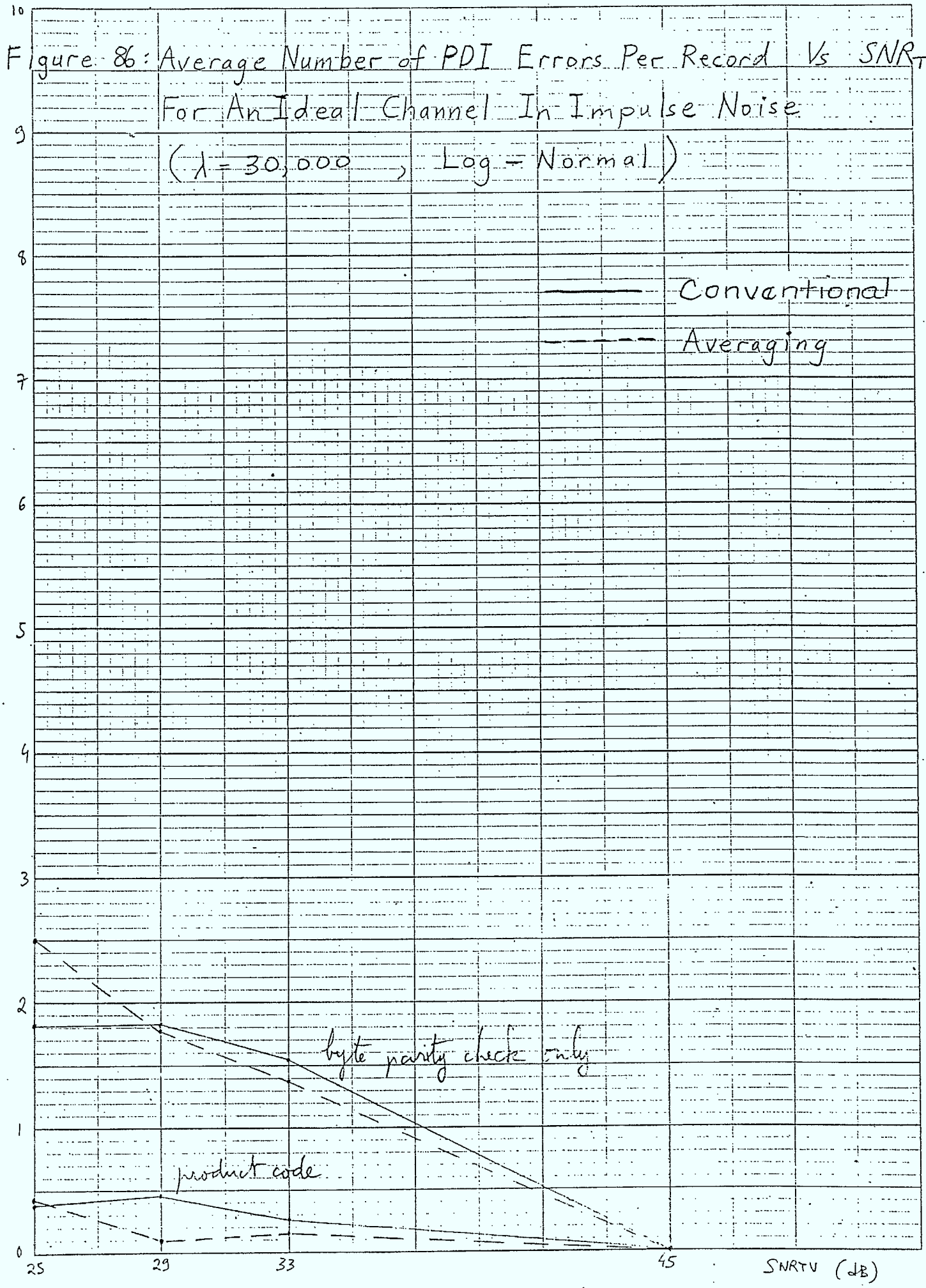

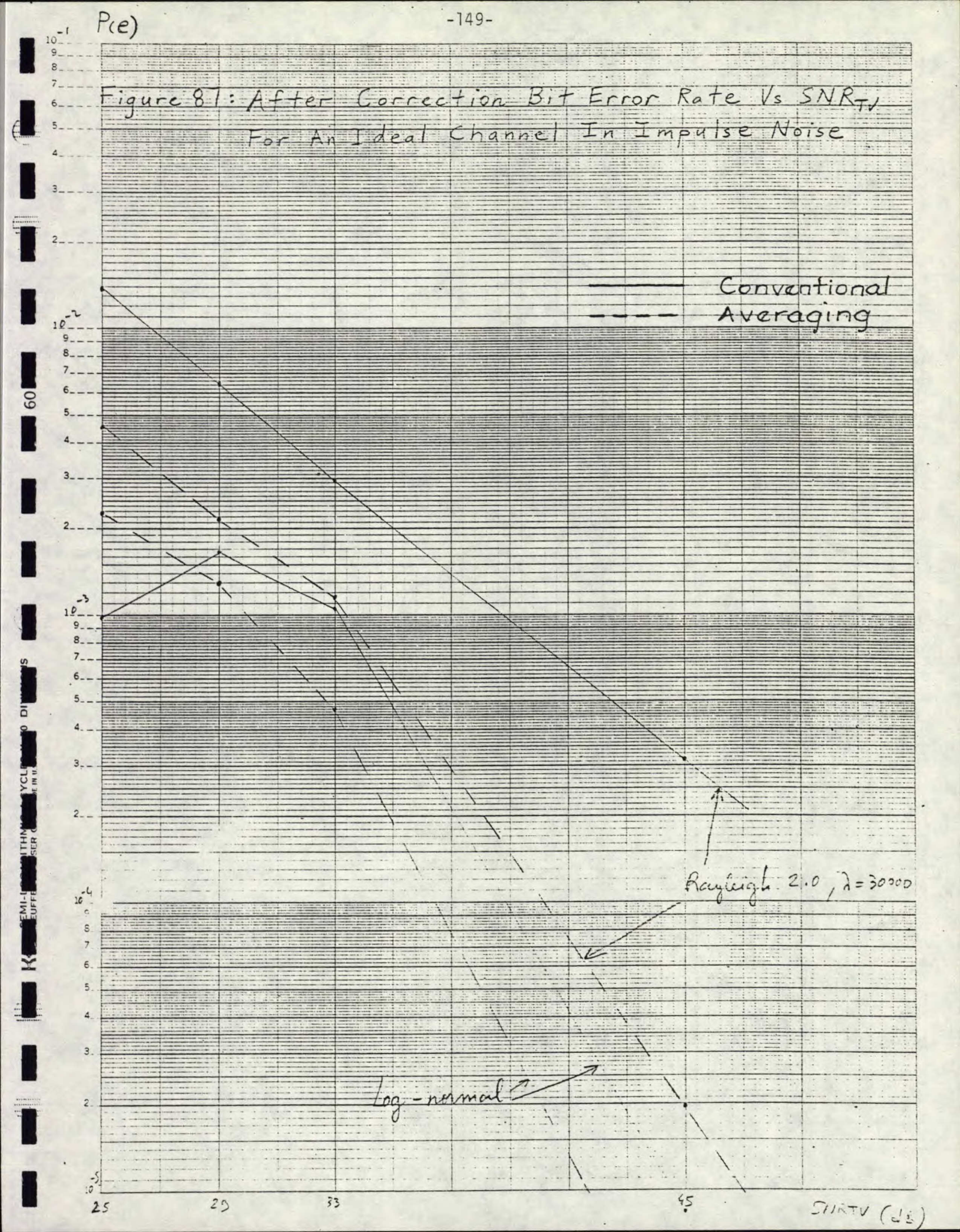

Figure 81: After Correction Bit Error Rate Vs SNR_{TV} For An Ideal Channel In Impulse Noise

Under relatively favourable conditions (not severe multipath), adequate performance (in terms of delay and corruption) seems to be achievable for television signal to noise ratios corresponding to passable TASO signal grades. To extend coverage to regions with lower signal to noise ratios, improved coding techniques and/or channel equalization would be necessary.

It is interesting and promising to discover that one is at least able to attain acceptable performance in impulse noise with the existing system, although it is at high SNR_{TV}. One needs to be able to establish acceptable subjective picture quality thresholds for impulse noise environments. One could then improve the system to give adequate performance whenever usable television pictures could be obtained, or a least as close to this subjective limit as possible.

REFERENCE LIST

[1] M. Sablatash, "Principles of Modelling and Pulse Shaping and Filter Optimization of Broadcast Teletext", CRC Technical Memorandum, June 8, 1983.

[2] E.S. Sousa and S. Pasupathy, "Transmitter-Receiver Design for Teletext Data Transmission", Communications Technical Report, Dept. of Electrical Engineering, The University of Toronto, May 1982.

[3] E.S. Sousa and S. Pasupathy, "Pulse Shape Design for Teletext Data Transmission", IEEE Trans. Commun., Vol. COM-31, pp. 871-878, July 1983.

[4] M. Sablatash, "A Short Essay on Pulse Shaping for Broadcast Teletext", Communications Research Centre, 1983.

[5] C. Eilers and P. Fockens, "Teletext Transmission Pulse Shape Optimization", IEEE Trans. Consumer Electron, Vol. CE-27, pp. 551-554, Aug. 1981.

[6] S.B. Ng, "Pulse Shape Optimization and Channel Equalization for Teletext Transmission over Multipath Channels", M.Sc Thesis, Department of Electrical Engineering and Computer Science, Massachusetts Institute of Technology, February, 1983.

[7] "Broadcast Specifications BS-14", Department of Communications, Government of Canada, Ottawa, Ontario, Issue 1, June 1981.

[8] E.S. Sousa and S. Pasupathy, "Enhanced Receivers for Nonoptimally Allocated Filtering", IEEE Trans. Commun., Vol. COM-31, pp. 879-885, July 1983.

[9] E.S. Sousa and S. Pasupathy, "Filtering Allocation in Teletext Data Transmission Under Power and Peak Constraints", IEEE Trans. Commun., Vol. COM-31, pp. 933-935.

[10] A.V. Oppenheim and R.W. Schafer, Digital Signal Processing, Prentice-Hall, Inc., Englewood Cliffs, New Jersey, 1975.

[11] "Radio Standards Specification: Television Broadcasting Transmitters Operating in the 54-88 MHz, 174-216 Mhz and 470-806 MHz Frequency Bands", Department of Communications, Government of Canada, Ottawa, Ontario, Issue 2, September 1980.

[12] P. Fockens and C.G. Eilers, "Intercarrier Buzz Phenomena Analysis and Cures", IEEE Trans. on Consumer Electronics, pp. 381-397, August 1981.

[13] T. Rzeszewski, "A System Approach to Synchronous Detection", IEEE Trans. on Consumer Electronics, pp. 186-193, May 1976.

[14] M. Schetzen, "Nonlinear System Modelling Based on the Wiener Theory", Proc. of the IEEE, pp. 1557-1573, Dec. 1981.

[15] K.W. Moreland et al., "Telidon System Study 2nd Interim Report", Miller Communications Systems Ltd. Report, DSS File No. DSS 21ST.36100-2-4380, MCS File No. 8342, June 1983.

[16] H.L. Van Trees, Detection, Estimation, and Modulation Theory, Part I, John Wiley and Sons, Inc., New York, 1968.

[17] C.S. Lindquist, Active Network Design with Signal Filtering Applications, Stewart and Sons, Inc., 1977.

[18] R.K. Tiedemann, "Simulation of VHF Multipath Propagation Model for Telidon", MCS, 29 April, 1983.

[19] R.K. Tiedemann, "Intuitive Confirmation of Far Field Approximation for VHF Multipath Reflections", MCS, 5 May, 1983.

[20] K.W. Moreland, "Subjective Quality of TV Pictures in Multipath Environments", MCS, 13 July 1983.

[21] S. Yamazaki and Y. Endo, "A Quanititative Measurement of Subjective Effects of TV Mulitple-Ghost Images by 'Perceived DU Ratio'", IEEE Trans. on Broadcasting, Vol. BC-26, No. 3, September 1980.

[22] S. K. Goyal, C. B. Neal, and E. R. Bowerman, "Television Transient Response Computations Using a New Simulation Program", IEEE Trans. On Broadcasting, Vol. BC-23, No. 2, June 1977.

[23] J. O. Voorman, P. J. Snijder, P. J. Barth, and J. S. Vromans, "A One-Chip Automatic Equalizer For Echo Reduction In Teletext", IEEE Trans. on Consumer Electronics, Vol. CE-27, No. 3, August 1981.

[24] K. W. Moreland, 'Baseband Model For Teletext Systems and Extracting Information For Channel Validation', MCS, March 31, 1983.

[25] EIA Teletext Subcommittee, "Draft Interim Report of Task Force C", August, 1981.

[26] "C.C.I.R. XIIIth Plenary Assembly, Volume XII-Geneva 1974", International Telecommunication Union, Geneva, 1975, pg. 37.

[27] T. Fujio, "A Universal Weighted Power Function of Television Noise And Its Application To High-Definition TV

System Design", IEEE Trans. on Broadcasting, Vol. BC-26, No. 2, June 1980, pg. 43.

[28] D. Falconer, "Course Notes for Advanced Digital Communication", Carleton University, Ottawa, January 1983.

[29] W.L. Behrend, "Performance Comparison of TV Transmitter, RF Demodulators and the Home Receivers", IEEE Trans. on Broadcasting, Vol. BC-17, No. 1, March 1971.

[30] "Reference Data for Radio Engineers, Fifth Edition", ITT, Howard W. Sams and Co., Inc., 1972.

[31] W.C. Treurniet and P.J. Hearty, "Qualitative and Quantitative Measures of Users Responses to Errors in Teletext Transmissions ... Draft", Presented at CVCC/TS/WGB Meeting, January 1983.

[32] J.R. Storey, "Distribution of Errors in Japanese Teletext", 20 July 1983.

[33] V.K. Bhargava et al., "Realization, Economic and Performance Analysis of Error - Correcting Codes and ARQ Systems for Broadcast Telidon and other Videotex Transmission", Concordia University, Montreal, Quebec, 15 June 1981.

[34] A. Vincent, "A Simulation Study of Teletext Transmission", CRC, DOC, Ottawa, February 1983.

APPENDIX I

PULSE SHAPING FOR TELETEXT

APPENDIX I: PULSE SHAPING FOR TELETEXT

1.0 INTRODUCTION

In recent years a considerable amount of effort has gone towards the development of Canada's television broadcast teletext system, Telidon. Like all data transmission systems a crucial goal is the reliable transmission of data. Although many factors have an impact on this goal, the choice of a suitable pulse shape has received a great deal of attention lately [1][2][3][4][5][6]. This appendix is primarily concerned with the pulse shaping issue but also discusses some other related issues such as audio buzz, adaptive "slicing level", and bit phase synchronization.

Much of the effort has concentrated on raised cosine pulse shapes with various roll-off factors. In fact the current specified pulse shape is a truncated 100 percent raised cosine [7]. It has been pointed out that although the raised cosine family of pulse shapes are fairly good, it may be possible to do better if one searches over a wider class of pulse shapes for the one that is in some sense optimal [4]. As a result of this observation a comprehensive collection of pertinent facts and formulas were compiled [1] to aid further research. Also, the Communications Research Centre let a contract to the University of Toronto to study the pulse shaping problem. The study culminated in an excellent report [2] and several papers [3][8][9]. However, certain aspects of pulse shaping were not adequately dealt with. These include:

- Minimizing the overshoot at the transmitter is not considered.
- The recommended pulse shape is not realizable.
- The zero phase assumption for the frequency response is not justified.

- The assumed receiver filter is not representative of typical television receivers.

Here, we will address these and other topics, using the University of Toronto report [2] as a starting point.

Ideally, the overall objectives of this pulse shape design are as follows:

- Minimize the probability of bit error subject to the other design objectives being satisfied.

- The overshoots, at both the output of the transmitter and the baseband channel of the receiver, should be constrained at acceptable levels.

- The pulse shape design should lead to specifications that are compatible with the current television broadcast specifications.

- The overall pulse shape should be reasonably robust in the presence of multipath.

- It is desirable that the receiver requirements be kept as simple as possible. That is that any necessary complexity and stringent specifications should be transferred to the transmit side if possible.

- The bandwidth should be constrained to the 4.2 MHz NTSC video bandwidth.

One possible approach for meeting the above objectives is to define a massive nonlinear optimization that attempts to simultaneously achieve the above goals, but this is beyond the scope of this contract. Another approach is to try to decompose the problem into several smaller more manageable

problems (that are hopefully approximately orthogonal) and handle each one separately. This is the approach taken here. Although some of the above objectives are not incorporated in the pulse shape design, all are discussed.

It is assumed here that some form of coherent demodulation is used at the receiver. Therefore the complex baseband model, that is shown in Figure 1, can be applied. Here, P(f) is the teletext transmit filter. Since this filter is implemented at baseband, it will have a purely real impulse response. T(f) is the effective television broadcast transmit filter. It includes the effects of the transmitter's IF filter, zonal filters, harmonic filter, and any fixed (but typically adjustable) equalizer. Since this frequency response must be asymmetrical about the carrier frequency, its baseband representation will have a complex impulse response. C(f) is the frequency response of the channel, including multipath and the transmit and receive antennas, and is assumed to be of the form

$$C(f) = \hat{C}(f)\left[\sum_{p=1}^{P} c_p(t)e^{-j2\pi f T_p}\right], \qquad (1)$$

where $\hat{C}(f)$ is the channel response in the absence of multipath (usually taken to be unity), P is the number of propagation paths, and $c_p(t)$ and T_p are the complex path gains and the path delays, respectively. Note that angles of the complex path gains incorporate any phase offset in the recovered carrier (which in turn is a function of the multipath structure of the channel). R(f) is the effective television receiver filter. Since this frequency response must be asymmetrical about the carrier frequency, its baseband representation will have a complex impulse response. L(f), is the teletext receive filter. This filter will probably be implemented at baseband and

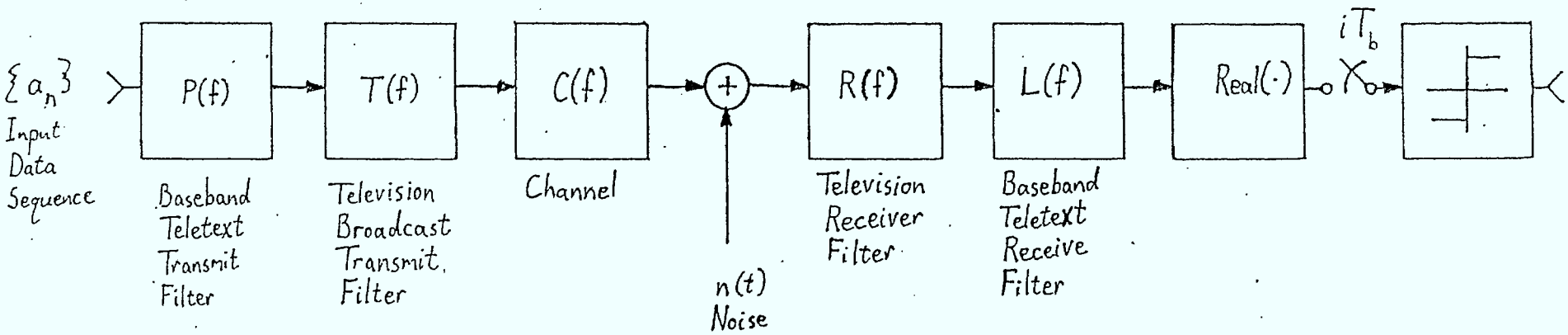

Figure 1: The baseband model for teletext transmission.

therefore will have a real impulse response. It is desirable that this filter be kept very simple. Note that the model of Figure 1 does not include an adaptive equalizer, however such a facility can easily be incorporated at a later date.

The organization of this appendix is as follows. Section 2.0 contains a general discussion about pulse shaping. In Section 3.0, overall pulse shape design is considered. Then, in Section 4.0, the apportioning of the pulse shape is discussed along with a reasonable approach to specifying it. Section 5.0 briefly discusses audio buzz, slicing level and symbol synchronization. Section 6 contains conclusions and recommendations.

2.0 A GENERAL DISCUSSION ABOUT SEVERAL ISSUES RELATED TO PULSE SHAPE DESIGN

Here, we consider some issues that affect the choice of the overall pulse shape. By overall, we mean from the input of the baseband teletext transmit filter to the input of the sampler (see Figure 1). One of the key requirements on the pulse shape is that it meets (or at least almost meets) Nyquist's first criterion. Because of the importance of this requirement, and in order to gain some further insight, we begin with a brief tutorial discussion on Nyquist's first criterion.

Let the transfer function of the overall real baseband channel be denoted by $H(\omega)$.

The model, to be discussed, can be seen in Figure 2. In order for there to be no intersymbol interference it is necessary that

$$h(kT_b) = \begin{cases} 1 & k=m \\ 0 & \text{otherwise} \end{cases}, \qquad (2)$$

where mT_b is the propagation delay of the channel. Here it has been assumed that the symbol timing recovery circuit (i.e. the sampling synchronization circuit) is operating correctly. If the constraint given in equation (2) is satisfied then

$$h(t) \sum_{k=-\infty}^{\infty} \delta(t-kT_b) = \delta(t-mT_b), \qquad (3)$$

where $\delta(t)$ is the Dirac delta function which is defined by

$$\int_{-\infty}^{\infty} f(t)\,\delta(t-T_o)dt = f(T_o). \qquad (4)$$

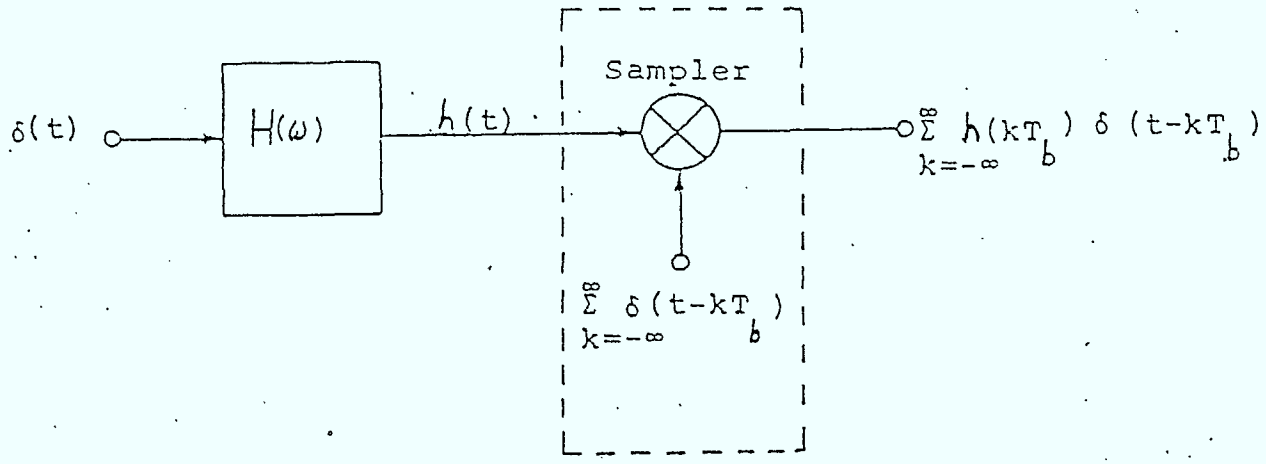

Figure 2: A model for the transmission of an impulse over a sampled linear channel

The Fourier transform of equation (3) is given by

$$H(\omega) * \sum_{k=-\infty}^{\infty} \frac{1}{T_b} \delta\left(\omega - \frac{2\pi k}{T_b}\right) = e^{-j\omega m T_b}, \qquad (5)$$

where * denotes the convolution operator. Equation (4) can be used to show that

$$\sum_{k=-\infty}^{\infty} H\left(\omega - \frac{2\pi k}{T_b}\right) = T_b e^{-j\omega m T_b}. \qquad (6)$$

Equation (6) is the Nyquist I requirement for no intersymbol interference. Note that this relationship indicates that the aliased version of $H(\omega)$ must have a constant amplitude (i.e. the sampled pulse shape has a "white" spectrum) and a linear phase if the channel is to be free of intersymbol interference. Clearly, the aliasing is due to sampling at the symbol rate. Typically, the propagation delay of the channel is conceptually removed, since a fixed delay should not affect the intersymbol interference at the receive end. In this case equation (6) reduces to

$$\sum_{k=-\infty}^{\infty} H\left(\omega - \frac{2\pi k}{T_b}\right) = T_b. \qquad (7)$$

At this point it becomes clear why it is desirable to choose a zero phase pulse shape. From equation (7) it can be seen that aliasing due to symbol rate sampling will not result in destructive interference, between frequency components of the pulse shape, only if $H(\omega)$ is real and nonnegative. An example of a pulse frequency response that is poor, in this

respect, can be seen in Figure 3. Clearly, if such a pulse shape were used, most of the transmitted energy would be lost due to aliasing upon symbol rate sampling. For the above reason, we will restrict our attention to zero phase pulse shapes. For this case, if $H(\omega)$ is zero beyond the interval $-2\pi/T_b \leq \omega \leq 2\pi/T_b$, then the channel will not exhibit intersymbol interference if the "folded" spectrum possesses symmetry about $T_b/2$. This concept is illustrated in Figure 4b. A common example of this type of transfer function is the raised-cosine transfer function. However, many other pulse shape transfer functions fall in this category.

In addition to satisfying (or almost satisfying) Nyquist's first criterion, it is desirable that the eye be wide so that performance is relatively insensitive to bit timing error and jitter. In some early works, Nyquist's second criterion was stated as an objective that would ensure a wide eye. However, it is well known that it is not possible to simultaneously satisfy both Nyquist I and II unless the channel bandwidth is equal to or greater than the symbol rate. In this effort, Nyquist II is not included as a direct objective although closely related objectives such as small overshoots and insensitivity to timing jitter are included.

A key objective of the pulse shape design is to keep most of the energy of the pulse shape within several symbol periods of the main lobe. (Recall that the pulse shape will be symmetric about the main lobe). There are several reasons for this but perhaps the most important reason is realizability. In general it is much easier to closely approximate a symmetric impulse response that is of short duration that one with a long precursor and tail. At this point it is appropriate to mention that a compact impulse response has implications to bit clock phase recovery. Note that during the clock run-in period many decoders (e.g. the

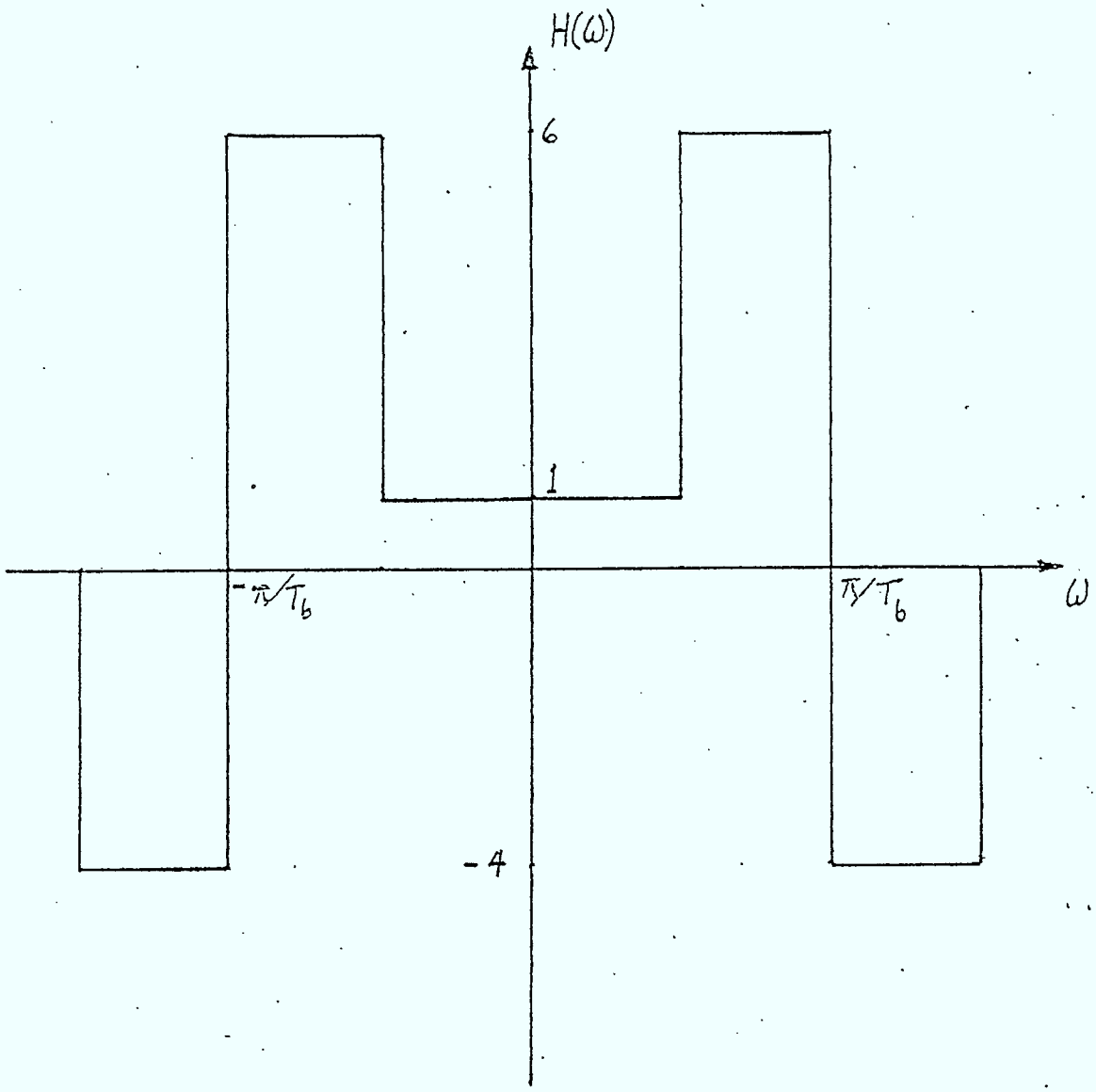

Figure 3: An example of a pulse frequency response for which most of the transmitted energy would be lost due to aliasing.

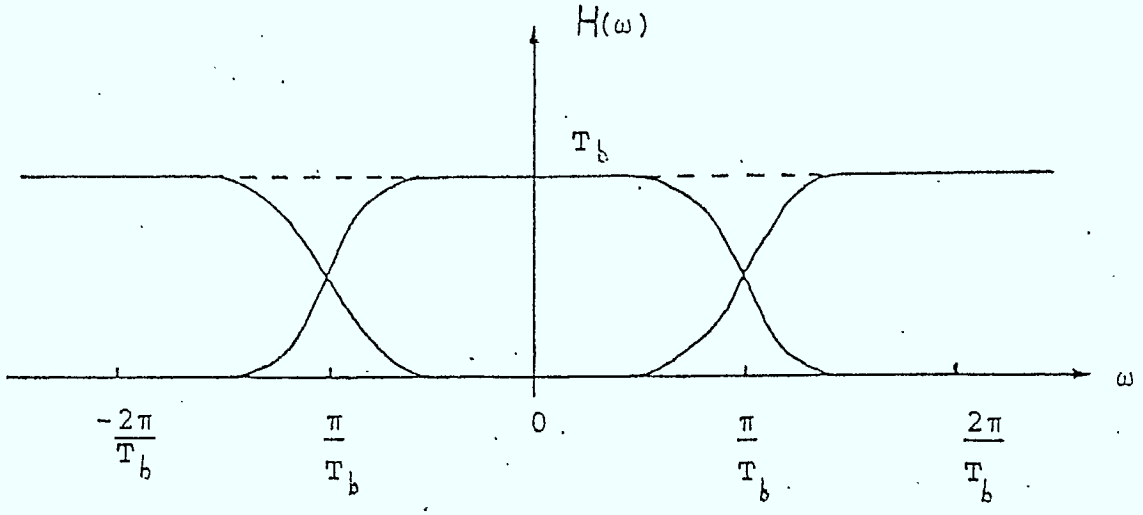

(a)

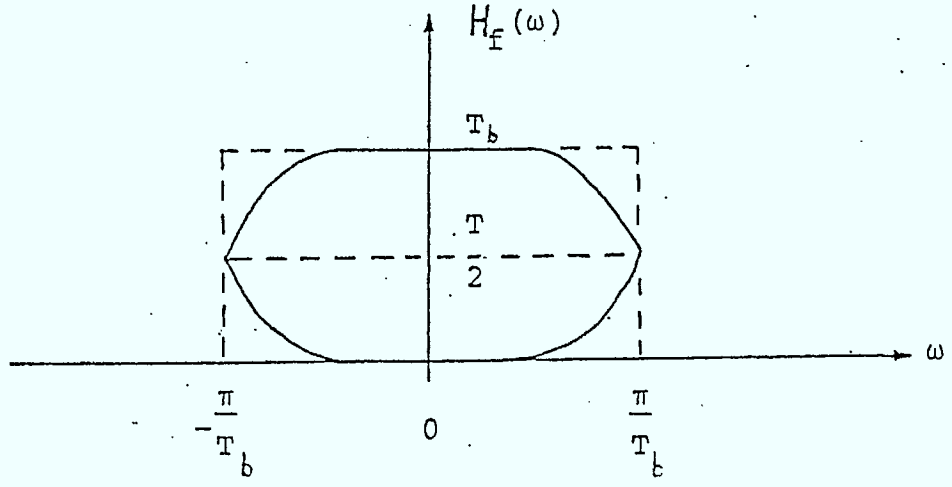

(b)

Figure 4: (a) A graphical representation of equation (7)
(b) The equivalent "folded" transfer function.

present decoder employed in the Telidon system) attempt to recover the clock phase. At baseband, this 2 byte period is essentially a CW signal at one half of the bit rate, in addition to a DC component that is due to the carrier. If the pulse shape is zero phase, then the phase of the clock run-in signal will be correct (just prior to the sampler) except for transients occurring at the start and the end of the 2 byte signal. Clearly the duration of these transients is equal to the duration of the precursor and tail of the pulse shape impulse response. It is interesting to note that if the clock phase is recovered during the clock run-in sequence, the phase error is not directly related to eye width. Intuitively, this is because the eye width takes into account all possible combinations of plus and minus ones, whereas during the clock run-in signal we are not faced with all possible combinations.

One of the objectives, that has already been stated, is the minimization of overshoots. Here, we are referring to overshoots in the receiver's baseband channel. Overshoot's at the transmitter will be addressed in a later section. There are several reasons for restricting the overshoots (and undershoots). Reasons given include the avoidance of false synchronization (i.e. overshoots being mistaken for sync pulses by the television receiver) and visibility on retrace (although this is expected to be a relatively weak function of overshoot). Excessive overshoots have also been blamed for causing audio buzz although the sources of audio buzz do not appear to be very well understood. Sousa and Pasupathy state that "the overshoots should be restricted so as to minimize the effect of multipath propagation" [3]. There is indeed some relationship between the size of the overshoots and the effects of multipath propagation, but it is not as strong a relationship as one might hope because of the vestigal sideband nature of the transmission system. The effects of multipath propagation on the vestigal sideband teletext transmission system of Figure 1 will now be discussed.

Let the transfer function from the input of the baseband teletext transmit filter to the output of the baseband teletext receive filter be given by

$$\hat{H}(f) = H(f)\left[\sum_{p=1}^{P} c_p e^{-j2\pi f T_p}\right]. \qquad (8)$$

Here,

$$H(f) = P(f)T(f)C(f)R(f)L(f) \qquad (9)$$

is the transfer function of the channel in the absence of multipath, and the summation on the right-hand side of equation (8) represents the multipath propagation. Also let the argument of c_p be denoted by θ_p.

Here, we begin by considering the case where no multipath is present. In this case $\hat{H}(f) = H(f)$. An example of a possible H(f) is illustrated in Figure 5a. Due to the vestigal sideband nature of the data transmission, this transfer function exhibits a local antisymmetry about f=0. The transfer function H(f) can be decomposed into two components, a symmetrical component

$$H_I(f) = 1/2[H(f) + H^*(-f)], \qquad (10)$$

and an antisymmetrical component

$$H_Q(f) = 1/2[H(f) - H^*(f)], \qquad (11)$$

where H^* denotes the complex conjugate of H. The global symmetry, about f=0, of $H_I(f)$ guarantees that the corresponding impulse response is purely real. Therefore,

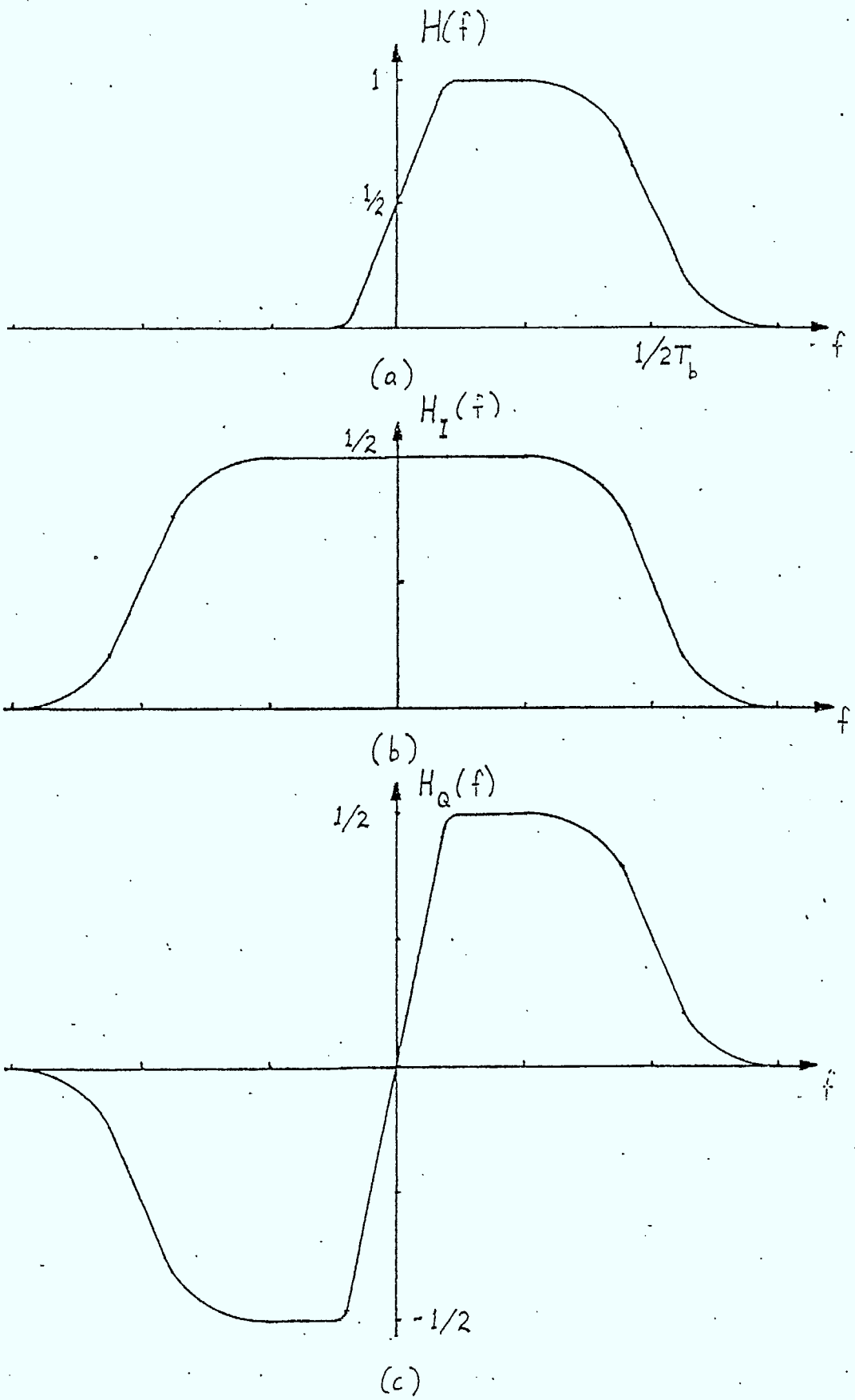

Figure 5: (a) The vestigal sideband transfer function H(f).
(b) The symmetrical component.
(c) The antisymmetrical component.

$H_I(f)$ represents the transfer function of the inphase channel. It is $H_I(f)$ that is the transfer function upon which the pulse shape design is performed. For example $H_I(f)$ has often been chosen to be some type of raised cosine. Usually $H_I(f)$ is chosen to meet or nearly meet Nyquist's first criterion.

The global antisymmetry, about f=0, of $H_Q(f)$ guarantees that the corresponding impulse response is purely imaginary. Therefore, $H_Q(f)$ represents the transfer function of the quadrature channel. In general $H_Q(f)$ will not satisfy Nyquist's first criterion and indeed for the ideal situation there is no reason why it should. However, consider the case where there is some phase offset θ, perhaps due to nonideal carrier recovery*. In this case

$$\tilde{H}(f) = c_1 H(f), \tag{12}$$

where $|c_1| = 1$ and $\arg(c_1) = \theta$. It is straight forward to show that the resulting inphase (i.e. that seen by the sampler) impulse response is

$$h_\theta(t) = (\cos\theta)h_I(t) + (\sin\theta)h_Q(t), \tag{13}$$

where $h_I(t)$ and $h_Q(t)$ are the impulse responses corresponding to $H_I(f)$ and $H_Q(f)$, respectively. Note that even though the "overall" pulse shape satisfies Nyquist's first criterion, significant intersymbol interference can result due to nonideal carrier recovery, because $h_Q(t)$ will not have the desired zero locations! This is in contrast to the usual mode of BPSK transmission where both sidebands are transmitted. An implication of the above observation is

*In practice such a phase offset would typically be slowly time varying.

that a quasi-synchronous detector is likely to exhibit performance that is far from optimal. Ideally what is desirable for carrier recovery is a phase locked loop circuit with a relatively narrow loop bandwidth. However a fairly wide loop bandwidth is necessary for some television applications such as for tracking phase variations originating in video games or resulting from incidental phase modulation due to a poor television transmitter. Perhaps the simplest way to solve this dilemma is to employ a phase locked loop circuit that is switchable between two loop bandwidths, a narrow one for teletext, and a wider one for other applications. Such circuits are fairly standard for high data rate applications because it is often desirable to have a relatively wide loop bandwidth for carrier acquisition and a narrower loop bandwidth for carrier tracking. The variability of the loop bandwidth is usually achieved by switching an additional resistor or capacitor in or out of the loop filter circuit. Also, sideband asymmetry due to the "Nyquist slope" region of the receiver's IF filter can be responsible for a significant amount of time-varying phase offset. Therefore it is desirable that sideband symmetry about the carrier be either retained or re-established prior to carrier recovery [13].

We now return to the multipath problem. Equation (8) can be written in the form

$$\hat{H}(f) = \sum_{p=1}^{P} c_p H(f) e^{-j2\pi f T_p}. \qquad (14)$$

Recalling that the exponential terms correspond to pure delays in the time domain and applying equations (12) and (13) yields the resulting inphase impulse response.

$$h_{MP}(t) = \sum_{p=1}^{P} a_p h_I(t-T_p) + \sum_{p=1}^{P} b_p h_Q(t-T_p), \tag{15}$$

where

$$a_p = |c_p| \cos\theta_p$$
$$b_p = |c_p| \sin\theta_p. \tag{16}$$

Note that the direct path may no longer have unity gain and zero phase because multipath propagation will affect both the phase of the carrier and the AGC. A couple of observations should be made about equation (15). One is that when multipath propagation is present with vestigal sideband transmission, the inphase channel does not experience pure multipath but rather a superposition of the multipath channel operating on both the inphase and quadrature channels. Thus the distortion due to multipath propagation can consist of two components, one from the "inphase channel multipath" and one from the "quadrature channel multipath". It is not difficult to show that the peak overshoot of the ideal inphase signal (i.e. no multipath or phase rotation) will place an upper bound on the amount of eye closure that is due to the "inphase channel multipath" component but the peak overshoot does not appear to be directly related to the amount of eye closure due the "quadrature channel mulipath component". It should be noted that the rather simplistic model used in [2] and [3] does not encompass quadrature multipath, since that model only allows real path gains. However characterization

of multipath at complex baseband usually requires complex path gains*. Thus although there is some relationship between the peak overshoot and the sensitivity to multipath, the relationship is a relatively weak one.

On several occasions it has been pointed out that in order to perform near optimal equalization for multipath propagation a complex equalizer (i.e. one that operates on both the inphase and quadrature signals) is required. However for vestigal sideband communication the complex signal is still required for optimal performance even when no equalization is necessary. Surprisingly the author has never seen this point brought out in the teletext literature even though a great deal of effort has gone into coding and pulse shaping in an effort to squeeze an extra couple of dBs of performance out of the system. From Figure 5 it can be seen that, in the absence of multipath propagation, an equivalent model to the one in Figure 1 is the model that is illustrated in Figure 6. Absolutely no use is being made of the signal energy that is transmitted in the quadrature channel, which is almost as much as the signal energy in the inphase channel. In fact the SNRs of these two channels will usually be almost the same. However the noise in the inphase and quadrature channels will be highly correlated, so the gain from utilizing the energy in the quadrature channel may be marginal. Ideally, maximum likelihood sequence estimation could be used on the received complex signal in order to make use of the energy in the quadrature channel. Unfortunately maximum likelihood sequence estimation is probably not practical at teletext bit rates. A more practical scheme is illustrated in Figure 7. Note that a fixed decision feedback equalizer is necessary to achieve

*Channel measurements performed by CRC have clearly demonstrated that complex path gains are required to characterize the multipath channel.

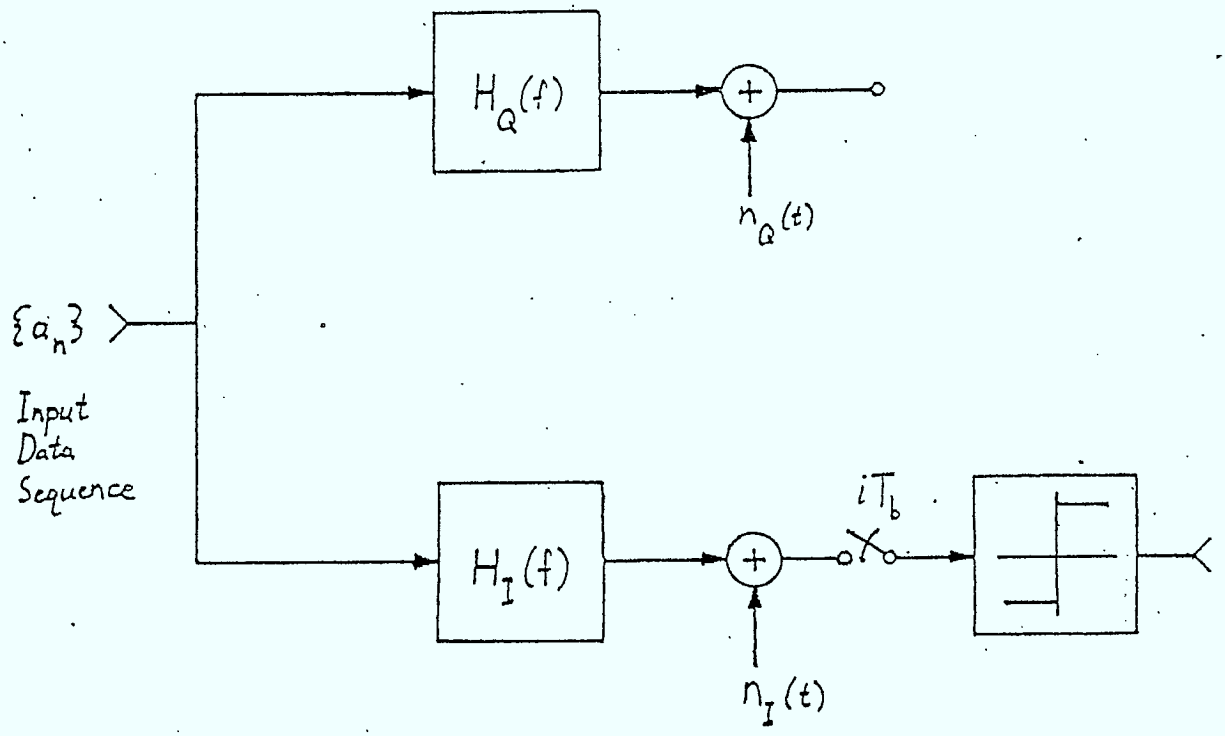

Figure 6: A complex baseband model that is equivalent to the one shown in Figure 1, under the assumption that no multipath propagation or carrier phase offset is present.

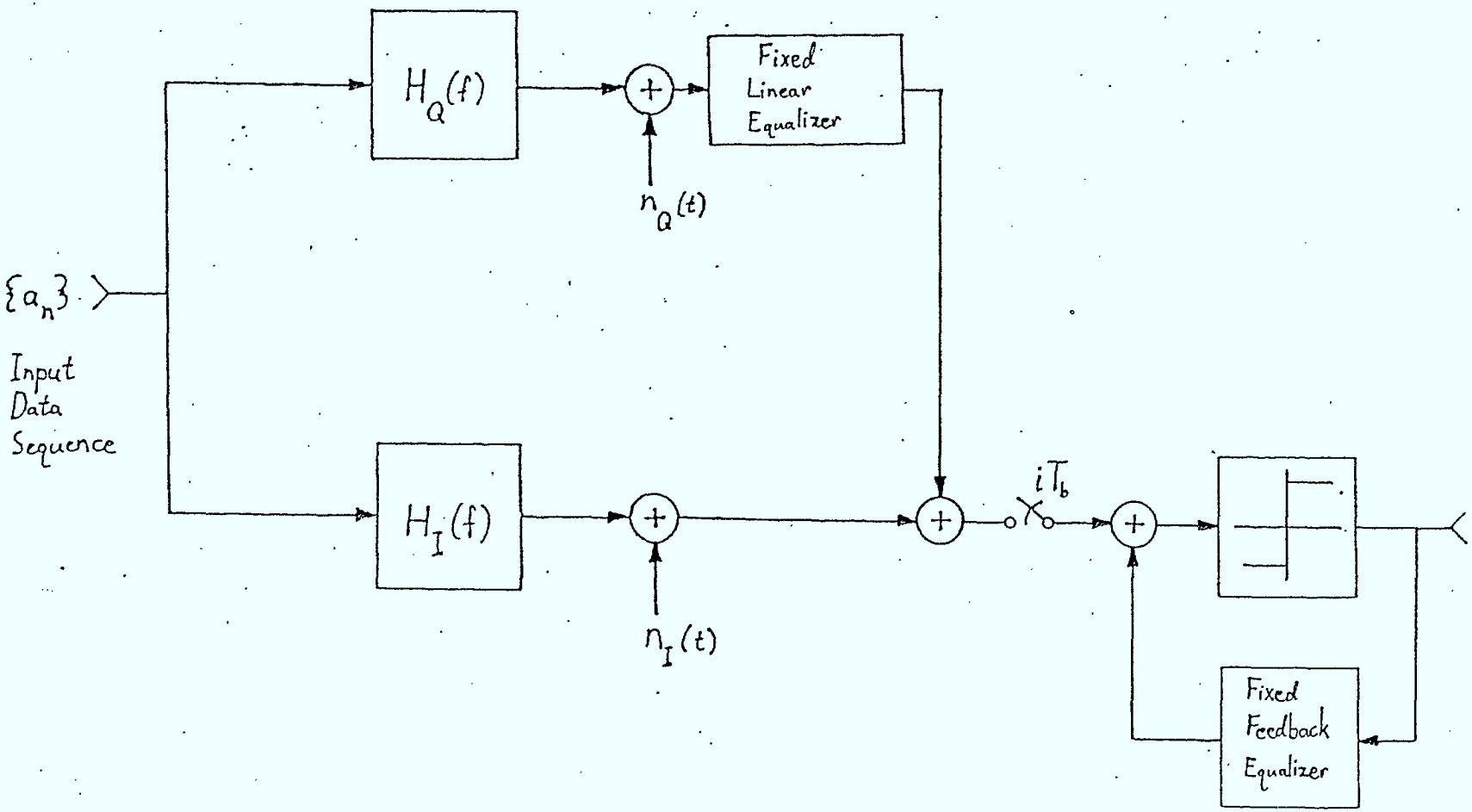

Figure 7: A scheme that makes use of the signal energy in the quadrature channel.

nearly optimum performance because of the null at f=0 in the quadrature channel. It should be emphasized that the fixed equalization discussed here is simply for utilizing signal energy in the quadrature channel and should not be confused with adaptive equalization for the compensation of multipath propagation.

The above discussion leads to an interesting question. Why was vestigal sideband BPSK chosen as the modulation technique in the first place? In many ways it seems like a rather cumbersome choice. The author suspects that this modulation technique was chosen by historical evolution rather than by some conscious effort to choose an appropriate technique. For example QPSK on a subcarrier (of approximately 2.1 MHz) has the following advantages over vestigal sideband BPSK.

- Most of the energy in both the inphase and quadrature channels can be used without the need of fixed equalizers.

- The fact that the television carrier is no longer placed in the data signal spectrum, greatly eases the slicing level problem. (This problem will be discussed in a later section.)

- Nyquist slope incidental phase modulation would be reduced because less teletext signal energy is in the vicinity of the carrier (see Section 5.0).

Other bandwidth efficient modulation techniques may yield different advantages. The choice of modulation technique is not discussed further here, and is left as an open (and probably academic) problem.

3.0 A GOOD OVERALL PULSE SHAPE

In the work of Sousa and Pasupathy [2][3] certain properties of the eye diagram (e.g. eye height and eye width) were used as figures of merit for various pulse shapes. Here, the profile of the eye will also be used as a basis for comparison. Justification for this is not given here because the interested reader can consult references [2] and [3] for such justification. The transfer function, impulse response, and eye diagram that correspond to a pulse shape that is almost the same as the one outlined in BS-14 [7], can be seen in Figure 8. Here we assume that the peak teletext signal levels in the receiver must be constrained to within specified limits. Note that there will also be a constraint on the signal levels at the transmitter, but this constraint will be discussed in the following section. For the purpose of overall pulse shape design it will be assumed that the peak constraint at the receiver is active. Given this peak constraint a reasonable figure of merit is a/c (i.e. the ratio of the eye opening to the peak-to-peak signal level). Ideally, a/c is equal to 1. However, this requires a bandwidth at least as great as the symbol rate (e.g. the triangular transfer function of [2]). Thus some degradation on this figure of merit must be accepted due to the bandwidth constraint of 4.2 MHz. For the pulse shape of Figure 8, a/c is approximately 0.65 (-3.7 dB). The eye width, which is another important figure of merit, is about 0.9. (Recall that the bandwidth limitation prevents us from simultaneously meeting Nyquist I and achieving an eye width of 1).

Sousa and Pasupathy [2][3] developed their recommended pulse shape by finding the one that minimized the squared error in the Nyquist II criterion subject to the Nyquist I criterion. The transfer function, impulse response, and eye diagram that corresponds to this pulse shape are shown in

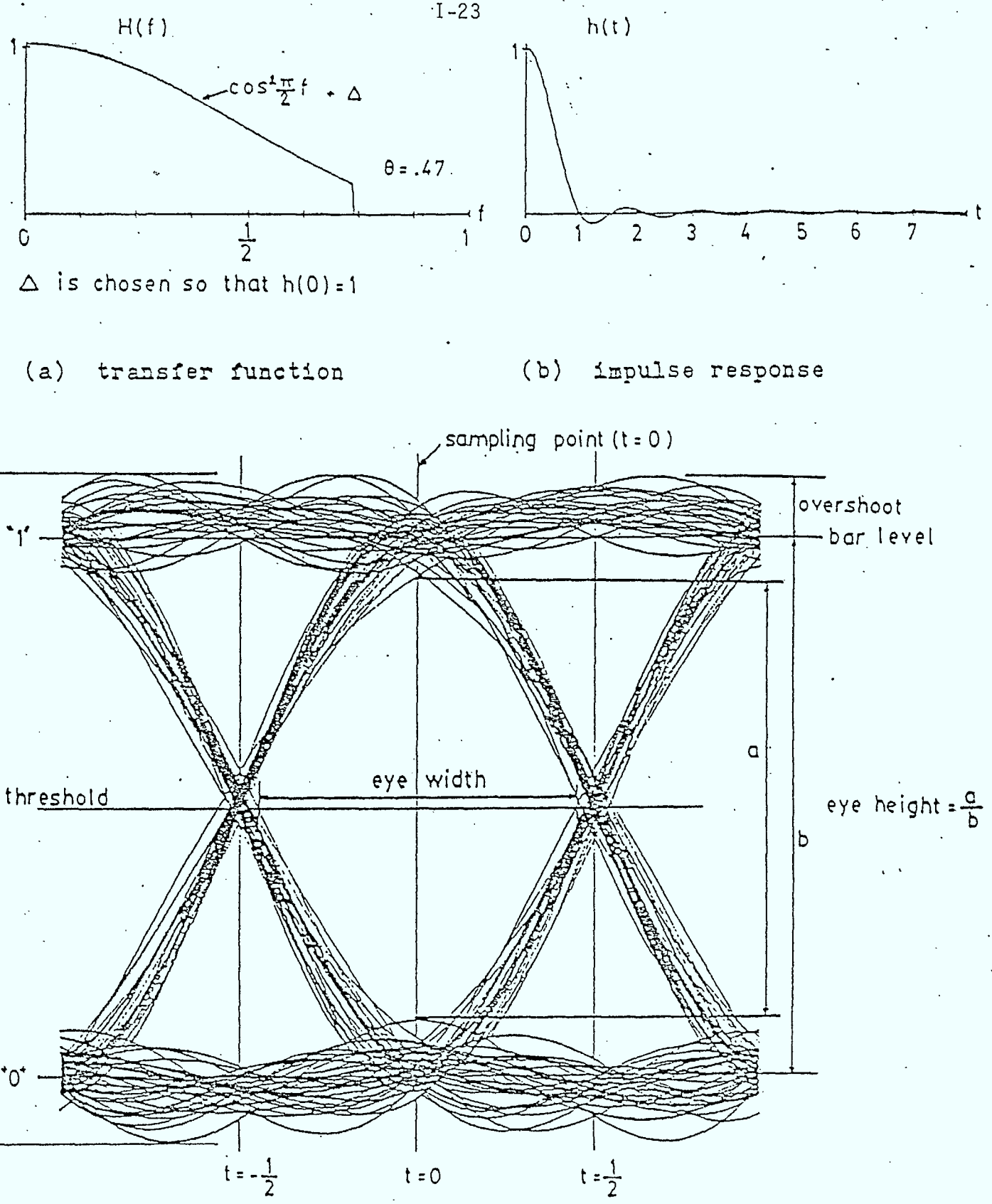

Figure 8: The transfer function, impulse response, and eye diagram corresponding to a pulse shape that is almost the same as the one specified in BS-1# (from [2]).

Figure 9. It can be seen that for this pulse shape a/c is about 0.75 (-2.5 dB) and the eye width is approximately 0.83. Thus, some eye width has been sacrificed, while a/c has improved by about 1 dB. Although the recommended pulse shape of Sousa and Pasupathy has some interesting properties, the discontinuities in the transfer function are troublesome from several points of view. Obviously such a pulse shape would be very difficult to approximate in practice. Also, the long tail and precursor that results from the discontinuity will tend to aggravate the peak and eyewidth problems. The approach used here was to use a Hamming window [10] on the impulse response of Figure 9. Since this window is simply a multiplication in the time domain, it preserves Nyquist's first criterion. Ideally, we would like a relatively short window in order to keep the duration of the resulting impulse response as short as possible. However, the shorter the window the more smeared will be the resulting frequency response. Therefore it is desirable to choose as short a window as possible that still leaves most of the signal energy in the 4.2 MHz bandwidth. A reasonable tradeoff between these two considerations resulted in the transfer function that is shown in Figure 10. The analytical expression for this transfer function is

$$\begin{aligned} H(f) = {} & 0.501 + 0.543 \cos[0.54856f] \\ & - 0.015 \cos[(3)(0.54856)f] \\ & - 0.035 \cos[(5)(0.54856)f] \\ & - 0.002 \cos[(7)(0.54856)f] \\ & + 0.012 \cos[(9)(0.54856)f] \\ & - 0.003 \cos[(13)(0.54856)f], \end{aligned} \tag{17}$$

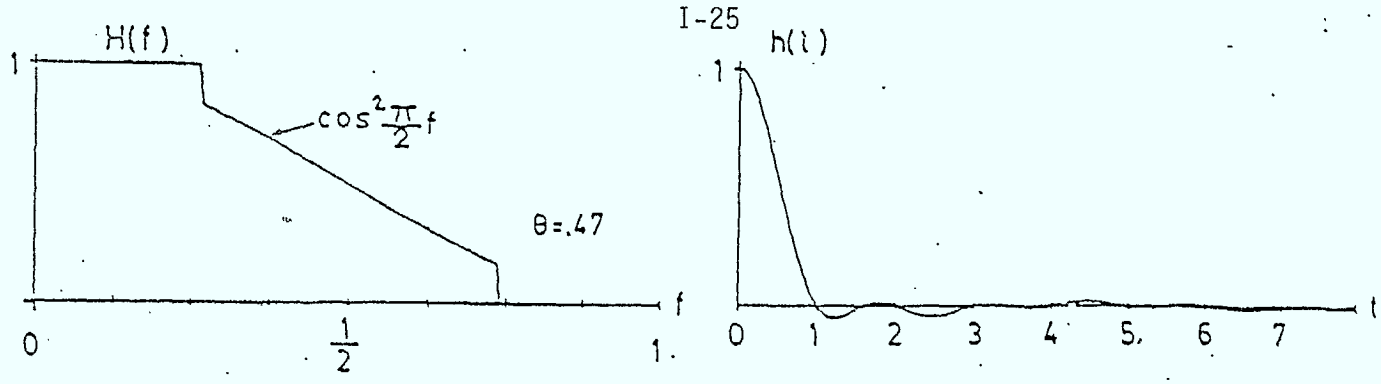

(a) transfer function (b) impulse response

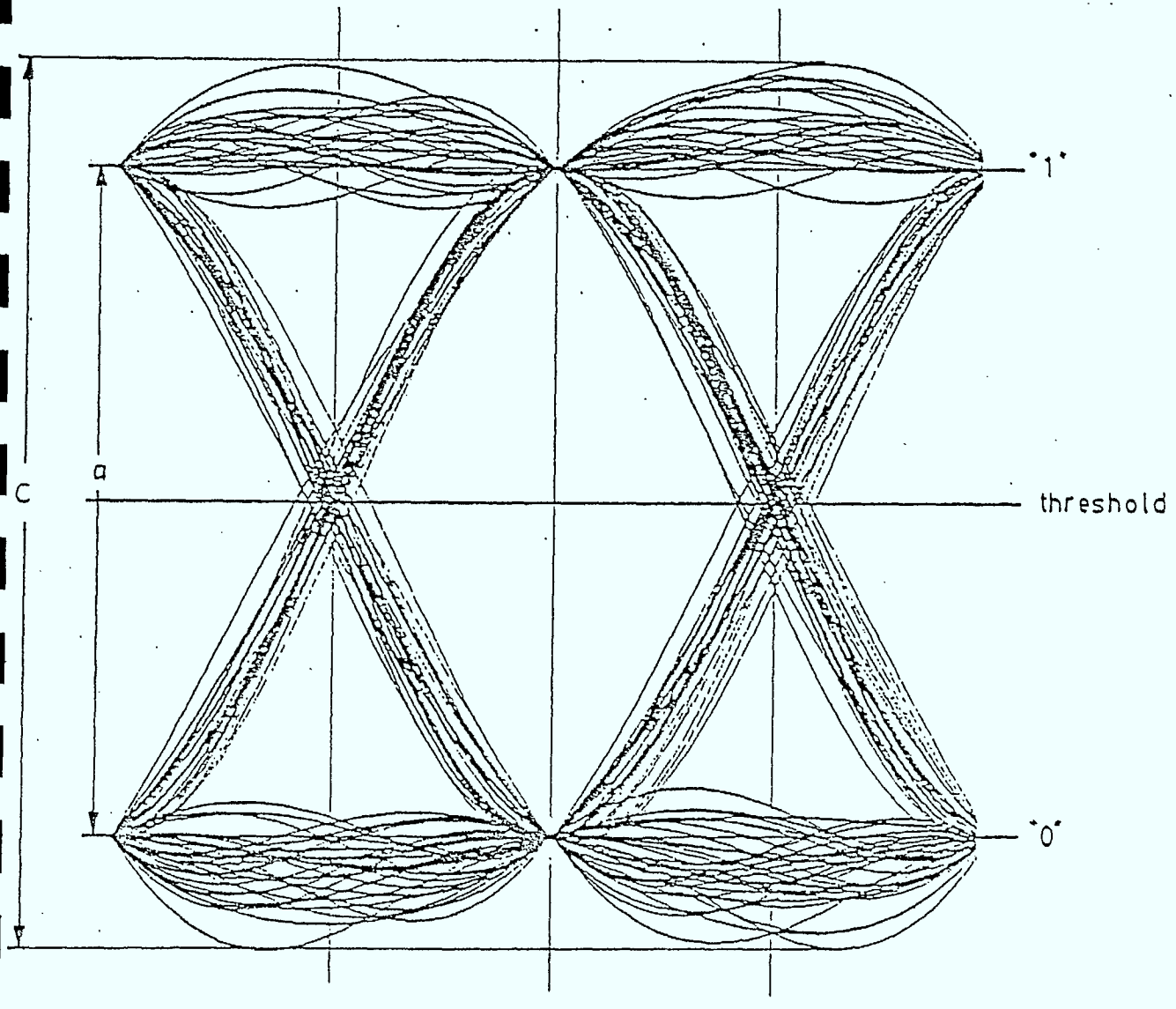

(c) eye diagram

Figure 9: The transfer function, impulse response, and eye diagram that correspond to the pulse shape recommended in [2] and [3].

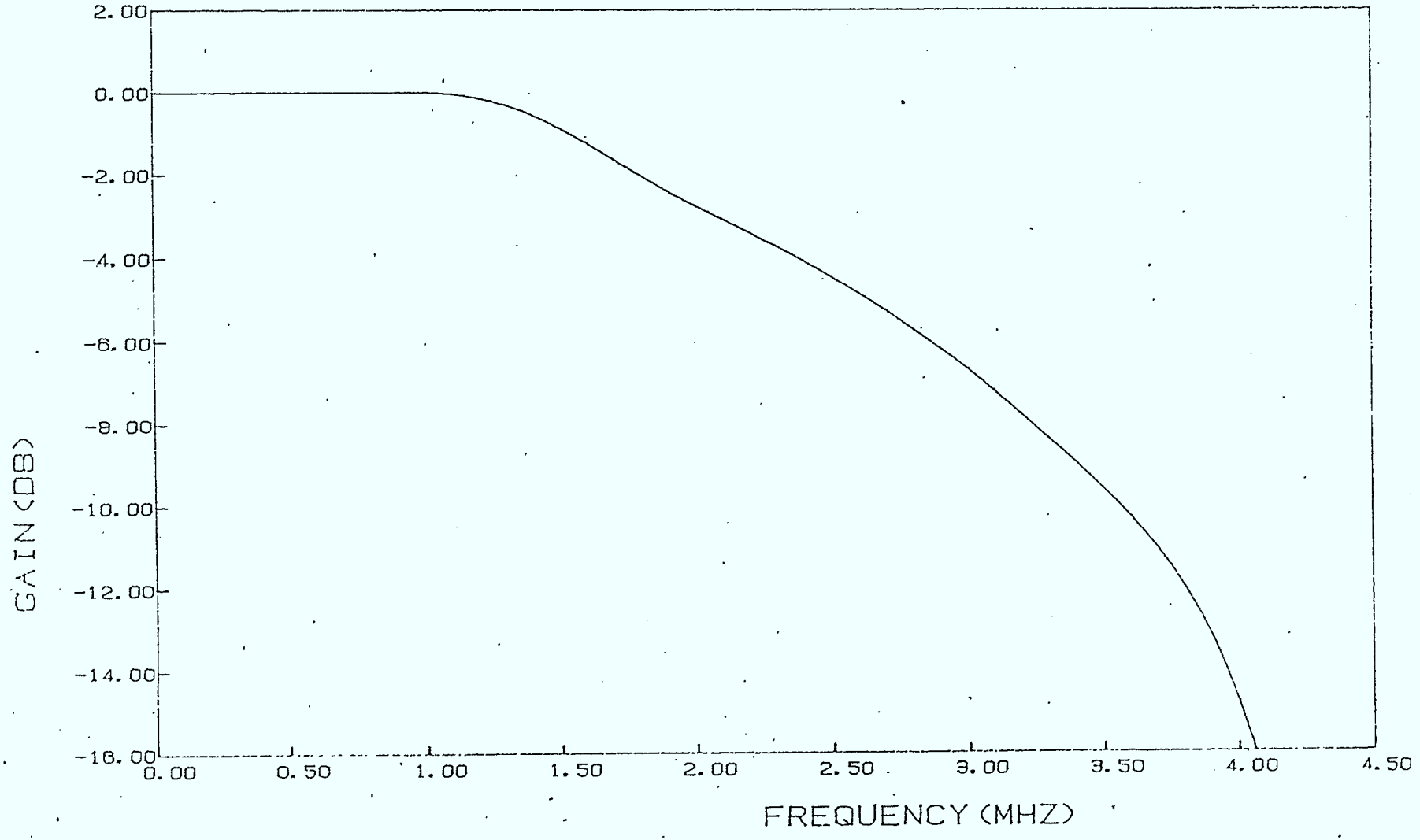

Figure 10: The transfer function that is given by equation (17).

where f is in MHz. This transfer function is down about 20 dB at 4.2 MHz, and down to about 33 dB at 4.5 MHz. The corresponding impulse response is shown in Figure 11. The eye profile corresponding to this pulse shape is shown in Figure 12. It can be seen that a/c is approximately 0.82 (-1.7 dB) and the eye width is about 0.9. Interestingly this pulse shape yields a 2 dB improvement in a/c over the pulse shape of Figure 8 without sacrificing eye width! The relatively flat peak of the eye profile suggests to the author that the -1.7 dB degradation in a/c is probably very close to the optimum for the given bandwidth. This suspicion follows from the fact that a minimax optimum point is characterized by the property that it is not possible to "push" one maximum point down without "pushing" another maximum point up. Unfortunately this pulse shape is not truly bandlimited due to spectral spreading by the Hamming window. The gain is down 33 dB at the sound carrier of 4.5 MHz. This is probably too high particularly after the "nominal receiver transfer function" is divided out. Thus it seems reasonable to consider a transfer function that is similar to the one given in equation (17), but is more strictly bandlimited. Such a transfer function is given by

$$
\begin{aligned}
H(f) = {} & 0.501 + 0.543 \cos[0.54856f] \\
& - 0.015 \cos[(3)(.54856)f] \\
& - 0.035 \cos[(5)(0.54856)f] \\
& - 0.002 \cos[(7)(0.54856)f] \\
& + 0.012 \cos[(9)(0.54856)f] \\
& - 0.003 \cos[(13)(0.54856)f]; \quad |f| \leq 4.0 \\
H(f) = {} & -0.1883|f|^2 + 1.125|f| - 1.3045; \quad 4.0 \leq |f| \leq 4.4 \\
H(f) = {} & 0. \qquad\qquad\qquad\qquad\qquad\qquad ; |f| \geq 4.4,
\end{aligned}
\tag{18}
$$

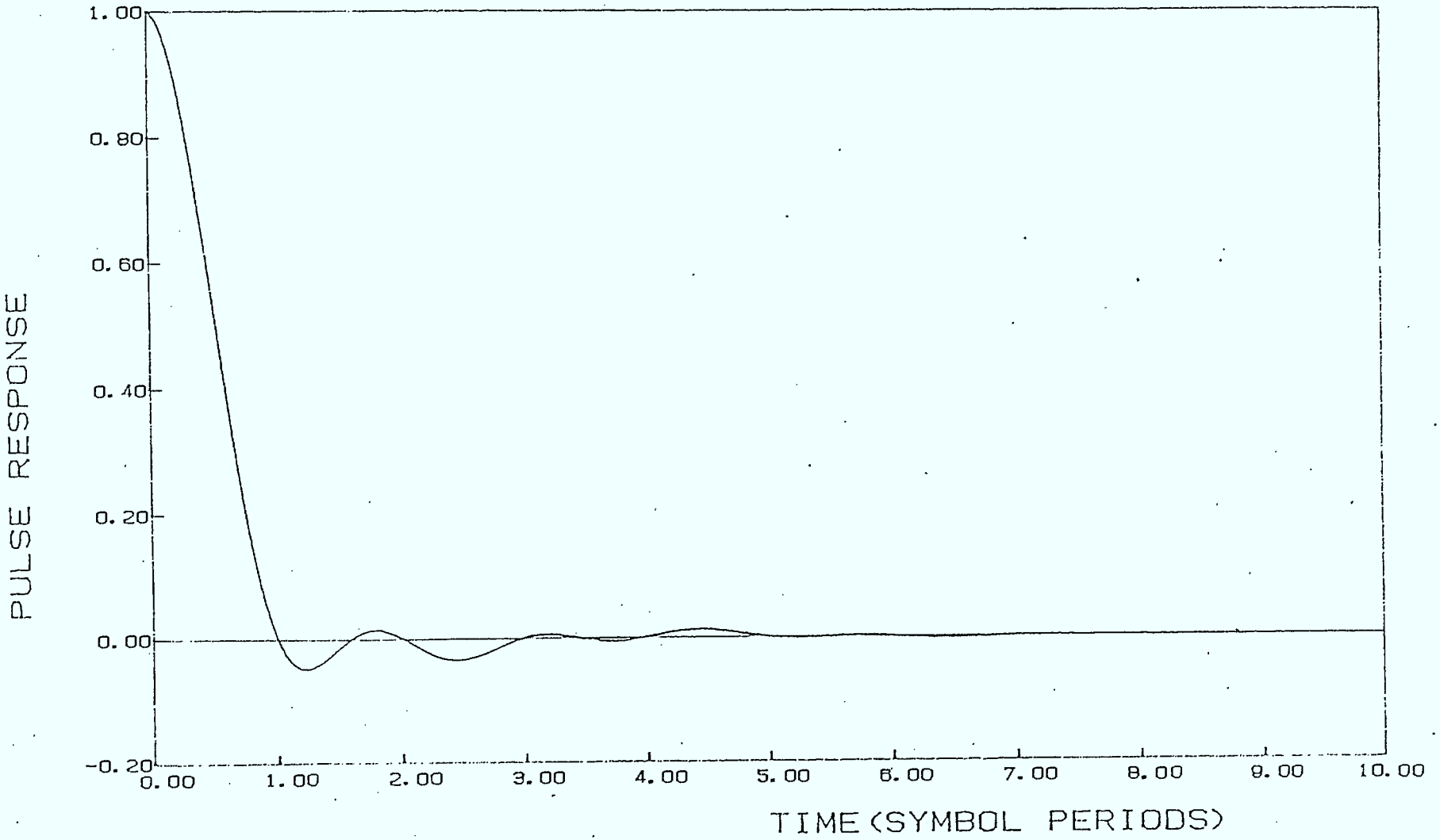

Figure 11: The impulse response corresponding to the transfer function that is given by equation (17).

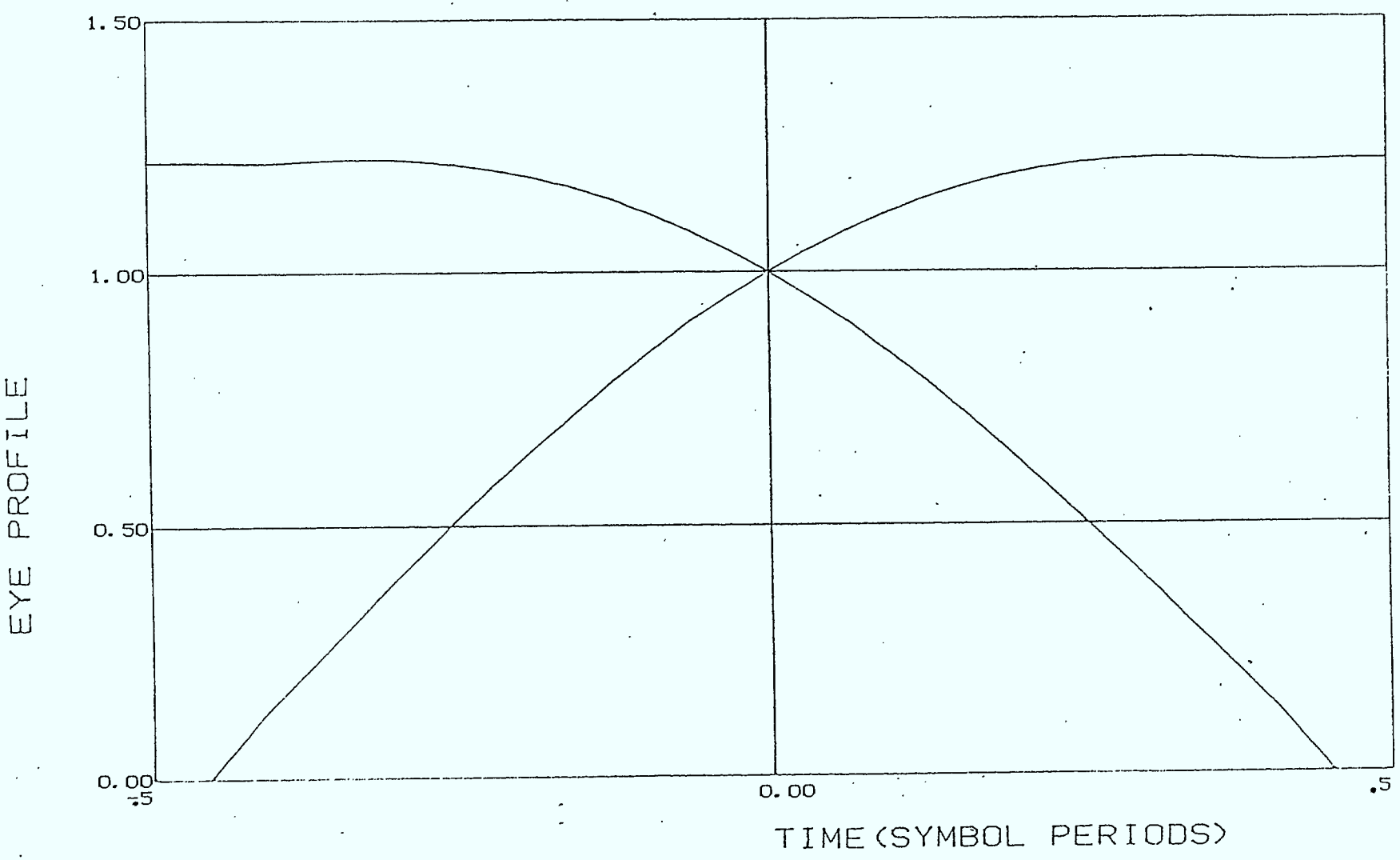

Figure 12: The eye profile that corresponds to the transfer function that is given by equation (17).

where f is in MHz. This transfer function is shown in Figure 13. Note that this frequency response is identical to the one in Figure 10, out to 4.0 MHz, and they are still within 0.5 dB at 4.2 MHz. But after 4.2 MHz, the transfer function in Figure 13 drops off very rapidly and is effectively zero by the time it is within 100 kHz of the sound carrier. The corresponding impulse response is shown in Figure 14. This impulse response is almost indistinguishable from the one in Figure 11 except that its overshoots and undershoots are slightly larger and its tail does not die out quite as quickly. The eye profile is shown in Figure 15. For this eye, a/c is approximately 0.77 (-2.3 dB). Thus the apparently minute change in the transfer function has resulted in a loss of about 0.5 dB! Note however that this a/c is still about 1.4 dB better than that for the truncated 100% raised cosine transfer function in Figure 8. The eye height and eye width for the eye profile shown in Figure 15 are 0.96, and 0.89, respectively. Both of these values are quite acceptable given bandwidth limitation. Due to the generally good properties of the transfer function given in equations (18), this transfer function is recommended as the nominal overall pulse shape transfer function.

Before leaving the general subject of choice of nominal overall pulse shapes, it is probably worthwhile having a general discussion about "optimal" overall pulse shapes. Several overall pulse shapes were derived in references [2] and [3] that are in some sense optimal. Hamming windows have been applied to some of the more promising of these pulse shapes in order to make their transfer functions continuous (i.e. realizable). The resulting transfer functions are shown in Figure 16. The curve labels (i.e. 2C, 2D, 2E, 2F, 2G) refer to Figure 2 of reference [3]. The curve labelled 2E is the transfer function that is given by equation (17). Note that for most of the frequency range of

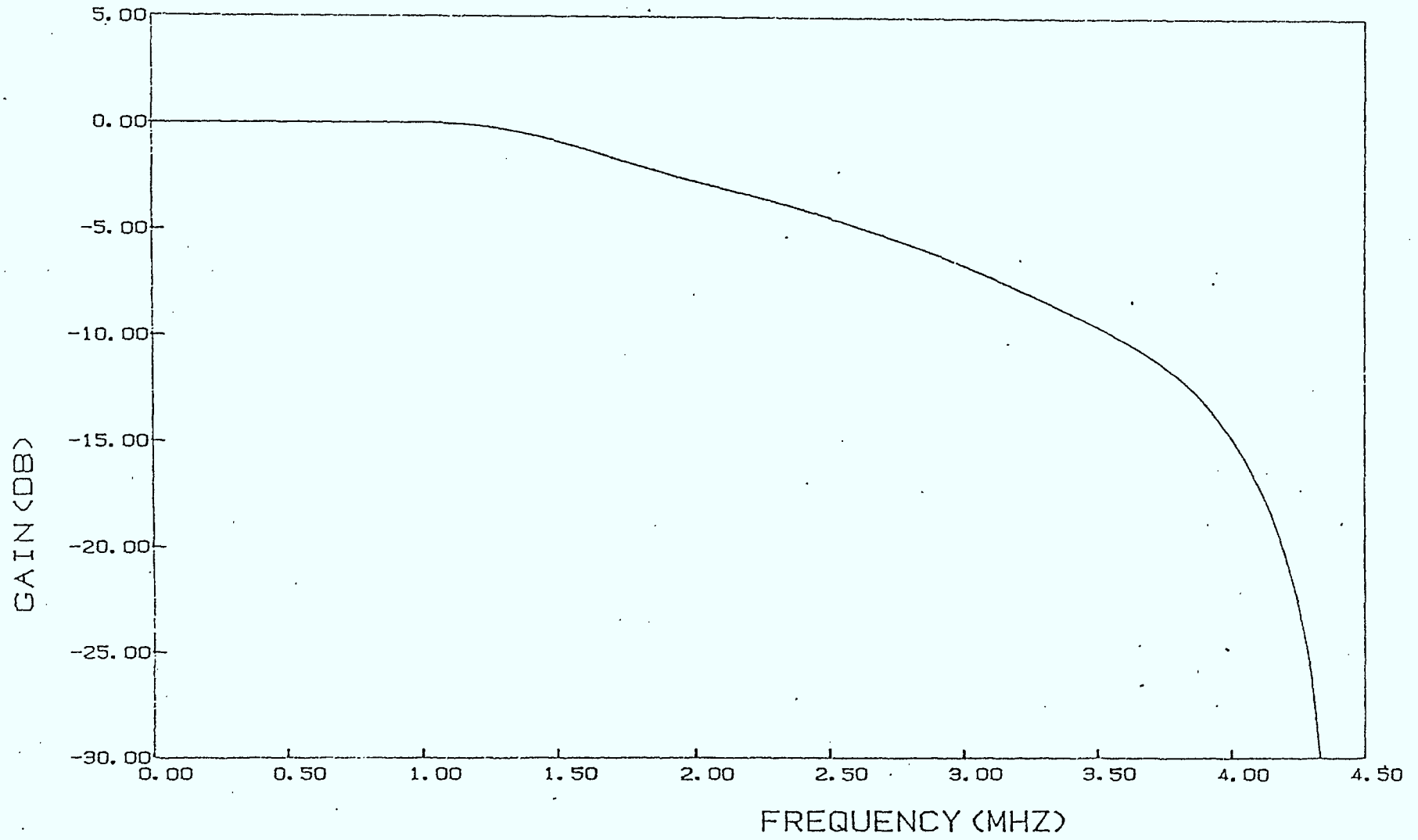

Figure 13: The transfer function that is given in equations (18).

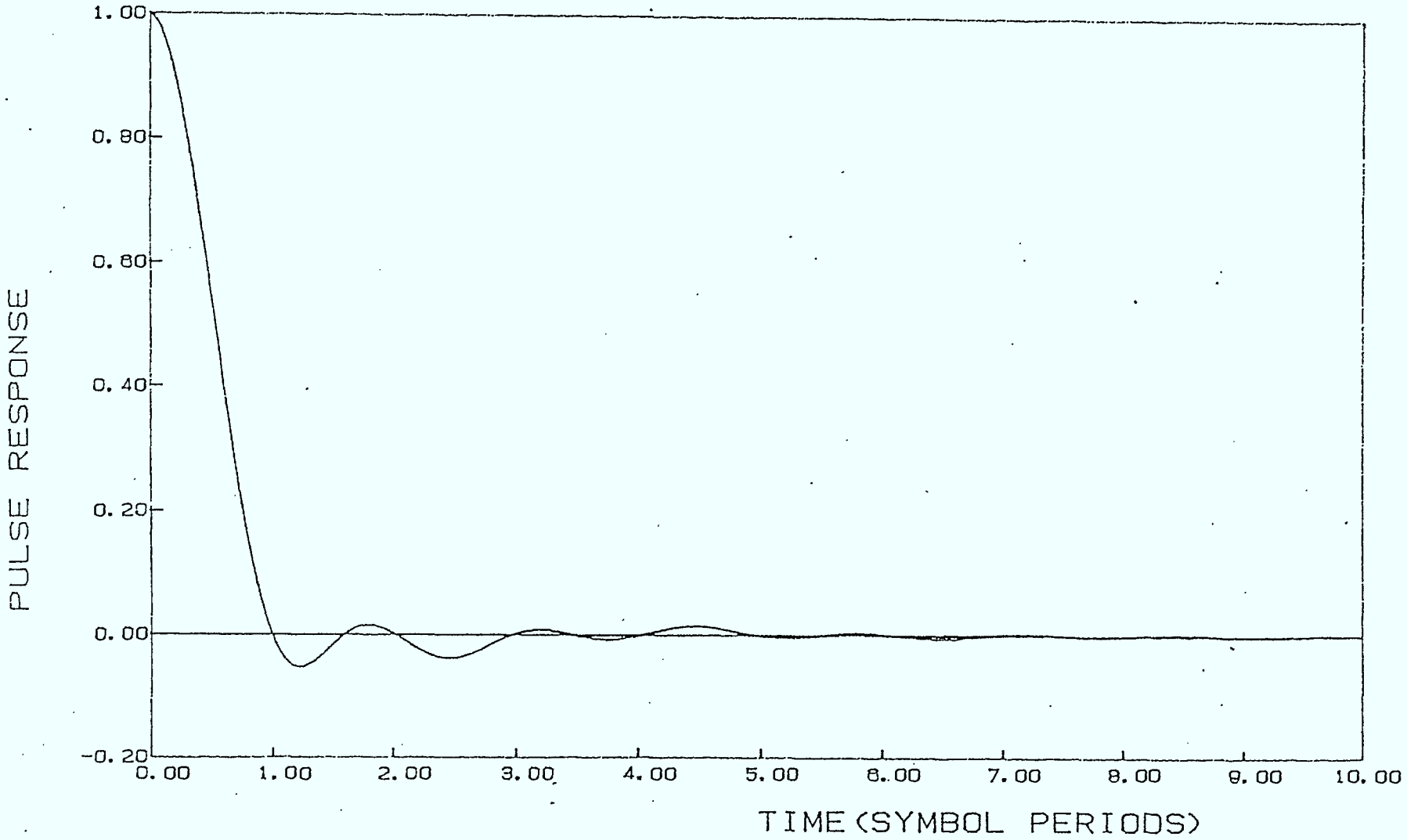

Figure 14: The impulse response corresponding to the transfer function that is given by equations (18).

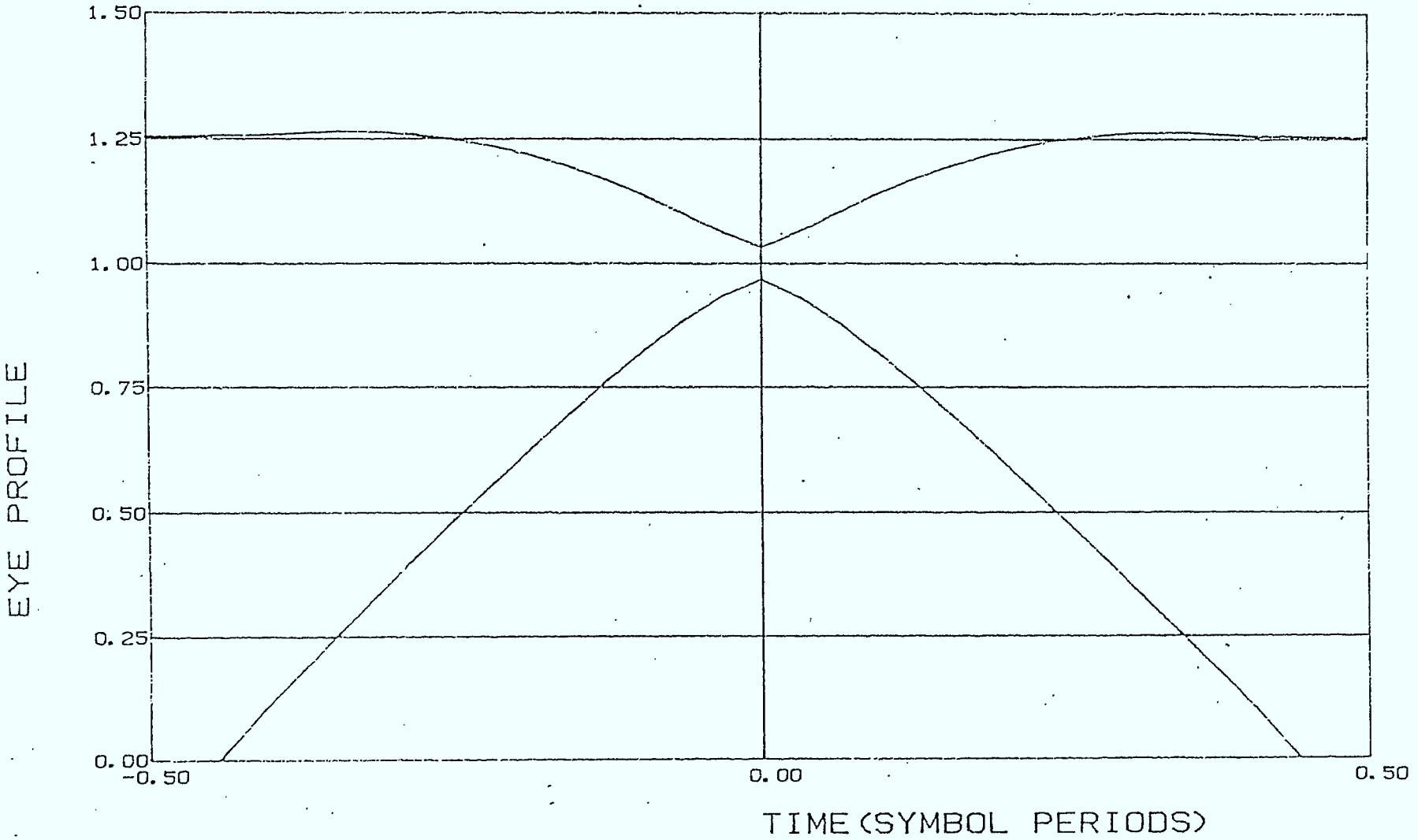

Figure 15: The eye profile that corresponds to the transfer function that is given by equations (18).

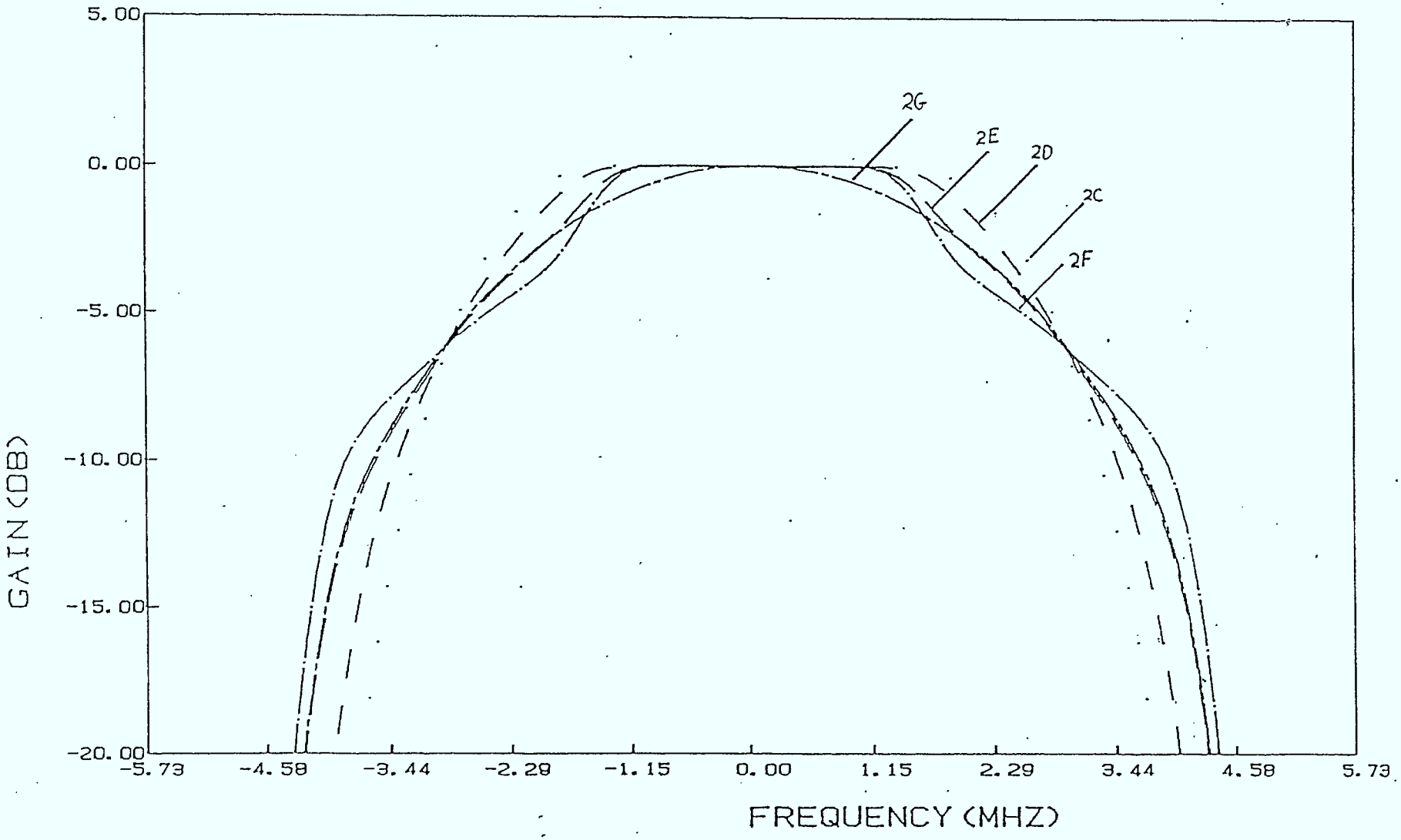

Figure 16: The transfer functions of some of the pulse shapes derived in [3], after a Hamming window has been applied to the impulse responses.

interest, all of the curves are within 2 dB of curve 2E (at least until the gain drops below 10 dB). The similarity of these transfer functions should not be to surprising because in order to result in little intersymbol interference all of the transfer functions must be approximaely 0 dB from 0 to 1.527 MHz, and -6 dB at 2.86 MHz. Furthermore, they all face the same bandwidth restriction and they all must be fairly smooth. Given that an optimal pulse shape transfer function will likely be within 2 dB of the recommended nominal transfer function and given that the uncertainty in the combined channel (i.e. the transmit equipment, the propagation path, and the receive equipment) will often exceed 2 dB, it may be that we are already reaching the point of diminishing returns in the optimization of the overall pulse shape. Recall that the transfer function due to a direct path of unity gain and a single reflected path is given by

$$M(f) = 1 + ce^{-j2\pi fT}. \qquad (19)$$

This transfer function has a "rippled" magnitude response and a "rippled" group delay characteristic. The size of the magnitude response ripple as a function of the strength of the reflected path is shown in Figure 17. Note that even for a relatively modest multipath channel consisting of a single reflected path that is 10 dB weaker than the direct path, the resulting overall transfer function would be 2.4 dB higher than nominal at some frequencies and -3.3 dB lower than nominal at some other frequencies. The above discussion suggests that optimal pulse shaping is not likely to be an effective weapon against multipath propagation. This would imply that the pulse shape should be designed for good channels (ie. no multipath) and that any channel that is severely corrupted by multipath should be equalized at the receiver.

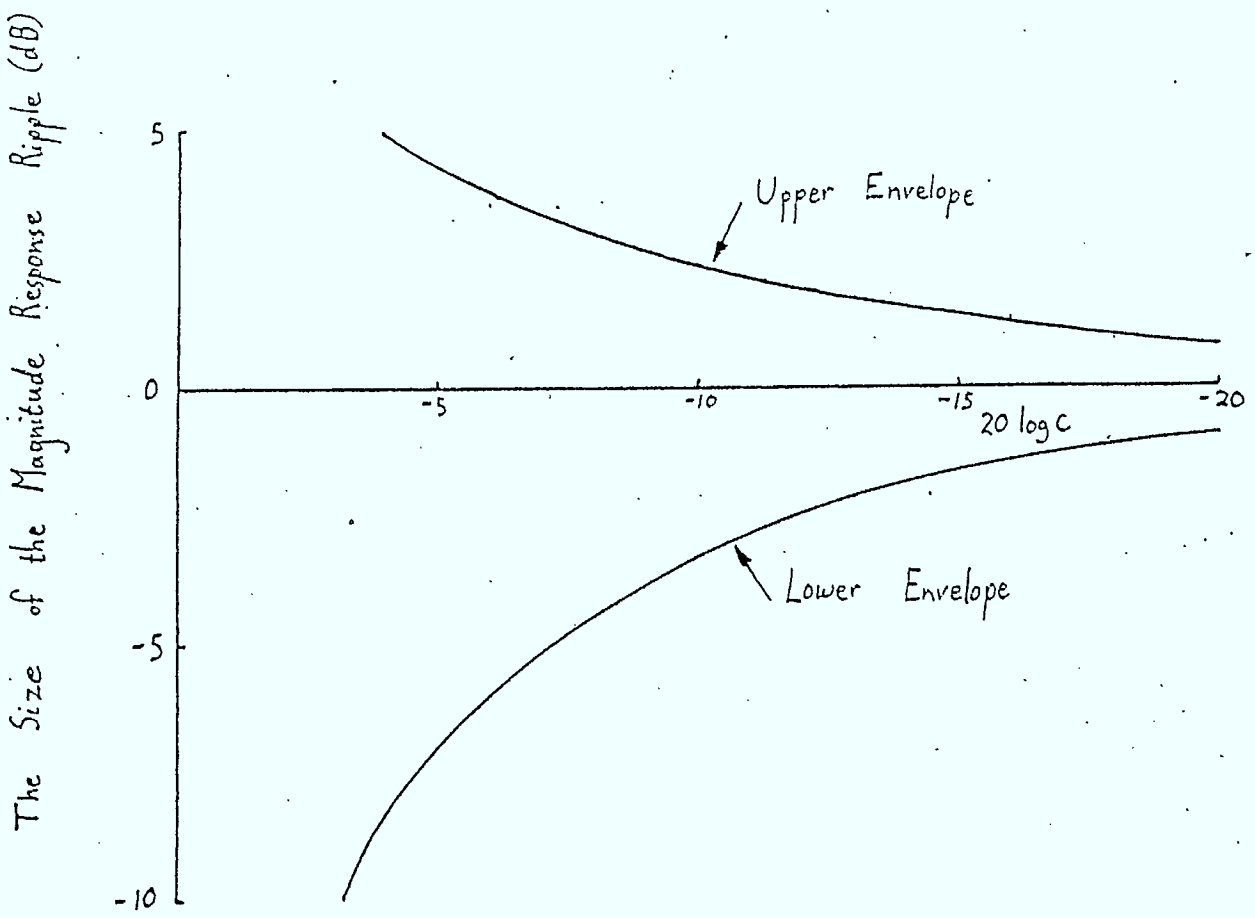

Figure 17: The size of the magnitude response ripple as a function of the strength of the reflected path.

4.0 PULSE SHAPE APPORTIONING AND SPECIFICATION

In this section pulse shape apportioning and specification are discussed. The discussion takes the form of a suggested approach, with examples, as opposed to a recommendation. The reason for this is that before any set of teletext specifications is adopted, significant involvement is required from the television broadcast community, the CATV community, and the television manufacturers in order that a reasonable balance between economic factors and performance can be achieved.

Before proceeding, it is probably useful to say a few words about the specifications in general. In the author's view the main purpose for the teletext specification is to provide guidelines to the manufacturers and suppliers (of consumer equipment, transmission equipment, and the teletext signal) so that a desirable degree of uniformity (i.e. compatibility) is achieved. The specification should not be any more restrictive than necessary as to how a given goal should be met. (This point should become clearer shortly.) Also, specifications should not be used for areas in which market forces are more likely to find the optimal balance of cost and performance than are the authorities responsible for the specification. However, in this case recommendations (as opposed to specificaions) are sometimes desirable. The author feels that the consumer teletext receive equipment falls in this category. In time, the market itself will determine how much performance the consumer is willing to pay for. Clearly, this will be a time-varying function that is highly dependent upon technical development. It would be prudent however, to recommend a nominal receiver characteristic that can be economically realized.

In order to produce a reasonable specification for the transmit filter, it is necessary to assume some nominal

characteristic for the receivers. Obviously, the television manufacturers should have some input to the choice of nominal characteristic. For the purpose of discussion, we will use the response of a Zenith receiver cascaded with a 4.5 MHz intercarrier sound trap and a single tuned video peaking circuit [5], as the nominal characteristic. The corresponding magnitude response is shown in Figure 18 (curve a). Also shown in Figure 18 is the magnitude response of the transmit pulse shape which is obtained by dividing the magnitude response of equations (18) by the nominal receiver magnitude response. Note that curve b is a composite response that includes the effects of the transmit antenna, the RF harmonic filter, the IF filter, the baseband teletext transmit filter, and the sine(x)/x characteristic due to NRZ signalling. Also, the group delay response of the transmit pulse shape should be such that when summed with the group delay response of the nominal receiver the resultant is a constant group delay. Note that it is the composite transmit pulse shape (e.g. curve b) that should be specified. The broadcaster should not be restricted as to how he meets the specification (i.e. how much of the shaping is performed at baseband, IF, etc.). For example, it may be the case in the future that it is desirable to insert the data at IF so that pulse shaping can be done at IF (e.g. using SAW filters) and so that IF equalization for teletext and television signals can be performed independently. In this case the horizontal axis becomes the frequency relative to visual carrier. The specification should be in the form of a magnitude response mask and a group delay response mask. The tolerances will in general be the result of a tradeoff between the performance and the cost of realization and maintenance. This tradeoff should be evaluated with care before the specification is made. However as a starting point we suggest the following tolerances as representing a reasonable compromise between cost and performance. For the magnitude response, the

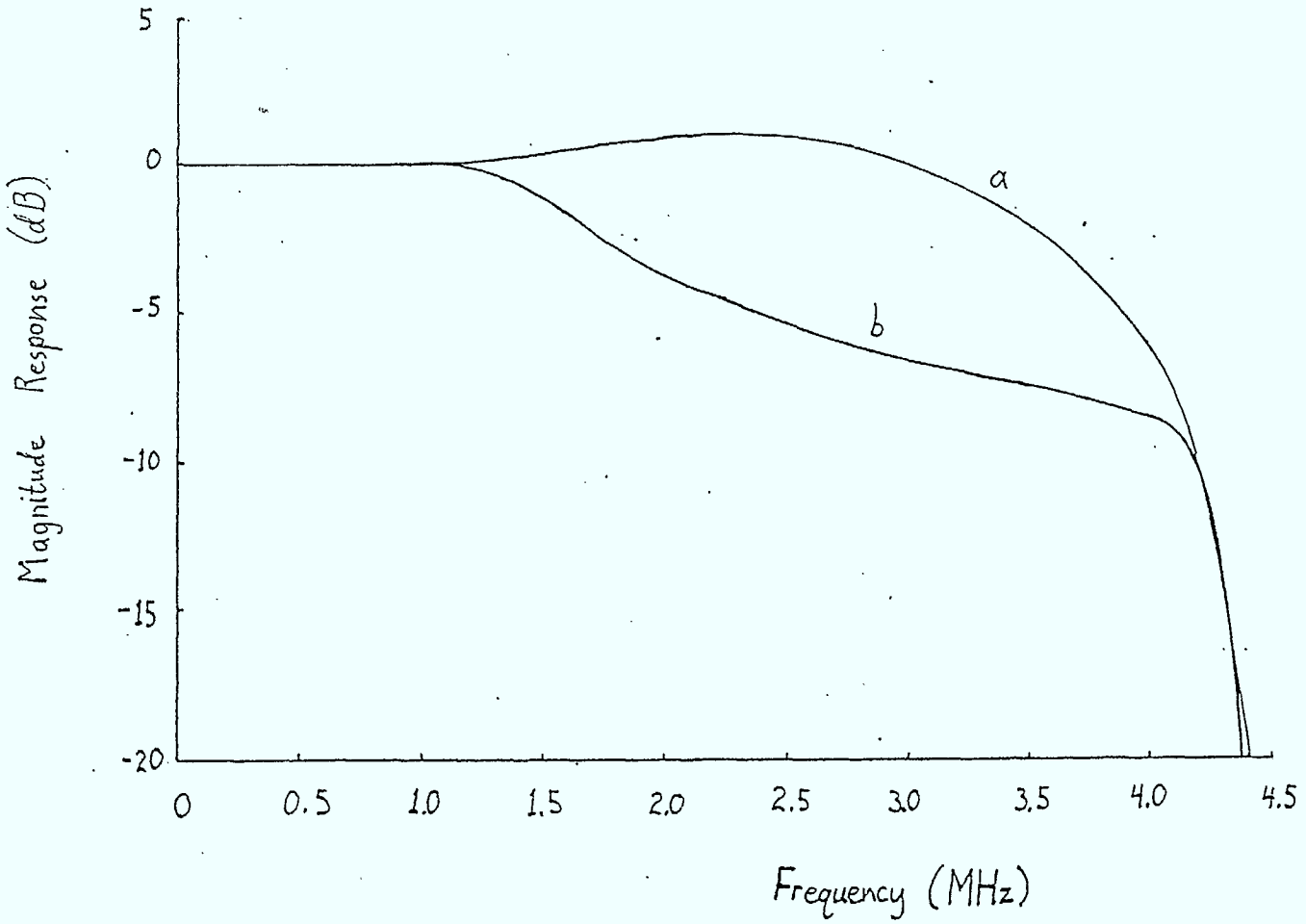

Figure 18: (a) An example of a nominal receiver magnitude characteristic [5].
(b) The magnitude characteristic resulting from dividing the characteristic of equations (18) by the nominal receiver characteristic.

measured response $|H(f)|$ should be within the following tolerances of the nominal response (e.g. curve b))

$$\begin{aligned} &\pm 0.5 \text{ dB} ; && -0.5 \leq f \leq 4.0 \\ &\pm 1.0 \text{ dB} ; && 4.0 \leq f \leq 4.2 \\ &\pm 3.0 \text{ dB} ; && 4.2 \leq f \leq 4.35 \\ &20 \log|H(f)| \leq (-227f + 958.8) \text{ dB}; && 4.35 \leq f \leq 4.4 \\ &|H(f)| \leq 40 \text{ dB} ; && f \geq 4.4, \end{aligned} \tag{20}$$

where f is the frequency relative to the visual carrier in MHz. For $f \leq -0.5$, the current magnitude mask of television broadcasting is probably appropriate (see Figure 19) [11]. For the group delay response, the measured response should be the complement of the nominal receiver's group delay response within the following tolerance

$$\pm 40 \text{ nsec} ; \quad -0.3 \leq f \leq 4.2, \tag{21}$$

where f is the frequency relative to the visual carrier in MHz. The above group delay tolerance was chosen because it ensures that all of the frequency components arrive within a quarter of a symbol period of the desired time.

It is desirable that the peak amplitude of the transmitted signal be constrained to the region in which the power amplifier is fairly linear, in order to avoid signal distortion, which in turn can result in interference to the sound carrier [12] and degrade the performance of the data transmission. Clearly the transmit pulse shape will affect the peak amplitude of the transmitted signal. An illustration of a possible transmit magnitude response can be seen in Figure 20. This response is subdivided into

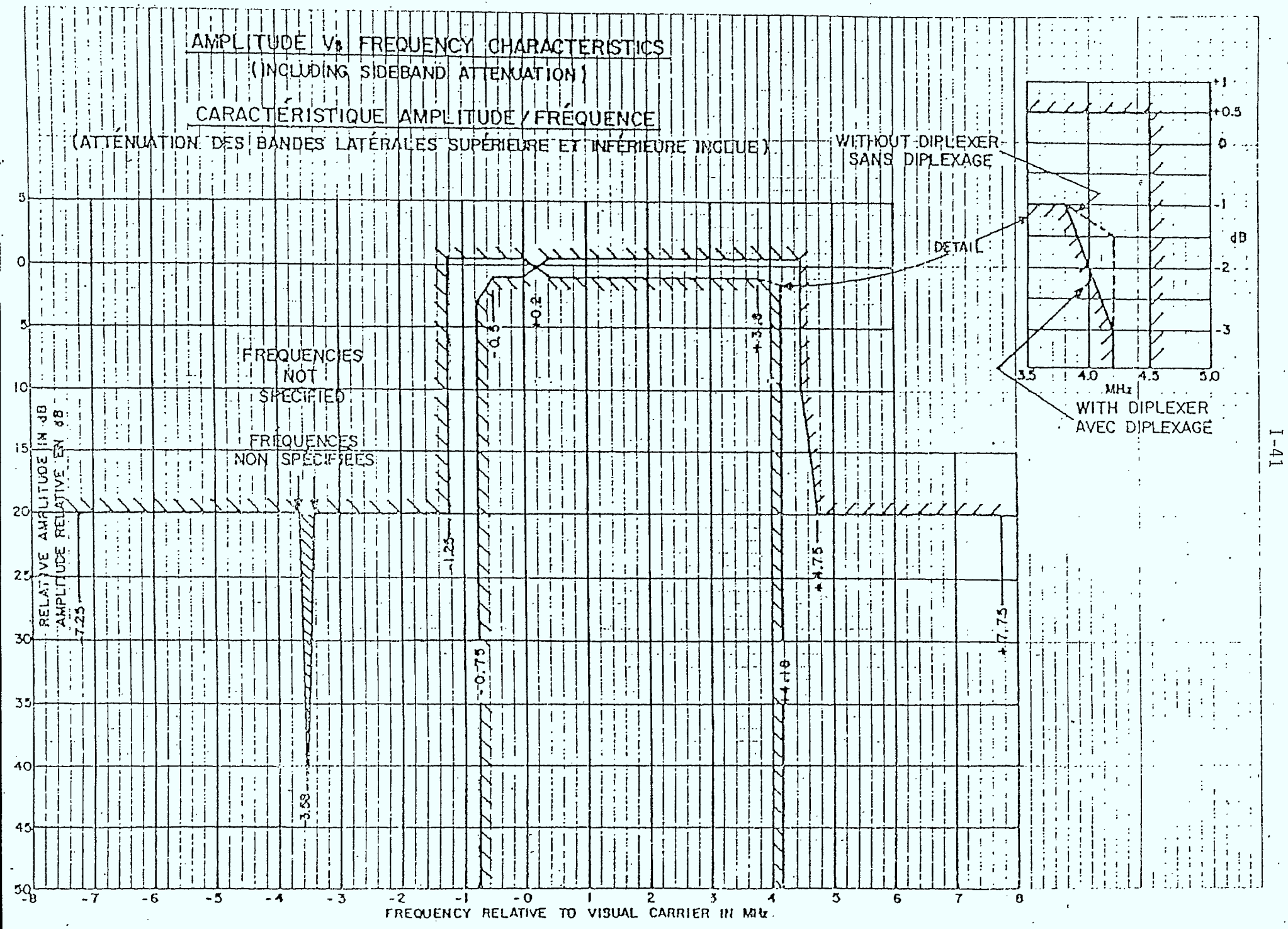

Figure 19: The magnitude mask for television broadcasting [11].

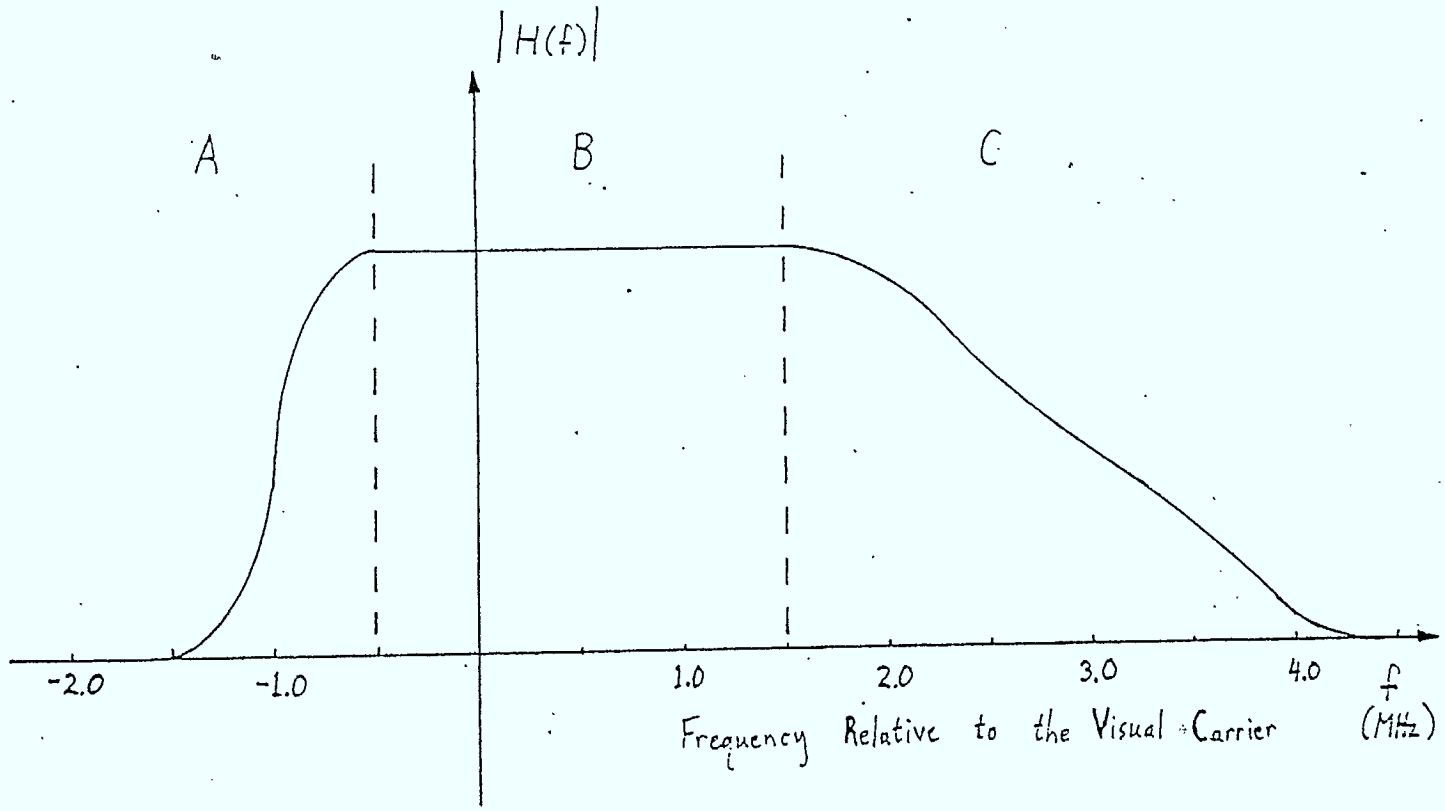

Figure 20: An illustration of a possible transmit magnitude response.

three regions. Region A is primarily dominated by the IF filter, and hence this region is not affected much by the overall pulse shape. Also, most of the energy that is transmitted in this region is thrown away at the receiver so that the characteristic here has very little effect on the received baseband signal. However, there is not much room to maneuver with respect to the magnitude response because it must fall within the mask (see Figure 19). On the other hand, the group delay response is completely unspecified in this region for both television broadcast and teletext. Therefore, it may be possible to tailor the group delay response in such a way as to minimize the peak transmitted signal for a given overall pulse shape and nominal receiver characteristic. Of course in order to realize this group delay, fixed IF equalization at the transmitter would be required. If such an approach is ruled out by the televison broadcast community, then the choice of pulse shape will have little effect* in this region and hence its characteristic will remain dominated by the transmitter's IF filter. It should be noted that this region could have quite an impact on the peak transmitted signal level because this is the region where the slope of the spectrum is the greatest.

In region B, the transmit pulse must be approximately uniform gain with a group delay characteristic that is the complement of the nominal receiver's group delay characteristic, if intersymbol interference is to be kept to a minimum and if the reconstruction of the baseband signal from the vestigal sideband signal is to be kept relatively distortion free. Thus in this region (as in region A), there is not much flexibility for reduction of the peak transmitted signal level via overall pulse shape design.

*Here it is assumed that we are restricting ourselves to BPSK signalling and a pulse shape that results in little intersymbol interference (i.e. Nyquist I is approximately satisfied).

Finally, region C is certainly affected by the choice of overall pulse shape. However it is also greatly affected by the choice of nominal receiver characteristic. The main point to be drawn here is that the peak transmit signal level cannot be properly included in the overall pulse shape design until a nominal receiver characteristic has been chosen and until a representative collection of transmit IF filter frequency responses (both magnitude and group delay) is gathered. The measured transmit IF filter frequency responses must include the responses at frequencies below the picture carrier (i.e. region A).

5.0 AUDIO BUZZ, SLICING LEVEL, AND BIT TIMING

In this section the topics of audio buzz, slicing level, and bit timing are briefly discussed. The purpose of this section is not to comprehensively discuss any of these issues but rather to bring out several pertinent points.

A good discussion on the general problem (i.e. not specifically for teletext transmission) of audio buzz can be found in [12]. This paper identifies several causes of audio buzz, but the two causes that are identified as the most likely to cause problems are "Nyquist slope" incidental phase modulation and incidental phase modulation due to nonlinearities in the transmitter's power amplifier. Here we will briefly outline an analytical procedure that encompasses both of the above causes of audio buzz. If a fairly long and "random" data sequence is transmitted then the signal entering the transmitter's power amplifier would have a Fourier transformation with a magnitude similar to the one illustrated in Figure 21. The frequency domain regions that are critical, with respect to audio buzz, are indicated with dashed lines. In general, a nonlinearity will distort the signal's frequency response. From the point of view of audio buzz, it is clearly undersirable for this distortion to result in signal energy falling within the sound channel itself. Also, it is undersirable for this distortion to result in complex conjugate antisymmetry (i.e. the real part of the Fourier transformation is antisymmetrical and the imaginary part is symmetrical) in the passband of the carrier recovery circuitry because this would correspond to phase modulation on the carrier that would be transferred to the audio signal by the carrier recovery circuitry [12]. Unfortunately, in general the power amplifiers can not be adequately modelled by a static input-output characteristic curve [12] (i.e. the nonlinearity is not memoryless and hence its output level

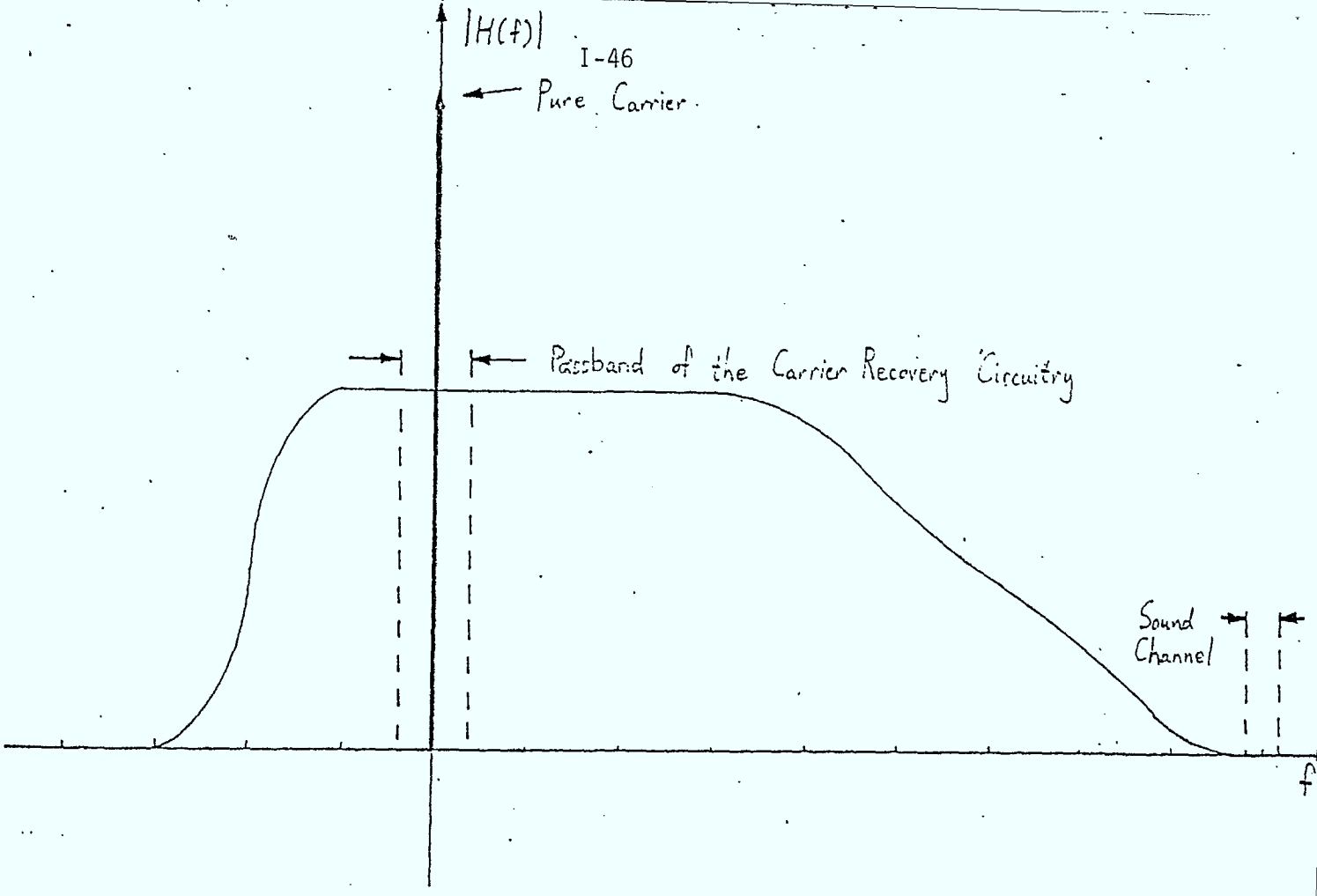

Figure 21: A possible magnitude response for the signal entering the transmitter's power amplifier.

cannot be represented by a polynomial in the input level). More general modelling techniques which allow nonlinearities with memory to be modelled can be used, such as a Volterra series or a Wiener model [14]. For example a causal time-invariant system with memory T can be represented by a Volterra series of the form

$$y(t) = h_o + \int_o^T h_1(\tau_1)x(t-\tau_1)d\tau_1 + \int_o^T\int_o^T h_2(\tau_1,\tau_2)\, x(t-\tau_1)x(t-\tau_2)d\tau_1 d\tau_2 + \int_o^T\int_o^T\int_o^T h_3(\tau_1,\tau_2,\tau_3)x(t-\tau_1)x_2(t-\tau_2)x(t-\tau_3)d\tau_1 d\tau_2 d\tau_3 + \ldots , \quad (22)$$

where x(t) is the input signal to the nonlinear system and y(t) is the output signal from the nonlinear system. If one makes the reasonable assumptions that a sampling rate equal to four times the symbol rate is sufficient, the effective memory of the power amplifier is not greater than a symbol interval (i.e. 175 nsec), and that the contribution of terms higher than third order is negligible, then the power amplifier can be modelled by*

---

*Equation (23) is for real signals (i.e. a "low IF model"). Extension to complex baseband is relatively straightforward. Note that sampling at 4 times the symbol rate at a low IF is equivalent to sampling at twice the symbol rate at complex baseband.

$$y_n = h_o + \sum_{i=0}^{4} h_{1,i} x_{n-i} + \sum_{i=0}^{4}\sum_{j=0}^{4} h_{2,i,j} x_{n-i} x_{n-j} + \sum_{i=0}^{4}\sum_{j=0}^{4}\sum_{k=0}^{4} h_{3,i,j,k} x_{n-i} x_{n-j} x_{n-k} \quad (23)$$

If the effects due to the nonlinearity of the transmitter's power amplifier are to be incorporated in a pulse shape design or a simulation then the parameters (i.e. the h's) in the above model (or an equivalent model) must be determined for a representative sampling of transmitters. A record of a given power amplifier's (down-converted) input and output signals can be used to obtain the model parameters by solving the resulting set of overdetermined linear equations.

A frequency domain interpretation of equation (23) can easily be obtained by recalling that multiplication in the time domain corresponds to convolution in the frequency domain, and delay in the time domain corresponds to an additive linear phase. The convolutions of the Fourier transforms of the various delayed version of x_n accounts for the classical spectral spreading effect of nonlinearities. Thus the signal coming out of a nonlinear power amplifier will have energy in the sound channel even though the signal entering the amplifier does not. The effect of this signal on the sound channel will be similar to that of additive Gaussian noise.

In addition to spectral spreading, the asymmetry about the carrier, due to the nonlinearity, is of concern. This type of degradation includes the commonly referred to AM to PM conversion. In an apparent deviation from the current topic, "Nyquist slope" incidental phase modulation is briefly considered. Recall that the Fourier transformation of the signal out of the receiver's IF filter will be highly asymmetrical and can therefore be decomposed into its complex conjugate symmetrical component and its complex conjugate antisymmetrical component. The complex conjugate antisymmetrical component is the spectrum of the signal that is in quadrature to the carrier. As an example consider the antisymmetrical component that is illustrated in Figure 5c. This component is shown again in Figure 22a. The Fourier transformation of the quadrature signal that is "passed" by the carrier recovery circuitry is shown in Figure 22b*. In all cases of interest the energy in this signal will be small compared to the energy of the carrier. Therefore, the small angle assumption (i.e. $\theta \simeq \sin\theta$ for $\theta \ll 1$ radian) can be employed to show that Figure 22b also represents the Fourier transformation of the "Nyquist slope" incidental phase modulation. Note that after frequency discrimination (i.e. differentiation of the phase function) the power spectrum of the resulting interference will have an x^4 characteristic, and will therefore be predominantly a high frequency interference. However deemphasis and voiceband lowpass filtering will somewhat ease this situation. It should be noted that "Nyquist slope" incidental phase modulation depends only upon a relatively narrow band (centred on the carrier) of the received signal and upon the Nyquist slope region of the receiver's IF filter. Therefore only a narrow band at the centre of the frequency response of the overall teletext pulse shape has any bearing on the amount of Nyquist slope induced audio buzz. Recall that all

*Any inphase signal that is in the passband of the carrier recovery circuitry is assumed to be removed by a limiter.

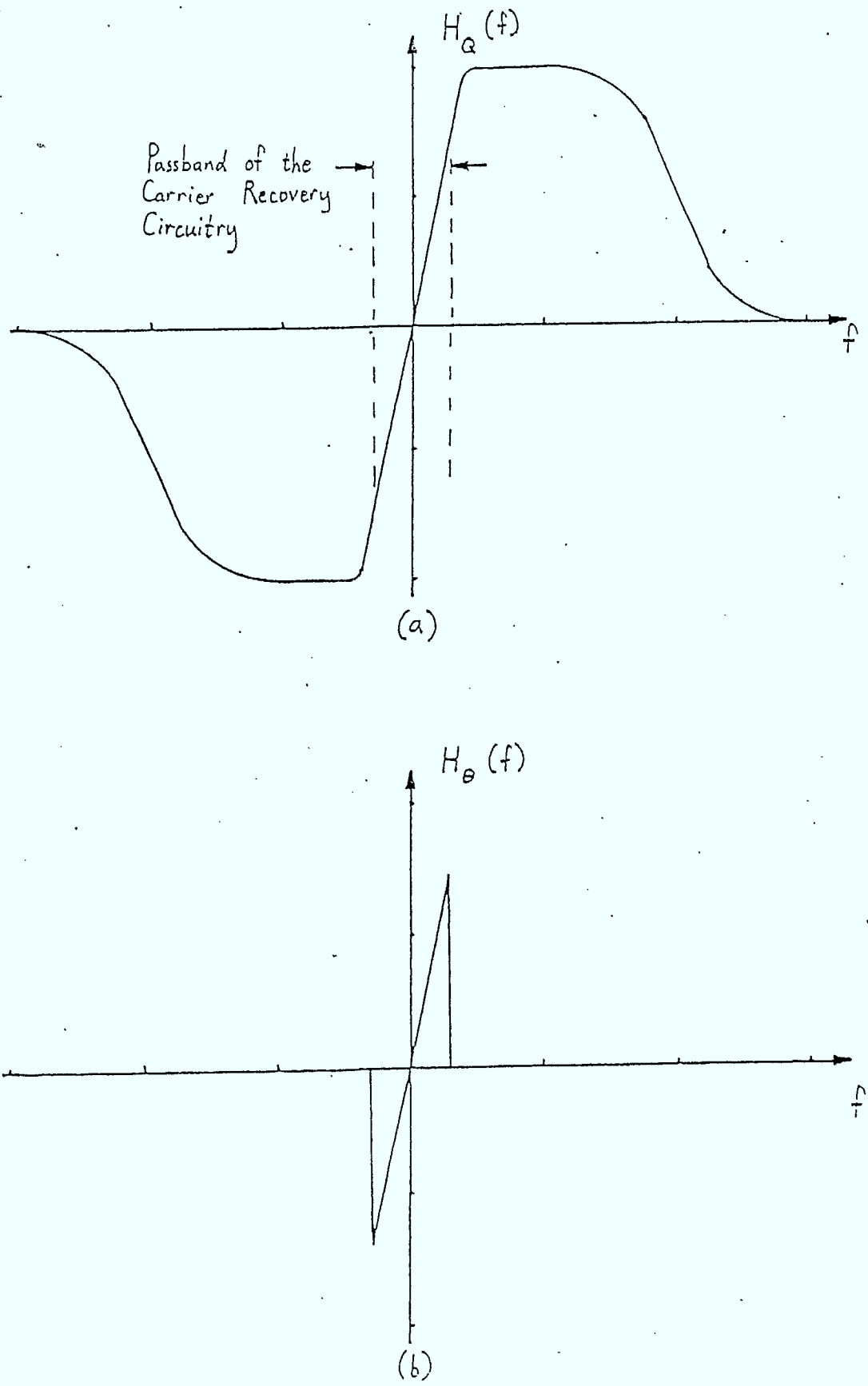

Figure 22: (a) The antisymmetrical component from Figure 5.
(b) The Fourier transformation of the resulting "Nyquist slope" phase modulation.

overall pulse shapes of interest are approximately uniform gain and constant group delay in this region. Therefore the choice of overall pulse shape will have very little effect on the level of audio buzz, that is caused by "Nyquist slope" incidental phase modulation, for televisions using either coherent or quasi-coherent detection.

Asymmetry caused by the nonlinearity will cause carrier phase modulation in exactly the same way as "Nyquist slope" incidental phase modulation. It is highly unlikely that the amount of asymmetry that is caused by the nonlinearity would be comparable to that caused by the receiver's IF filter, because this would require such a severe nonlinearity that the amplifier would be virtually useless for the transmission of either television signals or teletext. Therefore it is expected that incidental phase modulation due to the nonlinear power amplifier is negligible compared to "Nyquist slope" incidental phase modulation, for televisions using either coherent or quasi-coherent detection. Also, it is unlikely that spectral spreading is a major source of audio buzz. The apparent conclusion is that the choice of overall pulse shape will have little effect on the level of audio buzz for televisions using either coherent or quasi-coherent detection.

In recent off-air tests, using the most recent Telidon decoder, CRC personnel have found that in strong-signal urban environments the decoder either gives very good performance (i.e. extremely low bit error rates) or very poor performance (e.g. often it appears that proper synchronization has not occurred). Therefore it might be prudent to critically examine the synchronization techniques used by the existing teletext decoder and to suggest possible improvements. Here, we will concentrate on the slicing level and clock phase determination. First, the approach used by the existing teletext decoder is briefly

outlined. This decoder uses the two byte clock sync signal to estimate both the slicing level and the clock phase serially (as opposed to in parallel). It begins by estimating the slicing level, using two peak detection circuits (one for the "overshoots" and one for the "undershoots") which have a short attack time and a long decay time. The slicing level is taken to be the midpoint between the two peak values. Once the slicing level has been determined, the decoder uses a single zero crossing to choose one of five possible clock phases. There are several severe weaknesses in the procedure that result in the decoder's performance falling far short of optimal. Several of the problems with the slicing level determination technique are

- The peak detectors are very sensitive to impulse noise [15]. In fact simulations have shown that a loss of approximately 3 dB can be attributed to the slicing level and clock phase circuitry of the present decoder even under fairly ideal conditions (i.e. no multipath propagation and ideal carrier recovery) [15].

- Even relatively modest multipath propagation can cause a substantial error in the estimated slicing level. This is because the signal level immediately preceding the clock sync signal is at 0 IRE were as the average level during the clock sync signal (i.e. the slicing level to be determined) is 35 IRE (see Figure 23). Thus any multipath propagation will result in an apparent shift of level, for a duration that is proportional to the multipath differential delay. Note that if the delay spread is large enough that a delayed version of the sync pulse or the colour burst gets superimposed on the clock sync signal, then the situation gets even worse. It is this problem with synchronization in the presence of multipath propagation that is suspected to be responsible for the decoder behaviour noted by CRC personnel.

- The optimum slicing level may be time-varying due to a time-varying phase offset in the recovered carrier. This is illustrated in Figure 24. Thus any technique that attempts to determine the slicing level during the first two bytes and then freeze it for the remainder of the line, will yield inferior performance unless the carrier recovery is very good. Clearly, this point adds further impetus to the suggestion in Section 2 that improved carrier recovery techniques are desirable.

We will return shortly to discuss possible solutions to the above problems but first clock phase estimation will be discussed.

A couple of serious problems exist with the current Telidon decoder's technique to estimate clock phase. These are as follows.

- An error in the slicing level will result in an error in the clock phase. From the above discussion this is clearly a characteristic that should be avoided.

- The clock phase is estimated from a single zero crossing. Thus only a small fraction of the signal energy in the two byte clock sync signal is being used to estimate the clock phase. Therefore the estimated clock phase tends to be very sensitive to noise and other forms of interference.

One thing that should be noted about the first point is that there is absolutely no need for the slicing level estimation and the clock phase estimation to be highly dependent upon each other, because they are truly orthogonal problems! That is that during the clock sync signal the slicing level circuitry is attempting to estimate the average signal level (i.e. the DC component), while the clock phase circuitry is trying to estimate the phase of the 2.863636 MHz component of the signal. A block diagram illustrating a clock phase

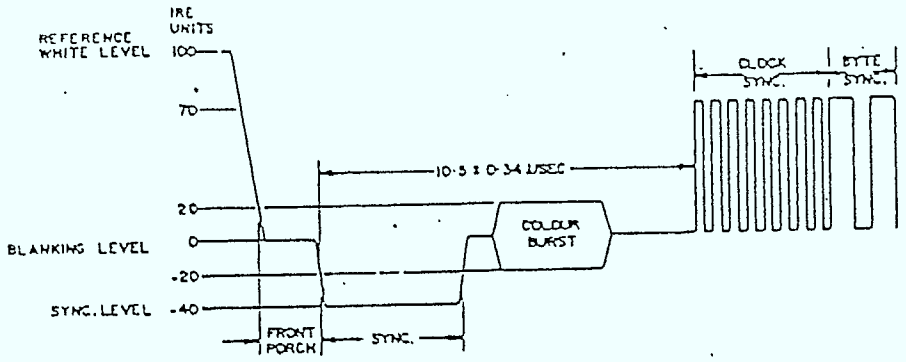

Figure 23: An illustration of the start of the teletext signal relative to the television synchronizing signals (from [7])

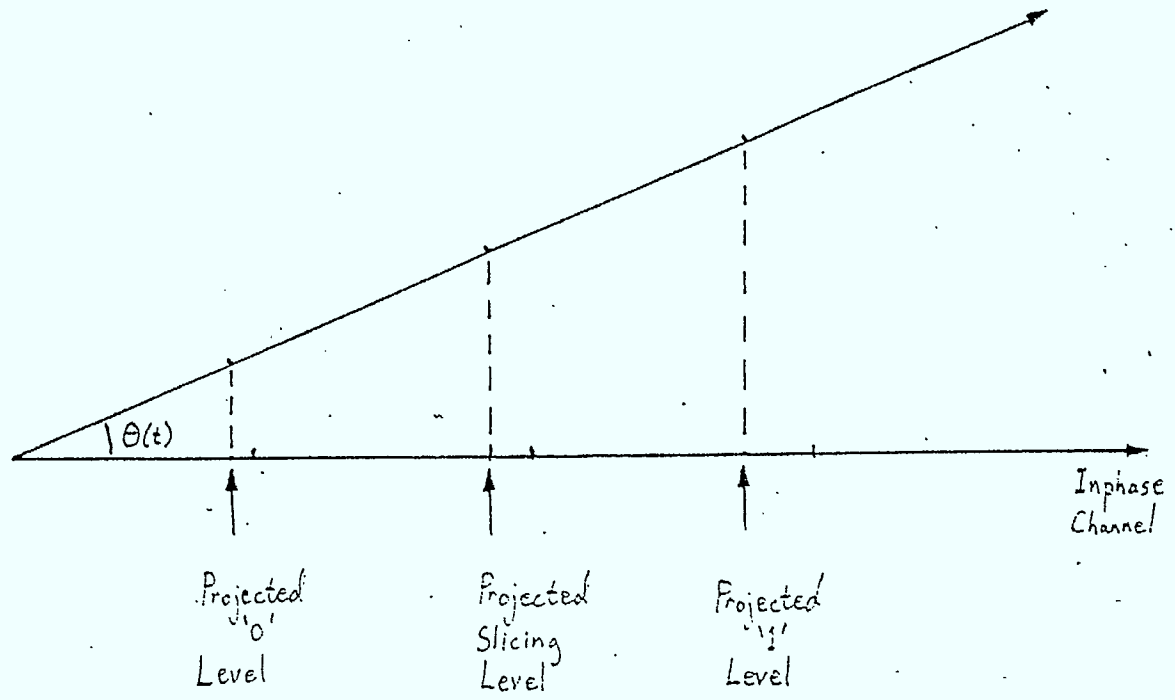

Figure 24: An illustration of the time-varying levels caused by a time-varying phase offset in the recovered carrier.

estimation technique that is independent of slicing level and that uses most of the available energy in the clock sync signal, can be seen in Figure 25. The RC circuit at the input is to block low frequency components prior to the limiter. The resistor and capacitor values should be chosen so that the RC network does not introduce a phase shift at 2.863636 MHz. After filtering by the RC circuit, the analog signal is converted to a binary NRZ signal by a limiting amplifier. The binary signal is then fed to each of five channels, one for each of the five possible clock phases*. In a given channel the binary signal is first multiplied by an alternating NRZ signal of the given clock phase. The "multiplers" in Figure 25 can be realized with exclusive-or gates. The product signal is integrated, rectified, and finally fed to a threshold detector. The first threshold detector to be triggered should indicate the best clock phase. Note that the technique described is that suggested by classical signal detection theory [16], where the optimal detector in the presence of additive white Gaussian noise consists of a bank of correlators followed by threshold detectors.

We now return to the slicing level problem. The problem of sensitivity to impulse noise can easily be eliminated by replacing the present peak detector based circuit with a lowpass filter. This seems like the intuitively obvious solution because what we are trying to estimate is the DC component of the clock phase signal. In choosing the filter it is desirable to have a filter with a narrow bandwidth in order to minimize the effects of the noise, to suppress the 2.863636 MHz clock sync signal, and possibly to suppress the 3.58 MHz colour burst signal. On the other hand the filter step response should settle fairly quickly so that the level change (i.e. from 0 IRE to 35 IRE) does not affect the

*The question regarding the adequacy of five clock phases is not addressed here.

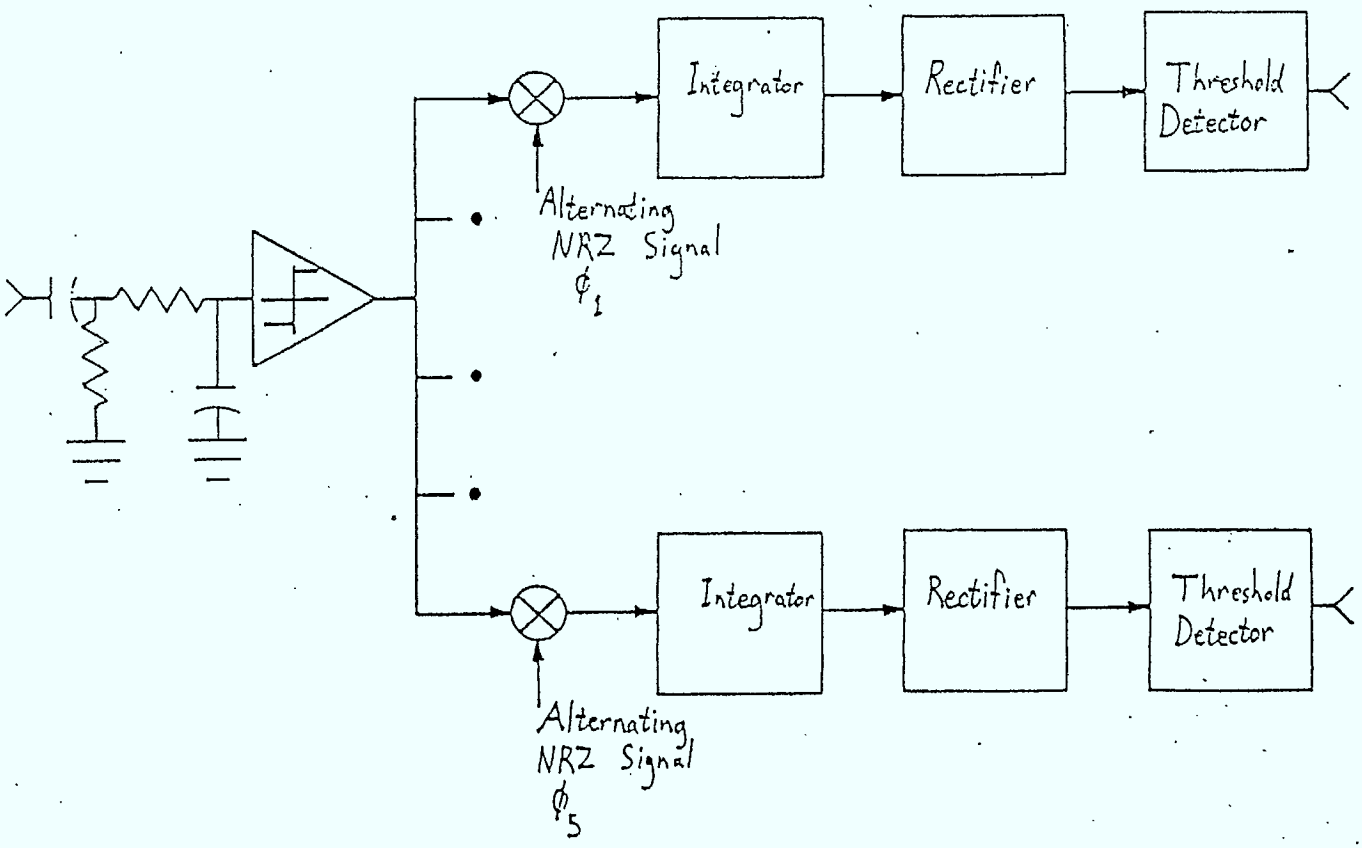

Figure 25: A block diagram illustrating a clock phase estimation technique that is independent of slicing level and that uses most of the available energy in the clock sync signal.

filters output for too long. Also, the order of the filter should be low so that it can be economically realized. A filter that represents a reasonable tradeoff between the above considerations is a second order Butterworth filter with a 270 kHz 3 dB bandwidth. The frequency and step responses for normalized Butterworth filters can be seen in Figure 26. From these curves it can be shown that step response ripple will be no greater than -26 dB after 10 symbol periods, and the clock sync signal at 2.863636 MHz is suppressed about 40 dB. Also, this bandwidth is narrow enough that noise should not represent a significant problem for usable signal to noise ratios. The output of this filter should be "frozen" near the end of the clock sync signal. The level of this output can then be used as the slicing level for lower-cost decoders or as the initial slicing level for more expensive adaptive decoders. The triggering of one of the threshold detectors (see Figure 25) can be used as an indication that the end of the clock signal is near.

If time-varying slicing levels, due to phase errors on the recovered carrier or due to wide multipath spreads, are to be tracked then adaptive slicing level circuitry is required. A block diagram that illustrates a possible approach is shown in Figure 27. This circuit attempts to estimate the logic "0" level and the logic "1" level in a decision-directed manner. The sum of these two levels can be used to control the slicing level (since the slicing level should be half of the sum), while the difference of these two levels can be used as an input to gain control circuitry.

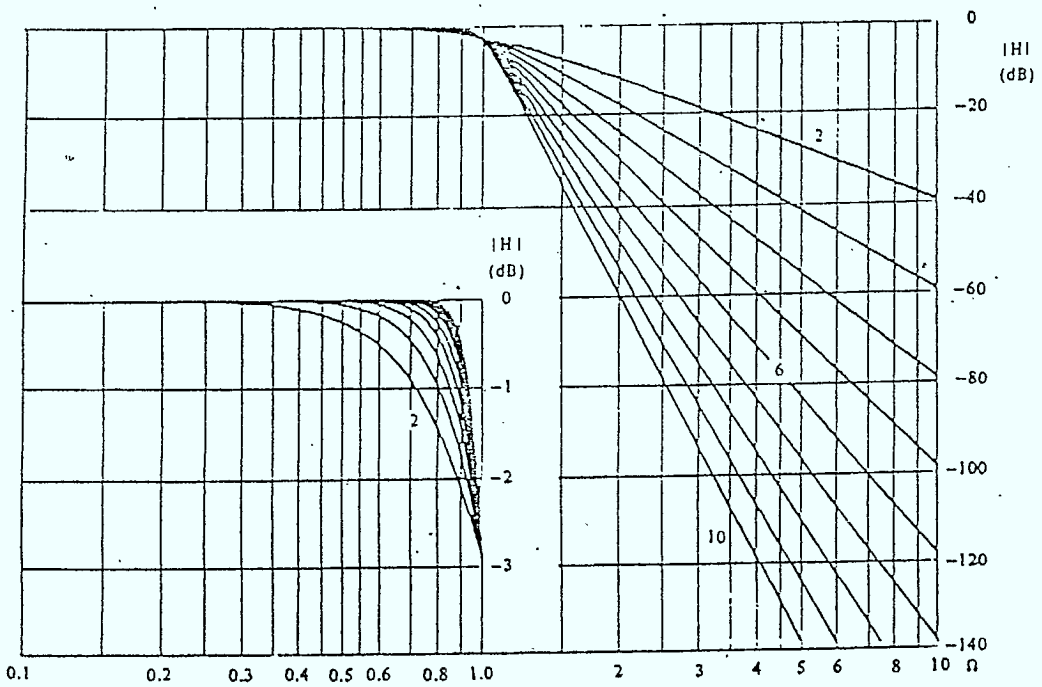

(a)

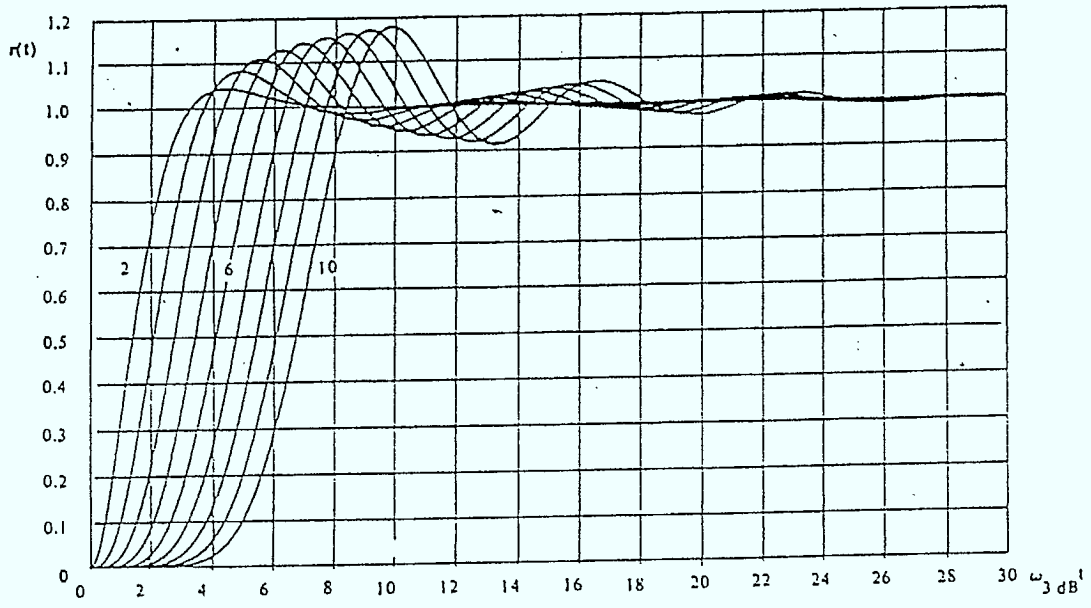

(b)

Figure 26 : (a) The magnitude responses for normalized Butterworth filters (from [17]).
(b) The step responses for normalized Butterworth filters (from [17]).

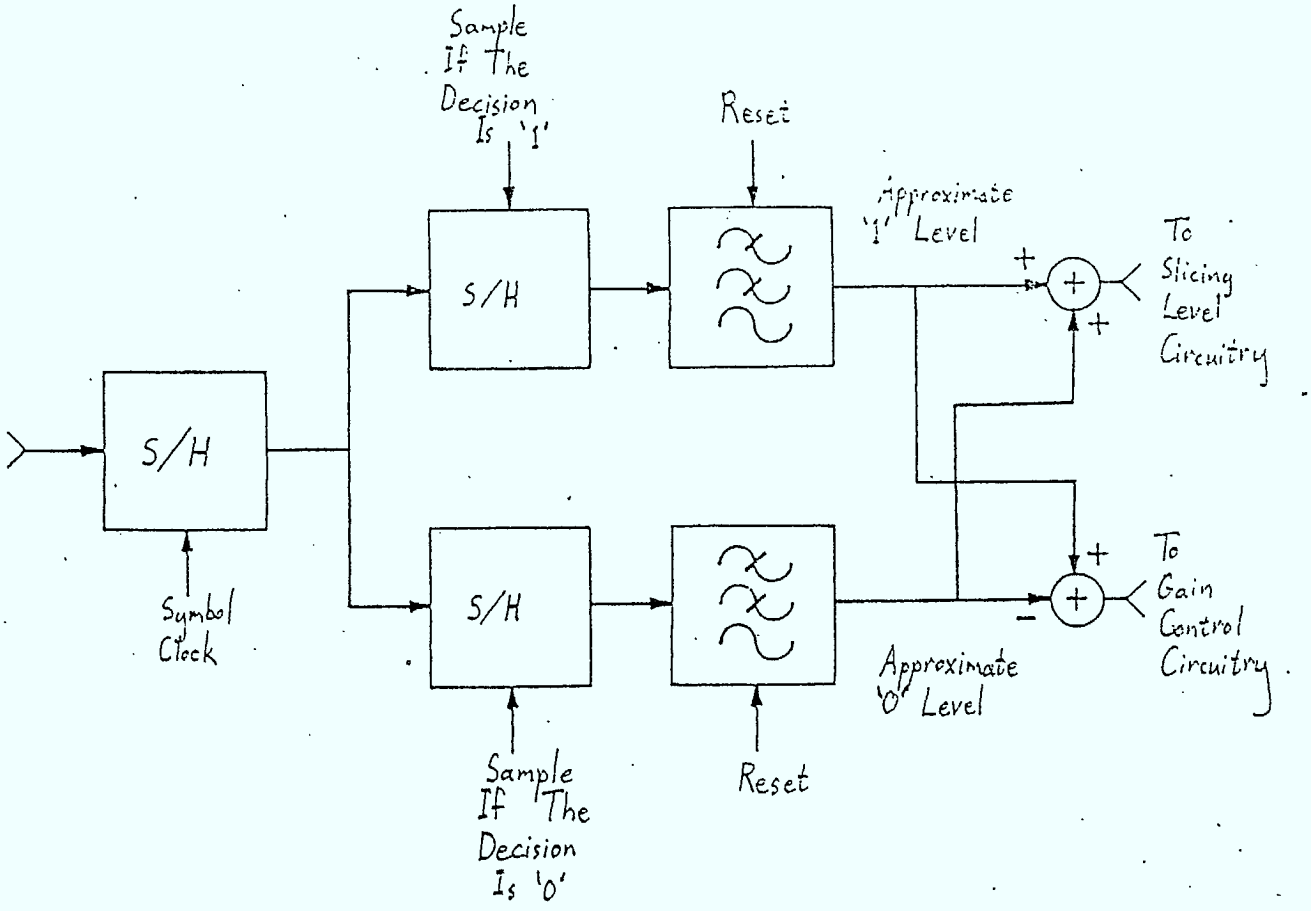

Figure 27: A block diagram illustrating a possible approach to achieving an adaptive slicing level.

6.0 CONCLUSIONS AND RECOMMENDATIONS

A tutorial discussion on Nyquist's first criterion was given. From this discussion it was apparent that aliasing due to symbol rate sampling will not result in destructive interference, between the frequency components of the pulse shape, only if the overall pulse shape is real and nonnegative. Therefore, the overall pulse shape design was restricted to those with zero-phase (i.e. the fixed delay is ignored) frequency responses.

The implications of vestigal sideband transmission were outlined. It was pointed out that even though the overall pulse shape (i.e. the inphase transfer function) satisfies Nyquist's first criterion, significant intersymbol interference can result due to nonideal carrier recovery because the quadrature transfer function will not satisify the criterion.

A promising pulse shape was recommended. Then some suggestions were given for specifying the pulse shape.

Overshoots at the transmitter's output were discussed. It was pointed out that it may be possible to reduce overshoots at the transmitter by appropriately tailoring the transmitter's group delay response, at frequencies that are negative relative to the carrier. It was noted that the peak transmit signal level cannot be properly included in the overall pulse shape design until a nominal receiver characteristic has been chosen and until a representative collection of transmit IF filter frequency responses (both magnitude and group delay) is gathered.

The problem of audio buzz was briefly discussed. In particular audio buzz resulting from "Nyquist slope" incidental phase modulation or from the nonlinearity of the transmitter's power amplifier was considered. It was concluded that incidental phase modulation due to the nonlinear power amplifier is likely to be negligible compared to "Nyquist slope" incidental phase modulation, for televisions using either coherent or quasi-coherent detectors. Furthermore, for these televisions, the choice of overall pulse shape will have little effect on the level of audio buzz that is due to "Nyquist slope" incidental phase modulation. In addition to being a source of audio buzz, the nonlinearity of the transmitter's power amplifier can also degrade the performance of the teletext transmission. If the effects due to the nonlinearity of the transmitter's power amplifier are to be incorporated in a pulse shape design or a simulation then the parameters of an appropriate model (e.g. one based on the Volterra series representation) must be determined for a representative sampling of the transmitters.

Some of the deficiencies of the synchronization circuitry employed in the current Telidon decoders were discussed. Possible approaches that overcome these deficiencies were suggested.

In addition to optimization of the overall pulse shape, several other areas for further effort were identified including:

- Improved carrier recovery techniques.
- Improved slicing level determination techniques.
- Improved clock phase recovery.

- The choice of a nominal receiver characteristic.

- Investigation of the cost versus performance tradeoff for the pulse shape magnitude and group delay response tolerances.

Of course there are many other areas that do not fall within the scope of this memo. As with any resource allocation problem the critical question is, how should the available resources be allocated in order to achieve the greatest benefit?

The level of sophistication with which pulse shape optimization could be pursued ranges from a fairly simple nonlinear programming problem (which perhaps is not very representative of the real world problem) to a massive nonlinear programming problem that would attempt to account for the many uncertainties in the teletext transmission chain. The complexity of the massive nonlinear programming problem is limited only by the available information and by the computational requirements. To further complicate the issue, it is not clear that a massive nonlinear optimization would produce a pulse shape that would yield significantly improved performance over a well chosen pulse shape. In fact it is possible that the performance could actually deteriorate if great care is not taken to avoid certain pitfalls. For example if the uncertainties are not represented in a complete and unbiased fashion, then the optimization would produce a biased result. Clearly, the modelling of the uncertainties and the subsequent collection of data for model parameter estimation is a major task on its own. Also most performance criteria, that would seem reasonable to apply, would tend to implicitly weight the poorer members of the ensemble of possible channels (i.e. those with a relatively high bit error rate) more than the good members. This will be particularly true of an

optimization that attempts to include multipath propagation. The likely result is that the optimization will tend to sacrifice the performance of the good channels in order to achieve a marginal improvement for the poor channels. From the above discussion, it is felt that if pulse shape optimization is to be pursued the first step should be a comparatively small problem definition and tradeoff study as opposed to jumping right into a full blown optimization. Areas that such a study should address include:

- Identifying suitable models for the various uncertainties in the teletext transmission path.
- Outlining procedures for determining the parameters of these models.
- Defining a tractable optimization problem (perhaps defining several problems of varying degrees of complexity) and then estimating the associated costs (in both money and amount of computation).
- Estimating the potential benefits (and risks) of performing such an optimization so that a rational decision can be made as to whether or not to pursue pulse shape optimization.

APPENDIX II

SUBJECTIVE QUALITY OF TV PICTURES IN MULTIPATH ENVIRONMENTS

APPENDIX II: SUBJECTIVE QUALITY OF TV PICTURES IN MULTIPATH ENVIRONMENTS

1.0 INTRODUCTION

Preliminary measurements of complex impulse responses, performed by CRC, for channels in the 200 MHz region, have provided results that tend to support rather than contradict the Telidon RF propagation model simulation results. Consequently, for establishing Telidon system performance in multipath environments, we plan to use the simulation program to generate realistic multipath channels. Because attention should be restricted to the subset of channels which provide acceptable video signals, a prescreening procedure for discarding channels not providing usable television pictures is required.

Until recently, the examination of the effects of echoes on the subjective quality of television pictures has received little attention. Some work was done in the early 70's by Lessman [21, 22]. However, only the restrictive cases of positive (in-phase) and negative (out-of-phase) single echoes were studied. A procedure for weighting multiple ghosts to obtain an estimate of the subjective picture quality is proposed in [21] and will be summarized later.

The subjective effect of long echoes on television pictures was studied by Allnatt (1965) [21]. The major observation was that there is almost no difference in the degree of degradation of picture quality for delay times between 5-15 μsec. Lessman's pioneering work is still useful and is often referenced. Lessman used a seven point comment scale, shown in Table II.1, for accessing the subjective quality of the picture. In [22], the effects on picture quality of transmitter amplitude and group delay responses which satisfy the FCC tolerances (fit inside amplitude and group delay masks) are discussed. The amplitude and group delay tolerances are shown in Figure II.1. In [22], an

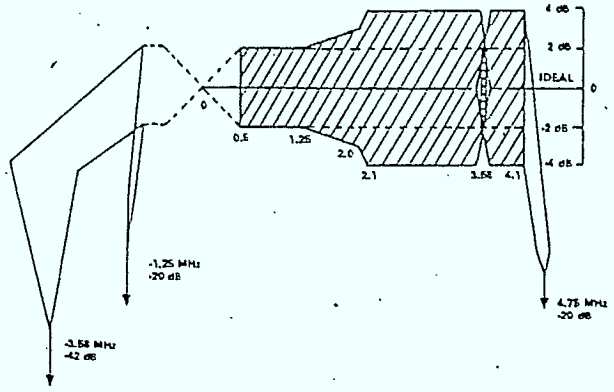

a) FCC Amplitude Response Mask

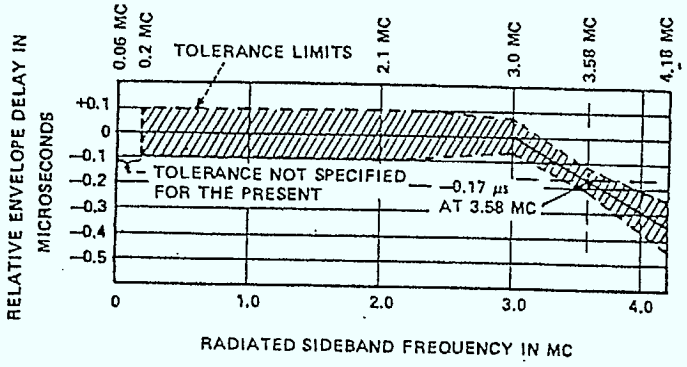

b) FCC Group Delay Mask

Figure II.1 : Transmitter Amplitude and Group Delay Tolerance Specifications (FCC) [after [22]]

arbitrary amplitude response varying ±2 dB in the frequency range (-1.0 MHz to 4.0 MHz) at a rate of 1 cycle per MHz and a constant group delay response were assigned to the transmitter characteristic. In evaluating the effects of this transmit characteristic, an ideal VSB receiver characteristic with constant group delay was used. The output signal exhibited paired echoes (11.5% of the main signal) displaced from both sides of the main response by 1 μsec. It is claimed in [22] that this echo level and delay corresponds to a cumulative comment class 4 or better by at least 50% of the audience. As is apparent from Table II1, this corresponds to fairly good picture quality (not at the threshold of acceptability).

Also in [22], computations were performed with an ideal transmitter amplitude response, but with group delay varying sinusoidally with peak amplitude of 100 nsec between 0-3 MHz, and 50 nsec between 3.0 - 4.2 MHz. The output for the above transmitter and an ideal receiver revealed a negative echo pair that was 5% of the main signal. According to [22], this corresponds to 60% comment 2 or better. It is evident that amplitude and group delay tolerances for transmit and receiver characteristics provide good quality pictures and cannot be used for prescreening multipath channel responses. In fact, in [22] it is claimed that a transmission system (incorporating an ideal receiver) should be capable of producing a picture of at least 80% comment 2 or better. This is a very high quality picture.

The echo strength versus echo delay for 80% comment 2 or better performance is shown in Figure II.2. One can see that for 100 nsec ripples in the group delay response, the echo delay must be greater than 2 μsec (undulation frequency less than 0.5 cycles per MHz) for acceptable colour TV

Comment Number	Comment Description
1	Not Perceptible
2	Just Perceptible
3	Definitely Perceptible, But Only Slight Impairment to Picture
4	Impairment To Picture, But Not Objectionable
5	Somewhat Objectionable
6	Definitely Objectionable
7	Extremely Objectionable

Table II.1: Lessman's Seven Point Comment Scale (after [22])

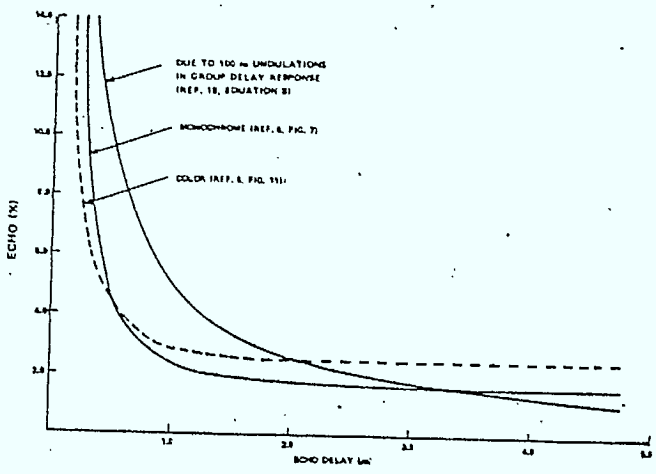

Figure II.2: Echo due to 100 nsec group delay undulations compared with subjective perceptibility data

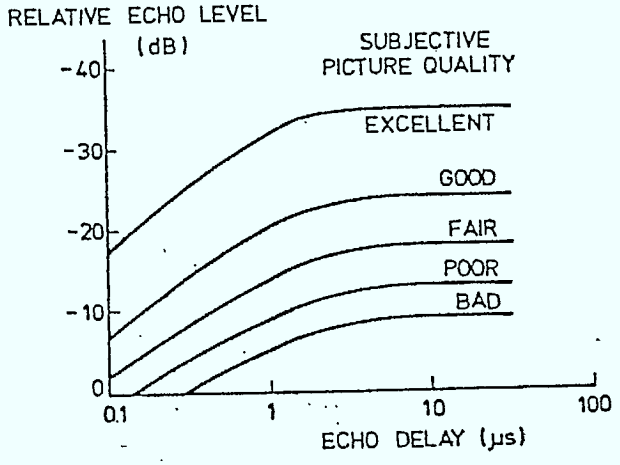

Figure II.3: Subjective quality of TV pictures for a single (in-phase) echo as a function of relative level and echo delay (after [23])

performance. It is quite clear from Figure II.2 that strong close-in echoes are not as objectionable as those with longer delays. Shorter echoes are subjectively masked by the main signal. Many people even appreciate some occurence of short echoes, as they accentuate contours in the picture [23]. Curves, presented in Figure II.3 [23], indicate the subjective influence on a television picture of a single (in-phase) echo as a function of relative level and echo delay. It is evident that close-in echoes are significantly less annoying than far out echoes. These short echoes, however, can seriously disturb Teletext transmission.

The curves of Figure II.3 are more useful than the curves of Figure II.2, as they allow us to approximately establish the threshold of acceptability. The major deficiency, however, is that the above curves are restricted to the single, positive echo case. This deficiency is addressed in [21] and will be summarized in the next section.

2.0 WEIGHTING OF MULTIPLE ECHOES FOR ESTIMATING THE ANNOYANCE IN THE TV PICTURE

In [21], a perceived DU (desired to undesired) ratio, PDUR, is proposed for evaluating the subjective quality of television video. It is essentially the power sum of the levels of individual ghost images (DU ratios) weighted by subjective effects due to r.f. phase (ψ) and delay (τ). Experiments conducted by the authors of [21], have revealed that the correlation coefficient between the numerical quantity, PDUR, and the subjective picture evaluation (using a 5 point comment scale shown in Table II.2) is quite high ($\simeq 80\%$). Hence, the numerical PDUR is probably the best gauge of subjective picture quality available at present. The relationship between PDUR and subjective picture quality is shown graphically in Figure II.4.

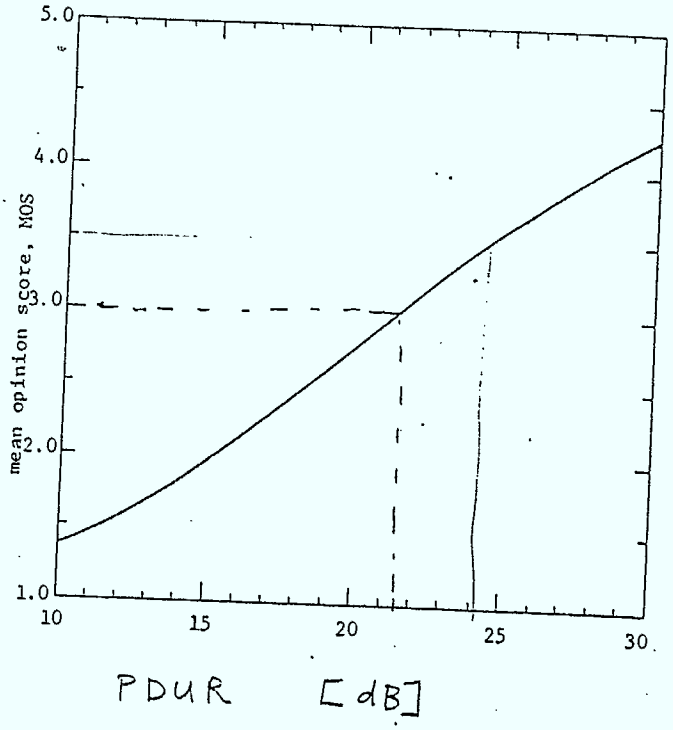

Figure II.4: Relationship between PDUR and mean opinion score for picture quality

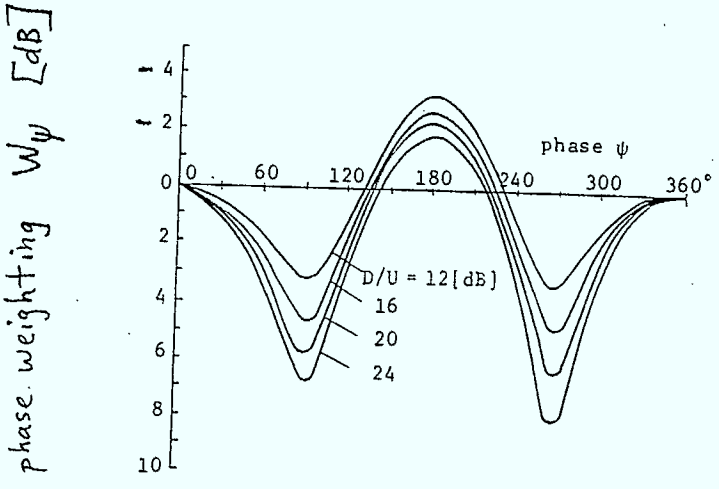

Figure II.5: Phase Weighting Curve

Comment Number	Description
5	imperceptible
4	perceptible but not annoying
3	somewhat annoying
2	severely annoying
1	unusable

Table II.2: 5-point comment scale used in [21] for subjective picture evaluation

2.1 Single Ghost Case

The single ghost case will be discussed first to establish the effects of r.f. phase and ghost delay. The degree of quality degradation is strongly dependent on the phase, ψ, of the ghost. In [21], experiments have been conducted to establish the DU ratio of a positive ghost that provides equivalent degradation to the ghost with phase ψ and specific DU ratio. The perceived DU ratio is the DU ratio of this equivalent positive ghost, and is given by

$$p = D/U + W_{\psi} \quad [dB]$$

where

D/U is the DU ratio of the ghost

W_{ψ} is a phase weighting function.

The phase weighting function, W_{ψ}, presented in [21] is shown in Figure II.5. Note that the weighting function is also a function of the DU ratio of the ghost. It is evident that for phase angles in the neighbourhoods of 80-100° and 260-280°, ghosts are much less visible than positive echo ghosts.

The ghost delay has a strong impact on the quality of a picture. The delay weighting function, W_{τ}, is shown in Figure II.6. The curve is normalized to 0 at a delay of 5 μsec, and there is only a small difference in the degree of quality degradation for delays greater than 4 μsec. The results are compared with those obtained by Lessman in Figure II.6, and reasonable agreement is evident. In [21], a delay of 5 μsec was taken as the standard delay. The perceived DU ratio, p, is given by:

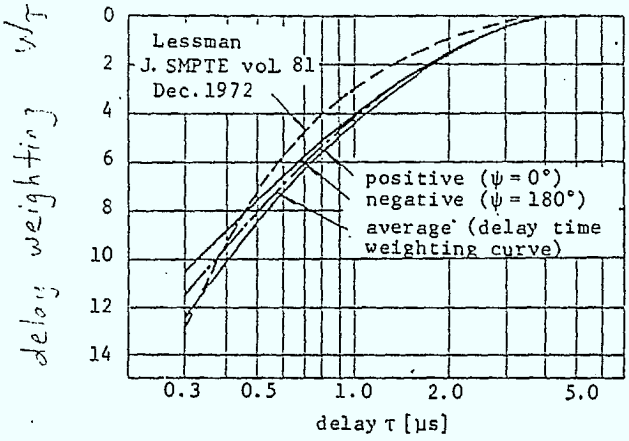

Figure II.6 : Delay time weighting curves

$$p = D/U + W_{\psi} + W_{\tau} \quad [dB],$$

and represents the DU ratio of a positive ghost with standard delay that produces equivalent impairment to that of a single ghost with arbitrary phase and delay. This can be used to establish the subjective picture quality using Figure II.4.

Using the comment scale of Table II.2, the following thresholds are established for good and unacceptable picture qualities:

Picture Quality	Threshold (5-point comment scale)
Good	≥ 3.5
Unacceptable	≤ 1.5

Choosing the threshold of acceptability halfway between comment 1 and 2 is probably a conservative estimate.

2.2 Multiple Ghosts

The PDUR, which gives an indication of the degree of quality degradation of a picture impaired by multiple ghosts, is given by [21]:

$$PDUR = -10 \log_{10} \sum_{i=1}^{n} 10^{-P_i/10} \quad [dB]$$

where

$$P_i = D/U(i) + W_{\psi}(i) + W_{\tau}(i)$$

(perceived DU ratio of i-th ghost)

n = the number of ghosts

$W_\psi(i)$ = the phase weighting of the i-th ghost (see Figure II.5)

$W_\tau(i)$ = the delay weighting of the i-th ghost (see Figure II.6).

The subjective picture quality can be ascertained using Figure II.4. If the PDUR is below 11 dB, the picture quality is deemed unacceptable, and if the PDUR is greater than 24 dB, the picture quality is good.

2.3 Generating Prospective Multipath Channels

The multipath simulation program can be used to establish prospective channel characteristics. In the simulation program, the ratio of the magnitude of the scattered field to the incident field is accumulated in a scatter table. Instead of a scatter table, an impulse response table is required. One possible way of generating this is to have very fine resolution delay bins (i.e. ± 0.05 μsec). When a path falls into a particular delay bin, the value of $|E_s/E_i|$ would be multiplied by $\exp j\phi$, where ϕ is a uniformily distributed random variable on $[-\pi, \pi]$, and added to the complex quantity previously there. The carrier frequency would be an important input parameter to the RF simulation program, and should be reflected in the complex baseband output response, whose format may be as shown in Table II.3. One should use randomized reflector dimensions and parameters, with the reflector positioned in the local domain about the receiver.

Multipath Channel File

Carrier Frequency = _____ MHz

Subjective Picture Quality = _____
{good or acceptable}

Delay (μsec)	Amplitude	Phase
0	1	0
0.05	___	___
0.15	___	___
0.20	___	___
-		
-		
-		
-		
-		
-		
-		
-		
-		
-		
15.0	___	___

Table II.3: Format of Multipath Channel File

For each multipath channel file, the PDUR can be computed and used to prescreen channels that will not provide acceptable video. Whenever the PDUR is less than 11 dB, the channel should be discarded. Channels for which the subjective picture quality is perceived to be quite good (PDUR $\geq$ 24 dB), will have this indicated in the impulse response file. Note that good subjective TV performance does not necessarily guarantee good Teletext performance.

3.0 DEVELOPING AN APPROACH FOR PRESCREENING CHANNELS DEFINED BY COMPLEX TIME DOMAIN SAMPLES OR THEIR FREQUENCY RESPONSE.

Complex baseband channel measurements have been performed by CRC over the past few weeks. These are provided in time domain sampled form, which can be easily converted to the frequency domain (amplitude - phase or amplitude-group delay format). From the time-domain impulse response measurements, the parameters of the underlying multipath channel process may be estimated visually. Some improvement may be achieved by dividing the received spectrum by the measured back-to-back frequency response [spectral division approach, reference [24]], and transforming back to the time domain. The major parameters (i.e. number of paths, relative magnitudes, phases, and delays of each path) can be estimated from the resulting complex impulse response and its envelope [24]. These estimated channel parameters can then be used to establish the PDUR, and, thus, the subjective picture quality.

3.1 Setting Amplitude and Group Delay Masks for Prescreening Channels

For transmit and receive filters, allowed tolerances are typically provided by amplitude and group delay masks. Since this is such a standard practice, it was thought that developing masks to compare with channel amplitude and group delay characteristics might prove valuable for prescreening channels (it would be somewhat simpler, but less exact, than the PDUR approach).

The amplitude and group delay responses for a single positive echo (delay-d, magnitude-m) are provided in Attachment II.I. From the curves provided in Figure II.4, the maximum echo strength for a standard delay of 5 μsec is -11 dB, (.282), for acceptable video. If we set a group delay mask based on this standard delay:

$$gd(thresh) \simeq \pm m\, d = \pm(.282)5\ \mu sec$$

$$\simeq \pm 1.41\ \mu sec$$

For echoes less than 5 μsec with echo magnitudes, m, corresponding to acceptable video, the group delay will be within the above mask. The prescreening power is not very good, as there will be channels within the group delay mask which do not provide acceptable video quality . Furthermore, for echoes with delays greater than 5 μsec (with acceptable subjective quality), the group delay will fall outside the above mentioned mask. However, for this case, the amplitude response should be in the mask [1-m, 1+m] where m = 0.282, to ensure acceptable video. Hence the prescreeing approach could be summarized as follows:

(1) if group delay falls within the prescribed mask, response deemed acceptable.

(2) if group delay falls outside the mask, check to see if amplitude response falls within limits [.718, 1.282].

This approach is a conservative approach as the channels that are rejected are clearly unacceptable).

The above mentioned approach was prescribed considering only a single positive echo. However one must consider multiple echo paths, and for this case, the bounds on the group delay are approximately

$$gd(bound) = \sum_{i=1}^{n} m_i d_i ,$$

where

n is the number of echo paths,

m_i is the magnitude of the i-th echo,

d_i is the delay associated with the i-th echo.

With multiple echo paths, there is clearly the possibility that the group delay will fall out the above mentioned spec for paths with delays less than 5 μsec, which would still provide acceptable subjective picture quality. Furthermore, it is likely in such cases, that the amplitude response will also fall outside the above mentioned boundaries.

Suppose that a channel response has a number of echoes, n, with similar perceived D/U ratios and similar delays. The combined PDUR is given by:

$$PDUR = -10 \log_{10} \sum_{i=1}^{n} 10^{-P_i/10}$$

$$= -10 \log_{10} \sum_{i=1}^{n} u_i^2$$

where u_i is essentially the ratio of the magnitude of each undesired echo to the magnitude of the desired signal.

If each individual perceived DU ratio is essentially the same ($u_i = \bar{u}$), then the magnitude of the overall equivalent single echo, m,

$$m = n^{\frac{1}{2}} \bar{u}.$$

The group delay bound for such a case would be approximately

$$gd(thres) \approx \bar{u} \sum_{i=1}^{n} d_i$$

$$\approx m \bar{d} n^{\frac{1}{2}}$$

Selecting m to be 0.282 (acceptable limit for $\bar{d}$ near 5 μsec) and selecting 4 as a conservative upper limit on the number of paths in this delay neighbourhood, one obtains the following group delay threshold:

$$gd(thres) = \pm 2.82 \text{ μsec.}$$

Channels whose group delay responses fall within this limit will be considered acceptable, although there will definitely be unacceptable channels that fall within the above bounds. Only clearly unacceptable channels would be prescreened. As before, there will be channels falling outside the group delay bounds that will have acceptable video quality (long echo paths). For channels falling in this category, those whose amplitude response falls outside the region $[1 - \sqrt{2}m, 1 + \sqrt{2}m]$, with $m=0.282$, will be discarded. The $\sqrt{2}$ scale factor is incorporated to reduce the possibility of discarding a channel response that would provide acceptable TV picture quality. Not all unacceptable channels are guaranteed to be detected by this ad hoc approach. As a result, this potentially simpler classification approach is not recommended. Furthermore, one cannot devise group delay and amplitude response masks that will reliably identify "good" video channels. Consequently, the recommended approach is to visually extract multipath parameters from baseband impulse responses, and evaluate the PDUR ratio, for a more reliable estimate of subjective picture quality.

ATTACHMENT II.1

AMPLITUDE AND GROUP DELAY RESPONSE FOR SINGLE POSITIVE ECHOES

Let the echo be characterized by delay, d, and magnitude, m. The channel frequency response is given by:

$$H_c(f) = 1 + me^{-j2\pi fd}$$

$$= (1 + m \cos 2\pi fd) - j\, m \sin 2\pi fd.$$

The amplitude response, A(f), is given by:

$$A(f) = (1 + m^2 + 2m \cos 2\pi fd)^{\frac{1}{2}}$$

$$\simeq 1 + m \cos 2\pi fd \quad \text{for small } m.$$

The phase response, $\phi(f)$, is given by:

$$\phi(f) = -\tan^{-1} \frac{m \sin 2\pi fd}{1+m \cos 2\pi fd}$$

The group delay response, G(f), is given by:

$$G(f) = -\frac{1}{2\pi} \frac{d\phi(f)}{df}$$

$$= \frac{m\, d\, (m + \cos 2\pi fd)}{1 + m^2 + 2\, m \cos 2\pi fd}$$

MORELAND, K.W.
--Telidon system study